UNIVERSITÀ DI PARMA

UNIVERSITA' DEGLI STUDI DI PARMA

DOTTORATO DI RICERCA IN

"Scienze del Farmaco, delle Biomolecole e dei Prodotti per la Salute"

CICLO XXXII

Convergent Medicinal Chemistry Approaches against Susceptible and Resistant Mycobacterial Infections

Coordinatore:
Chiar.mo Prof. Marco Mor

Tutore:
Chiar.mo Prof. Gabriele Costantino

Dottorando: Miriam Girardini

Anni 2016/2018

Table of contents

1. Introduction 6

1.1 Epidemiology 7

1.2 Tuberculosis 9

1.2.1 Diagnosis 9

1.2.2 Classification of resistant *Mycobacterium tuberculosis* 10

1.2.3 Pathogenesis 11

1.2.4 Current therapy 12

1.2.4.1 Classification of antitubercular drugs 13

1.2.4.1.1 First-line drugs 14

1.2.4.1.2 Second-line drugs 16

1.2.4.2 Recently approved drugs 19

1.2.5 TB pipeline 21

1.2.6 Mechanism of resistance 24

1.2.6.1 Target alteration 24

1.2.6.2 Degradation/modification of the antibiotic 25

1.2.6.3 Alteration of antibiotic intracellular concentration 25

1.2.7 Innovative approaches in antitubercular drug-discovery 27

1.3 Aim of the work 29

1.4 References 31

2. Characterization and optimization of antitubercular 2-aminothiazole based compounds 43

2.1 Introduction 43

2.2 Results and discussion 44

2.2.1 Alternative route for the synthesis of compound UPAR-453 44

2.2.2 Assessment of the reactivity to thiols 45

2.2.3 Hit-to-lead optimization through SAR and SMR 46

2.2.3.1 Investigation of the Structure-Activity Relationships 46

2.2.3.2 Investigation of solubility and Structure-Metabolism Relationships 50
2.2.4 Exploring the mechanism of action 60
2.3 Chemistry 62
2.3.1 Synthesis of UPAR-453 63
2.3.2 Synthesis of the panel of derivatives for the SAR investigation 63
2.3.3 Synthesis of metabolites and metabolically protected compounds 64
2.4 Conclusions 66
2.5 Materials and methods 68
2.5.1 Synthetic chemistry 68
2.5.2 Analytical chemistry 102
2.5.2 Biology 107
2.6 References 110
3. Inhibition of efflux systems through bacterial energetic shutdown 112
3.1 Introduction 112
3.2 Results and discussion 115
3.3 Chemistry 119
3.4 Conclusions 121
3.5 Materials and methods 122
3.5.1 Synthetic chemistry 122
3.5.2 Biology 132
3.6 References 134
4. Exploring the inhibition of Proteasome accessory factor A (PafA) as innovative antitubercular drug target 138
4.1 Introduction 138
4.2 Results and discussion 142
4.3 Conclusions 144
4.4 Materials and methods 145

4.4.1 Synthetic chemistry 145
4.4.2 Biology 150
4.5 References 154
5. Hijacking E3 ligases against each other using PROTACs 156
5.1 Introduction 156
5.2 Results and discussion 160
5.2.1 VHL-CRBN Hetero-PROTACs 160
5.2.1.1 Design of compounds 160
5.2.1.2 Evaluation of PROTACs cellular activity 164
5.2.1.3 Conclusions 167
5.2.2 CM11 optimization 167
5.2.2.1 Design of compounds 167
5.2.2.2 Evaluation of PROTACs cellular activity 168
5.2.2.3 Conclusions 170
5.2.3 CRBN Homo-PROTACs 171
5.2.3.1 Design of compounds 171
5.2.3.2 Evaluation of PROTACs cellular activity 172
5.2.3.3 Conclusions 173
5.3 Chemistry 173
5.4 Materials and methods 180
5.4.1 Synthetic chemistry 180
5.4.2 Biology 225
5.5 References 227
6. Conclusions 232
7. Acknowledgements 234
Appendix A. 235
Appendix B. 242

1. Introduction

Mycobacterial infections are a group of multisystem diseases caused by organisms of the genus *Mycobacterium*[1] which includes strictly aerobic, non-motile, acid-fast and rod-shaped bacilli with fastidious growth requirements and characterized by slow growth rate.[2] The term "mycobacterium" derives from the Greek word "myco" which means "fungus", and it has been referred to its peculiar way of growing in a mold-like manner on the surface of cultures, as fungi do. Although mycobacteria are evolutionarily classified as Gram-positive bacteria, the architecture of their cell wall, at a closer look, resembles that of Gram-negative organisms. In fact, in addition to an inner cytoplasmic membrane, they also possess a bilayer outer membrane mostly constituted by mycolic acids, which makes the cell surface particularly waxy and therefore resistant to Gram staining, disinfectants and, more importantly, to various antibiotics. This protective envelope represents a mechanism of intrinsic resistance, making these bacteria particularly harsh to treat.[3] There are over 190 species recognized within this genus, with very few not reported as pathogenic in humans or animals.[1] Mycobacteria are generally classified into three groups: (i) *Mycobacterium tuberculosis* complex, the causative agent of tuberculosis (TB); (ii) *Mycobacterium leprae*, the causative agent of leprosy and (iii) Nontuberculous mycobacteria (NTM).

Along with the most known *Mycobacterium tuberculosis,* Mycobacterium tuberculosis complex comprises *M. bovis*, including the *M. bovis bacillum Clamette- Guérin (BCG), M. africanum, M. caprae*, *M. canetti* and *M. microti*, among the others.[4] Although they are characterized by 99.9% similarity at the nucleotide level,[5,6] they are widely different in terms of their host tropisms, phenotypes, and pathogenicity.[7–9]

M. tuberculosis, first described by Robert Koch in 1882, represents the most common etiological agent of TB, a highly contagious airborne disease. TB generally affects the lung, but it can also affect other organs throughout the body and, in this case, is classified as extrapulmonary TB.[10] TB infection might be active, a contagious state characterized by clinical manifestations like cough, fever and weight loss, or latent, a

non-contagious state of persistent immune response to *M. tuberculosis* without clinical evidences of TB.[11] Nowadays TB represents one of the top ten causes of death worldwide and the leading cause from a single infectious agent (above HIV/AIDS).[12] The morbidity and mortality associated with TB has made its control a top priority for the World Health Organization, which in 2015 started the "END TB Strategy", a global program to fight TB worldwide.

In recent years, due to the heightened clinical recognition and improved laboratory diagnostic capabilities, also NTM are gaining increasing attention. NTM comprise a heterogeneous group of ubiquitous bacteria found in soil, water, food and animals. There are more than 150 species, but only a few of them are known to cause disease in humans. The incidence of NTM lung diseases and associated hospitalizations are on the rise, mainly in regions with low prevalence of TB, such as Europe and US.[13]

1.1 Epidemiology of mycobacterial infections

Worldwide, TB is the leading cause of death from a single infectious agent (above HIV/AIDS). It was estimated that, in 2017, TB caused about 1.3 million deaths among HIV-negative people and additional 300 000 deaths among HIV-positive people. It is also estimated that one third of the world population is infected with latent TB, and thus at risk of developing active TB disease during their lifetime.[12]

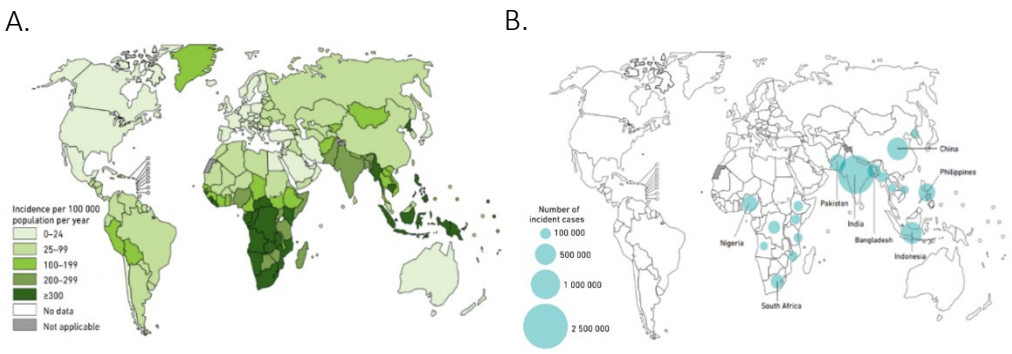

Figure 1. *(A) Estimated TB incidence rates in 2017;[12] (B) Estimated TB incidence in 2017 for countries with at least 100 000 incident cases.[12]*

Although vaccination with *Mycobacterium bovis* bacillus Calmette-Guérin (BCG) exists and protects against TB disease and mortality in some populations, its efficacy is suboptimal and clearly not adequate for disease control.[14–16] The incidence in 2017 (Figure 1A,B) counted about 10 million new cases: 5.8 million men, 3.2 million women and 1.0 million children. TB cases were registered in all countries and aged groups: 87% of cases were registered in the 30 countries listed in the in WHO's list of 30 high TB burden countries with India (27%), China (9%), Indonesia (8%), the Philippines (6%), Pakistan (5%), Nigeria (4%), Bangladesh (4%) and South Africa (3%), on the top of the list.

Moreover, the situation is worsened by the increasing emergence of drug-resistance, which continues to be a public health issue. In 2017, about 558,000 people developed TB resistant to rifampicin (RR-TB), which is the most effective first-line drug. 82% of them had multidrug-resistant TB (MDR-TB), among which 8.5% are extensively drug resistant tuberculosis (XDR-TB) (definitions of resistant *M. tuberculosis* are discussed in the Section 1.2.2). Most cases of RR-TB/MDR-TB regarded India (24%), China (13%) and the Russian Federation (10%). RR-TB/MDR-TB are 3.5% of new TB cases and 18% of previously treated cases had RR/MDR-TB, and the phenomenon is constantly increasing.[12] These resistant phenotypes represent an important issue as they are more difficult to eradicate and need longer therapeutic regimen and more toxic and poorly tolerated drugs for their treatment.[17,18] Moreover, among the 920,000 new cases of TB in 2017, 51% (464 633 cases) regarded HIV patients, of whom 84% were on antiretroviral therapy. Africa is the country where the burden of HIV-associated TB is the highest.

Unlike *M. tuberculosis* infections, public authorities are not usually made aware of NTM diseases, thus their epidemiology is difficult to define. The frequency of laboratory isolates appears to be increasing around the world,[19–23] and similar trends have been documented with respect to the disease. The US prevalence of NTM infections raised from about 1.8 per 100,000 people in 1980s[24] to 8.6 per 100,000 people in 2005/2006. There was a considerable geographic variation in disease with the west coast and

south-eastern USA having the highest prevalence and the Midwest the lowest. Globally, the increase of NTM disease incidence has been documented in many locations, including south-western Ireland, multiple countries in Asia, Australia and Canada.[19–23] Recent studies have also shown the high prevalence of drug resistance in NTM species that threatens adequate control of the disease.[25,26]

1.2 Tuberculosis

1.2.1 Diagnosis

As above reported, TB can be roughly defined as "active" or "latent". From a merely diagnostic point of view, the active form is characterized by the observation of viable bacteria in the sputum, while latent TB results negative to the sputum test and can be instead recognized by a delayed type hypersensitivity test, called purified protein derivative (PPD) skin test. The prompt diagnosis, in particular for active pulmonary TB, is crucial, both for treating the individual and for public health intervention in order to reduce further spread of the bacteria in the community.[27] However, accurate diagnosis suffers from the lack of an adequate assay that can be used in all circumstances. For example, the microscopic scanning of acid-fast stained bacilli in sputum smears, the most used technique in low and middle income countries, is convenient but insensitive, diagnosing only about 60-70% of pulmonary TB cases in adults[28,29] and with reduced sensitivity in children[30] and HIV-positive patients.[31–33] The skin test is a fast and cheap method which can reveal active and latent TB. It is performed by injecting a small amount of fluid containing a purified protein derivative (PPD) into the skin and checking the reaction within 48 to 72 hours. It is a widely used test, but it often gives false negative in children and people with HIV.[34] Moreover, the problem with its use in countries with high rates of TB infection is that the majority of people may have latent TB. Blood test, also called Interferon Gamma Release Assay (IGRA), provides more quantitative and dynamic measurement of cellular immune response, which would be important for serial testing studies, but it is rather costly, and it also requires blood samples and laboratory facilities to process them right after collection. It highlights the

presence of both latent and active TB by measuring the patient's immune system reaction to *M. tuberculosis*, based on the evidence that white blood cells from most patients that have been infected with *M. tuberculosis* will release interferon-gamma (IFN-γ) when mixed with antigens derived from *M. tuberculosis*.[35–37] In addition, a posterior-anterior chest radiograph is used to detect chest abnormalities, which may suggest the presence of pulmonary active TB or exclude this possibility in a person who has had a positive reaction to the skin or blood test. Beside these consolidated diagnostic approaches new methods has been developed recently, especially for detecting resistant bacilli. However, they involve expensive techniques and, for this reason, their use is limited.[30,38]

For all patients, it is generally recommended to isolate *M. tuberculosis* strain and test it for drug susceptibility, in order to promptly identify resistant strains and ensure effective treatment.

1.2.2 Classification of resistant *Mycobacterium tuberculosis*

Drug resistant TB represents a significant challenge to TB therapy and control programs. Resistant infections are generally classified as primary or acquired. Primary infection occurs when patients contract the disease after being exposed to resistant strains; on the other hand, acquired infection occurs when TB patients are treated with a drug regimen that is not effective to eventually eradicate the infection, leading to the selection of multi-drug resistant strains.[39]

Resistant *M. tuberculosis* are classified based on the number and type of drugs they are resistant to. They are called single-drug resistant (**SDR-TB**), if resistant to one first-line anti-TB drug only, or poly-resistant, if resistant to more than one first-line anti-TB drug, other than both isoniazid and rifampicin.

By definition, multi-drug resistant *M. tuberculosis* (**MDR-TB**) is referred to strains that are resistant to at least two of the first-line drugs, *i.e.* isoniazid (INH) and rifampicin (RMP). On the other hand, extensively-drug resistant *M. tuberculosis* (**XDR-TB**) is referred to MDR-TB strains that are resistant, in addition, to any fluoroquinolone and

at least one of three injectable second line drugs (i.e. amikacin, capreomycin or kanamycin).[40]

Isolated cases of TB with resistance to all first line and second line anti-TB drugs have been reported for the first time in Italy in 2007[41] and also a study from Iran in 2009 reported a group of patients with resistance to all anti-TB drugs tested.[42] These resistant *M. tuberculosis* strains are non-consensually defined extremely drug resistant (**XXDR-TB**) or totally drug resistant (**TDR-TB**), a designation for strains that are virtually untreatable since the loss of susceptibility to all of the molecules belonging to the anti-TB arsenal.

1.2.3 Pathogenesis

TB is a multicomponent airborne disease that primarily affects the lungs. People get infected by inhaling droplets containing *M. tuberculosis*, transported through the air, after coughs or sneezes from patients who have developed active pulmonary TB. Besides the direct transmission from person to person, the TB bacilli can also be transmitted by re-aerosolization from dust as they can survive for weeks outside the body.

Infection with *M. tuberculosis* follows a well-defined sequence of events. After being inhaled as droplets, the infectious bacilli reach the lower respiratory tract of the lungs, where they find the alveolar macrophages (AV) as first-line defence. Alveolar macrophages phagocytize the mycobacterial invaders but, in many cases, fail to kill them. They also produce cytokines which attract the first round of inflammatory cells, i.e., neutrophils, monocyte derived macrophages, NK cells, and T cells, which are the building blocks of the granuloma, also called tubercle, that the pathology is named after. The granuloma is a nodular inflammation characterized by an internal core of infected macrophages, foamy giant cells, and other macrophages, surrounded by a rim of lymphocytes. It is from this primary infection site, that bacteria can access the blood stream through the draining lymphatic system and infect the apical region of the lungs, forming secondary lesions. Although granuloma has the main role to contain the

infection (there are no symptoms of the disease during this phase, neither patients are contagious), it also provides a safe shelter for the bacteria, which can survive inside the granuloma in a latent state.[43] Due to some environmental factors, among those HIV infection and malnutrition, or genetic factors, in 5-10 % of cases the latent infection can reactivate into active TB.[44] Progression toward active disease involves the progress of a necrotic zone called "caseum" in the granuloma centre. The increasing necrosis in the centre of the granuloma disintegrates the structure, allowing bacterial spread.[45] One important aspect of TB infection is the ability of *M. tuberculosis* to deeply change its metabolism, allowing bacteria to survive in a dormant state inside the macrophages. Low availability of nutrients and oxygen in necrotic or caseous regions represents the main event leading to a change in the metabolic state of the bacteria and therefore to a state of dormancy. Inside the macrophages, *M. tuberculosis* increases its lipid metabolism, which may represent an adaptive response to the lack of carbohydrates. In addition, all those genes involved in the stress response, cell wall production and anaerobic respiration, are upregulated.[46,47]

1.2.4 Current therapy

Ideal treatment aims to cure the disease, rapidly stop the transmission, and prevent relapse.[48] Considering the multifaced aspects of the infection and the issue of resistance, current treatment for TB requires a long and multidrug regimen, which should be guided by predicted or demonstrated antibiotic susceptibility. Currently available drugs are classified as first-line drugs (isoniazid, rifampicin, pyrazinamide and ethambutol) and second-line drugs.[49,50] Rifampicin and isoniazid are the two most potent first-line drugs and they are administered for susceptible TB for a period of six months, in combination with pyrazinamide and ethambutol taken for the first two months of the treatment. Pyrazinamide synergistically reinforces the sterilizing activity of rifampicin and it contributes to short the duration of treatment to six months, while ethambutol reduces the development of drug resistant throughout the course of the therapy. These long drug regimens are challenging for both patients, who often do not

have the expected adherence to the therapeutic regimen, and healthcare systems, especially in low- and middle-income countries.[49]

Currently, the Directly Observed Treatment Short course (DOTS) is the internationally recommended strategy for TB control. The DOTS strategy promotes standardized treatment combined with supervision and patient support, which includes the strict visual control from the healthcare worker of the patient taking the medication to ensure the appropriate adherence to the therapy.[51] The regimen for the drug resistant strains need combination of more drugs, including second line drugs, which are less potent and less tolerated and required to be administered for a prolonged period, up to 24 months.[52]

1.2.4.1 Classification of antitubercular drugs

As above-mentioned, anti-TB drugs can be divided in two classes.[49]

First-line drugs. First-line drugs (Figure 2) comprise the most effective and less toxic drugs available, which are used for the standard treatment of fully susceptible *M. tuberculosis*. First-line drugs includes isoniazid (INH), rifampicin, also called rifampin, (RIF), pyrazinamide (PZA), ethambutol (EMB). In some cases, also Streptomycin is considered a first line drug, especially in those countries where the cost of the treatment must be contained.

Second-line drugs. Second-line drugs (Figure 3) includes different class of antibiotics which are less effective on fully susceptible *M. tuberculosis* or more toxic than first-line drugs, and they are used in the treatment of resistant infections:

- aminoglycosides (amikacin (AMK) and kanamycin (KM)),
- polypeptides (capreomycin (CM) and viomycin),
- flouroquinolones (moxifloxacin (MFX), levofloxacin (LFX) and ofloxacin (OFX)),
- thioamides (ethionamide (ETO), prothionamide (PTO)),
- cycloserine (DCS)
- linezolid
- *p*-aminosalicylic acid (PAS).

1.2.4.1.1 First-line drugs

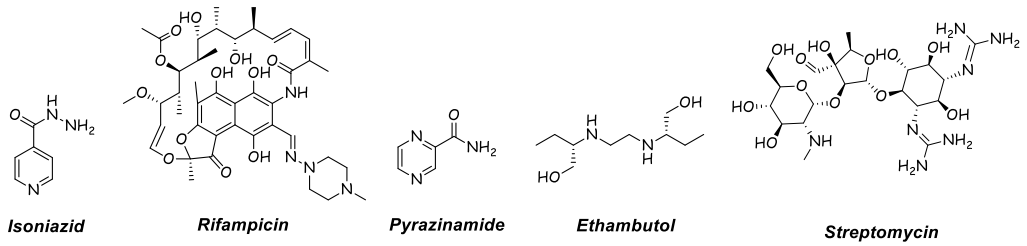

Figure 2. *First-line antitubercular drugs*

Isoniazid. Isoniazid, chemically the hydrazide of the isonicotinic acid, represents one of the most clinically successful antitubercular drugs ever developed.[53,54] It was first synthesized in 1912, but its antitubercular activity was only later discovered and it was launched on the market in 1952.[55] It has a dual action against *M. tuberculosis* as it is bactericidal toward rapidly-dividing bacilli and bacteriostatic against slow-growing mycobacteria. INH has multiple effects on TB bacillus and the exact nature of activity resulting in cell death is still unclear. The most investigated targets of INH are the enoyl acyl carrier protein (ACP) reductase (InhA)[56] and beta-ketoacyl ACP synthase (KasA).[57] INH is a pro-drug that requires cellular conversion into the active form by the bifunctional enzyme called KatG, having catalase and peroxidase activities. The introduction of INH on the market is considered a milestone in the TB treatment for its activity, limited toxicity and low cost. However, although once INH was synonymous with TB chemotherapy and prophylaxis, it has paradoxically become a defining feature of the multidrug-resistance (MDR) and extensively drug-resistance (XDR) globally.

Rifampicin. Rifampicin (RIF), also called rifampin in the US, is a semisynthetic antibiotic of the rifamycins group. The first rifamycin described, namely rifamycin B, was extracted from the soil actinomycete *Amycolatopsis mediterranei*.[58] The natural product had modest antibiotic activity, but semisynthetic derivatives of the rifamycin family, in particular rifampicin, have proved to be highly successful in the clinic. Rifampicin has an excellent sterilizing activity against *M. tuberculosis* and it is effective against active and latent TB. It binds to the β-subunit of the bacterial RNA

polymerase, where it blocks the exit tunnel for RNA elongation, inhibiting bacterial transcription.[59,60]

Pyrazinamide. The activity of pyrazinamide (PZA), an analogue of the nicotinamide, was serendipitously observed because its chemical synthesis was followed immediately by the *in vivo* testing, bypassing the *in vitro* assays. It was first tested on animal models by Vital Chorine, who observed the ability of subcutaneous nicotinamide to prolong the survival of guinea pigs infected with *M. tuberculosis*.[61] Unexpectedly, PZA was found to be inactive in *in vitro* culture, at neutral pH, as it requires a slightly acidic pH which usually characterizes the inflammatory environment at the TB infection site.[62] Due to this major difficulty, the susceptibility test for PZA is not routinely performed in many laboratories in the world, and, for this reason, comprehensive surveillance studies of pyrazinamide resistance are rare.[63] PZA has a remarkable sterilising activity, responsible for killing the bacilli during the initial intensive phase of chemotherapy, allowing to shorten the therapy from 9 to 6 months. PZA is a pro-drug, activated by the conversion into the pyrazinoic acid, catalysed by some amidases, i.e. pyrazinamidase or nicotinamidase. The limitations in reproducing the therapeutic activity *in vitro* models has also slowed down the study of the mechanism of action, which is not fully understood as yet. Pyrazinoic acid was thought to inhibit the enzyme fatty acid synthase (FAS), a crucial enzyme involved in the synthesis of fatty acids. A different hypothesis suggested that the accumulation of pyrazinoic acid inside the bacterial cell causes disruption of the membrane potential.

Ethambutol. Like PZA, ethambutol (EMB) was immediately tested in animal after its discovery. Early studies revealed that it is taken up by both replicating and non-replicating bacteria but active only against replicating bacilli. It binds to the arabinosyl transferase, inhibiting the biosynthesis of arabinogalactan, an important step in the cell wall biosynthesis.[64,65]

Streptomycin. Streptomycin (STM) is an antibiotic compound belonging to the class of aminoglycosides and it is a natural compound derived from the actinobacterium

Streptomyces griseus. It has a bactericidal activity, that inhibits both Gram-positive and Gram-negative bacteria and it is active also against multi-drug resistant Gram-negative pathogens, making it a useful broad-spectrum antibiotic.[66–68] When used for the treatment of *M. tuberculosis*, it is generally not considered a first line drug, mostly because of its toxicity, with the exception of those countries where more expensive treatments are not available. By binding the small 16S rRNA of the 30S subunit of the bacterial ribosome, STM interfere with the protein synthesis, disrupting the initiation and elongation steps in protein synthesis. Differently from most inhibitors of the protein synthesis, STM and the other aminoglycosides are bactericidal. This behaviour is not fully understood but the most likely explanation appears to be that aminoglycosides induce the production of abnormal membrane proteins that may result in alterations in membrane permeability.[69]

1.2.4.1.2 Second-line drugs

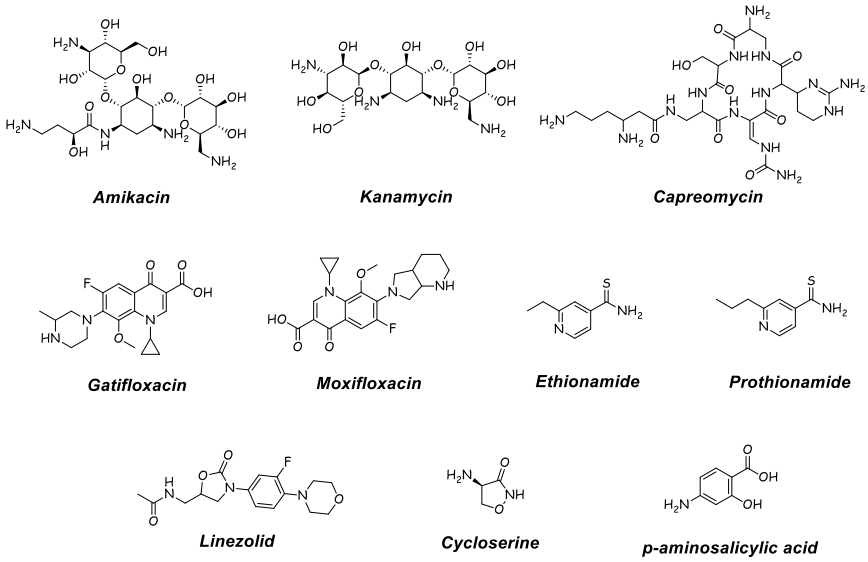

Figure 3. *Second-line antitubercular drugs*

Aminoglycosides. Aminoglycosides, like streptomycin (SM) amikacin (AMK), kanamycin (KAN), are important injectable drugs in the treatment of MDR-TB.[49] Chemically they are characterized by a core structure of amino sugars connected *via* glycosidic linkages to a dibasic aminocyclitol. The core structure is decorated with a variety of amino and

hydroxyl substitutions having a direct influence on the mechanism of action. They inhibit the protein synthesis by binding the 16S ribosomal rRNA of the 30S ribosome[70] with high affinity. As a result of this interaction, they promote the miscoding of mRNA codons, allowing for incorrect amino acids to assemble into a polypeptide, which after being release, caused damage to the cell membrane. Some of them can also interfere with the protein synthesis by blocking elongation or inhibiting initiation.[70,71] Aminoglycosides are potent bactericidal, having also a prolonged post-antibiotic affect, however they have substantial renal toxicity and they also potentially cause irreversible hearing loss. For this reason, regular monitoring of hearing and renal function is recommended.

Polypeptides. Antibacterial polypeptides are non-ribosomal secondary metabolites usually produced by microorganism like bacteria and fungi. Among those, viomycin and capreomycin belong to the tuberactinomycin family of antibiotics,[72] which are among the most effective antibiotics against MDR-TB. Although viomycin was the first member of this family to be identified, it has been replaced by binding the less toxic capreomycin. Capreomycin exerts its activity by binding both the ribosomal subunits and disrupting the bacterial protein biosynthesis.[73]

Fluoroquinolones. Fluoroquinolones (FQs) are molecules with a broad-spectrum antimicrobial activity and they are widely used for different types of infections. By inhibiting the ligase activity of the type II topoisomerases, gyrase, and topoisomerase IV, they prevent the bacterial DNA from unwinding and duplicating. This triggered a series of poorly defined cellular events that ultimately result in cell death. FQs have excellent *in vivo* and *in vitro* activity and they also able to penetrate inside macrophages and kill intracellular bacteria. They also showed bactericidal activity against RIF-tolerant persistent bacilli able to survive despite chemotherapy.[74] Among this class, gatifloxacin and moxifloxacin showed the lowest minimum inhibitory concentrations (MICs) on *M. tuberculosis.* Fluoroquinolones are generally well tolerated, even with long term use in treating TB, but rare and serious adverse effects have been reported.[75]

Thioamides. Thioamide drugs, ethionamide (ETH) and prothionamide (PTH), have been widely used for many years in the treatment of TB. They are structurally similar to isoniazid and, like isoniazid, inhibit the synthesis of mycolic acids by targeting the enoyl-acyl carrier protein reductase. For this reason, they often show cross-resistance with isoniazid even partial cross resistance is uncommon. Thioamides are prodrugs which requires activation to exert their action. They are generally well tolerated apart from the common occurrence of gastrointestinal irritation.[76,77]

Cycloserine. Cycloserine is a natural product, initially isolated from *Streptomyces orchidaceus* in the 1950s.[78] It is a broad-spectrum agent, active against both Gram-positive and Gram-negative organisms, but only marginally active against *M. tuberculosis*. It is an analogue of the amino acid D-alanine and it exerts its activity by blocking two enzymes: (i) L-alanine racemase, the enzyme responsible for the conversion of L-alanine in D-alanine, (ii) D-alanylalanine synthetase, responsible for the incorporation of D-alanine into the pentapeptide necessary for peptidoglycan formation and bacterial cell wall synthesis. It is a bacteriostatic agent, with a limited use due to its weak activity, frequent adverse reactions and short shelf life (<24 months).[17] Side effects mainly consist in severe psychiatric adverse reactions, which makes necessary a psychiatric evaluation before starting the treatment.

Linezolid. Linezolid is a synthetic oxazolidinone antimicrobial drug used for Gram-positive infections. It acts by binding the P-site on the bacterial 23S ribosomal RNA of the 50S subunit, preventing the formation of bacterial ribosomes. As a result of its unique mechanism, it shows no cross-resistance with other classes of antibiotics. Linezolid is bacteriostatic on *M. tuberculosis* disrupting bacterial growth *via* inhibition of the initiation process during protein synthesis.[50,79] Side effects include reversible myelosuppression and peripheral and optic neuropathy.[80–82] However, despite these side effects, linezolid-containing regimens have proved efficacy in patients with MDR-TB.[83]

p-aminosalicylic acid. *para*-aminosalicylic acid (PAS) is one of the first antitubercular agents found to be effective, in the 1940s.[84] It has a very low effectiveness and it is poorly tolerated, making it the last-choice drug among second-line group. Side effects of PAS includes persistent nausea, vomiting, diarrhoea and hepatitis, usually preceded by a rash or a fever. Other occasional side effects include increased prothrombin time and malabsorption syndrome. Moreover, PAS is expensive, and requires to be kept refrigerated *via* a cold chain which is not always available in low income countries.

1.2.4.2 Recently approved drugs

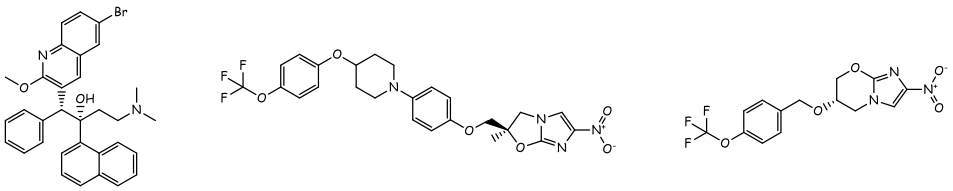

Figure 4. *Recently approved antitubercular drugs*

Considering that the antitubercular first-line drugs were developed more than half a century ago and most of the clinical studies defining their optimal combination were completed in the 1970s,[85] the recent approval of bedaquiline has represented an important achievement.

In 2012, bedaquiline (Figure 4) was the first new antitubercular drug to be approved since rifapentine approval in 1998 and the first antitubercular drug with a novel mechanism of action to be approved after more than 40 years (rifampicin was introduced in clinic in 1968).[60,86] In addition, few years after bedaquiline approval, two compounds of the nitroimidazole class, delamanid[87] and pretomanid,[88] were also marketed.

Bedaquiline. Bedaquiline (BDQ, formerly TMC-207, marketed as Sirturo®) is a diarylquinoline, discovered from a whole-cell high-throughput screening against *M. smegmatis*,[89] a non-pathogenic bacterium closely related to *M. tuberculosis*. It is an ATP synthase inhibitor which acts by binding to the subunit *c* of the mycobacterial ATP

synthase enzyme (complex V), thus blocking its action.[90,91] It showed an MIC of 0.03–0.12 μg/mL against drug-sensitive and drug-resistant *M. tuberculosis* strains, being active against replicating and non-replicating bacilli. Recently, it was demonstrated that mycobacteria cultured on lipid-rich media are more susceptible to the killing action of bedaquiline, suggesting an important role of the energy source on mycobacterial susceptibility.[92] Mutation in *atp*E was found to be linked with resistance to bedaquiline, as well as drug efflux, which plays a crucial role in the natural and acquired resistance to bedaquiline.[93] Moreover, when exposed to bedaquiline, mycobacteria tend to minimize the consumption of cellular ATP and to enhance their capacity of generating ATP *via* different pathways, which contributes to maintain bacterial viability in spite of antibiotic stress.[92] Side effects of bedaquiline includes nausea, hepatitis and a remarkable cardiotoxicity, with the prolongation of the QT interval which is enhanced by the association with other drugs, like clofazimine or moxifloxacin.[94] This drug has also a black-box warning for increased risk of death and arrhythmias. Bedaquiline is indicated as part of combination therapy in adults with pulmonary MDR-TB.[95]

Delamanid and pretomanid. Delamanid (deltyba®, formerly OPC-67683) and pretomanid (formerly PA-824) are bicyclic nitroimidazoles. They were originally investigated as radiosensitizers for cancer chemotherapy[96] but they were later found to show potent bactericidal activity against multidrug resistant *M. tuberculosis*.[97,98] In 2014, Delamanid has received conditional approval for the treatment of multi- and extensively drug resistant TB in EU, Japan and South Korea. Pretomanid was approved on August 2019, for MDR-TB that is treatment-intolerant or non-responsive to standard therapy. They are prodrugs that requires biotransformation by the mycobacterial F420 coenzyme system.[99] Upon activation, they inhibits methoxy-mycolic and keto-mycolic acid synthesis *via* the formation of a radical intermediate between delamanid and desnitro-imidazooxazole. This leads ultimately to the depletion of mycobacterial cell wall components and mycobacterial death. Moreover, nitroimidazooxazole derivative is thought to generate poisoning reactive nitrogen species, such as nitrogen oxide (NO). They are active both toward the actively replicating and the non-replicating bacteria.

Severe side effects were observed, including cardiac arrhythmia and general central nervous system toxicity, especially when used in combination with isoniazid or fluoroquinolones.[76]

1.2.5 TB pipeline

A.

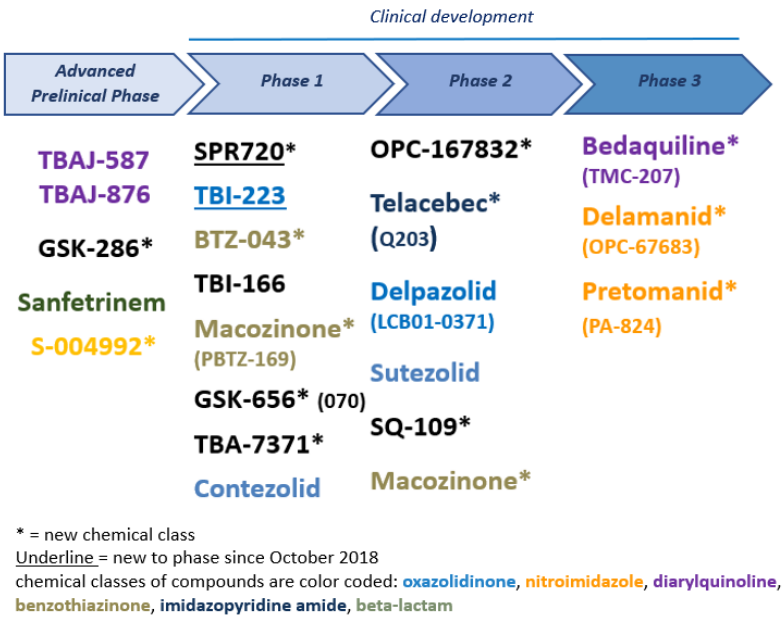

B.

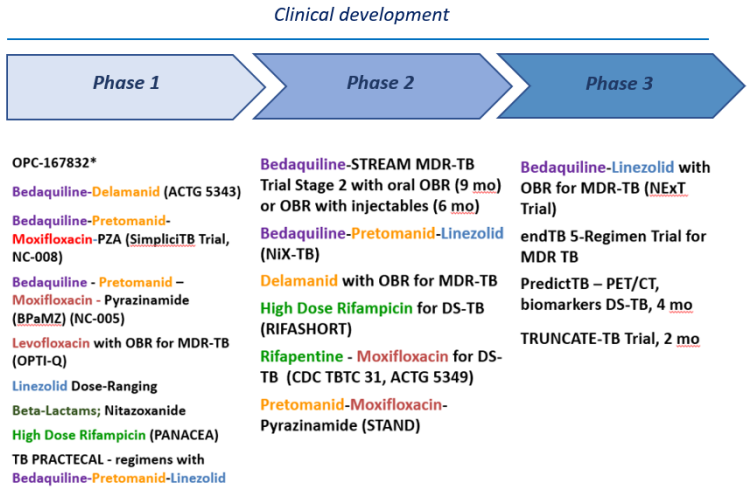

Figure 5. *(A) TB single drugs pipeline (B) TB drug regimens pipeline*

After decades of oblivion, TB drug development has recently experienced a major intensification resulting in a growing pipeline of new potential antitubercular agents.[100]

In Figure 5A and 6, the set of molecules currently in the pipeline[101] is represented, focusing the attention on compounds in advanced preclinical/clinical phases. Interestingly, at the current state the research is oriented toward an improvement of already known class of molecules, as in the case of telacebec (Q-203), structurally related to delamanid and pretomanid or in the case of the compounds TBAJ-587 and TBAJ-876, derived from bedaquiline. Most of the chemical classes in the pipeline, such as diarylquinoline and nitroimidazoles, were discovered *via* a phenotypic screening. This strategy seems to be the preferred approach in antibacterial drug-discovery, and antitubercular in particular, mostly for the lack of correspondence between target inhibition and cellular activity, which is primarily linked to the difficulty of drugs in penetrating the mycobacterial cell wall.[102] Phenotypic screening relies on two main steps: (i) The identification of a molecule with a promising MIC in whole cell screening and (ii) the subsequent investigation of the mode of action. The validation the molecular target represents a main challenge of the phenotypic whole-cell screening.[103] Giving the complexity of the TB infection and considering the risk of relapses and possible development of resistance, single-drug treatment is not recommended. TB has been treated with combined therapy for over fifty years as it was observed that regimens based on a single drug results in the rapid development of resistance and treatment failure.[104] Thus, besides the pipeline of the single antitubercular agents, a second pipeline regarding the drug regimen is generally contemplated (Figure 5B), in which combination of already approved antitubercular drugs are tested, in order to evaluate the effectiveness of drugs in combination and define the proper doses for the therapy. Currently the research is oriented in facing two important challenges: shortening the duration of the therapy for both susceptible and resistant infections and preventing the raise of resistances. It is believed that those two aspects can be strongly modulated by the composition of the drug cocktail.

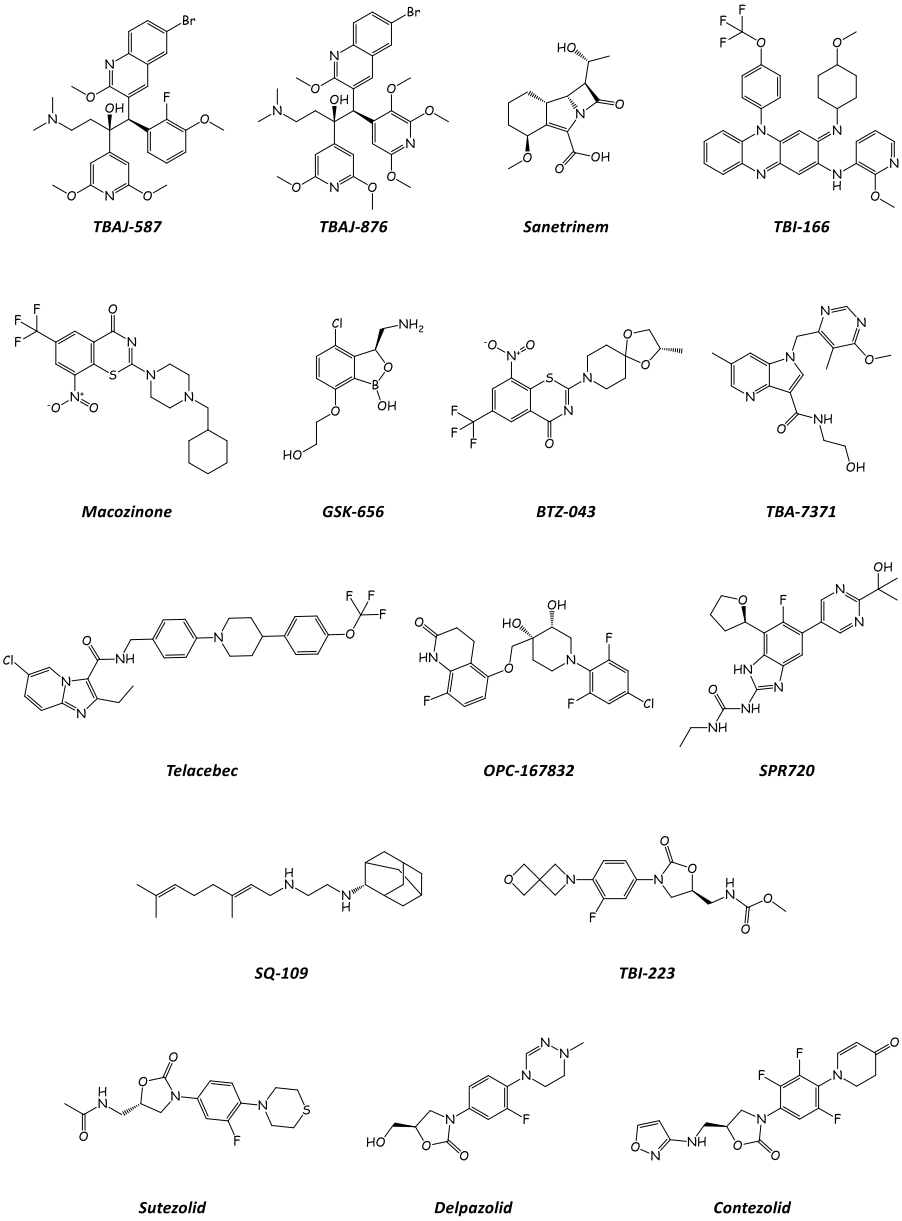

Figure 6. *Compounds in TB single-drug pipeline*

1.2.6 Mechanisms of resistance

Antibiotic resistance in *M. tuberculosis* occurs *via* various mechanisms,[105] among which the most common are:

- Target alterations
- Degradation/modification of the antibiotic
- Alteration in the antibiotic permeability

1.2.6.1 Target alteration

Introducing modifications to the target site is one of the most common mechanisms of antibiotic resistance in bacteria. The primary mechanism of target alteration consists in the acquisition of point mutation in the genes encoding for the target sites. This results in structural modifications of the target that interfere with the binding of the antimicrobial agents, thus reducing the susceptibility of the bacteria for the antibiotic. One of the most classical examples of mutational resistance regards rifampicin (RIF). The binding pocket of rifampicin is a highly conserved structure of the RNA polymerase β subunit, encoded by *rpoB*. Many single step-point mutations affecting the *rpoB* has been reported to be involved in high-level resistance to this drug. Of note, a common feature of these mutations is that despite they caused a decreased affinity of the drug for its target, they do not the catalytic activity of the polymerase, permitting transcription to continue.[106] Another example of resistance derived from mutations regards fluoroquinolones, toward which resistance emerges *via* genetic changes in the genes *gyrA-gyrB* and *parC-parE* encoding for DNA gyrase and topoisomerase IV, respectively.[74,107,108] Given the multiple targets of the fluoroquinolones, a single mutation produces minor increases in the MIC and clinically relevant resistance to fluoroquinolones frequently requires an accumulation of mutations over time. Mutational changes are also responsible for resistance to linezolid, which primary occurred *via* mutations in the *rplC* and *rrl* target genes, associated with high or low-level linezolid resistance respectively.[109]

1.2.6.2 Degradation/ modification of the antibiotic

The production of enzymes capable of degrading or introducing chemical changes to the antibiotics is a well-known mechanism of resistance in bacteria.[110] Degradation of the antibiotic mainly consists in hydrolysis and it is clinically relevant especially for β-lactams, while alterations in the chemical structure consists in reaction transferring chemical groups on the antibiotic molecules, among which the most frequent are acetylation, phosphorylation and adenylation. In this case the final effect of the modification is often related to steric hindrance that decreases the affinity of the drug for its target, resulting in higher bacterial MICs. One example of this type of resistance is the presence in *M. tuberculosis* of aminoglycoside modifying enzymes (AMEs) that covalently modify the hydroxyl or amino groups of the aminoglycoside molecule. To date, multiple AMEs have been described and they have become the predominant mechanism of aminoglycoside resistance worldwide.[111]

1.2.6.3 Alteration of antibiotic intracellular concentration

Many of the antibiotics used in clinical practice have intracellular bacterial targets and therefore requires the antibiotic to cross the cell wall and reach the intracellular environment at a proper concentration. Bacteria have developed mechanisms to prevent the antibiotic from reaching its intracellular target in effective concentrations by decreasing the uptake or enhancing the efflux of antimicrobial molecules.[110]

The mycobacterial cell envelop has a key role in natural resistance to antibiotics. Mycobacterial have evolved a complex cell envelop which consists of three main structural components: (i) a network of peptidoglycan, (ii) the arabinogalactan polysaccharide, and (c) the long-chain mycolic acids.[112–114] This cell permeability barrier protects the bacteria from environmental stress, contributing to the virulence, and confers natural resistance to many antibiotics. Another key component of mycobacterial resistance regards efflux pumps, which are membrane transport proteins, involved in the outward transport of a wide variety of substrates to the exterior of the cell in an energy-dependent manner. They have a broad substrate

specificity from cell toxins and lipids to dyes and they are also able to extrude antibiotics to the extracellular environment, being part of the innate mechanism of antibiotic resistance. Usually they confer low-to-medium level of resistance to antibiotics, but the sustained pressure of subinhibitory concentrations of antibiotic triggered by the overexpression of efflux pumps, may result in the selection of spontaneous mutants.[115–117] For example, it was demonstrated that exposure of *M. tuberculosis* strains to isoniazid, the most important first line drug, induces the activity of efflux pumps that make the bacteria more resistant to this antibiotic.[118,119] Depending on their energy source and substrates, efflux pumps are classified in different families: the resistance-nodulation-division (RND) family, the major facilitator superfamily (MFS), the ATP-binding cassette (ABC) superfamily, the drug/metabolite transporter (DMT) superfamily, and the multidrug and toxic compound extrusion (MATE) family (Figure 7). With the exception for the RND superfamily, only found in Gram-negative bacteria, the other four families are widely distributed in both Gram-positive and negative bacteria.[120]

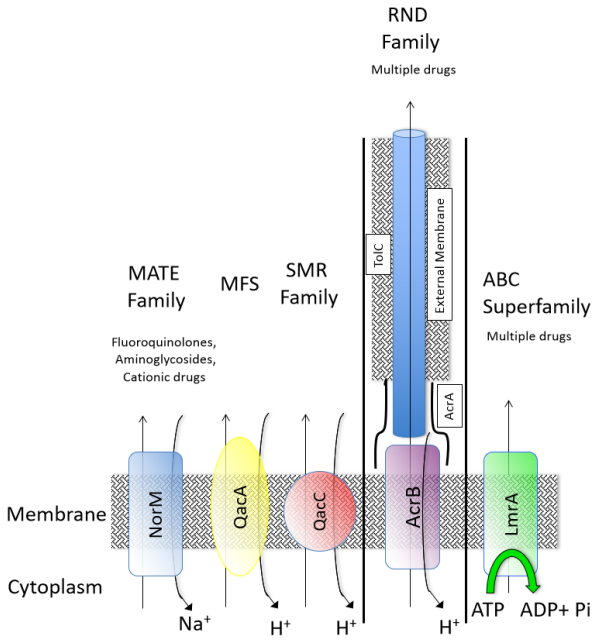

Figure 7. *Different classes of efflux pumps*

The involvement of efflux pumps in the mycobacterial virulence and antibiotic resistance makes them attractive drug targets, making the identification and characterization of mycobacterial efflux pump inhibitors (EPIs) valuable approach for the development of new effective therapies.[121,122]

1.2.7 Innovative approaches in antitubercular drug-discovery

As discussed throughout this chapter, the increasing emergence of drug-resistance mycobacteria represents a serious global health issue, which requires novel effective drug discovery strategies. The development of drugs acting against new molecular targets toward which the resistance has not yet developed, might represent a valuable strategy, as above discussed for the recently approved bedaquiline. However, the lack of innovation in the drug discovery approach and/or in the combination of the therapeutic cocktail makes predictable the onset of resistance also for the newly marketed drugs, as already confirmed by the identification of *M. tuberculosis* resistant to both bedaquiline and delamanid.[123] It appears evident that, beside the need of compounds with novel mechanisms of action, also therapeutic tools able to prevent the onset of resistance are required. Recently, adjuvant therapies (AT) and host-directed therapies (HDT) has gained increasing consideration in the antibacterial landfill, introducing a novel paradigm primarily focused not on the bacteria itself but instead on the host-pathogen interaction.[124,125] Unlike most of the antibiotics currently used, both AT and HDT are not supposed to have any intrinsic microbicidal activity, and they are intended to be used in combination with bactericidal molecules. They are called AT if target the bacteria, or HDT if the molecular targets belong to the host. HDT can provide beneficial effects by (i) helping the host in clearing the pathogen or (ii) controlling inflammation to prevent permanent lung tissue damage. The complex immunological events unfolding during *M. tuberculosis* infection offer many opportunities for HDTs and, in the last years, several drugs, mainly repurposed, have been evaluated for the treatment of TB in combination with the currently approved antituberculars either in pre-clinical experiments or in clinical trials.[126–129]

Ideal ATs are based on non-bactericidal compounds designed to enhance the effectiveness of first or second line antitubercular drugs and prevent the emergence of resistance.[130] Efflux Pumps Inhibitors (EPIs) are molecules that represent the most studied example of such approach. Considering the crucial role of efflux pumps in antibiotic tolerance, their inhibition may be able to provide several therapeutic benefits. Different well-known compounds have been proved to have efflux pumps inhibitory activity on *M. tuberculosis*. Among those there are the antiarrhythmic verapamil and the neuroleptic thioridazine, both acting as Ca^{2+} channel blockers and inhibiting efflux pump activity by reduction of the transmembrane potential.[131–133] The protonophores carbonyl cyanide *m*-chlorophenyl hydrazone (CCCP), 2,4-dinitrophenol (DNP) and valinomycin, inhibit efflux pump activity by disrupting the proton motif force (PMF).[134] Since efflux pumps require an energy source, it is thought that compounds targeting the energy metabolism and ATP production of the bacterial cell are able to affect the efflux pumps activity.[135] Numerous *in vitro* studies have demonstrated the effect of efflux pump inhibition in mycobacteria, and also in *in vivo* experiments the use of EPI as adjuvants has explored.[136–139] For example, verapamil (VP) was found to have efflux pump inhibitory properties and antimicrobial-potentiating effects in the treatment of *M. tuberculosis* both *in vitro* and *in vivo*. Verapamil profoundly decreases the MIC of bedaquiline on *M. tuberculosis* by 8- to 16-fold.[137] In addition, inhibition of mycobacterial efflux pumps by verapamil reduces the bacterial drug tolerance induced in the intracellular compartment inside the macrophages and in zebrafish granuloma-like lesions.[140] The most studied EPI is thioridazine (TZ), belonging to the class of phenothiazine. Thioridazine is able to potentiate the activity of co-administered antitubercular drugs and enhance intracellular killing by macrophages.[141] Moreover, it showed good results when administered on compassionate basis in a clinical trial in Argentina to patients with XDR-TB in combination with linezolid and moxifloxacin.[142] Beside efflux inhibition, some phenothiazines display also direct antimycobacterial activity *via* various mechanisms as yet not fully understood.

Summarizing, EPI can decrease the emergence of resistance, partially restore the activity of antibiotics toward which the bacteria had developed resistance, enhance the amount of bacterial cells killed by macrophages and shorten the therapy. However, despite many advantages there are still numerous factors to be addressed to overcome limitations of important adverse effects associated with efflux pump inhibitors *in vivo*.

1.3 Aim of the work

Mycobacterial infections are a global public health issue. In particular TB, an airborne disease mostly caused by *M. tuberculosis*, represents one of the top ten causes of death worldwide and the leading cause from a single infectious agent. The complexity of TB pathogenesis requires a long and multi-drug regimen, including a combination of four drugs at minimum, challenging for both healthcare system and the patients. This threatening scenario is further worsened by the rapid spread of bacterial resistances, that require innovative approaches for an effective containment. Despite many efforts from the World Health Organization, there are still several challenges to be addressed for the TB control globally. In particular, lateral strategies for the identification of promising hit compounds in early phases of drug discovery are needed. At this regard, along with novel bactericidal compounds with innovative mechanism of action, chemical tools able to prevent the emergence of resistance and/or reverse resistance already established, might suitably address the need of novel antitubercular strategies. In recent years, Host-Directed Therapies and Adjuvant Therapies have gained increasing consideration as alternative approaches able to prevent the emergence of resistance when used in combination with antitubercular bactericidal drugs. Among the many targets that can be exploited for adjuvant therapy, efflux pumps are particularly worth of note for the many roles they play in mycobacterial resistance and drug tolerance. In the last years, a number of compounds with efflux pumps inhibitory activity, mostly marketed drugs repositioned for this purpose, have been described. However, off target toxicity has been frequently observed and it currently represents

an important limitation for the possibility to move these compounds further toward drug development.

The aim of this thesis was to identify novel hit compounds for antitubercular treatment taking into account what above reported, with a particular focus on overcoming resistances. To do that in the most comprehensive way, three converging medicinal chemistry approaches were envisaged:

- a hit-to-lead optimization process of potent antitubercular hit compounds (Chapter 2)
- the development of a non-cytotoxic efflux pump inhibitor (Chapter 3)
- the exploration of Proteasome Accessory Factor A (PafA) as antitubercular drug target (Chapter 4)

1.4 References

(1) Forbes, B. A. Mycobacterial Taxonomy. *J. Clin. Microbiol.* **2017**, *55* (2), 380–383.

(2) Forbes, B. A.; Hall, G. S.; Miller, M. B.; Novak, S. M.; Rowlinson, M.-C.; Salfinger, M.; Somoskövi, A.; Warshauer, D. M.; Wilson, M. L. Practice Guidelines for Clinical Microbiology Laboratories: Mycobacteria. *Clin. Microbiol. Rev.* **2018**, *31* (2), e00038-17.

(3) Fu, L. M.; Fu-Liu, C. S. Is Mycobacterium Tuberculosis a Closer Relative to Gram-Positive or Gram-Negative Bacterial Pathogens? *Tuberc. Edinb. Scotl.* **2002**, *82* (2–3), 85–90.

(4) Esteban, J.; Muñoz-Egea, M.-C. Mycobacterium Bovis and Other Uncommon Members of the Mycobacterium Tuberculosis Complex. *Microbiol. Spectr.* **2016**, *4* (6).

(5) Böddinghaus, B.; Rogall, T.; Flohr, T.; Blöcker, H.; Böttger, E. C. Detection and Identification of Mycobacteria by Amplification of RRNA. *J. Clin. Microbiol.* **1990**, *28* (8), 1751–1759.

(6) Velayati, A. A.; Farnia, P. F.; Atlas of Mycobacterium Tuberculosis - 1st Edition, Elsevier, **2017**.

(7) Brosch, R.; Gordon, S. V.; Marmiesse, M.; Brodin, P.; Buchrieser, C.; Eiglmeier, K.; Garnier, T.; Gutierrez, C.; Hewinson, G.; Kremer, K.; Parson, L. M.; Pym, A. S.; Samper, S.; Van Sooligen, D.; Cole, S. T. A New Evolutionary Scenario for the Mycobacterium Tuberculosis Complex. *Proc. Natl. Acad. Sci. U. S. A.* **2002**, *99* (6), 3684–3689.

(8) Aktaş, E.; Zozio, T.; Cömert, F. B.; Külah, C.; Aydin, O.; Rastogi, N.; Sola, C. A First Insight into the Genetic Diversity and Population Structure of Mycobacterium Tuberculosis in Zonguldak, Turkey. *Clin. Microbiol. Infect. Off. Publ. Eur. Soc. Clin. Microbiol. Infect. Dis.* **2008**, *14* (1), 55–59.

(9) Wirth, T.; Hildebrand, F.; Allix-Béguec, C.; Wölbeling, F.; Kubica, T.; Kremer, K.; van Soolingen, D.; Rüsch-Gerdes, S.; Locht, C.; Brisse, S.; Meyer, A.; Supply, P.; Niemann, S. Origin, Spread and Demography of the Mycobacterium Tuberculosis Complex. *PLoS Pathog.* **2008**, *4* (9), e1000160.

(10) Banta, J. E.; Ani, C.; Bvute, K. M.; Lloren, J. I. C.; Darnell, T. A. Pulmonary vs. Extra-Pulmonary Tuberculosis Hospitalizations in the US [1998-2014]. *J. Infect. Public Health* **2019**.

(11) WHO. Fact sheets on tuberculosis. http://www.who.int/tb/publications/factsheets/en/.

(12) WHO. Global tuberculosis report 2018. http://www.who.int/tb/publications/global_report/en/.

(13) Wassilew, N.; Hoffmann, H.; Andrejak, C.; Lange, C. Pulmonary Disease Caused by Non-Tuberculous Mycobacteria. *Respir. Int. Rev. Thorac. Dis.* **2016**, *91* (5), 386–402.

(14) Colditz, G. A.; Berkey, C. S.; Mosteller, F.; Brewer, T. F.; Wilson, M. E.; Burdick, E.; Fineberg, H. V. The Efficacy of Bacillus Calmette-Guérin Vaccination of Newborns and Infants in the Prevention of Tuberculosis: Meta-Analyses of the Published Literature. *Pediatrics* **1995**, *96* (1 Pt 1), 29–35.

(15) Pitt, J. M.; Blankley, S.; McShane, H.; O'Garra, A. Vaccination against Tuberculosis: How Can We Better BCG? *Microb. Pathog.* **2013**, *58*, 2–16.

(16) Lambert, P.-H.; Hawkridge, T.; Hanekom, W. A. New Vaccines Against Tuberculosis. *Clin. Chest Med.* **2009**, *30* (4), 811–826.

(17) Caminero, J. A.; Sotgiu, G.; Zumla, A.; Migliori, G. B. Best Drug Treatment for Multidrug-Resistant and Extensively Drug-Resistant Tuberculosis. *Lancet Infect. Dis.* **2010**, *10* (9), 621–629.

(18) Rieder, H. L.; Lauritsen, J. M.; Naranbat, N.; Katamba, A.; Laticevschi, D.; Mabaera, B. Quantitative Differences in Sputum Smear Microscopy Results for Acid-Fast Bacilli by Age and Sex in Four Countries. *Int. J. Tuberc. Lung Dis. Off. J. Int. Union Tuberc. Lung Dis.* **2009**, *13* (11), 1393–1398.

(19) Kennedy, M. P.; O'Connor, T. M.; Ryan, C.; Sheehan, S.; Cryan, B.; Bredin, C. Nontuberculous Mycobacteria: Incidence in Southwest Ireland from 1987 to 2000. **2012**.

(20) O'Brien, D. P.; Currie, B. J.; Krause, V. L. Nontuberculous Mycobacterial Disease in Northern Australia: A Case Series and Review of the Literature. *Clin. Infect. Dis. Off. Publ. Infect. Dis. Soc. Am.* **2000**, *31* (4), 958–967.

(21) Lai, C.-C.; Hsueh, P.-R. Diseases Caused by Nontuberculous Mycobacteria in Asia. *Future Microbiol.* **2014**, *9* (1), 93–106.

(22) Lai, C. C.; Tan, C. K.; Chou, C. H.; Hsu, H. L.; Liao, C. H.; Huang, Y. T.; Yang, P. C.; Luh, K. T.; Hsueh, P. R. Increasing Incidence of Nontuberculous Mycobacteria, Taiwan, 2000-2008. *Emerg. Infect. Dis.* **2010**, *16* (2), 294–296.

(23) Adjemian, J.; Olivier, K. N.; Seitz, A. E.; Holland, S. M.; Prevots, D. R. Prevalence of Nontuberculous Mycobacterial Lung Disease in U.S. Medicare Beneficiaries. *Am. J. Respir. Crit. Care Med.* **2012**, *185* (8), 881–886.

(24) O'Brien, R. J.; Geiter, L. J.; Snider, D. E. The Epidemiology of Nontuberculous Mycobacterial Diseases in the United States. Results from a National Survey. *Am. Rev. Respir. Dis.* **1987**, *135* (5), 1007–1014.

(25) Cândido, P. H. C.; Nunes, L. de S.; Marques, E. A.; Folescu, T. W.; Coelho, F. S.; de Moura, V. C. N.; da Silva, M. G.; Gomes, K. M.; Lourenço, M. C. da S.; Aguiar, F. S.; et al. Multidrug-Resistant Nontuberculous Mycobacteria Isolated from Cystic Fibrosis Patients. *J. Clin. Microbiol.* **2014**, *52* (8), 2990–2997.

(26) Brown-Elliott, B. A.; Nash, K. A.; Wallace, R. J. Antimicrobial Susceptibility Testing, Drug Resistance Mechanisms, and Therapy of Infections with Nontuberculous Mycobacteria. *Clin. Microbiol. Rev.* **2012**, *25* (3), 545–582.

(27) WHO. Early detection of tuberculosis: an overview of approaches, guidelines and tools. https://apps.who.int/iris/handle/10665/70824.

(28) WHO. Toman's tuberculosis: case detection, treatment and monitoring: questions and answers (2nd edition), Geneva, **2004**.

(29) Viney, K.; Bissell, K.; Tabutoa, K.; Kienene, T.; Linh, N. N.; Briand, K.; Harries, A. D. Sputum Smear Examination and Time to Diagnosis in Patients with Smear-Negative Pulmonary Tuberculosis in the Pacific. *Public Health Action* **2012**, *2* (4), 133–137.

(30) Detjen, A. K.; DiNardo, A. R.; Leyden, J.; Steingart, K. R.; Menzies, D.; Schiller, I.; Dendukuri, N.; Mandalakas, A. M. Xpert MTB/RIF Assay for the Diagnosis of Pulmonary Tuberculosis in Children: A Systematic Review and Meta-Analysis. *Lancet Respir. Med.* **2015**, *3* (6), 451–461.

(31) Padmapriyadarsini, C.; Narendran, G.; Swaminathan, S. Diagnosis & Treatment of Tuberculosis in HIV Co-Infected Patients. *Indian J. Med. Res.* **2011**, *134* (6), 850–865.

(32) Elliott, A. M.; Namaambo, K.; Allen, B. W.; Luo, N.; Hayes, R. J.; Pobee, J. O.; McAdam, K. P. Negative Sputum Smear Results in HIV-Positive Patients with Pulmonary Tuberculosis in Lusaka, Zambia. *Tuber. Lung Dis. Off. J. Int. Union Tuberc. Lung Dis.* **1993**, *74* (3), 191–194.

(33) Matee, M.; Mtei, L.; Lounasvaara, T.; Wieland-Alter, W.; Waddell, R.; Lyimo, J.; Bakari, M.; Pallangyo, K.; von Reyn, C. F. Sputum Microscopy for the Diagnosis of HIV-Associated Pulmonary Tuberculosis in Tanzania. *BMC Public Health* **2008**, *8*, 68.

(34) Nayak, S.; Acharjya, B. Mantoux Test and Its Interpretation. *Indian Dermatol. Online J.* **2012**, *3* (1), 2–6.

(35) Pai, M.; Menzies, D. The New IGRA and the Old TST. *Am. J. Respir. Crit. Care Med.* **2007**, *175* (6), 529–531.

(36) Wilson, F. A.; Miller, T. L.; Stimpson, J. P. Mycobacterium Tuberculosis Infection, Immigration Status, and Diagnostic Discordance: A Comparison of Tuberculin Skin Test and QuantiFERON®-TB Gold In-Tube Test Among Immigrants to the U.S. *Public Health Rep.* **2016**, *131* (2), 303–310.

(37) Sharma, S. K.; Vashishtha, R.; Chauhan, L. S.; Sreenivas, V.; Seth, D. Comparison of TST and IGRA in Diagnosis of Latent Tuberculosis Infection in a High TB-Burden Setting. *PLoS ONE* **2017**, *12* (1).

(38) Nurwidya, F.; Handayani, D.; Burhan, E.; Yunus, F. Molecular Diagnosis of Tuberculosis. *Chonnam Med. J.* **2018**, *54* (1), 1–9.

(39) Chung, M. J.; Lee, K. S.; Koh, W.-J.; Kim, T. S.; Kang, E. Y.; Kim, S. M.; Kwon, O. J.; Kim, S. Drug-Sensitive Tuberculosis, Multidrug-Resistant Tuberculosis, and Nontuberculous Mycobacterial Pulmonary Disease in NonAIDS Adults: Comparisons of Thin-Section CT Findings. *Eur. Radiol.* **2006**, *16* (9), 1934–1941.

(40) Seung, K. J.; Keshavjee, S.; Rich, M. L. Multidrug-Resistant Tuberculosis and Extensively Drug-Resistant Tuberculosis. *Cold Spring Harb. Perspect. Med.* **2015**, *5* (9).

(41) Migliori, G. B.; De Iaco, G.; Besozzi, G.; Centis, R.; Cirillo, D. M. First Tuberculosis Cases in Italy Resistant to All Tested Drugs. *Euro Surveill. Bull. Eur. Sur Mal. Transm. Eur. Commun. Dis. Bull.* **2007**, *12* (5), e070517.

(42) Masjedi, M. R.; Tabarsi, P.; Baghaei, P.; Jalali, S.; Farnia, P.; Chitsaz, E.; Amiri, M.; Mansouri, D.; Velayati, A. A. Extensively Drug-Resistant Tuberculosis Treatment Outcome in Iran: A Case Series of Seven Patients. *Int. J. Infect. Dis. IJID Off. Publ. Int. Soc. Infect. Dis.* **2010**, *14* (5), e399-402.

(43) Ehlers, S.; Schaible, U. E. The Granuloma in Tuberculosis: Dynamics of a Host–Pathogen Collusion. *Front. Immunol.* **2013**, *3*.

(44) Silva Miranda, M.; Breiman, A.; Allain, S.; Deknuydt, F.; Altare, F. The Tuberculous Granuloma: An Unsuccessful Host Defence Mechanism Providing a Safety Shelter for the Bacteria? *Clin. Dev. Immunol.* **2012**, *2012*.

(45) Russell, D. G.; Cardona, P.-J.; Kim, M.-J.; Allain, S.; Altare, F. Foamy Macrophages and the Progression of the Human Tuberculosis Granuloma. *Nat. Immunol.* **2009**, *10* (9), 943–948.

(46) Schnappinger, D.; Ehrt, S.; Voskuil, M. I.; Liu, Y.; Mangan, J. A.; Monahan, I. M.; Dolganov, G.; Efron, B.; Butcher, P. D.; Nathan, C.; et al. Transcriptional Adaptation of Mycobacterium Tuberculosis within Macrophages. *J. Exp. Med.* **2003**, *198* (5), 693–704.

(47) Ward, S. K.; Abomoelak, B.; Marcus, S. A.; Talaat, A. M. Transcriptional Profiling of Mycobacterium Tuberculosis during Infection: Lessons Learned. *Front. Microbiol.* **2010**, *1*, 121.

(48) Organization, W. H. Improving the Diagnosis and Treatment of Smear-Negative Pulmonary and Extrapulmonary Tuberculosis among Adults and Adolescents : Recommendations for HIV-Prevalent and Resource-Constrained Settings. **2007**.

(49) Jnawali, H. N.; Ryoo, S. First– and Second–Line Drugs and Drug Resistance. *Tuberc. - Curr. Issues Diagn. Manag.* **2013**.

(50) Singh, B.; Cocker, D.; Ryan, H.; Sloan, D. J. Linezolid for Drug-resistant Pulmonary Tuberculosis. *Cochrane Database Syst. Rev.* **2019**, *2019* (3).

(51) Karumbi, J.; Garner, P. Directly Observed Therapy for Treating Tuberculosis. *Cochrane Database Syst. Rev.* **2015**, *2015* (5).

(52) Esposito, S.; Bosis, S.; Tadolini, M.; Bianchini, S.; Migliori, G. B.; Principi, N. Efficacy, Safety, and Tolerability of a 24-Month Treatment Regimen Including Delamanid in a Child with Extensively Drug-Resistant Tuberculosis. *Medicine (Baltimore)* **2016**, *95* (46).

(53) Chakraborty, S.; Rhee, K. Y. Tuberculosis Drug Development: History and Evolution of the Mechanism-Based Paradigm. *Cold Spring Harb. Perspect. Med.* **2015**, *5* (8).

(54) Vilchèze, C.; Jacobs, W. R. The Mechanism of Isoniazid Killing: Clarity through the Scope of Genetics. *Annu. Rev. Microbiol.* **2007**, *61*, 35–50.

(55) McDermott, W. The Story of INH. *J. Infect. Dis.* **1969**, *119* (6), 678–683.

(56) Banerjee, A.; Dubnau, E.; Quemard, A.; Balasubramanian, V.; Um, K. S.; Wilson, T.; Collins, D.; Lisle, G. de; Jacobs, W. R. InhA, a Gene Encoding a Target for Isoniazid and Ethionamide in Mycobacterium Tuberculosis. *Science* **1994**, *263* (5144), 227–230.

(57) Mdluli, K.; Slayden, R. A.; Zhu, Y.; Ramaswamy, S.; Pan, X.; Mead, D.; Crane, D. D.; Musser, J. M.; Barry, C. E. Inhibition of a Mycobacterium Tuberculosis Beta-Ketoacyl ACP Synthase by Isoniazid. *Science* **1998**, *280* (5369), 1607–1610.

(58) Sensi, P.; Margalith, P.; Timbal, M. T. Rifomycin, a New Antibiotic; Preliminary Report. *Il Farm. Ed. Sci.* **1959**, *14* (2), 146–147.

(59) Calvori, C.; Frontali, L.; Leoni, L.; Tecce, G. Effect of Rifamycin on Protein Synthesis. *Nature* **1965**, *207* (4995), 417–418.

(60) Qi, X.; Lin, W.; Ma, M.; Wang, C.; He, Y.; He, N.; Gao, J.; Zhou, H.; Xiao, Y.; Wang, Y.; et al. Structural Basis of Rifampin Inactivation by Rifampin Phosphotransferase. *Proc. Natl. Acad. Sci. U. S. A.* **2016**, *113* (14), 3803–3808.

(61) Chorine, V. Action of nicotinamide on bacilli of the type Mycobacterium. *C. r. Acad. Sci.* **1945**, *220*, 150–151.

(62) Zhang, Y.; Mitchison, D. The Curious Characteristics of Pyrazinamide: A Review. *Int. J. Tuberc. Lung Dis. Off. J. Int. Union Tuberc. Lung Dis.* **2003**, *7* (1), 6–21.

(63) Martin, A.; Takiff, H.; Vandamme, P.; Swings, J.; Palomino, J. C. L.; Portaels, F. A New Rapid and Simple Colorimetric Method to Detect Pyrazinamide Resistance in Mycobacterium Tuberculosis Using Nicotinamide. *J. Antimicrob. Chemother.* **2006**, *58* (2), 327–331.

(64) Forbes, M.; Kuck, N. A.; Peets, E. A. MODE OF ACTION OF ETHAMBUTOL. *J. Bacteriol.* **1962**, *84* (5), 1099–1103.

(65) Forbes, M.; Kuck, N. A.; Peets, E. A. Effect of Ethambutol on Nucleic Acid Metabolism in Mycobacterium Smegmatis and Its Reversal by Polyamines and Divalent Cations. *J. Bacteriol.* **1965**, *89* (5), 1299–1305.

(66) Singh, B.; Mitchison, D. A. Bactericidal Activity of Streptomycin and Isoniazid Against Tubercle Bacilli. *Br. Med. J.* **1954**, *1* (4854), 130–132.

(67) Schatz, A.; Bugie, E.; Waksman, S. A. Streptomycin, a Substance Exhibiting Antibiotic Activity against Gram-Positive and Gram-Negative Bacteria. 1944. *Clin. Orthop.* **2005**, No. 437, 3–6.

(68) Woodruff, H. B. Selman A. Waksman, Winner of the 1952 Nobel Prize for Physiology or Medicine. *Appl. Environ. Microbiol.* **2014**, *80* (1), 2–8.

(69) Montie, T.; Patamasucon, P. Aminoglycosides: The Complex Problem of Antibiotic Mechanisms and Clinical Applications. *Eur. J. Clin. Microbiol. Infect. Dis.* **1995**, *14* (2), 85–87.

(70) Kotra, L. P.; Haddad, J.; Mobashery, S. Aminoglycosides: Perspectives on Mechanisms of Action and Resistance and Strategies to Counter Resistance. *Antimicrob. Agents Chemother.* **2000**, *44* (12), 3249–3256.

(71) Davis, B. D. Mechanism of Bactericidal Action of Aminoglycosides. *Microbiol. Rev.* **1987**, *51* (3), 341–350.

(72) Felnagle, E. A.; Rondon, M. R.; Berti, A. D.; Crosby, H. A.; Thomas, M. G. Identification of the Biosynthetic Gene Cluster and an Additional Gene for Resistance

to the Antituberculosis Drug Capreomycin. *Appl. Environ. Microbiol.* **2007**, *73* (13), 4162–4170.

(73) Stanley, R. E.; Blaha, G.; Grodzicki, R. L.; Strickler, M. D.; Steitz, T. A. The Structures of the Anti-Tuberculosis Antibiotics Viomycin and Capreomycin Bound to the 70S Ribosome. *Nat. Struct. Mol. Biol.* **2010**, *17* (3), 289–293.

(74) Ginsburg, A. S.; Grosset, J. H.; Bishai, W. R. Fluoroquinolones, Tuberculosis, and Resistance. *Lancet Infect. Dis.* **2003**, *3* (7), 432–442.

(75) Golomb, B. A.; Koslik, H. J.; Redd, A. J. Fluoroquinolone-Induced Serious, Persistent, Multisymptom Adverse Effects. *BMJ Case Rep.* **2015**, *2015*.

(76) Chan, E. D.; Laurel, V.; Strand, M. J.; Chan, J. F.; Huynh, M.-L. N.; Goble, M.; Iseman, M. D. Treatment and Outcome Analysis of 205 Patients with Multidrug-Resistant Tuberculosis. *Am. J. Respir. Crit. Care Med.* **2004**, *169* (10), 1103–1109.

(77) Nathanson, E.; Gupta, R.; Huamani, P.; Leimane, V.; Pasechnikov, A. D.; Tupasi, T. E.; Vink, K.; Jaramillo, E.; Espinal, M. A. Adverse Events in the Treatment of Multidrug-Resistant Tuberculosis: Results from the DOTS-Plus Initiative. *Int. J. Tuberc. Lung Dis. Off. J. Int. Union Tuberc. Lung Dis.* **2004**, *8* (11), 1382–1384.

(78) Epstein, I. G.; Nair, K. G.; Boyd, L. J. Cycloserine, a New Antibiotic, in the Treatment of Human Pulmonary Tuberculosis: A Preliminary Report. *Antibiot. Med. Clin. Ther. N. Y. NY* **1955**, *1* (2), 80–93.

(79) Wilcox, M. H. Update on Linezolid: The First Oxazolidinone Antibiotic. *Expert Opin. Pharmacother.* **2005**, *6* (13), 2315–2326.

(80) Rucker, J. C.; Hamilton, S. R.; Bardenstein, D.; Isada, C. M.; Lee, M. S. Linezolid-Associated Toxic Optic Neuropathy. *Neurology* **2006**, *66* (4), 595–598.

(81) Bressler, A. M.; Zimmer, S. M.; Gilmore, J. L.; Somani, J. Peripheral Neuropathy Associated with Prolonged Use of Linezolid. *Lancet Infect. Dis.* **2004**, *4* (8), 528–531.

(82) Gerson, S. L.; Kaplan, S. L.; Bruss, J. B.; Le, V.; Arellano, F. M.; Hafkin, B.; Kuter, D. J. Hematologic Effects of Linezolid: Summary of Clinical Experience. *Antimicrob. Agents Chemother.* **2002**, *46* (8), 2723–2726.

(83) Schecter, G. F.; Scott, C.; True, L.; Raftery, A.; Flood, J.; Mase, S. Linezolid in the Treatment of Multidrug-Resistant Tuberculosis. *Clin. Infect. Dis. Off. Publ. Infect. Dis. Soc. Am.* **2010**, *50* (1), 49–55.

(84) Lehmann, J. Para-Aminosalicylic Acid in the Treatment of Tuberculosis. *Lancet Lond. Engl.* **1946**, *1* (6384), 15.

(85) J Libardo, M. D.; Boshoff, H. I.; Barry, C. E. The Present State of the Tuberculosis Drug Development Pipeline. *Curr. Opin. Pharmacol.* **2018**, *42*, 81–94.

(86) Deoghare, S. Bedaquiline: A New Drug Approved for Treatment of Multidrug-Resistant Tuberculosis. *Indian J. Pharmacol.* **2013**, *45* (5), 536–537.

(87) Xavier, A. S.; Lakshmanan, M. Delamanid: A New Armor in Combating Drug-Resistant Tuberculosis. *J. Pharmacol. Pharmacother.* **2014**, *5* (3), 222–224.

(88) Keam, S. J. Pretomanid: First Approval. *Drugs* **2019**.

(89) Andries, K.; Verhasselt, P.; Guillemont, J.; Göhlmann, H. W. H.; Neefs, J.-M.; Winkler, H.; Van Gestel, J.; Timmerman, P.; Zhu, M.; Lee, E.; et al. A Diarylquinoline Drug Active on the ATP Synthase of Mycobacterium Tuberculosis. *Science* **2005**, *307* (5707), 223–227.

(90) Koul, A.; Dendouga, N.; Vergauwen, K.; Molenberghs, B.; Vranckx, L.; Willebrords, R.; Ristic, Z.; Lill, H.; Dorange, I.; Guillemont, J.; et al. Diarylquinolines Target Subunit c of Mycobacterial ATP Synthase. *Nat. Chem. Biol.* **2007**, *3* (6), 323–324.

(91) de Jonge, M. R.; Koymans, L. H. M.; Guillemont, J. E. G.; Koul, A.; Andries, K. A Computational Model of the Inhibition of Mycobacterium Tuberculosis ATPase by a New Drug Candidate R207910. *Proteins* **2007**, *67* (4), 971–980.

(92) Koul, A.; Vranckx, L.; Dhar, N.; Göhlmann, H. W. H.; Özdemir, E.; Neefs, J.-M.; Schulz, M.; Lu, P.; Mørtz, E.; McKinney, J. D.; et al. Delayed Bactericidal Response of Mycobacterium Tuberculosis to Bedaquiline Involves Remodelling of Bacterial Metabolism. *Nat. Commun.* **2014**, *5* (1), 1–10.

(93) Andries, K.; Villellas, C.; Coeck, N.; Thys, K.; Gevers, T.; Vranckx, L.; Lounis, N.; Jong, B. C. de; Koul, A. Acquired Resistance of Mycobacterium Tuberculosis to Bedaquiline. *PLOS ONE* **2014**, *9* (7), e102135.

(94) Guglielmetti, L.; Jaspard, M.; Le Dû, D.; Lachâtre, M.; Marigot-Outtandy, D.; Bernard, C.; Veziris, N.; Robert, J.; Yazdanpanah, Y.; Caumes, E.; et al. Long-Term Outcome and Safety of Prolonged Bedaquiline Treatment for Multidrug-Resistant Tuberculosis. *Eur. Respir. J.* **2017**, *49* (3).

(95) Information, N. C. for B.; Pike, U. S. N. L. of M. 8600 R.; MD, B.; Usa, 20894. *"How-to" Guide on the Use of Bedaquiline for MDR-TB Treatment*; World Health Organization, 2014.

(96) Agrawal, K. C.; Bears, K. B.; Sehgal, R. K.; Brown, J. N.; Rist, P. E.; Rupp, W. D. Potential Radiosensitizing Agents. Dinitroimidazoles. *J. Med. Chem.* **1979**, *22* (5), 583–586.

(97) Walsh, J. S.; Wang, R.; Bagan, E.; Wang, C. C.; Wislocki, P.; Miwa, G. T. Structural Alterations That Differentially Affect the Mutagenic and Antitrichomonal Activities of 5-Nitroimidazoles. *J. Med. Chem.* **1987**, *30* (1), 150–156.

(98) Ashtekar, D. R.; Costa-Perira, R.; Nagrajan, K.; Vishvanathan, N.; Bhatt, A. D.; Rittel, W. In Vitro and in Vivo Activities of the Nitroimidazole CGI 17341 against Mycobacterium Tuberculosis. *Antimicrob. Agents Chemother.* **1993**, *37* (2), 183–186.

(99) Lewis, J. M.; Sloan, D. J. The Role of Delamanid in the Treatment of Drug-Resistant Tuberculosis. *Ther. Clin. Risk Manag.* **2015**, *11*, 779–791.

(100) Laughon, B. E.; Nacy, C. A. Tuberculosis — Drugs in the 2016 Development Pipeline. *Nat. Rev. Dis. Primer* **2017**, *3* (1), 1–1.

(101) Pipeline. Working Group for New TB Drugs https://www.newtbdrugs.org/pipeline/clinical.

(102) Grzelak, E. M.; Choules, M. P.; Gao, W.; Cai, G.; Wan, B.; Wang, Y.; McAlpine, J. B.; Cheng, J.; Jin, Y.; Lee, H.; et al. Strategies in Anti-Mycobacterium Tuberculosis Drug Discovery Based on Phenotypic Screening. *J. Antibiot. (Tokyo)* **2019**, *72* (10), 719–728.

(103) Machado, D.; Girardini, M.; Viveiros, M.; Pieroni, M. Challenging the Drug-Likeness Dogma for New Drug Discovery in Tuberculosis. *Front. Microbiol.* **2018**, *9*, 1367.

(104) Sotgiu, G.; Centis, R.; D'ambrosio, L.; Migliori, G. B. Tuberculosis Treatment and Drug Regimens. *Cold Spring Harb. Perspect. Med.* **2015**, *5* (5).

(105) Dookie, N.; Rambaran, S.; Padayatchi, N.; Mahomed, S.; Naidoo, K. Evolution of Drug Resistance in Mycobacterium Tuberculosis: A Review on the Molecular Determinants of Resistance and Implications for Personalized Care. *J. Antimicrob. Chemother.* **2018**, *73* (5), 1138–1151.

(106) Floss, H. G.; Yu, T.-W. RifamycinMode of Action, Resistance, and Biosynthesis. *Chem. Rev.* **2005**, *105* (2), 621–632.

(107) Buetow, L.; Huang, D. T. Structural Insights into the Catalysis and Regulation of E3 Ubiquitin Ligases. *Nat. Rev. Mol. Cell Biol.* **2016**, *17* (10), 626–642.

(108) Hooper, D. C. Mechanisms of Quinolone Resistance. *Quinolone Antimicrob. Agents Third Ed.* **2003**, 41–67.

(109) Ismail, N.; Omar, S. V.; Ismail, N. A.; Peters, R. P. H. Collated Data of Mutation Frequencies and Associated Genetic Variants of Bedaquiline, Clofazimine and Linezolid Resistance in Mycobacterium Tuberculosis. *Data Brief* **2018**, *20*, 1975–1983.

(110) Munita, J. M.; Arias, C. A. Mechanisms of Antibiotic Resistance. *Microbiol. Spectr.* **2016**, *4* (2).

(111) Ramirez, M. S.; Tolmasky, M. E. Aminoglycoside Modifying Enzymes. *Drug Resist. Updat. Rev. Comment. Antimicrob. Anticancer Chemother.* **2010**, *13* (6), 151–171.

(112) Alderwick, L. J.; Harrison, J.; Lloyd, G. S.; Birch, H. L. The Mycobacterial Cell Wall--Peptidoglycan and Arabinogalactan. *Cold Spring Harb. Perspect. Med.* **2015**, *5* (8), a021113.

(113) Daffé, M. The Cell Envelope of Tubercle Bacilli. *Tuberc. Edinb. Scotl.* **2015**, *95 Suppl 1*, S155-158.

(114) Jankute, M.; Cox, J. A. G.; Harrison, J.; Besra, G. S. Assembly of the Mycobacterial Cell Wall. *Annu. Rev. Microbiol.* **2015**, *69*, 405–423.

(115) Soto, S. M. Role of Efflux Pumps in the Antibiotic Resistance of Bacteria Embedded in a Biofilm. *Virulence* **2013**, *4* (3), 223–229.

(116) Yan, M.; Sahin, O.; Lin, J.; Zhang, Q. Role of the CmeABC Efflux Pump in the Emergence of Fluoroquinolone-Resistant Campylobacter under Selection Pressure. *J. Antimicrob. Chemother.* **2006**, *58* (6), 1154–1159.

(117) Poole, K. Efflux Pumps as Antimicrobial Resistance Mechanisms. *Ann. Med.* **2007**, *39* (3), 162–176.

(118) Viveiros, M.; Portugal, I.; Bettencourt, R.; Victor, T. C.; Jordaan, A. M.; Leandro, C.; Ordway, D.; Amaral, L. Isoniazid-Induced Transient High-Level Resistance in Mycobacterium Tuberculosis. *Antimicrob. Agents Chemother.* **2002**, *46* (9), 2804–2810.

(119) Machado, D.; Couto, I.; Perdigão, J.; Rodrigues, L.; Portugal, I.; Baptista, P.; Veigas, B.; Amaral, L.; Viveiros, M. Contribution of Efflux to the Emergence of Isoniazid and Multidrug Resistance in Mycobacterium Tuberculosis. *PLOS ONE* **2012**, *7* (4), e34538.

(120) Sun, J.; Deng, Z.; Yan, A. Bacterial Multidrug Efflux Pumps: Mechanisms, Physiology and Pharmacological Exploitations. *Biochem. Biophys. Res. Commun.* **2014**, *453* (2), 254–267.

(121) Pieroni, M.; Machado, D.; Azzali, E.; Santos Costa, S.; Couto, I.; Costantino, G.; Viveiros, M. Rational Design and Synthesis of Thioridazine Analogues as Enhancers of the Antituberculosis Therapy. *J. Med. Chem.* **2015**, *58* (15), 5842–5853.

(122) Machado, D.; Pires, D.; Perdigão, J.; Couto, I.; Portugal, I.; Martins, M.; Amaral, L.; Anes, E.; Viveiros, M. Ion Channel Blockers as Antimicrobial Agents, Efflux Inhibitors,

and Enhancers of Macrophage Killing Activity against Drug Resistant Mycobacterium Tuberculosis. *PloS One* **2016**, *11* (2), e0149326.

(123) Bloemberg, G. V.; Keller, P. M.; Stucki, D.; Trauner, A.; Borrell, S.; Latshang, T.; Coscolla, M.; Rothe, T.; Hömke, R.; Ritter, C.; et al. Acquired Resistance to Bedaquiline and Delamanid in Therapy for Tuberculosis. *N. Engl. J. Med.* **2015**, *373* (20), 1986–1988.

(124) Ordonez, A. A.; Maiga, M.; Gupta, S.; Weinstein, E. A.; Bishai, W. R.; Jain, S. K. Novel Adjunctive Therapies for the Treatment of Tuberculosis. *Curr. Mol. Med.* **2014**, *14* (3), 385–395.

(125) Wallis, R. S.; Hafner, R. Advancing Host-Directed Therapy for Tuberculosis. *Nat. Rev. Immunol.* **2015**, *15* (4), 255–263.

(126) Padmapriyadarsini, C.; Bhavani, P. K.; Natrajan, M.; Ponnuraja, C.; Kumar, H.; Gomathy, S. N.; Guleria, R.; Jawahar, S. M.; Singh, M.; Balganesh, T.; et al. Evaluation of Metformin in Combination with Rifampicin Containing Antituberculosis Therapy in Patients with New, Smear-Positive Pulmonary Tuberculosis (METRIF): Study Protocol for a Randomised Clinical Trial. *BMJ Open* **2019**, *9* (3), e024363.

(127) Datta, M.; Via, L. E.; Kamoun, W. S.; Liu, C.; Chen, W.; Seano, G.; Weiner, D. M.; Schimel, D.; England, K.; Martin, J. D.; et al. Anti-Vascular Endothelial Growth Factor Treatment Normalizes Tuberculosis Granuloma Vasculature and Improves Small Molecule Delivery. *Proc. Natl. Acad. Sci. U. S. A.* **2015**, *112* (6), 1827–1832.

(128) Kearns, M. D.; Tangpricha, V. The Role of Vitamin D in Tuberculosis. *J. Clin. Transl. Endocrinol.* **2014**, *1* (4), 167–169.

(129) Maiga, M.; Agarwal, N.; Ammerman, N. C.; Gupta, R.; Guo, H.; Maiga, M. C.; Lun, S.; Bishai, W. R. Successful Shortening of Tuberculosis Treatment Using Adjuvant Host-Directed Therapy with FDA-Approved Phosphodiesterase Inhibitors in the Mouse Model. *PLoS ONE* **2012**, *7* (2).

(130) González-Bello, C. Antibiotic Adjuvants – A Strategy to Unlock Bacterial Resistance to Antibiotics. *Bioorg. Med. Chem. Lett.* **2017**, *27* (18), 4221–4228.

(131) Ramón-García, S.; Martín, C.; Aínsa, J. A.; De Rossi, E. Characterization of Tetracycline Resistance Mediated by the Efflux Pump Tap from Mycobacterium Fortuitum. *J. Antimicrob. Chemother.* **2006**, *57* (2), 252–259.

(132) Pasca, M. R.; Guglierame, P.; Arcesi, F.; Bellinzoni, M.; De Rossi, E.; Riccardi, G. Rv2686c-Rv2687c-Rv2688c, an ABC Fluoroquinolone Efflux Pump in Mycobacterium Tuberculosis. *Antimicrob. Agents Chemother.* **2004**, *48* (8), 3175–3178.

(133) Rodrigues, L.; Aínsa, J. A.; Amaral, L.; Viveiros, M. Inhibition of Drug Efflux in Mycobacteria with Phenothiazines and Other Putative Efflux Inhibitors. *Recent Patents Anti-Infect. Drug Disc.* **2011**, *6* (2), 118–127.

(134) Pule, C. M.; Sampson, S. L.; Warren, R. M.; Black, P. A.; van Helden, P. D.; Victor, T. C.; Louw, G. E. Efflux Pump Inhibitors: Targeting Mycobacterial Efflux Systems to Enhance TB Therapy. *J. Antimicrob. Chemother.* **2016**, *71* (1), 17–26.

(135) Black, P. A.; Warren, R. M.; Louw, G. E.; van Helden, P. D.; Victor, T. C.; Kana, B. D. Energy Metabolism and Drug Efflux in Mycobacterium Tuberculosis. *Antimicrob. Agents Chemother.* **2014**, *58* (5), 2491–2503.

(136) Amaral, L.; Boeree, M. J.; Gillespie, S. H.; Udwadia, Z. F.; van Soolingen, D. Thioridazine Cures Extensively Drug-Resistant Tuberculosis (XDR-TB) and the Need for Global Trials Is Now! *Int. J. Antimicrob. Agents* **2010**, *35* (6), 524–526.

(137) Gupta, S.; Cohen, K. A.; Winglee, K.; Maiga, M.; Diarra, B.; Bishai, W. R. Efflux Inhibition with Verapamil Potentiates Bedaquiline in Mycobacterium Tuberculosis. *Antimicrob. Agents Chemother.* **2014**, *58* (1), 574–576.

(138) Martins, M.; Schelz, Z.; Martins, A.; Molnar, J.; Hajös, G.; Riedl, Z.; Viveiros, M.; Yalcin, I.; Aki-Sener, E.; Amaral, L. In Vitro and Ex Vivo Activity of Thioridazine Derivatives against Mycobacterium Tuberculosis. *Int. J. Antimicrob. Agents* **2007**, *29* (3), 338–340.

(139) Caleffi-Ferracioli, K. R.; Cardoso, R. F.; de Souza, J. V.; Murase, L. S.; Canezin, P. H.; Scodro, R. B.; LD Siqueira, V.; Pavan, F. R. Modulatory Effects of Verapamil in Rifampicin Activity against Mycobacterium Tuberculosis. *Future Microbiol.* **2019**, *14* (3), 185–194.

(140) Adams, K. N.; Takaki, K.; Connolly, L. E.; Wiedenhoft, H.; Winglee, K.; Humbert, O.; Edelstein, P. H.; Cosma, C. L.; Ramakrishnan, L. Drug Tolerance in Replicating Mycobacteria Mediated by a Macrophage-Induced Efflux Mechanism. *Cell* **2011**, *145* (1), 39–53.

(141) Amaral, L.; Viveiros, M. Thioridazine: A Non-Antibiotic Drug Highly Effective, in Combination with First Line Anti-Tuberculosis Drugs, against Any Form of Antibiotic Resistance of Mycobacterium Tuberculosis Due to Its Multi-Mechanisms of Action. *Antibiotics* **2017**, *6* (1).

(142) Abbate, E.; Vescovo, M.; Natiello, M.; Cufré, M.; García, A.; Gonzalez Montaner, P.; Ambroggi, M.; Ritacco, V.; van Soolingen, D. Successful Alternative Treatment of Extensively Drug-Resistant Tuberculosis in Argentina with a Combination of Linezolid, Moxifloxacin and Thioridazine. *J. Antimicrob. Chemother.* **2012**, *67* (2), 473–477.

2. Characterization and optimization of antitubercular 2-aminothiazole based compounds

2.1 Introduction

In the research group where I have conducted my research, starting from a library of 2-aminothiazoles variously substituted, it was possible to identify 2 compounds (**UPAR-49** and **UPAR-50**, Figure 1) holding promise for further investigation.[1]

Figure 1.

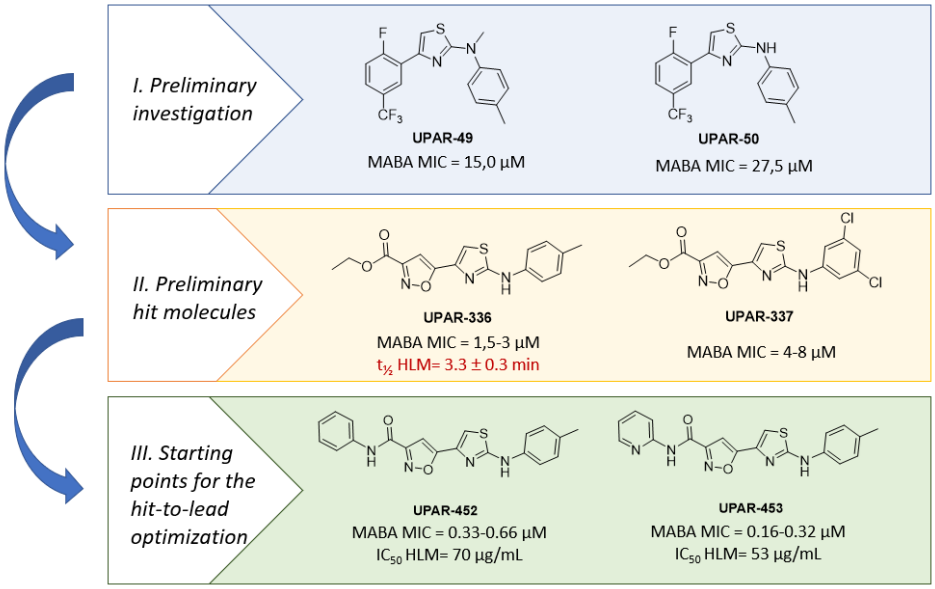

Figure 1. *Preliminary optimization of antitubercular 2-aminothiazoles.*

In a preliminary round of optimization, two potent antitubercular compounds were identified (**UPAR-336**, **UPAR-337**) even though characterized by a remarkable metabolic liability. Thus, the most relevant metabolic soft-spot of the molecule (the ethyl ester) was identified and replaced, leading to the synthesis of **UPAR-452** and **UPAR-453**, that represent the starting points for the hit-to-lead optimization process that I herein report.

2.2 Results and discussion

Since the encouraging results obtained for compounds **UPAR-452** and **UPAR-453**, they were selected as starting points for a hit-to-lead optimization campaign, mainly focused on two purposes: investigating the Structure-Activity Relationships (SAR) and exploring the Structure-Metabolism Relationships (SMR). Beside this study, the characterization of the parent compounds was further enriched by exploring their chemical reactivity, to exclude a nonspecific and promiscuous behaviour, and by preliminarily investigating their mechanism of action. Finally, an improved and more straightforward synthetic route for the synthesis of the hit **UPAR-453** was explored.

2.2.1 Alternative route for the synthesis of compound UPAR-453

The initial protocol for the synthesis of **UPAR-453**, previously reported by our research group,[1] required a total of four steps starting from ketone **39** (Scheme 1, section 2.3.1). The first three steps allowed to obtain the acid intermediate **3a** in reasonable yield, whereas the formation of the amide was characterized by low and poorly reproducible yields, generally ranging from 10 to 20%, although only in one case a surprising 85% yield was obtained. This might represent an important limitation, especially in the view of further biological characterizations which requires a solid, efficient and reproducible protocol for the synthesis of the hit compounds. First, to address these limitations, four alternative coupling procedures were explored using different coupling reagents (HATU or COMU) and varying the equivalents (1.5 or 3 eq.) of the base triethylamine (TEA). Since no significant improvements in the yield was obtained (see Table 1), a different synthetic route for **UPAR-453** was planned, starting from compound **39** (see Scheme 2, section 2.3.1). In this alternative synthetic approach, the coupling reaction was performed before the bromination, after hydrolysing **39** to its corresponding carboxylic acid. Since it was observed that some degradation process occurred over the time for this carboxylic acid, the coupling reaction was performed right after the deprotection of **39**. This allowed to obtain the amide **40** in 67% yield. After compound **40** was obtained, it was reacted with bromine using the same condition reported for the

synthesis of compound **1**, but no conversion into the desired α-bromoketone was observed. Harsher conditions were needed to obtain compound **42** which was synthesized reacting **40** with bromine in dioxane at 70°C. Compound **42** was then reacted with the proper thiourea according to the Hantzsch protocol to give the desired product **UPAR-453**.

Table 1

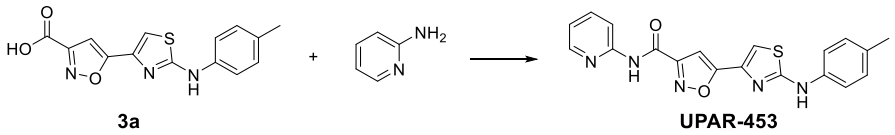

#	Coupling reagent	Base	Equivalents of base	Yield (%)
1	HATU	TEA	1.5	21
2	HATU	TEA	3	20
3	COMU	TEA	1.5	16
4	COMU	TEA	3	18

Table 1. *Summary of the coupling reaction conditions tried in the first attempt of optimization.*

Although the same number of reaction steps, the overall yield was significantly improved from 5-9 % to 35 %, proving the efficiency of this alternative synthetic pathway. This improvement in the yield highlights a better reactivity of the carboxylic acid derived from **39** over compound **3a**, which might be explained with the inductive effect due to the extended conjugation. Moreover, intermediate **42** resulted to be particularly useful for the synthesis of **UPAR-453** derivatives modified at the Right Hand Site (RHS) moiety (Section 2.2.3.2).

2.2.2 Assessment of the reactivity to thiols

The parent compounds **UPAR-452** and **UPAR-453** are characterized by a central 2-aminothiazole ring, which, along with some chemotypes like oxazoles, epoxides, β-aminoketones, among the others,[2–4] has been recently identified as a common motif in Pan-Assay Interference Compounds (PAINS).[5] Compounds

defined as PAINS generally give false positive results in the high throughput screening as they tend to react non-specifically with numerous biological target proteins. The mechanism of action is not fully understood, but it seems that PAINS may react as Michael acceptors with thiols and amines. This behaviour was not only related to false positive results in HTS, but it was also found to affect the outcome of some biochemical assays and, more in general, it reflects the tendency to a high and promiscuous chemical reactivity, an undesired feature for pharmacologically active compounds. In the view of an expansion of the series, the investigation of the reactivity of the parent compounds was carried out. **UPAR-452** and **UPAR-453** were incubated with glutathione (GSH), one of the most abundant cellular thiols, for 24 hours before analysing the formation of the GSH-adducts by HPLC-MS. Beside the parent compounds, the analogues **33** and **34** (described in the Section 2.2.3.1) were also evaluated. At the MS analysis only the molecular ion $[M+H]^+$ was observed for the compound tested, while for the GSH-adducts the presence of either the singly charged ($[M+H]^+_{adduct}$) either the doubly charged ion ($[M+2H]^{2+}_{adduct}$) was detected in all cases (data are reported in the Table 2). Therefore, the percentage ratio of the GSH adduct formed, was calculated as: $\frac{([M+H]+\text{adduct})+([M+2H]2+\text{adduct})}{([M+H]+\text{compound})}$.

Table 2

Compound	Peak Areas			
	$[M+H]^+_{compound}$	$[M+H]^+_{adduct}$	$[M+2H]^{2+}_{adduct}$	Ratio (%)
UPAR-452	$1.18 \cdot 10^9$	$2.22 \cdot 10^6$	$1.02 \cdot 10^6$	0.27
33	$1.26 \cdot 10^9$	$1.38 \cdot 10^7$	$1.01 \cdot 10^7$	1.90
UPAR-453	$1.36 \cdot 10^9$	$1.18 \cdot 10^8$	$8.66 \cdot 10^6$	9.34
34	$3.47 \cdot 10^9$	$6.70 \cdot 10^7$	$3.68 \cdot 10^6$	2.12

Table 2. *Peak areas for test compounds and related GSH-adducts in extracted ion chromatograms*

At 24 hours, only a negligible percentage of the compounds reacted with GSH. In fact, the percentage of compound-GSH adducts remained below 3% for **UPAR-452**, **33** and

34. The highest value was observed for **UPAR-453**, which, however, did not exceed 10%. Giving the poor reactivity of these compounds towards GSH, it can be concluded that their activity (Section 2.2.3.1) is the result of a specific interaction with a molecular target rather than a false positive derived from a promiscuous interaction.

2.2.3 Hit-to-lead optimization through SAR and SMR

2.2.3.1 Investigation of the Structure-Activity Relationships

For the sake of clarity, the parent compounds **UPAR-452** and **UPAR-453** will be ideally divided into three regions: the central 2-aminothiazolyl isoxazole bicyclic core (BC), the left-hand side (LHS), attached to the isoxazole core, and the right-hand side (RHS) attached to the 2-aminothiazole ring (Figure 2).

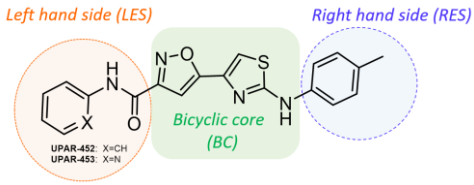

Figure 2. *General structure of UPAR-452 and UPAR-453 divided into three regions.*

Starting from the very preliminary SAR already reported[1] the majority of efforts were devoted to the LHS, as it proved to give significant contribution to the activity. Moreover, modifications at LHS give the possibility to explore a variety of substrates on the phenyl and pyridine rings, starting from the carboxylic acid **3a**. 34 compounds (Table 3) were obtained by modifying the amine involved in the coupling reaction. The aromatic amines used are mainly anilines or aminopyridines substituted at one or two positions. In addition, 2-aminothiazoles (**13**, **25**), aminothiophenes (**26**, **27**) and 4-aminopyridazine (**12**) were also explored, as isosteric replacements and/or privileged scaffolds in the medicinal chemistry landfill.[6–8] In one case the possibility to use the pyrrolidine to give a tertiary amide was investigated (compound **24**). Substituents were carefully chosen based on properties such as lipophilicity, electronic effect and steric hindrance. Lipophilic substituents were, in general, preferred over hydrophilic ones, as improving lipophilicity has proven to be beneficial for the antitubercular activity.[9] For this reason, methyl and halogenated substituents were prioritized over less lipophilic

moieties. In addition, the electronic effect was taken into account, exploring both electron-donor (methyl, dimethyl, ethoxy, hydroxyl) and electron-withdrawing (fluorine, chlorine) groups. Modifications on the RHS were as well investigated, even though to a lesser extent. In particular, fluorine, methyl and chlorine were introduced at position 3 and 5 on the RHS. SAR was further refined by the synthesis of compounds **33** and **34**, where the thiazole ring on the BC was replaced with the oxazole, in order to evaluate the effect of this isosteric replacement on pharmacokinetic parameters such as solubility and metabolic stability.

All compounds synthesized were evaluated through a whole cell biological assay to determine the Minimum Inhibitory Concentration required to inhibit the growth of 90% of bacteria (MIC_{90}) on *M. tuberculosis* (Table 3). From the results obtained, important SAR findings can be retrieved. Looking at the MIC_{90} values, it can be observed that there is a consistent group of compounds maintaining a very promising antitubercular activity, showing an MIC_{90} value in the range of the parent compounds, whereas some molecules were found to be less or no active ($MIC_{90} \geq 20$ µg/mL). Focusing on the chemical features responsible for the activity, it can be noticed that low MIC_{90} values were maintained when small groups, such as fluorine or methyl (**4**, **5**, **23**; **17-19**), were introduced at one of the three available positions of the phenyl ring at the LHS. We were also pleased to notice an MIC_{90} of 0.6 µg/mL for the three hydroxyl derivatives on the LHS phenyl (**35**-**37**), indicating a positive impact of this polar group on the activity. The comparable results obtained for the methyl derivatives **17-19**, the hydroxyl derivatives **35-37** and the fluorine derivatives **4-5, 23**, regardless their position around the ring of the substituents suggested that stereoelectronic effects might prevail on the specific interaction of the functional groups with a precise group in the target binding pocket. This hypothesis will be confirmed only after the identification of the molecular target of this class of compounds, which at this moment is out of the scope of this work.

Table 3

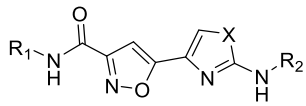

Cmpd.	R_1	R_2	X	MIC_{90} (μg/mL)	IC_{50} (μM)
UPAR-453	Pyridin-2-yl	4-methylphenyl	S	0.5	22.1
UPAR-452	Phenyl	4-methylphenyl	S	1.0	88.0
4	4-fluorophenyl	4-methylphenyl	S	1.0	46.8
5	3-fluorophenyl	4-methylphenyl	S	2.5	n.d.
6	Pyridin-2-yl	3,5-dichlorophenyl	S	20	n.d.
7	Phenyl	3,5-dichlorophenyl	S	20	n.d.
8	2-chloro-4-methylphenyl	4-methylphenyl	S	20	n.d.
9	2,4-dimethylphenyl	4-methylphenyl	S	>20	n.d.
10	4-methylpyridin-2-yl	4-methylphenyl	S	1.0	86.3
11	Pyridin-4-yl	4-methylphenyl	S	1.0	29.9
12	Pyridazin-4-yl	4-methylphenyl	S	>20	n.d.
13	Thiazol-2-yl	4-methylphenyl	S	>40	n.d.
14	4-chlorophenyl	4-methylphenyl	S	>40	n.d.
15	3,5-dimethylphenyl	4-methylphenyl	S	>20	n.d.
16	Pyridin-3-yl	4-methylphenyl	S	10	n.d.
17	4-methylphenyl	4-methylphenyl	S	1.0	47.5
18	3-methylphenyl	4-methylphenyl	S	0.5	10.7
19	2-methylphenyl	4-methylphenyl	S	1.0	63.7
20	3-(trifluoromethyl)phenyl	4-methylphenyl	S	>20	n.d.
21	3-ethoxyphenyl	4-methylphenyl	S	>10	n.d.
22	3-methylpyridin-2-yl	4-methylphenyl	S	0.5	66.8
23	2-fluorophenyl	4-methylphenyl	S	1.0	33.9
25	5-methylthiazol-2-yl	4-methylphenyl	S	>20	n.d.
26	Thiophen-3-yl	4-methylphenyl	S	1.0	>100
27	Thiophene-2-ylmethyl	4-methylphenyl	S	>20	n.d.
28	6-methylpyridin-2-yl	4-methylphenyl	S	>20	n.d.
29	Pyridin-2-yl	3,5-difluorophenyl	S	>20	n.d.
30	Phenyl	3,5-difluorophenyl	S	>20	n.d.
31	Pyridin-2-yl	3,5-dimethylphenyl	S	>20	n.d.
32	Phenyl	3,5-dimethylphenyl	S	1.0	70.9
33	Phenyl	4-methylphenyl	O	1.0	>100
34	Pyridin-2-yl	4-methylphenyl	O	2.5	n.d.
35	2-hydroxyphenyl	4-methylphenyl	S	0.6	53.1
36	3-hydroxyphenyl	4-methylphenyl	S	0.6	48.7
37	4-hydroxyphenyl	4-methylphenyl	S	0.6	79.1
24	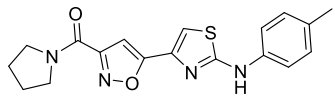			>20	n.d.

Table 3. *Panel of derivatives synthesized, their antitubercular activity (MIC_{90}) and toxicity (IC_{50} on THP-derived macrophages).*

Bulkier groups like trifluoromethyl (**20**), ethoxy (**21**) or disubstitutions with 2,4-dimethyls (**9**), 3,5-dimethyls (**15**) or 2-chloride-4-methyl (**8**) were found to be detrimental for the activity. In these cases, steric hindrance might be accounted for the lack of activity. Thiophene is a valuable replacement of the benzene if directly attached to the amide (**26**), while the activity was lost if a methylene spacer was introduced (**27**). The 4-pyridinyl derivative **11** maintained an antitubercular activity comparable to that observed for the parent compounds, while the 3-pyridinyl derivative **16** is less active. Pyridazine (**12**), thiazole (**13**) and 5-methyl thiazole (**25**) negatively impact on the activity suggesting that aromatic rings bearing two heteroatoms might be poorly tolerated. Moving on the RHS, substitutions in positions 3 and 5 with chlorine (**6-7**) and fluorine (**29**-**30**) cause a drop of the activity (MIC_{90} ≥20). When two methyl groups were introduced at positions 3 and 5, surprisingly the activity was maintained only if phenyl (**7**), but not 2-pyridine (**6**), was present on the LHS. Interestingly, the analogues characterized by the 2-aminothiazole in the BC (**33** and **34**) presented MIC_{90} values comparable to those observed for the parent compounds.

In summary, a reliable SAR could be defined, especially for the LHS, while, giving the lower number of substitutions introduced on the RHS, only a few considerations could be made. Interestingly, we observed that the activity of compounds **33** and **34**, characterized by the 2-aminooxazole ring in the BC, is comparable to those of the parent compounds. Due to the close structural similarity of these two compounds with **UPAR-452** and **UPAR-453**, they were evaluated along with the parent compounds for some pharmacokinetic parameters like solubility and metabolic stability as reported in the following paragraph.

2.2.3.2 Investigation of solubility and Structure-Metabolism Relationships

In the SAR study presented above, the antitubercular activity of **33** and **34** was found to be similar to that observed for the parents **UPAR-452** and **UPAR-453** respectively.

For this reason, also considering the isosterism between 2-aminothiazole and 2-aminooxazole, compounds **33** and **34** were introduced in the set of molecules undergoing kinetic solubility and metabolic stability investigation. In fact, the

replacement of the sulfur with the oxygen is a well-known modification in medicinal chemistry[10–12] and generally, it allows to decrease the calculated LogP value of the molecule, which potentially may give compounds with higher solubility in water, an important and desired feature for drug candidates. The impact of the replacement was evaluated by measuring the kinetic solubility of the compounds in water and in PBS at pH 7.4, as reported in the Table 4. Comparing the results obtained for compound **UPAR-452** and **33**, it can be observed that they have a similar solubility which is slightly higher in water than in PBS. Surprisingly, the solubility of **UPAR-453** in water is approximately 5 times lower than **UPAR-452**, although the similarity in chemical structure. Comparing the solubility of compound **34** and **UPAR-453**, it seems that substitution with oxazole is beneficial for solubility. However, a similar trend cannot be seen in case of compound **33** and its counterpart **UPAR-452**. Therefore, it might be concluded that substitution of the thiazole with the oxazole does not affect in a decisive fashion the solubility, especially if the LogS scale is considered.

Table 4

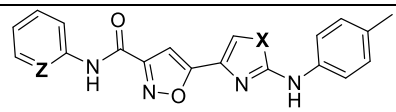

Cmpd.	Structure		Kinetic solubility in water (μM)	LogS	Kinetic solubility in PBS pH 7.4 (μM)	LogS	HLM $t_{½}$ (min)	CL'_{int}* (mL/min/ kg)
	Z	X						
UPAR-452	CH	S	15.36 (±1.64)	-4.81	9.13 (±1.09)	-5.04	12.42 (±0.87)	50.2
33	CH	O	9.57 (±1.33)	-5.02	6.51 (±0.78)	-5.19	12.83 (±1.30)	48.6
UPAR-453	N	S	2.89 (±0.46)	-5.54	2.40 (±0.50)	-5.62	14.63 (±1.58)	42.6
34	N	O	24.00 (±3.79)	-4.62	9.35 (±1.20)	-5.03	15.02 (±0.05)	41.5

* Intrinsic clearance (CL'_{int}) was calculate as: (0.693/ in vitro $t_{½}$)·(mL incubation/ mg microsomes)·(45 mg microsomes/g liver)·(20 g liver/kg body).

Table 4. *Pharmacokinetic parameters for compound **UPAR-452**, **UPAR-453**, **33** and **34***

These four compounds were also evaluated for their stability in human liver microsomes (HLM). The data obtained revealed that the half-life of the compounds

ranged from 12 to 15 minutes, with a slightly better stability for compounds bearing the phenyl ring at the LHS. As those values are far from the ideal results required for a drug candidate, also considering the SAR hints previously reported, the optimization process was mainly focused on the understanding and overcoming this metabolic liability. This was achieved via different steps, starting from the identification of the metabolites generated in the incubation of compounds **UPAR-452** and **UPAR-453** in HLM.

Preliminary incubations showed a similar metabolic profile for the two parent compounds. Three major metabolites were detected for each series and characterized by High Resolution Mass Spectra (HR-MS) and tandem mass spectrometry (MS/MS) analysis. Two of them showed molecular mass M = M+16 [M+O] with respect to the parent compound and they were called, in descending order of abundance, $M1_{UPAR-452}$, $M2_{UPAR-452}$ if derived from **UPAR-452** (Figure 3, A) or $M1_{UPAR-453}$, $M2_{UPAR-453}$ if derived from **UPAR-453** (Figure 3, B). A third metabolite having a molecular mass M = M+30 [M+2O-2H], was detected for each parent compound and called $M3_{UPAR-452}$ or $M3_{UPAR-453}$. However, since the hydroxylation was found to be the major phase 1 metabolic modification for either series, this study was mainly focused on the characterization of M1 and M2. For either series, although the nature of the metabolic modification of M1 and M2 was easily identified by HR-MS, it was not possible to predict the site of hydroxylation, even if the MS/MS spectra excluded the involvement of the LHS moiety, at least for metabolites $M2_{UPAR-452}$, $M1_{UPAR-453}$, $M2_{UPAR-453}$. For this reason, the final identification of the metabolites was accomplished *via* the synthesis of a panel of plausible metabolites of the parent compounds, followed by the comparison of the features of the synthesized molecules with those of the corresponding metabolites in the HLM incubates. The comparative identification was carried out analysing the following features: 1) High Resolution (HR) mass value, as derived from HR-MS analysis; 2) MS/MS spectrum; 3) Retention Time (RT) in HPLC runs; 4) Co-elution of the standard compounds with the putative metabolites in the HLM incubates. The panel of hydroxylated derivatives synthesized is reported in the Table 5. Based on the

information obtained from the MS/MS spectra, and considering that the toluene ring is known to be a privileged moiety for the phase 1 metabolism, the synthesis of the hydroxylated derivatives was focused on structures bearing the hydroxyl group at the aromatic ring on the RHS. However, for $M1_{UPAR-452}$ the MS/MS spectrum gave no information about the region involved in the metabolic hydroxylation and, therefore, compounds **35**, **36** and **37**, presented in the Section 2.2.3.1, were included in the study.

Figure 3

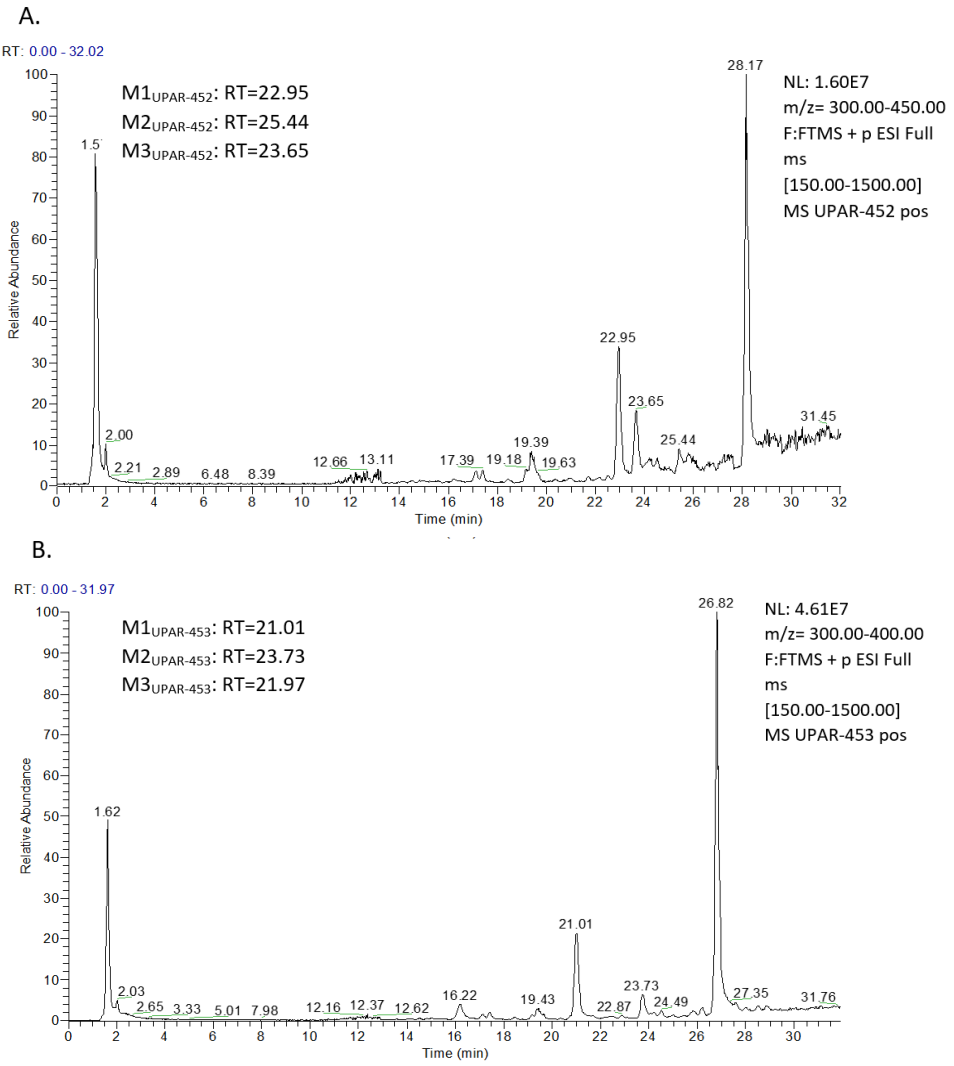

Figure 3. *Full scan traces of HLM incubates: (A)* ***UPAR-452****, (B)* ***UPAR-453***

Figure 4

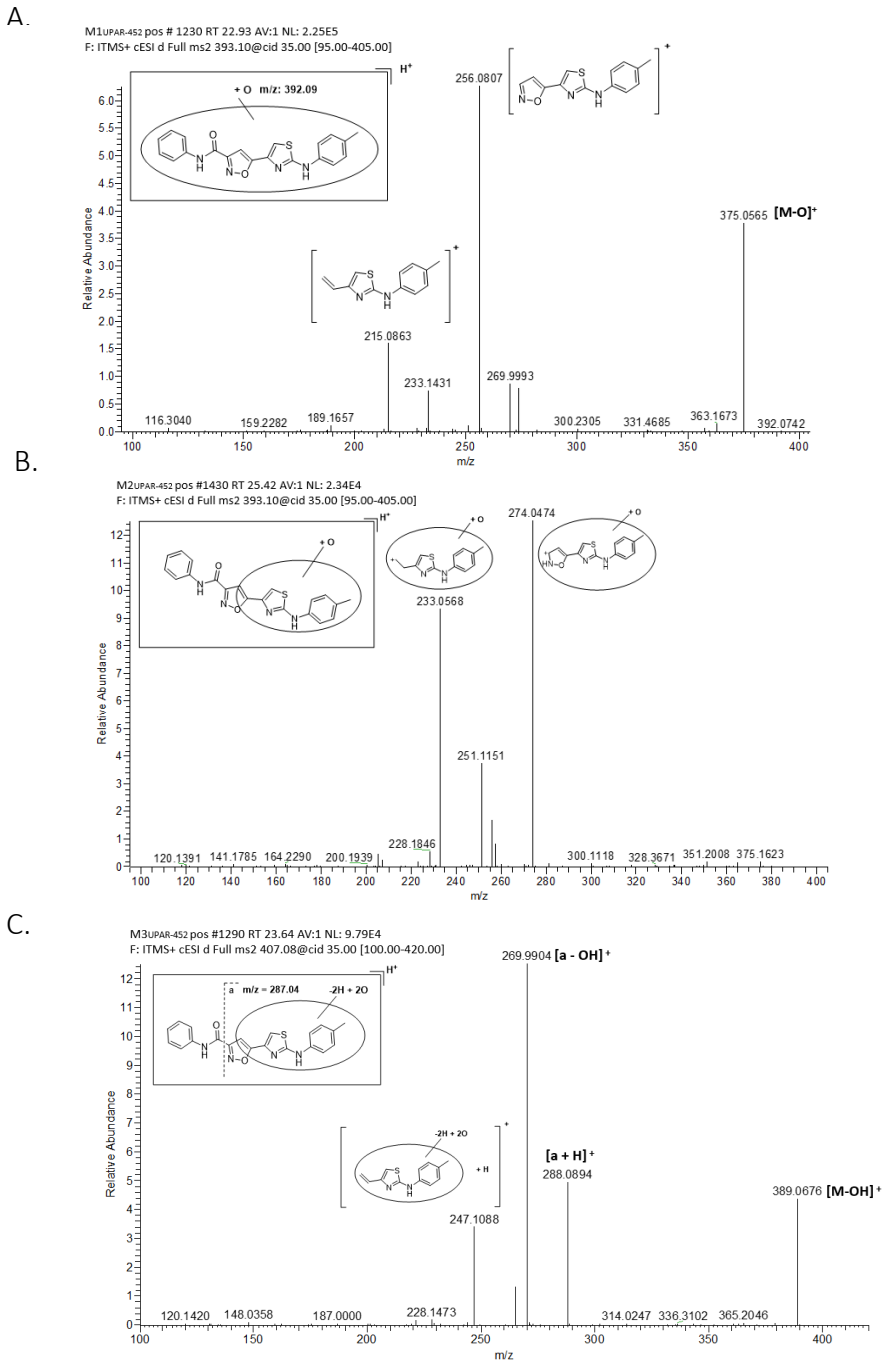

Figure 4. *MS/MS spectra of the three metabolites of **UPAR-452**: (A) M1, (B) M2, (C) M3.*

Figure 5

A.

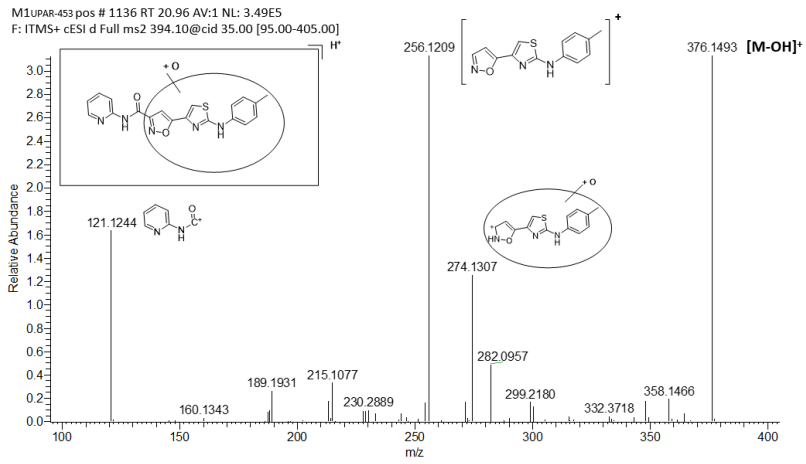

B.

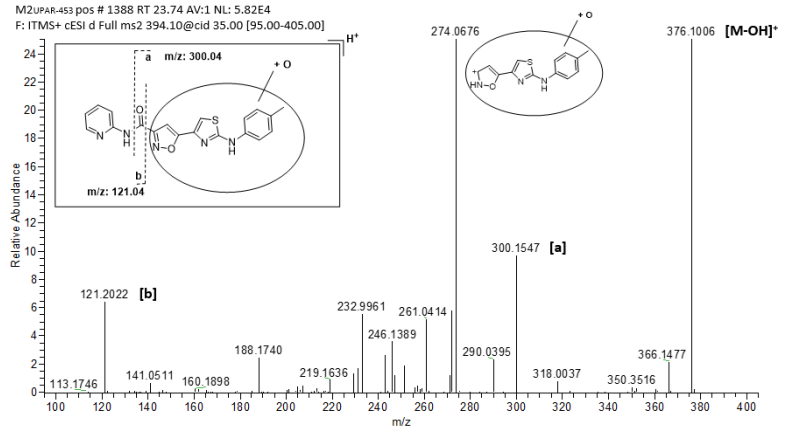

C.

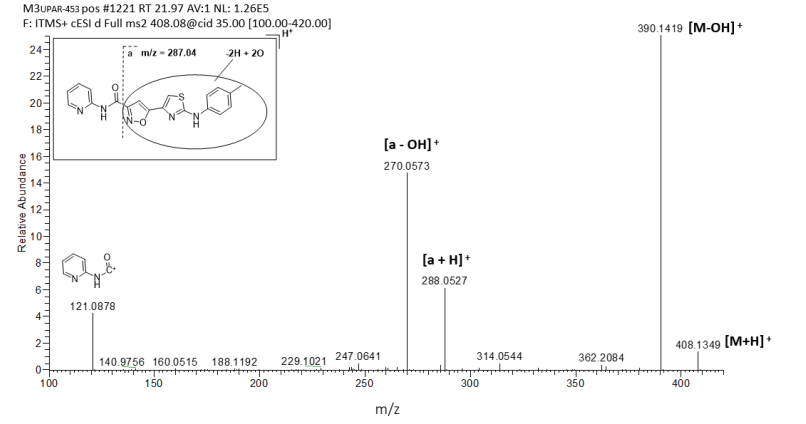

Figure 5. *MS/MS spectra of the three metabolites **UPAR-453**: (A) M1, (B) M2, (C) M3.*

Table 5

A.

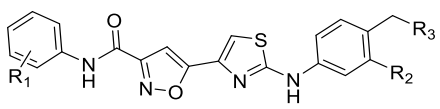

Compound	R_1	R_2	R_3	MIC_{90} (µg/mL)	IC_{50} (µM)
35	ortho-OH	H	H	0.6	53.1
36	meta-OH	H	H	0.6	48.7
37	para-OH	H	H	0.6	79.1
38	H	OH	H	2.5	>100
43h	H	H	OH	>20	34.9

B.

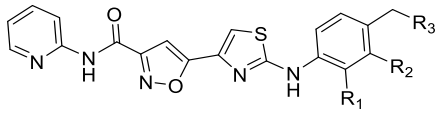

Compound	R_1	R_2	R_3	MIC_{90} (µg/mL)	IC_{50} (µM)
42h	H	H	OH	>20	>100
42e	H	OH	H	5	>100
42i	OH	H	H	>20	72.3

Table 5. *Plausible metabolites of UPAR-452 (A) and UPAR-453 (B), synthesized for the comparative identification study. Structures, MIC_{90} values in M. tuberculosis H37Rv and IC_{50} in THP-derived macrophages.*

Regarding compound **UPAR-453**, the metabolites M1 and M2 were identified, first by comparing the MS/MS spectrum with those of the synthesized standards. The MS/MS spectrum of the metabolite $M1_{UPAR-453}$ matched that of compound **42h** (Figure 5S Appendix A), hydroxylated on the methyl group of the toluene, while the MS/MS spectrum of $M2_{UPAR-453}$ matched both those of the compounds **42e** (Figure 6S Appendix A) and **42i** (Figure 7S Appendix A), bearing the hydroxyl group at ortho and meta positions with respect to the methyl. The identity of the metabolite $M1_{UPAR-453}$ was finally confirmed by the HPLC analysis, comparing the retention time of the metabolite with that of compound **42h** and then coeluting compound **42h** in the HLM incubate using an appropriate gradient of 15 minutes (Figure 12S Appendix A). This gradient, optimized for the identification of the metabolite M1, did not allow to separate **42e** from **42i**, and for this reason a 120 min gradient was optimized (see section Materials and Methods), allowing to finally identify the M2 metabolite as **42e**, via the comparison of the retention times and the coelution of the standard with $M2_{UPAR-453}$ in the HLM

incubate (Figure 13S Appendix A). The HR-MS values for the identified metabolites were also acquired (see section 1.1 Appendix A) and are reported, together with the experimental error, in Table 6.

Table 6

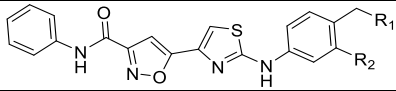

Comp.	Structure assigned		Calculated mass	Ion	Elemental composition	Experimental mass	Error (Δppm)
	R_1	R_2					
UPAR-452	H	H	377.1067	$[M+H]^+$	$C_{20}H_{16}N_4O_2S$	377.1075	2.1
M1	OH	H	393.10159	$[M+H]^+$	$C_{20}H_{16}N_4O_3S$	393.10241	2.1
M2	H	OH	393.10159	$[M+H]^+$	$C_{20}H_{16}N_4O_3S$	393.10126	-0.8

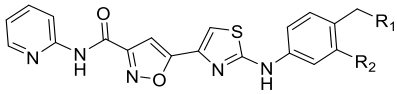

Comp.	Structure assigned		Calculated mass	Ion	Elemental composition	Experimental mass	Error (Δppm)
	R_1	R_2					
UPAR-453	H	H	378.10192	$[M+H]^+$	$C_{19}H_{15}N_5O_2S$	378.1026	1.8
M1	OH	H	394.09684	$[M+H]^+$	$C_{19}H_{15}N_5O_3S$	394.09705	0.5
M2	H	OH	394.09684	$[M+H]^+$	$C_{19}H_{15}N_5O_3S$	394.09695	0.5

Table 6. *Calculated and experimental HR-MS values for the identified metabolites.*

The determination of the metabolic sites of the parent compound **UPAR-453** confirmed the hypothesis that the toluene moiety was the region affected by the oxidative phase 1 metabolism. Following the same approach $M1_{UPAR-452}$ and $M2_{UPAR-452}$ were identified using: (i) the HR-MS spectra (Chart 4 and section 1.1 Appendix A), (ii) MS/MS spectra (see section 1.2 Appendix A), (iii) retention times and coelution with in the HLM incubate (see section 1.3 Appendix A). Analogously to the results obtained for **UPAR-453**, the major metabolite $M1_{UPAR-452}$ was found to be the hydroxylated derivative on

the methyl group (compound **43h**) and the minor metabolite $M2_{UPAR-452}$ corresponded to the hydroxylated derivative on the ortho position with respect to the methyl group of the toluene (compound **38**). After the identification of the metabolites, they were tested for their activity on *M. tuberculosis* H37Rv. For either series the most abundant metabolites M1 resulted inactive, while the minor metabolites M2 still retained a certain activity. Since the metabolites M1 of both series are the most abundant, the phase 1 metabolism could significantly impact on the activity of these series of derivatives, hampering their future development. In order to overcome this issue, a panel of derivatives with predicted improved metabolic stability was designed and synthesized, according to two different strategies: (i) removing the site of metabolism, (ii) capping the metabolic soft-spots with halogens. A total of 8 compounds (4 compounds for each series) were synthesized and their metabolic stability was measured in HLM (Table 7 A, B). Interestingly, all the molecules synthesized showed an improved stability compared to the parent compounds and, for the majority of derivatives, the residual fraction after 60 minutes of incubation was above 50%. The residual percentage of compounds **42o** and **43o** at 60 minutes suggested that, when toluene core is removed, no metabolic alterations occur on the rest of the molecule. The derivatives bearing halogens at the metabolic sites (**42m-n**, **43m-n**) showed a remarkable stability as it can be observed from the residual percentage of compound at $t=60_{min}$.

After the encouraging results obtained from the stability of the metabolically protected compounds, the study was completed by the measurement of their activity on *M. tuberculosis* H37Rv (MIC_{90}) and toxicity on THP-derived macrophages (IC_{50}). The structure-activity relationships (section 2.2.3.1) already anticipated that, while the LHS moiety was more prone to be chemically manipulated, the RHS region less tolerated the introduction of different substituents. This preliminary observation was confirmed by the MIC_{90} results of the metabolically protected compounds. In fact, both the removal of the toluene ring, as in the case of compounds **42o** and **43o**, and the introduction of halogens at different positions, as in the case of the 3,4,5-

trichlorophenyl ring and the 4-(trifluoromethyl)phenyl moiety, were detrimental for the activity. Interestingly, the non-substituted phenyl ring, allowed to retain the antitubercular activity only for **43l**, while **42l** resulted completely inactive. With a few exceptions, compounds are generally well tolerated, with IC_{50} values in the high micromolar range. To notice, the most active compound **43l** is also the one showing the higher toxicity to the reference cell line, although several-fold fairly above the MIC_{90}.

Table 7

A.

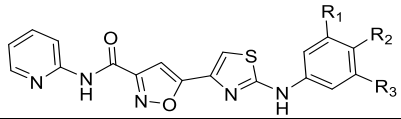

Cmpd.	R_1	R_2	R_3	Half-life (min)	Residual fraction at t = 60_{min}	MIC_{90} (μg/mL)	IC_{50} (μM)
42l	H	H	H	n.d.	60.4 ± 16.4	>20	11.0
42m	H	CF_3	H	n.d.	85.0 ± 6.4	>20	>100
42n	Cl	Cl	Cl	n.d.	101.5 ± 27.9	>20	14.6
42o	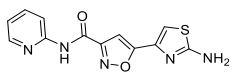			n.d.	96.4 ± 24.5	>20	43.32

B.

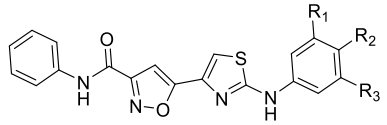

Cmpd.	R_1	R_2	R_3	Half-life (min)	Residual fraction at t = 60_{min}	MIC_{90} (μg/mL)	IC_{50} (μM)
43l	H	H	H	46.8 ± 8.6	42.7 ± 11.6	1.25	11.9
43m	H	CF_3	H	n.d.	70.7 ± 10.6	>20	70.3
43n	Cl	Cl	Cl	n.d.	100.8 ± 0.3	>20	71.7
43o	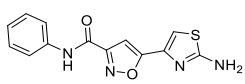			n.d.	98.7 ± 13.3	>20	>100

Table 7. *Metabolically protected derivatives of UPAR-453 (A) and UPAR-452 (B): stability, MIC_{90} values on M. tuberculosis H37Rv and IC_{50} on THP-derived macrophages. The stability is reported as half-life if the residual fraction at 60 min was above 50%, otherwise the residual fraction at 60 min was indicated.*

In conclusion, the study of the metabolism on the parent compounds **UPAR-452** and **UPAR-453** allowed to identify two metabolic soft-spots and revealed that the hydroxylation was the major phase 1 metabolic transformation. For both parent compounds, the major metabolic transformation, i.e the hydroxylation of the methyl group of the toluene ring, caused the loss of the antitubercular activity, while the minor metabolite hydroxylated at the ortho position retain the activity and showed to be not toxic in THP-derived macrophages. Metabolically protected compounds, designed with the aim of preventing/slowing down the metabolism, showed significantly improved stability profiles. However, as suggested by the SAR study reported above, the RHS moiety seems to poorly tolerate any kind of modifications. This results in the completely loss of activity for all the metabolically protected compounds, with the exception of **43l**, that showed an MIC_{90} of 1.25 μg/mL, although with higher toxicity.

2.2.4 Exploring the mechanism of action

The selection of the hit compounds **UPAR-452** and **UPAR-453** and the following SAR investigation were based on a phenotypic approach. Despite the many advantages of this approach, already addressed in this thesis work, the mechanism of action (MoA) remains unknown. However, the identification of the molecular target represents an important step for the characterization of a hit compound, as it allows more focused design in the hit-to-lead optimization phase. For this reason, a preliminary investigation of the mechanism of action was carried out on the two hit **UPAR-452** and **UPAR-453**. Compound **UPAR-326**, the ethyl ester precursor, was also included in the study in order to verify that the molecular target for the ester and its optimized derivatives was the same. Moreover, derivatives **18** and **22**, which showed a promising activity in the SAR study (Section 2.3.1) were also evaluated. Before starting the study, the MIC_{90} of the selected compounds were calculated via the Alamar Blue viability assay in two different media, one of them (7H9 ADC GLU Tw) containing Albumin Dextrose Catalase (ADC) and the other (7H9 CAS GLU Tx) containing Casitone (CAS) as an enrichment alternative (see Chart 6).

Chart 6

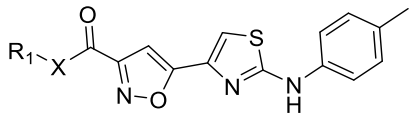

Cmpd.	Structure		Visual Alamar Blue: MIC_{90} (µg/mL)	Calculated Alamar Blue: MIC_{90} (µg/mL)	Visual Alamar Blue: MIC_{90} (µg/mL)	Calculated Alamar Blue: MIC_{90} (µg/mL)
	X	**R_1**	**[Media: 7H9 CAS GLU Tx, Day 7]**		**[Media: H9 ADC GLU Tw, Day 7]**	
UPAR-326	O	ethyl	0.488	<0.244	>125	>125
UPAR-452	NH	phenyl	3.906	1.636	>125	>125
UPAR-453	NH	pyridin-2-yl	31.25	31.86	>125	>125
18	NH	3-methylphenyl	125	>125	>125	>125
22	NH	3-methylpyridin-2-yl	0.488	0.488	31.25	31.25

Chart 6. *MIC_{90} values of selected compounds evaluated in two different media*

The MIC_{90} values for compounds **UPAR-326**, **UPAR-452** and **22** (Chart 6) in the Casitone-containing media, confirmed the activity of the compounds. For compounds **UPAR-453** and **18** some discrepancies were observed, although this is generally accepted when different methods or conditions are used. Moreover, an increasing of the MIC_{90} values in albumin-containing media was observed for all compounds, which might be determined by the high affinity of the compounds for the albumin.

From this preliminary study, compound **UPAR-326** and **22** were selected for the follow up on the MoA investigation. Firstly, these two compounds were tested on different single drug resistant *M. tuberculosis* mutants (see Chart 4) to evaluate whether cross resistance occurred.

Chart 7

Name	Strain/ mutation	UPAR-326 MIC_{90} (µM) 7H9/CAS/GLU medium; Day 7	22 MIC_{90} (µM) 7H9/CAS/GLU medium; Day 7	Interpretation
Wild-type	H37RvMa	≤ 0.2	≤ 0.2	Susceptible
Fusidic acid resist. mutants	GKFA *fus*A1	≤ 0.2	≤ 0.2	Susceptible
Spectinomycin resist. mutants	G1379T *rss*	≤ 0.2	≤ 0.2	Susceptible
Rifampicin resist. mutants	S531L *rpoB*	≤ 0.2	≤ 0.2	Susceptible
Linezolid resist. mutants	T460C *rplC*	12.5	25	Resistant
	GG2270T *rrl*	3.1	25	Resistant

Chart 7. *MIC_{90} values on resistant mutants*

Cross-resistance was observed in the linezolid resistant mutants, suggesting an overlapping mechanism of action with linezolid, while the activity on the other mutants is comparable to the wild-type. Further investigations based on the selection of resistant mutants will allow to identify the molecular target and to evaluate whether inhibition of protein synthesis is the sole mechanism of bacterial inhibition or whether a pleiotropic mode of action occurs.

2.3 Chemistry

For the sake of clarity, the description of the synthetic pathway and the reaction schemes will be divided as followed:

- Optimized synthesis of the parent compound **UPAR-453**
- Synthesis of panel of derivatives for the SAR investigation (compounds **4-37**)
- Synthesis of compounds for the SMR investigation (compounds **38-44**)

2.3.1 Synthesis of UPAR-453

The reported synthesis of **UPAR-453** and the optimized protocol developed in this work, already described in the Section 2.2.1, are shown in the Scheme 1 and in the Scheme 2 respectively.

Scheme 1. [a]

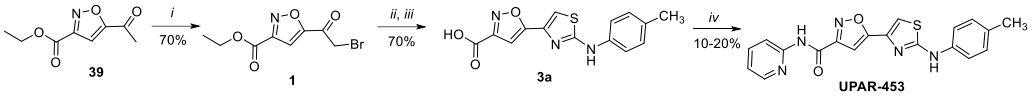

Scheme 1. [a] *Reagents and conditions*: *i)* Br_2, chloroform, AcOH, 50°C, 1h; *ii)* p-tolylthiourea, absolute EtOH, reflux, 2h; *iii)* LiOH, THF/H_2O/ MeOH (3:1:1 ratio), r.t., 1h; *iv)* TBTU, EDC·HCl, N_2 atm, dry DMF, 10 min; then 2-aminopyridine, TEA, r.t., 4h.

Scheme 2. [a]

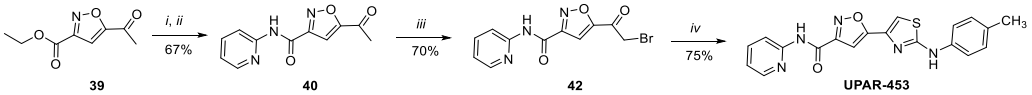

Scheme 2. [a] Reagents and conditions: *i)* NaOH powder, absolute EtOH, r.t, 30 min; *ii)* HATU, dry DMF, Ar atm, 10 min; then, 2-aminopyridine, TEA, r.t, 2h; *iii)* Acetic acid, Br_2, dioxane, 40°C-70°C, 2h; *iv)* p-tolylthiourea, absolute EtOH, 80°C.

2.3.2 Synthesis of the panel of derivatives for the SAR investigation

Compounds **2a-d** were obtained following an established protocol,[1] starting from compound **1** and the appropriate thiourea, commercially available or synthesized in one step from the corresponding anilines. The ethyl esters obtained were then hydrolysed with LiOH in THF/MeOH/H_2O at room temperature to give the carboxylic acids, which were then reacted with the suitable amine, using TBTU and EDC as coupling reagents. Using this synthetic route, 33 final compounds were obtained as shown in the Scheme 3.

Because of the different reactivity of the oxygen in comparison with sulfur, the 2-aminooxazole core of compound **2f** (Scheme 4) cannot be obtained by reacting the alpha-bromoketone **1** with the *p*-tolylurea. Thus, the synthesis of **2f** was carried out using a synthetic protocol previously developed and optimized in our research group as reported.[1] Similarly to the synthesis presented in the Schema 3, the ethyl ester, obtained as previously reported, was then hydrolysed and reacted with the suitable amine to give compounds **33** and **34**.

Scheme 3. [a]

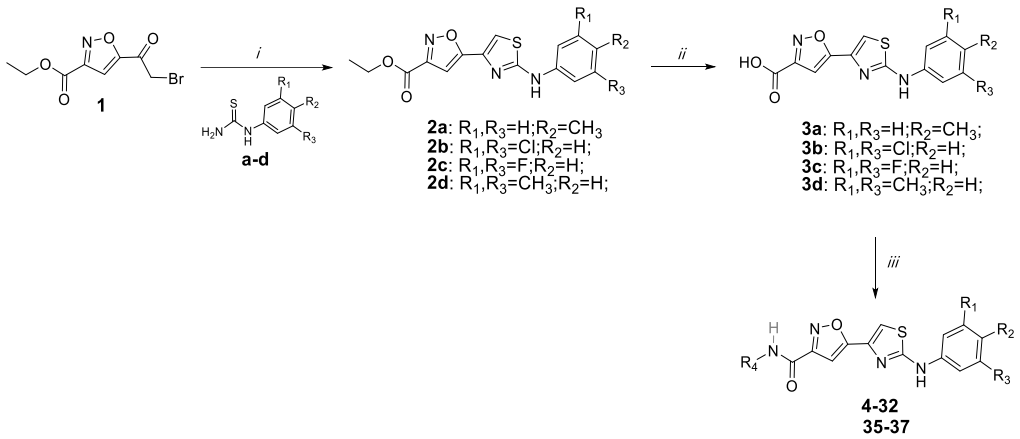

Scheme 3. [a] *Reagents and conditions: i)* thioureas **a-d**, absolute EtOH, 80°C, yield: 40-60%; *ii)* LiOH, THF/H_2O/MeOH 3:1:1, r.t., 1h, yield: quantitative; *iii)* for compounds **4-32**: TBTU, EDC·HCl, N_2 atm, dry DMF, 10 min; then R_4-NH_2, TEA, r.t., 4h, yield: 18-79%; for compounds **35-37**: the appropriate aminophenol, TEA, COMU, N_2 atm, dry DMF, r.t., 4h, yield: 10-28%.
[b] *For complete structures see Table 3.*

Scheme 4. [a]

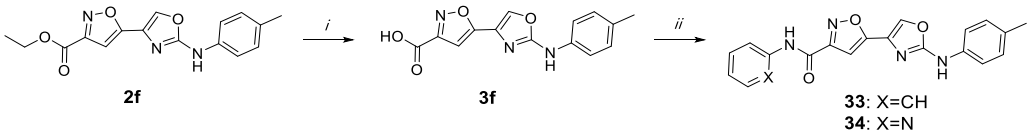

Scheme 4. [a] *Reagents and conditions: i)* LiOH, THF/H_2O/MeOH 3:1:1, r.t., 1h, yield: quantitative; *ii)* TBTU, EDC·HCl, N_2 atm, dry DMF, 10 min; then the appropriate amine (aniline or 2-aminopyridine), r.t., 4h, yield: 17-57%.

2.3.3 Synthesis of metabolites and metabolically protected compounds

The first attempt to synthesize compound **2e** was carried out refluxing compound **1** and the thiourea **e** in absolute ethanol. However, compound **44** (see section 2.5.1), bearing a bromine at position 2 on the RHS aromatic ring, was obtained as major product. In order to avoid the bromination, a microwave assisted protocol in nitrogen atmosphere was developed as reported in Scheme 5. Compound **2e** was hydrolysed to **3e** using LiOH as the base. The carboxylic acid obtained was activated with COMU and reacted with aniline to give the amide **38**.

Scheme 5. [a]

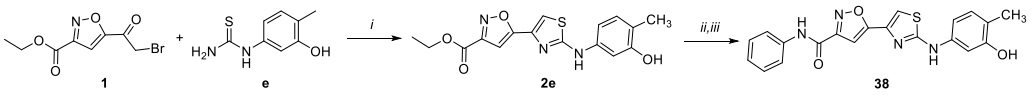

Scheme 5. [a] *Reagents and conditions: i)* absolute EtOH, MW (60 °C, 3 minutes), yield: 42%; *ii)* LiOH, THF/H_2O/MeOH 3:1:1, r.t., 1h; yield: quantitative *iii)* aniline, TEA, COMU, N_2 atm, dry DMF, r.t., 4h, yield: 34%.

Compound **43** (Scheme 6) was obtained following the same synthetic route used for compound **42**, previously discussed in the Sections 2.2.1 and 2.3.1. Reacting **42** and **43** with the suitable thioureas, 10 final compounds were obtained, using the classic Hantzsch protocol (**42l-o**, **43l-o**) or the microwave assisted synthesis (**42e**, **42i**), previously described for the synthesis of compound **2e.**

Scheme 6. [a,b]

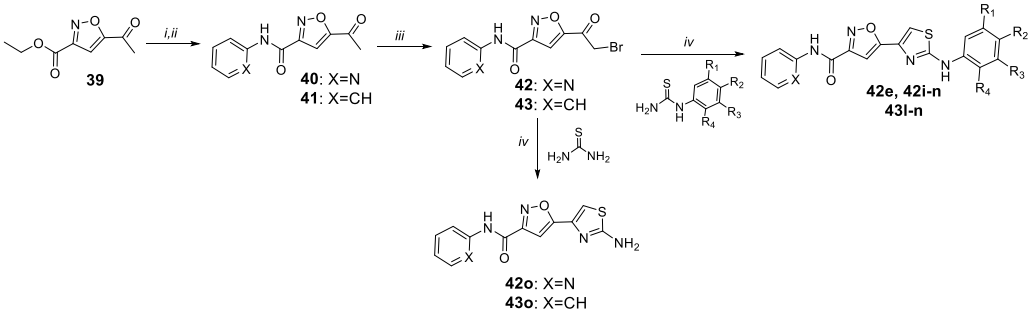

Scheme 6. [a] *Reagents and conditions: i)* NaOH powder, absolute EtOH, r.t, 30 min; *ii)* HATU, dry DMF, Ar atm, 10 min; then, aniline or 2-aminopyridine, TEA, r.t, 2h, yield:67-76%; *iii)* Acetic acid, Br_2, dioxane, 70°C, 2h, 70-81% *iv)* For compounds **42l-o** and **43l-o**: thioureas **l-o**, absolute EtOH, 80°C, yield: 35-70%; for compounds **42e**, **42i**: the thiourea **e** or **i** respectively, absolute EtOH, MW (60 °C, 3 minutes), yield: 17-61%. [b] *For complete structures see Table 5 and Table 6.*

Refluxing compound **42** with the thiourea **g** in EtOH failed to give the desired compound **42h**, as ethyl etherification of the hydroxyl group occurred as side reaction (compound **45**). Likely, the high temperature, the large excess of EtOH as nucleophile, and the acidic conditions generated by the release of HBr favoured the formation of the ethyl ether. To avoid this, the thiourea **g** was protected on the hydroxy group and reacted with compound **42** using the microwave assisted protocol described for the synthesis of compound **2e** (Scheme 5). The same synthetic strategy was followed in order to obtain compound **43h**.

Scheme 8. [a]

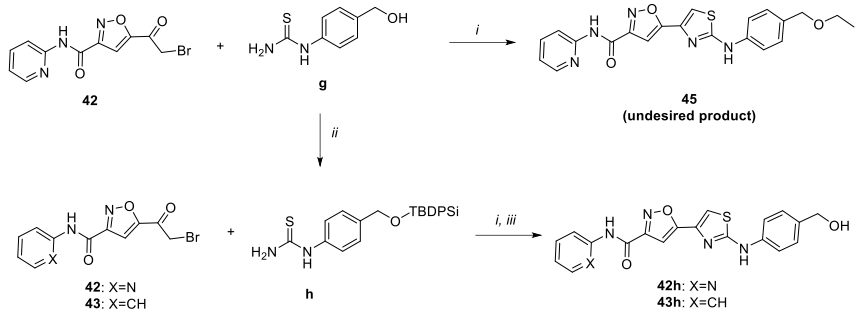

Scheme 8. [a] *Reagents and conditions: i)* absolute EtOH, MW (60 °C, 3 minutes), yield: 29%; *ii)* TBDPSiCl, imidazole in dry DMF, 0°C, 15 min; then compound **g**, r.t, 1h, yield: 65%. *iii)* absolute EtOH, MW (60 °C, 3 minutes); then TBAF on silica gel in dry DMF, 0°C to r.t., yield: 32-48%.

2.4 Conclusions

Two promising antitubercular compounds, **UPAR-452** and **UPAR-453**, previously reported in the group where I have carried out my PhD thesis, were characterized and optimized with regard to their activity and metabolic stability. In particular, (i) refinement of the Structure-Activity Relationships (SAR), (ii) characterization of the metabolic profile in vitro and Structure-Metabolism Relationships and (iii) improvement of the synthetic procedure in view of future scale up processing were investigated.

The SAR study revealed that the aromatic ring attached to the isoxazole-3-carboxyamide is more prone to be chemically modified than the toluene attached to the aminothiazole and it offers a wider scope for modification in order to modulate the activity of the compounds against *M. tuberculosis*. Despite the fact that the molecular mechanism of action of this class of compounds is still unknown, the comparable results obtained for both the methyl derivatives **17-19**, the hydroxyl derivatives **35-37** and the fluorine derivatives **4-5** and **23**, regardless their position around the ring suggested that stereoelectronic effects might prevail on the specific interaction of the functional groups with a precise group in the target binding pocket. Of notice, the hydroxyl derivative **37** was found to be the most promising compound of the series. This can be considered an exception in the field of medicinal chemistry for antitubercular

compounds, where hydrophilic substituents generally have a detrimental impact on the activity probably because they make molecules less prone to penetrate the mycobacterial cell wall.[9,13,14] On the other hand, this modification may be important in the improvement of the physicochemical characteristics of the molecule, such as solubility and formulability.

Figure 6

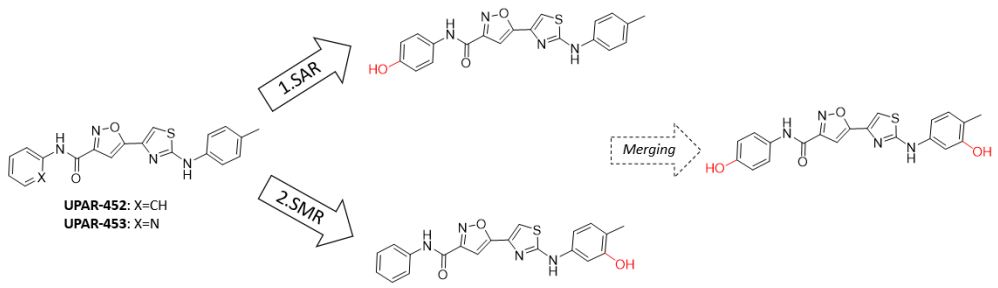

Although the metabolic stability was preliminarily investigated only in cellular models, interesting considerations can be made. The hydroxylation resulted to be the primary phase I transformation and the toluene ring attached to the 2-aminothiazole core was found to be the main substrate of the metabolism. In particular, the two metabolic soft-spots, both for **UPAR-452** and **UPAR-453**, are represented by the methyl group of the toluene and the ortho position to the methyl. The evaluation of the antitubercular activity of the metabolites revealed that for each series, while the major metabolite resulted inactive, the minor metabolite (compounds **38** and **42e**) was found to be moderately active and not toxic to mammal cells. This hydroxylated structure may also be less prone to be hydroxylated on the methyl group of the toluene opening the way for the design of antitubercular long-lasting molecules.

These findings have proved to be extremely important in the hit-to-lead process, driving the synthesis of further derivatives with ameliorated stability toward microsomes degradation. Importantly, the synthesis of derivatives specifically designed to improve the microsomal stability was successfully achieved, confirming the data obtained via instrumental analysis.

Merging the set of information above reported, it is possible to plan the design and synthesis of one or more improved analogues (Figure 6), where the introduction of the two hydroxyl moieties might also be beneficial for the general drug-likeness of the molecule.

2.5 Materials and methods

2.5.1 Synthetic chemistry

All the reagents were purchased from Sigma-Aldrich and Alfa-Aesar at reagent purity and, unless otherwise noted, were used without any further purification. Thioureas **a**, **b**, **c**, **d**, **o**, **l** were purchased while thioureas **e**, **g**, **h**, **i**, **m**, **n** were synthesized as described below. Dry solvents used in the reactions were purchased from Sigma Aldrich. Reactions were monitored by thin layer chromatography on silica gel-coated aluminum foils (silica gel on Al foils, SUPELCO Analytical, Sigma-Aldrich) at both 254 and 365 nm wavelengths. Where indicated, intermediates and final products were purified through silica gel flash column chromatography (silica gel, 0.040-0.063 mm) or Combiflash® Rf 200, using appropriate solvent mixtures. ^{1}H-NMR and ^{13}C-NMR spectra were recorded on BRUKER AVANCE spectrometers (^{1}H at 300 or 400 MHz and ^{13}C at 75 or 101 MHz respectively) or on a JEOL spectrometer (^{1}H at 600 and ^{13}C at 125), using residual solvents as internal standards in all cases. ^{1}H-NMR spectra are reported in this order: δ ppm (multiplicity, number of protons). Standard abbreviation indicating the multiplicity was used as follows: s = singlet, d = doublet, dd = doublet of doublets, t = triplet, q = quadruplet, m = multiplet and br = broad signal. HPLC/MS experiments were performed with HPLC: Agilent 1100 series, equipped with a Waters Symmetry C18, 3.5 µm, 4.6 mm x 75 mm column and MS: Applied Biosystem/MDS SCIEX, with API 150EX ion source. HR-MS experiments were performed with LTQ ORBITRAP XL THERMO.
All compounds were tested as 95–100% purity samples (by HPLC/MS).

General method A: amide synthesis. *O*-(Benzotriazol-1-yl)-*N,N,N′,N*′-tetramethyluronium tetrafluoroborate (TBTU) (1 eq) and *N*-(3-Dimethylaminopropyl)-*N*′-ethylcarbodiimide hydrochloride (EDC HCl) (1 eq) were added to a solution of the carboxylic acid (1 eq) in dry DMF (4 mL/mmol) under nitrogen atmosphere. Reaction mixture was stirred at room temperature for 15 minutes, then triethylamine (1.5 eq) and the amine (1 eq) were added. The mixture was stirred at the same temperature for 4h. Then, reaction mixture was taken up with brine (5 mL) and the mixture was

extracted with EtOAc (3 x 10 mL). The organic layers were collected, washed with brine (2 x 5 mL) and dried over Na_2SO_4. After filtration, the volatiles were removed under vacuum and the crude material was purified by flash column chromatography eluting from 5% to 40% v/v EtOAc in petroleum ether. Purification conditions, yields and analytical data are reported below.

General method B: amide synthesis. 1-[(1-(Cyano-2-ethoxy-2-oxoethylideneaminooxy) dimethylaminomorpholino)] uronium hexafluorophosphate (COMU) (1 eq) was added to a solution of the carboxylic acid (1 eq), the appropriate amine (1 eq) and triethylamine (1.5 eq) in dry DMF (4 mL/mmol) under N_2 atmosphere. After stirring at room temperature for 4h, brine (5 mL) was added and the mixture was extracted with EtOAc (3 x 10 mL). The organic layers were collected, washed with brine (2 x 5 mL) and dried over Na_2SO_4. After filtration, the volatiles were removed under vacuum and the crude material was purified by flash column chromatography. Purification conditions, yields and analytical data are reported below.

General method C: ester hydrolysis. LiOH (4 eq) was added to a solution of the ethyl ester (1eq) in a mixture of THF/MeOH/H_2O (3:1:1 ratio, 2 mL per mmol). After stirring at room temperature for 1 h, HCl 1M was slowly added to pH=1 and the mixture was extracted with EtOAc (20 mL x3). The organic layers were collected, washed with brine (x2) and dried over Na_2SO_4. The crude obtained was used in the next step without any further purification. Yields and analytical data are reported below.

General method D: standard protocol for Hantzsch thiazole synthesis. A solution of the α-bromo ketone (1 eq) and the appropriate thiourea (1 eq) in absolute EtOH (4 mL per mmol) was refluxed at 80°C until reaction completion was observed by TLC (30% v/v EtOAc in petroleum ether). After cooling, the desired compound was collected by filtration after precipitating in the reaction mixture. When the precipitation of the desired compound was not observed, reaction mixture was evaporated under reduced pressure, partitioned between water (5 mL) and EtOAc (5 mL), extracted with EtOAc (20 mL x3) and purified by Combiflash®. Purification conditions, yields and analytical data are reported below.

General method E: microwave-assisted protocol for thiazole synthesis. The α-bromo ketone (1 eq) and the appropriate thiourea (1 eq) were dissolved in EtOH (4 mL per mmol) under nitrogen atmosphere and the mixture was heated up to 60°C using microwave irradiation (power: 200 W) for 3 minutes. Purification conditions, yields and analytical data are reported below.

General method F: bromination. The appropriate ketone (1 eq) was dissolved in dioxane (2 mL per mmol) and a catalytic amount of acetic acid (0.1 mL per mmol) was added. The mixture was heated up to 40°C and bromine (1 eq) was added dropwise. Reaction mixture was stirred at 70°C for 2 h. Then, the mixture was carefully washed with aq. sat. $NaHCO_3$ and extracted with EtOAc (3 x 20 mL). Organic layers were collected, dried over Na_2SO_4 and purified by Combiflash® eluting from 10% to 30% v/v EtOAc in petroleum ether. Yields and analytical data are reported below.

Ethyl 5-(2-bromoacetyl)isoxazole-3-carboxylate(1)

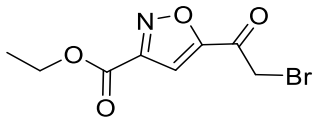

The title compound was synthesized as previously reported.[1] Analytical data matched those reported in literature.

3-hydroxy-4-methylphenylthiourea (e)

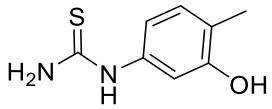

The title compound was synthesized as previously reported.[15] Analytical data matched those reported in literature.

1-(4-(hydroxymethyl)phenyl)thiourea (g)

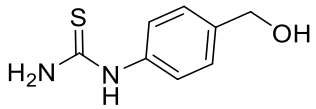

The title compound was synthesized as previously reported. Analytical data matched those reported in literature.[16]

1-(4-(((tert-butyldiphenylsilyl)oxy)methyl)phenyl)thiourea (h)

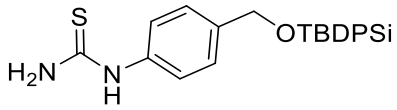

TBDPSiCl was added to a solution of Imidazole (45 mg, 0.66 mmol, 3 eq) in dry DMF (0.5 mL) at 0°C (ice bath). After stirring for 15 min, compound **g** was added and the reaction was allowed to stir for 1 h. Then, the reaction mixture was quenched with aq. sat. NH_4Cl and the mixture was extracted with EtOAc (3 x 10 mL). Organic layers were collected, dried over Na_2SO_4 and purified by flash chromatography eluting with 100% DCM to give the title compound as a white powder (yield 60 mg, 65%). ^{1}H-NMR (400 MHz, $CDCl_3$) δ: 7.89 (1H, s), 7.70 (4H, d, *J*=7.3 Hz), 7.47 - 7.39 (8H, m), 7.22 (2H, d, *J*=8.1 Hz), 6.06 (2H, s), 4.79 (2H, s); ^{13}C-NMR (101 MHz, $CDCl_3$) δ: 181.9, 141.2, 135.5, 134.8, 133.2, 129.9, 127.8, 125.1, 64.9, 26.8, 19.3.

1-(2-hydroxy-4-methylphenyl)thiourea (i)

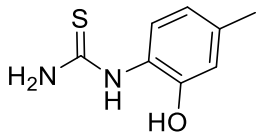

NH_4SCN (468.5 mg, 6.50 mmol, 4 eq) was added to a solution of 2-amino-5-methylphenol (200 mg, 1.62 mmol, 1 eq) in HCl 1N (1.6 mL) and the mixture was heated up to 100°C. After refluxing for 10 h, it was neutralized with a aq. sat. $NaHCO_3$ and extracted with EtOAc (3 x 10 mL). Organic layers were collected, dried over Na_2SO_4 and purified by flash column chromatography eluting from 0% to 5% v/v MeOH in DCM to give the title compound as a pale yellow powder (yield: 120 mg, 41%). ^{1}H-NMR (300 MHz, DMSO-d_6) δ: 9.58 (1H, s), 8.90 (1H, s), 7.49-735 (3H, m), 6.68 (1H, d, *J*=1.4 Hz), 6.57 (1H, dd, *J*=1.4, 8.1 Hz), 2.21 (3H, s); ^{13}C-NMR (75 MHz, MeOD) δ: 181.0, 151.7, 138.5, 126.4, 120.3, 116.9, 19.9.

1-(4-(trifluoromethyl)phenyl)thiourea (m)

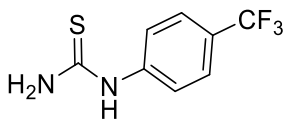

The title compound was synthesized as previously reported. Analytical data matched those reported.[17]

1-(3,4,5-trichlorophenyl)thiourea (n)

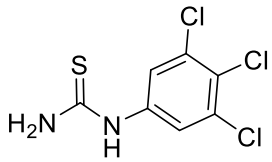

NH_4SCN (1.1 g, 15.27 mmol, 2 eq) was added to a solution of 3,4,5-trichloroaniline (1.5 g, 7.63 mmol, 1 eq) in HCl 1N (10 mL) and the mixture was heated up to 100°C. After refluxing for 5h, the mixture was carefully neutralized with NaOH 1M and it was extracted with EtOAc (x3). Organic layers were collected, dried over Na_2SO_4 and purified by Combiflash® eluting from 30% to 100% v/v EtOAc in petroleum ether to give the title compound as a pale yellow powder (yield: 1.9 g, 97%). ^{1}H-NMR (400 MHz, DMSO) δ: 9.98 (1H, s), 7.84 (2H, s), 7.78 (2H, bs); ^{13}C-NMR (101 MHz, DMSO-d_6) δ: 181.8, ^{1}140.1, 132.8, 124.5, 122.9. HR-MS analysis: calculated for $C_7H_5Cl_3N_2S$: 253.92; found: 254.96118 [$M+H^+$].

Ethyl 5-(2-(*p*-tolylamino)thiazol-4-yl)isoxazole-3-carboxylate (2a)

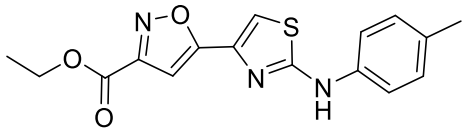

The title compound was synthesized as previously reported.[1] Analytical data matched those reported in literature.

5-(2-(*p*-tolylamino)thiazol-4-yl)isoxazole-3-carboxylic acid (3a)

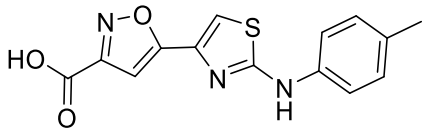

Starting from compound **2a** (308 mg, 0.93 mmol), the title compound was obtained as a yellow powder following the **general method C** (275 mg, quantitative yield). ^{1}H-NMR (400 MHz, DMSO-d_6) δ: 14.08 (1H, s), 10.38 (1H, s), 7.65 (1H, s), 7.57 (2H, d, *J*=8.5 Hz),

7.17 (2H, d, *J*=8.5 Hz), 7.06 (1H, s), 2.27 (3H, s); ^{13}C-NMR (101 MHz, DMSO-d_6) δ: 167.2, 165.0, 161.2, 158.0, 138.8, 138.3, 131.2, 130.0, 117.9, 110.0, 101.4, 20.9.

5-(2-((3,5-dichlorophenyl)amino)thiazol-4-yl)isoxazole-3-carboxylic acid (3b)

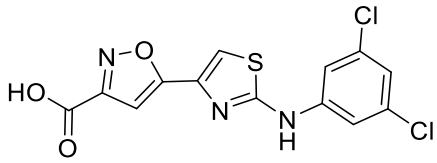

The title compound was synthesized as previously reported.[1] Analytical data matched those reported in literature.

Ethyl 5-(2-((3,5-difluorophenyl)amino)thiazol-4-yl)isoxazole-3-carboxylate (2c)

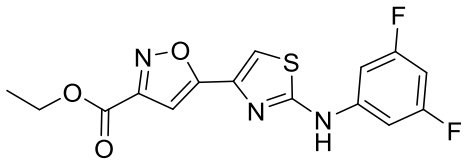

Compound **1** (400 mg, 1.53 mmol) and 3,5-difluorophenylthiourea (**c**) were reacted following the **general method D**. The crude obtained was purified by Combiflash® eluting from 20% to 60% v/v EtOAc in petroleum ether and the desired compound was obtained as pale yellow powder (yield: 325 mg, 65%). ^{1}H-NMR (400 MHz, DMSO-d_6) δ: 10.91 (1H, s), 7.85 (1H, s), 7.42 (2H, dd, *J*=2.2, 9.6 Hz), 7.18 (1H, s), 6.82 (1H, tt, *J*=2.2, 9.6 Hz), 4.42 (2H, q, *J*=7.1 Hz), 1.36 (3H, t, *J*=7.1 Hz).

5-(2-((3,5-difluorophenyl)amino)thiazol-4-yl)isoxazole-3-carboxylic acid (3c)

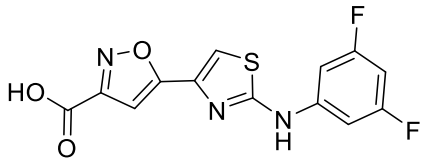

Starting from compound **2c** (161 mg, 0.46 mmol), the title compound was obtained as a yellow powder following the **general method C** (yield: 147 mg, quantitative). ^{1}H-NMR (400 MHz, DMSO-d_6) δ: 14.14 (1H, bs), 10.91 (1H, s), 7.82 (1H, s), 7.43 (2H, dd, *J*=2.2, 9.6 Hz), 7.11 (1H, s), 6.83 (1H, tt, *J*=2.2, 9.6 Hz); ^{13}C-NMR (101 MHz, DMSO-d_6) δ: 166.8, 164.0, 162.2, 162.0, 161.1, 158.0, 143.3, 138.3, 111.8, 101.6, 100.6, 100.3, 97.1. HR-MS analysis: calculated for $C_{13}H_7F_2N_3O_3S$: 323.02; found: 324.02539 [M+H$^+$].

Ethyl 5-(2-((3,5-dimethylphenyl)amino)thiazol-4-yl)isoxazole-3-carboxylate (2d)

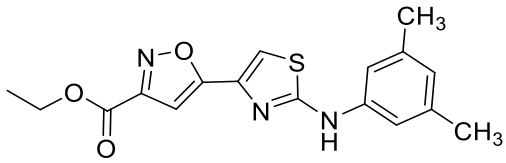

Compound **1** (400 mg, 1.53 mmol) and (3,5-dimethylphenyl)thiourea (**d**) were reacted following the **general method D**. The crude obtained was purified by Combiflash® eluting from 20% to 60% v/v EtOAc in petroleum ether and the desired compound was obtained as a pale yellow powder (yield: 315 mg, 60%). ^{1}H-NMR (400 MHz, DMSO-d_6) δ: 10.33 (1H, s), 7.71 (1H, s), 7.27 (2H, s), 7.09 (1H, s), 6.67 (1H, s), 4.41 (2H, q, *J*=7.1 Hz), 2.29 (6H, s), 1.36 (3H, t, *J*=7.1 Hz); ^{13}C-NMR (101 MHz, DMSO-d_6) δ: 167.4, 165.0, 159.8, 157.0, 141.0, 138.6, 138.1, 124.1, 115.6, 110.6, 101.2, 62.4, 21.7, 14.4. HR-MS analysis: calculated for $C_{17}H_{17}N_3O_3S$: 343.10; found: 344.10745 [M+H$^+$].

5-(2-((3,5-dimethylphenyl)amino)thiazol-4-yl)isoxazole-3-carboxylic acid (3d)

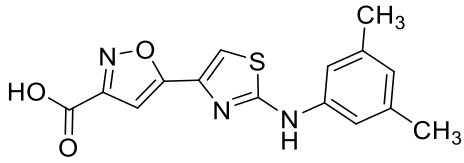

Starting from **2d** (150 mg, 0.44 mmol), the title compound was obtained as a pale yellow powder following the **general method C** (yield: 137 mg, quantitative). ^{1}H-NMR (400 MHz, DMSO-d_6) δ: 14.1 (1H, bs), 10.33 (1H, s), 7.68 (1H, s), 7.28 (2H, s), 7.02 (1H, s), 6.67 (1H, s), 2.27 (6H, s); ^{13}C-NMR (151 MHz, DMSO-d_6) δ: 167.2, 165.0, 161.2, 157.9, 141.1, 138.6, 138.3, 124.1, 115.6, 110.2, 101.3, 21.7. HR-MS analysis: calculated for $C_{15}H_{13}N_3O_3S$: 315.07; found: 316.07549 [M+H$^+$].

Ethyl 5-(2-((3-hydroxy-4-methylphenyl)amino)thiazol-4-yl)isoxazole-3-carboxylate (2e)

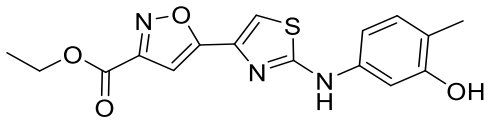

Compound **1** (80 mg, 0.31 mmol) and 3-hydroxy-4-methylphenylthiourea (**e**) were reacted following the **general method E**. After reaction completion, the volatiles were

evaporated under reduced pressure and the crude obtained was purified by flash column chromatography eluting from 40% to 90% v/v EtOAc in petroleum ether. The desired compound was obtained as a yellow powder (yield: 44 mg, 42%). ^{1}H-NMR (400 MHz, DMSO-d_6) δ: 10.30 (1H, s), 9.45 (1H, s), 7.67 (1H, s), 7.46 (1H, d, *J*=1.9 Hz), 7.21 (1H, s), 6.99 (1H, d, *J*=8.1 Hz), 6.83 (1H, dd, *J*=1.9, 8.1 Hz), 4.42 (2H, q, *J*=7.2 Hz), 2.06 (3H, s), 1.36 (3H, t, *J*=7.2 Hz); ^{13}C-NMR (151 MHz, DMSO-d_6) δ: 167.4, 164.7, 159.5, 157.3, 156.0, 140.0, 138.0, 130.9, 117.5, 110.0, 108.8, 104.9, 101.6, 62.5, 16.0, 14.5. HR-MS analysis: calculated for $C_{16}H_{15}N_3O_4S$: 345.08; found: 346.08611 [M+H$^+$].

5-(2-((3-hydroxy-4-methylphenyl)amino)thiazol-4-yl)isoxazole-3-carboxylic acid (3e)

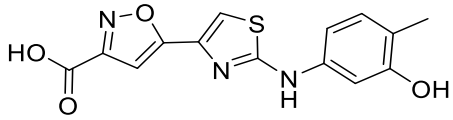

Starting from **2e** (27 mg, 0.08 mmol), the title compound was obtained as a yellow powder following the **general method C** (yield: 24 mg, quantitative). ^{1}H-NMR (400 MHz, DMSO-d_6) δ: 14.10 (1H, bs), 10.32 (1H, s), 9.46 (1H, s), 7.69 (1H, s), 7.46 (1H, d, *J*=1.9 Hz), 7.22 (1H, s), 7.01 (1H, d, *J*=8.1 Hz), 6.85 (1H, dd, *J*=1.9, 8.1 Hz), 2.07 (3H, s); ^{13}C-NMR (151 MHz, DMSO-d_6) δ: 167.1, 164.8, 159.7, 157.4, 156.1, 140.2, 138.0, 131.0, 117.5, 110.0, 108.9, 104.9, 101.6, 16.2. HR-MS analysis: calculated for $C_{14}H_{11}N_3O_4S$: 317.0470; found: 318.0543[M+H$^+$].

Ethyl 5-(2-(*p*-tolylamino)oxazol-4-yl)isoxazole-3-carboxylate (2f)

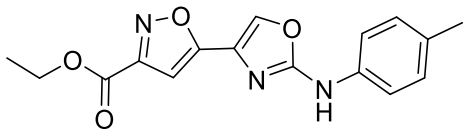

The title compound was synthesized as previously reported.[18] Analytical data matched those reported in literature.

5-(2-(*p*-tolylamino)oxazol-4-yl)isoxazole-3-carboxylic acid (3f)

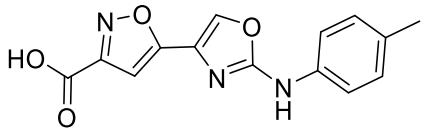

Starting from **2f** (95 mg, 0.30 mmol), the title compound was obtained as a yellow powder and following the **general method C** (yield: 85 mg, quantitative). ^{1}H-NMR (400 MHz, DMSO-d_6) δ: 14.11 (1H, bs), 10.33 (1H, s), 8.40 (1H, s), 7.54 (2H, d, *J*=8.3 Hz), 7.16 (2H, d, *J*=8.3 Hz), 7.02 (1H, s), 2.27 (3H, s); ^{13}C-NMR (101 MHz, DMSO-d_6) δ: 165.1, 161.1, 158.1, 157.8, 136.9, 132.5, 131.0, 129.9, 128.6, 117.4, 101.7, 20.8. HR-MS analysis: calculated for $C_{14}H_{11}N_3O_4$: 285.08; found: 286.08318 [M+H$^+$].

***N*-(4-fluorophenyl)-5-(2-(*p*-tolylamino)thiazol-4-yl)isoxazole-3-carboxamide (4)**

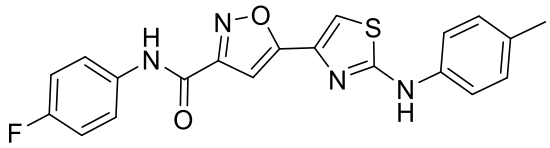

Starting from **3a** (50 mg, 0.17 mmol) and 4-fluoroaniline, the title compound was obtained as a pale yellow powder following the **general method A** (yield: 30 mg, 46%).^{1}H-NMR (400 MHz, DMSO-d_6) δ: 10.82 (1H, s), 10.40 (1H, s), 7.84 (2H, dd, *J*=5.2, 9.0 Hz), 7.68 (1H, s), 7.58 (2H, d, *J*=8.4 Hz), 7.24 - 7.17 (5H, m), 2.28 (3H, s); ^{13}C-NMR (101 MHz, DMSO-d_6) δ: 166.9, 165.0, 160.0, 159.2 (d, J_1=241.3Hz), 157.5, 138.8, 138.3, 134.9 (d, J_4=2.5 Hz), 131.3, 130.0, 123.0 (d, J_3= 7.9 Hz), 117.9, 115.9 (d, J_2= 22.4 Hz), 110.1, 100.7, 20.9. HR-MS analysis: calculated for $C_{20}H_{15}FN_4O_2S$: 394.09; found: 395.09704 [M+H$^+$].

***N*-(3-fluorophenyl)-5-(2-(*p*-tolylamino)thiazol-4-yl)isoxazole-3-carboxamide (5)**

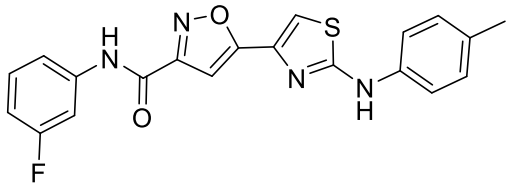

Starting from **3a** (20 mg, 0.07 mmol) and 3-fluoroaniline, the title compound was obtained as a pale yellow powder following the **general method A** (yield: 9 mg, 34%). ^{1}H-NMR (400 MHz, DMSO-d_6) δ: 10.95 (1H, s), 10.38 (1H, s), 7.77 - 7.73 (1H, m), 7.68 (1H, s), 7.65 - 7.63 (1H, m), 7.57 (2H, d, *J*=8.4 Hz), 7.46-7.40 (1H, m), 7.20 (1H, s), 7.17 (2H, d, *J*=8.4 Hz), 7.03 - 6.98 (1H, m), 2.28 (3H, s); HR-MS analysis: calculated for $C_{20}H_{15}FN_4O_2S$: 394.09; found: 395.09785 [M+H$^+$].

5-(2-((3,5-dichlorophenyl)amino)thiazol-4-yl)-N-(pyridin-2-yl)isoxazole-3-carboxamide (6)

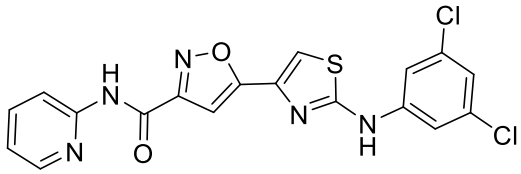

Starting from **3b** (150 mg, 0.42 mmol) and 2-aminopyridine, the title compound was obtained following the **general method A** (yield 50 mg, 27%; white powder). ^{1}H-NMR (400 MHz, DMSO-d_6) δ: 10.90 (1H, s), 10.82 (1H, s), 8.43 (1H, dd, *J*=1.0, 4.8 Hz), 8.16 - 8.12 (1H, m), 7.94 - 7.88 (1H, m), 7.84 (1H, s), 7.79 (2H, d, *J*=1.8 Hz), 7.28 (1H, s), 7.24 (1H, ddd, *J*=1.0, 4.8, 7.3 Hz), 7.20 (1H, t, *J*=1.8 Hz); ^{13}C-NMR (101MHz, DMSO-d_6) δ: 167.1, 164.1, 163.1, 159.8, 157.5, 150.7, 146.6, 142.9, 138.4, 138.3, 121.3, 116.2, 111.8, 100.9, 100.5 , 97.2. HR-MS analysis: calculated for $C_{18}H_{11}Cl_2N_5O_2S$: 431.00; found: 432.00750 [M+H$^+$].

5-(2-((3,5-dichlorophenyl)amino)thiazol-4-yl)-N-phenylisoxazole-3-carboxamide (7)

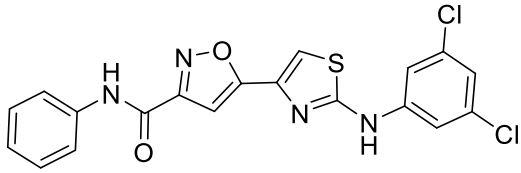

Starting from **3b** (85mg, 0.24 mmol) and aniline, the title compound was obtained as a white powder following the **general method A** (yield: 47 mg, 46%). ^{1}H-NMR (400 MHz, DMSO-d_6) δ: 10.88 (1H, s), 10.74 (1H, s), 7.85 (1H, s), 7.83 - 7.79 (2H, m), 7.78 (2H, d, *J*=1.8 Hz), 7.39 (2H, t, *J*=7.9 Hz), 7.20 - 7.15 (3H, m); ^{13}C-NMR (101MHz, DMSO-d_6) δ: 166.5, 163.9, 160.1, 157.5, 143.2, 138.5, 138.3, 134.8, 129.2, 124.9, 121.1, 115.6, 112.0, 100.9. HR-MS analysis: calculated for $C_{19}H_{12}Cl_2N_4O_2S$: 430.01; found: 431.01309 [M+H$^+$].

***N*-(2-chloro-4-methylphenyl)-5-(2-(*p*-tolylamino)thiazol-4-yl)isoxazole-3-carboxamide (8)**

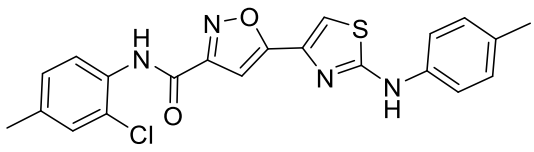

Starting from **3a** (30 mg, 0.10 mmol) and 2-chloro-4-methylaniline, the title compound was obtained as a white powder following the **general method A** (yield: 8.5 mg, 20%). ^{1}H-NMR (400 MHz, DMSO-d_6) δ: 10.27 (1H, s), 10.12 (1H, s), 7.64 (1H, s), 7.60 (1H, d, *J*=8.1 Hz), 7.57 (2H, d, *J*=8.6 Hz), 7.42 - 7.40 (1H, m), 7.24 - 7.21 (1H, m), 7.17 (2H, d, *J*=8.6 Hz), 7.15 (1H, s), 2.35 (3H, s), 2.28 (3H, s); ^{13}C-NMR (101MHz, DMSO-d_6) δ: 167.3, 164.7, 160.1, 158.3, 140.5, 138.5, 135.4, 131.7, 130.4, 129.8, 127.3, 122.9, 117.9, 110.9, 101.0, 20.8. HR-MS analysis: calculated for $C_{21}H_{17}ClN_4O_2S$: 424.08; found: 425.08273 [M+H$^+$].

***N*-(2,4-dimethylphenyl)-5-(2-(*p*-tolylamino)thiazol-4-yl)isoxazole-3-carboxamide (9)**

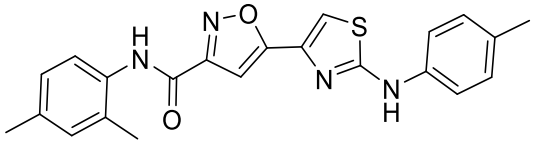

Starting from **3a** (30 mg, 0.10 mmol) and 2,4-dimethylaniline, the title compound was obtained as an orange powder following the **general method A** (yield: 30 mg, 74%).^{1}H-NMR (400 MHz, DMSO-d_6) δ: 10.37 (1H, s), 10.17 (1H, s), 7.66 (1H, s), 7.57 (2H, d, *J*=8.3 Hz), 7.25 (1H, d, *J*=8.1 Hz), 7.17 (2H, d, *J*=8.3 Hz), 7.16 (1H, s), 7.12 - 7.10 (1H, m), 7.06 - 7.03 (1H, m), 2.31 (3H, s), 2.28 (3H, s), 2.22 (3H, s); ^{13}C-NMR (101MHz, DMSO-d_6) δ: 166.3, 164.8, 159.3, 158.2, 138.2, 143.5, 140.0, 138.8, 134.2, 131.7, 131.2, ,130.0, 126.3, 117.8, 114.6, 110.7, 100.8, 21.6 20.9, 17.8. HR-MS analysis: calculated for $C_{22}H_{20}N_4O_2S$: 404.13; found: 405.13729 [M+H$^+$].

***N*-(4-methylpyridin-2-yl)-5-(2-(*p*-tolylamino)thiazol-4-yl)isoxazole-3-carboxamide (10)**

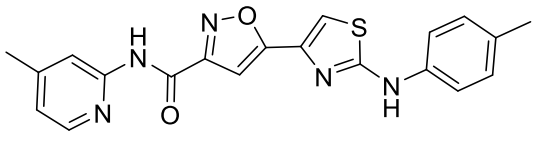

Starting from **3a** (30mg, 0.10 mmol) and 2-amino-4-methylpyridine, the title compound was obtained as a white powder following the **general method A** (yield: 7 mg, 18%). ^{1}H-NMR (400 MHz, DMSO-d_6) δ: 10.67 (1H, s), 10.37 (1H, s), 8.28 (1H, d, *J*=5.0 Hz), 7.99 (1H, s), 7.66 (1H, s), 7.58 (2H, d, *J*=8.4 Hz), 7.28 (1H, s), 7.18 (2H, d, *J*=8.4 Hz), 7.10 - 7.07

(1H, m), 2.39 (3H, s), 2.28 (3H, s); ^{13}C-NMR (101MHz, DMSO-d_6) δ: 167.0, 165.0, 159.6, 158.0, 151.4, 149.7, 148.3, 138.8, 138.4, 131.2, 130.0, 122.1, 117.9, 115.7, 110.1, 100.6, 21.4, 20.9. HR-MS analysis: calculated for $C_{20}H_{17}N_5O_2S$: 391.11; found: 392.11647 [M+H$^+$].

N-(pyridin-4-yl)-5-(2-(*p*-tolylamino)thiazol-4-yl)isoxazole-3-carboxamide (11)

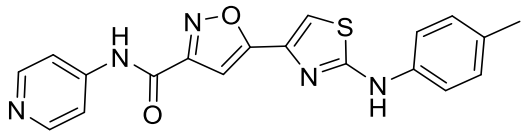

Starting from **3a** (30 mg, 0.10 mmol) and 4-aminopyridine, the title compound was obtained as a pale yellow powder following the **general method A** (yield: 27mg, 72%).^{1}H-NMR (400 MHz, DMSO-d_6) δ: 11.15 (1H, s), 10.41 (1H, s), 8.53 (2H, dd, *J*=1.6, 4.7 Hz), 7.83 (2H, dd, *J*=1.6, 4.7 Hz), 7.70 (1H, s), 7.58 (2H, d, *J*=8.5 Hz), 7.23 (1H, s), 7.18 (2H, d, *J*=8.5 Hz), 2.28 (3H, s); ^{13}C-NMR (101MHz, DMSO-d_6) δ: 167.1, 165.0, 159.6, 158.5, 151.0, 145.4, 138.7, 138.2, 131.3, 130.0, 117.9, 114.8, 110.3, 100.8, 20.9. HR-MS analysis: calculated for $C_{19}H_{15}N_5O_2S$: 377.09; found: 378.10092 [M+H$^+$].

***N*-(pyridazin-4-yl)-5-(2-(*p*-tolylamino)thiazol-4-yl)isoxazole-3-carboxamide (12)**

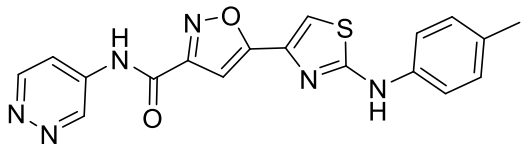

Starting from **3a** (30 mg, 0.10 mmol) and 4-amino-pyridazine, the title compound was obtained as a yellow powder following the **general method A** (yield: 16 mg, 42%). ^{1}H-NMR (400 MHz, DMSO-d_6) δ: 11.43 (1H, s), 10.41 (1H, s), 9.59 (1H, dd, *J*=0.8, 2.7 Hz), 9.14 (1H, dd, *J*=0.8, 5.9 Hz), 8.14 (1H, dd, *J*=2.7, 5.9 Hz), 7.71 (1H, s), 7.57 (2H, d, *J*=8.4 Hz), 7.24 (1H, s), 7.17 (2H, d, *J*=8.4 Hz), 2.26 (3H, s); ^{13}C-NMR (101MHz, DMSO-d_6) δ: 166.6, 164.8, 150.3, 159.4, 158.4, 145.1, 138.2, 140.0, 139.1, 138.8, 130.0, 117.8, 114.9, 110.7, 100.8, 20.9. HR-MS analysis: calculated for $C_{18}H_{14}N_6O_2S$: 378.09; found: 379.09650 [M+H$^+$].

***N*-(thiazol-2-yl)-5-(2-(*p*-tolylamino)thiazol-4-yl)isoxazole-3-carboxamide (13)**

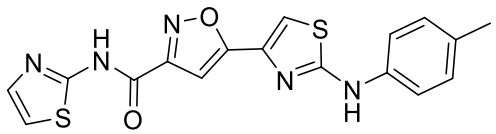

Starting from **3a** (30 mg, 0.10 mmol) and 2-aminothiazole, the title compound was obtained as a yellow powder following the **general method A** (yield: 23mg, 60%). ^{1}H-NMR (400 MHz, DMSO-d_6) δ: 13.08 (1H, s), 10.38 (1H, s), 7.66 (1H, s), 7.59 (1H, s), 7.58 (2H, d, *J*=8.2 Hz), 7.35 - 7.33 (2H, m), 7.17 (2H, d, *J*=8.2 Hz), 2.27 (3H, s); ^{13}C-NMR (101MHz, DMSO-d_6) δ: 167.0, 165.0, 158.8, 158.2, 138.8, 138.3, 131.2, 130.0, 117.9, 115.0, 110.1, 100.8, 20.9. HR-MS analysis: calculated for $C_{17}H_{13}N_5O_2S_2$: 383.05; found: 384.05920 [M+H$^+$].

***N*-(4-chlorophenyl)-5-(2-(*p*-tolylamino)thiazol-4-yl)isoxazole-3-carboxamide (14)**

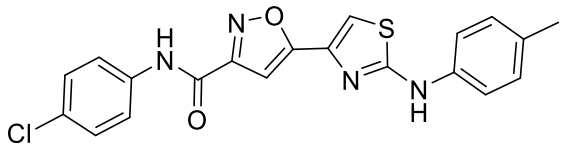

Starting from **3a** (30 mg, 0.10 mmol) and 4-chloroaniline, the title compound was obtained as a pale yellow powder following the **general method A** (yield: 25mg, 61%). ^{1}H-NMR (400 MHz, DMSO-d_6) δ: 10.90 (1H, s), 10.39 (1H, s), 7.85 (2H, d, *J*=8.9 Hz), 7.68 (1H, s), 7.57 (2H, d, *J*=8.4 Hz), 7.45 (2H, d, *J*=8.9 Hz), 7.19 (1H, s), 7.17 (2H, d, *J*=8.4 Hz), 2.27 (3H, s); ^{13}C-NMR (101MHz, DMSO-d_6) δ: 167.0, 165.0, 159.9, 157.6, 138.8, 138.3, 137.5, 131.3, 130.0, 129.2, 128.6, 122.6, 117.9, 110.2, 100.8, 20.9. HR-MS analysis: calculated for: $C_{20}H_{15}ClN_4O_2S$: 410.06; found: 411.06770 [M+H$^+$].

***N*-(3,5-dimethylphenyl)-5-(2-(*p*-tolylamino)thiazol-4-yl)isoxazole-3-carboxamide (15)**

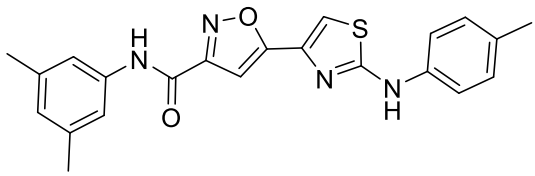

Starting from **3a** (30 mg, 0.10 mmol) and 3,5-dimethylaniline, the title compound was obtained as a white powder following the **general method A** (yield: 30 mg, 74%). ^{1}H-

NMR (400 MHz, DMSO-d_6) δ: 10.52 (1H, s), 10.37 (1H, s), 7.66 (1H, s), 7.58 (2H, d, *J*=8.4 Hz), 7.43 (2H, s), 7.18 (2H, d, *J*=8.4 Hz), 7.16 (1H, s), 6.81 (1H, s), 2.29 (9H, s); ^{13}C-NMR (101MHz, DMSO-d_6) δ: 166.8, 165.1, 160.1, 157.4, 138.8, 138.4, 138.3, 138.2, 131.3, 130.0, 126.5, 118.9, 117.9, 110.0, 100.7, 21.6, 20.9. HR-MS analysis: calculated for $C_{22}H_{20}N_4O_2S$: 404.13; found: 405.13773 [M+H$^+$].

***N*-(pyridin-3-yl)-5-(2-(*p*-tolylamino)thiazol-4-yl)isoxazole-3-carboxamide (16)**

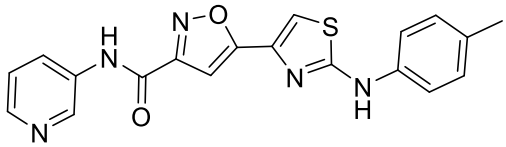

Starting from **3a** (30 mg, 0.10 mmol) and 3-aminopyridine, the title compound was obtained as a white powder following the **general method A** (yield: 10 mg, 27%). ^{1}H-NMR (400 MHz, DMSO-d_6) δ: 11.03 (1H, s), 10.39 (1H, s), 8.97 (1H, s), 8.38 (1H, d, *J*=4.8 Hz), 8.22 (1H, d, *J*=8.1 Hz), 7.70 (1H, s), 7.58 (2H, d, *J*=8.4 Hz), 7.45 (1H, dd, *J*=4.8, 8.1 Hz), 7.22 (1H, s), 7.18 (2H, d, *J*=8.4 Hz), 2.28 (3H, s); ^{13}C-NMR (101MHz, DMSO-d_6) δ: 167.1, 165.0, 159.7, 158.0, 145.8, 142.7, 138.8, 138.3, 135.2, 131.3, 130.0, 128.2, 124.1, 117.9, 110.2, 100.8, 20.9. HR-MS analysis: calculated for $C_{19}H_{15}N_5O_2S$: 377.09; found: 378.10112 [M+H$^+$].

***N*-(*p*-tolyl)-5-(2-(*p*-tolylamino)thiazol-4-yl)isoxazole-3-carboxamide (17)**

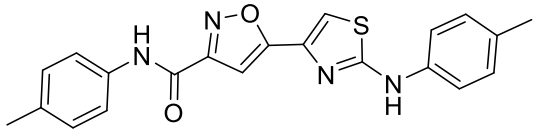

Starting from **3a** (30 mg, 0.10 mmol) and *p*-toluidine, the title compound was obtained as a pale yellow powder following the **general method A** (yield: 19 mg, 49%). ^{1}H-NMR (400 MHz, DMSO-d_6) δ: 10.67 (1H, s), 10.40 (1H, s), 7.69 (2H, d, *J*=8.4 Hz), 7.66 (1H, s), 7.58 (2H, d, *J*=8.4 Hz), 7.21 - 7.15 (5H, m), 2.30 (3H, s), 2.27 (3H, s); ^{13}C-NMR (101MHz, DMSO-d_6) δ: 166.8, 165.0, 160.1, 157.4, 138.8, 138.3, 136.0, 134.0, 131.3, 130.0, 129.6, 121.1, 117.9, 110.0, 100.7, 21.0, 20.9. HR-MS analysis: calculated for $C_{21}H_{18}N_4O_2S$: 390.12; found: 391.12298 [M+H$^+$].

***N*-(m-tolyl)-5-(2-(*p*-tolylamino)thiazol-4-yl)isoxazole-3-carboxamide (18)**

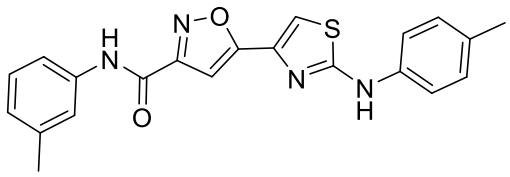

Starting from **3a** (30 mg, 0.10 mmol) and m-toluidine, the title compound was obtained as pale yellow powder following the **general method A** (yield: 19 mg, 49%). ^{1}H-NMR (400 MHz, DMSO-d_6) δ: 10.65 (1H, s), 10.40 (1H, s), 7.68 (1H, s), 7.66 - 7.57 (4H, m), 7.28 (1H, t, *J*=7.8 Hz), 7.20 - 7.15 (3H, m), 6.99 (1H, d, *J*=7.8 Hz), 2.33 (3H, s), 2.28 (3H, s); ^{13}C-NMR (101MHz, DMSO-d_6) δ: 166.9, 165.0, 160.1, 157.5, 138.8, 138.4, 138.3, 131.3, 130.0, 129.1, 125.6, 121.6, 118.3, 117.9, 110.0, 100.7, 21.7, 20.9. HR-MS analysis: calculated for $C_{21}H_{18}N_4O_2S$: 390.12; found: 391.12149 [M+H$^+$].

***N*-(o-tolyl)-5-(2-(*p*-tolylamino)thiazol-4-yl)isoxazole-3-carboxamide (19)**

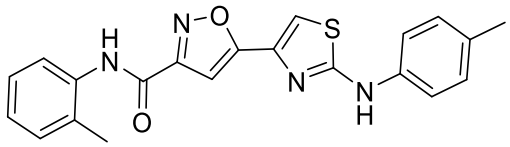

Starting from **3a** (30 mg, 10 mmol) and o-toluidine, the title compound was obtained as a pale yellow powder following the **general method A** (yield: 25 mg, 64%). ^{1}H-NMR (400 MHz, DMSO-d_6) δ: 10.39 (1H, s), 10.29 (1H, s), 7.68 (1H, s), 7.59 (2H, d, *J*=8.4 Hz), 7.41 - 7.38 (1H, m), 7.32 - 7.29 (1H, m), 7.27 - 7.20 (2H, m), 7.19 - 7.15 (3H, m), 2.28 (3H, s), 2.26 (3H, s); ^{13}C-NMR (101MHz, DMSO-d_6) δ: 166.9, 165.0, 159.8, 157.6, 138.8, 138.4, 135.6, 134.0, 131.2, 130.9, 130.0, 127.0, 126.9, 126.6, 117.9, 110.0, 100.7, 20.9, 18.3. HR-MS analysis: calculated for $C_{21}H_{18}N_4O_2S$: 390.12; found: 391.12263 [M+H$^+$].

5-(2-(*p*-tolylamino)thiazol-4-yl)-N-(3-(trifluoromethyl)phenyl)isoxazole-3-carboxamide (20)

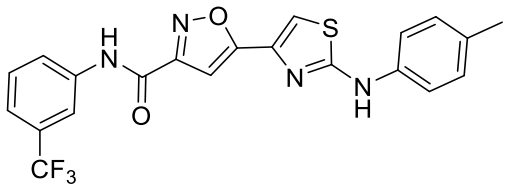

Starting from **3a** (30 mg, 0.0996 mmol) and 3-(trifluoromethyl)aniline, the title compound was obtained as a pale yellow powder following the **general method A** (yield: 18 mg, 41%). ^{1}H-NMR (400 MHz, DMSO-d_6) δ: 11.09 (1H, s), 10.39 (1H, s), 8.28 (1H, s), 8.10 (1H, d, *J*=8.1 Hz), 7.70 (1H, s), 7.65 (1H, t, *J*=8.1 Hz), 7.58 (2H, d, *J*=8.4 Hz), 7.53 (1H, d, *J*=8.1 Hz), 7.22 (1H, s), 7.18 (2H, d, *J*=8.4 Hz), 2.29 (3H, s); ^{13}C-NMR (101MHz, DMSO-d_6) δ: 167.1, 165.1, 159.8, 158.0, 139.3, 138.8, 138.3, 131.3, 130.5, 130.0, 125.9, 124.7, 121.3, 117.9, 117.2, 110.2, 100.8, 20.9. HR-MS analysis: calculated for $C_{21}H_{15}F_3N_4O_2S$: 444.09; found: 445.09304 [M+H$^+$].

***N*-(3-ethoxyphenyl)-5-(2-(*p*-tolylamino)thiazol-4-yl)isoxazole-3-carboxamide (21)**

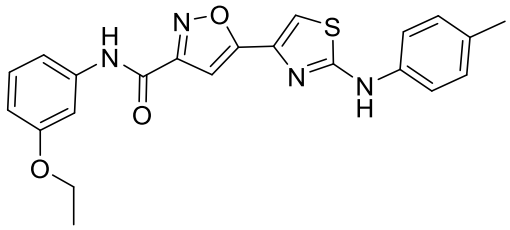

Starting from **3a** (30 mg, 0.10 mmol) and 3-ethoxyaniline, the title compound was obtained as a pale yellow powder following the **general method A** (yield: 18 mg, 43%). ^{1}H-NMR (400 MHz, DMSO-d_6) δ: 10.70 (1H, s), 10.39 (1H, s), 7.68 (1H, s), 7.58 (2H, d, *J*=8.4 Hz), 7.47 (1H, t, *J*=2.2 Hz), 7.41 - 7.38 (1H, m), 7.27 (1H, t, *J*=8.2 Hz), 7.18 (1H, s), 7.18 (2H, d, *J*=8.4 Hz), 6.75 - 6.71 (1H, m), 4.03 (2H, q, *J*=7.0 Hz), 2.29 (3H, s), 1.35 (3H, t, *J*=7.0 Hz); ^{13}C-NMR (101MHz, DMSO-d_6) δ: 166.9, 165.1, 160.1, 159.2, 157.5, 139.6, 138.8, 138.3, 131.3, 130.0, 130.0, 117.9, 113.2, 110.9, 110.1, 107.3, 100.7, 63.5, 20.9, 15.1. HR-MS analysis: calculated for $C_{22}H_{20}N_4O_3S$: 420.13; found: 421.13205 [M+H$^+$].

***N*-(3-methylpyridin-2-yl)-5-(2-(*p*-tolylamino)thiazol-4-yl)isoxazole-3-carboxamide (22)**

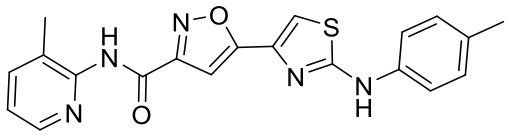

Starting from **3a** (60 mg, 0.20 mmol) and 2-amino-3-methylpyridine, the title compound was obtained as a pale yellow powder following the **general method A**

(yield: 16 mg, 21%). ^{1}H-NMR (400 MHz, DMSO-d_6) 10.85 (1H, s), 10.38 (1H, s), 8.35 (1H, dd, *J*=1.1, 4.7 Hz), 7.77 (1H, dd, *J*=1.1, 7.5 Hz), 7.67 (1H, s), 7.58 (2H, d, *J*=8.4 Hz), 7.32 (1H, dd, *J*=4.7, 7.5 Hz), 7.21 (1H, s), 7.17 (2H, d, *J*=8.4 Hz), 2.27 (3H, s), 2.26 (3H, s); ^{13}C-NMR (101MHz, DMSO-d_6) δ: 167.0, 165.0, 159.5, 157.8, 149.4, 146.7, 140.0, 138.8, 138.4, 131.2, 130.3, 130.0, 123.2, 117.9, 110.1, 100.7, 20.9, 17.8. HR-MS analysis: calculated for $C_{20}H_{17}N_5O_2S$: 391.11; found: 392.11670 [M+H$^+$].

***N*-(2-fluorophenyl)-5-(2-(*p*-tolylamino)thiazol-4-yl)isoxazole-3-carboxamide (23)**

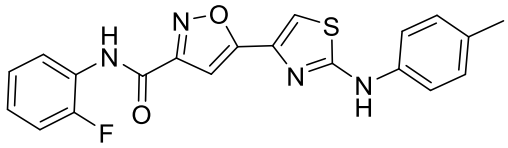

Starting from **3a** (30 mg, 0.10 mmol) and 2-fluoroaniline, the title compound was obtained as a white powder following the **general method A** (yield: 15 mg, 38%). ^{1}H-NMR (400 MHz, DMSO-d_6) δ: 10.35 (1H, s), 10.28 (1H, s), 7.68 (1H, dd, *J*=7.4, 8.2 Hz), 7.65 (1H, s), 7.57 (2H, d, *J*=8.4 Hz), 7.35 - 7.30 (2H, m), 7.28 - 7.23 (1H, m), 7.18 (2H, d, *J*=8.4 Hz), 7.16 (1H, s), 2.28 (3H, s); ^{13}C-NMR (101MHz, DMSO-d_6) δ: 167.1, 165.0, 159.4, 157.7, 156.2 (d, *J*=247.9 Hz), 138.8, 138.3, 131.3, 130.0, 128.2 (d, *J*=7.4 Hz), 127.5, 125.0, 124.9 (d, *J*=14.9 Hz), 117.9, 116.4 (d, *J*=19.7 Hz), 110.2, 100.7, 40.0, 20.9. HR-MS analysis: calculated for $C_{20}H_{15}FN_4O_2S$: 394.09; found: 395.09637 [M+H$^+$].

Pyrrolidin-1-yl(5-(2-(*p*-tolylamino)thiazol-4-yl)isoxazol-3-yl)methanone (24)

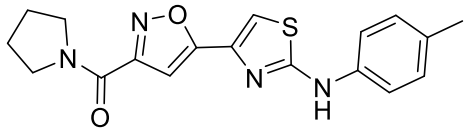

Starting from **3a** (30 mg, 0.10 mmol) and pyrrolidine, the title compound was obtained as a white powder following the **general method A** (yield: 15 mg, 42%). ^{1}H-NMR (400 MHz, DMSO-d_6) δ: 10.37 (1H, s), 7.63 (1H, s), 7.57 (2H, d, *J*=8.4 Hz), 7.16 (2H, d, *J*=8.4 Hz), 6.99 (1H, s), 3.71 (2H, t, *J*=6.6 Hz), 3.52 (2H, t, *J*=6.6 Hz), 2.27 (3H, s), 1.94 - 1.86 (4H, m); ^{13}C-NMR (101MHz, DMSO-d_6) δ: 166.3, 164.8, 159.3, 158.2, 138.2, 140.0, 138.8, 130.0, 117.8, 110.7, 100.8, 47.5, 25.6, 20.9. HR-MS analysis: calculated for $C_{18}H_{18}N_4O_2S$: 354.12; found: 355.12140 [M+H$^+$].

***N*-(5-methylthiazol-2-yl)-5-(2-(*p*-tolylamino)thiazol-4-yl)isoxazole-3-carboxamide (25)**

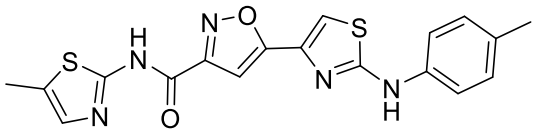

Starting from **3a** (30 mg, 0.10 mmol) and 2-amino-5-methylthiazole, the title compound was obtained as a pale yellow powder following the **general method A** (yield: 15 mg, 38%). ^{1}H-NMR (400 MHz, DMSO-d_6) δ: 12.89 (1H, s), 10.39 (1H, s), 7.66 (1H, s), 7.59 (2H, d, *J*=8.4 Hz), 7.32 (1H, s), 7.28 (1H, s), 7.18 (2H, d, *J*=8.4 Hz), 2.40 (3H, s), 2.28 (3H, s); ^{13}C-NMR (101MHz, DMSO-d_6) δ: 166.9, 166.6, 165.0, 157.6, 138.8, 138.3, 135.5, 131.2, 130.0, 117.9, 110.0, 100.8, 20.9, 11.7. HR-MS analysis: calculated for $C_{18}H_{15}N_5O_2S_2$: 397.07 found: 398.07301 [M+H$^+$].

N-(thiophen-3-yl)-5-(2-(*p*-tolylamino)thiazol-4-yl)isoxazole-3-carboxamide (26)

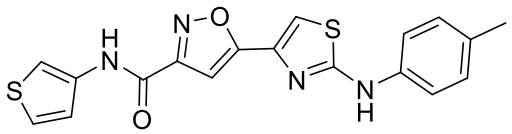

Starting from **3a** (30 mg, 0.10 mmol) and 3-amino-5-thiophene and following the **general method A**, the title compound was obtained as a pale yellow powder following the **general method A** (yield: 16 mg, 42%). ^{1}H-NMR (400 MHz, DMSO-d_6) δ: 11.23 (1H, s), 10.39 (1H, s), 7.79 (1H, dd, *J*=1.3, 3.2 Hz), 7.68 (1H, s), 7.58 (2H, d, *J*=8.4 Hz), 7.53 (1H, dd, *J*=3.2, 5.2 Hz), 7.38 (1H, dd, *J*=1.3, 5.2 Hz), 7.18 (1H, s), 7.18 (2H, d, *J*=8.4 Hz), 2.27 (3H, s); ^{13}C-NMR (101MHz, DMSO-d_6) δ: 167.0, 165.0, 159.7, 156.6, 138.8, 138.3, 136.3, 131.3, 130.0, 125.4, 122.6, 117.9, 111.3, 110.1, 100.7, 20.9. HR-MS analysis: calculated for $C_{18}H_{14}N_4O_2S_2$: 382.06; found: 383.06242 [M+H$^+$].

N-(thiophen-2-ylmethyl)-5-(2-(*p*-tolylamino)thiazol-4-yl)isoxazole-3-carboxamide (27)

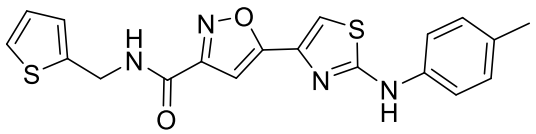

Starting from **3a** (30 mg, 0.10 mmol) and 2-methyl-thiophenamine, the title compound was obtained as a pale yellow powder following the **general method A** (yield: 31 mg, 79%). ^{1}H-NMR (400 MHz, DMSO-d_6) δ: 10.35 (1H, s), 9.45 (1H, t, *J*=6.1 Hz), 7.63 (1H, s), 7.56 (2H, d, *J*=8.5 Hz), 7.41 (1H, dd, *J*=1.3, 5.1 Hz), 7.17 (2H, d, *J*=8.5 Hz), 7.07 (1H, s), 7.05 (1H, dd, *J*=1.0, 3.5 Hz), 6.98 (1H, dd, *J*=3.4, 5.0 Hz), 4.64 (2H, d, *J*=5.7 Hz), 2.27 (3H, s); ^{13}C-NMR (101MHz, DMSO-d_6) δ: 166.9, 165.0, 159.5, 158.7, 142.0, 138.8, 138.4, 131.2, 129.9, 127.2, 126.4, 125.7, 117.9, 109.9, 100.4, 37.9, 20.9. HR-MS analysis: calculated for $C_{19}H_{16}N_4O_2S_2$: 396.07; found: 397.07781 [M+H$^+$].

***N*-(6-methylpyridin-2-yl)-5-(2-(*p*-tolylamino)thiazol-4-yl)isoxazole-3-carboxamide (28)**

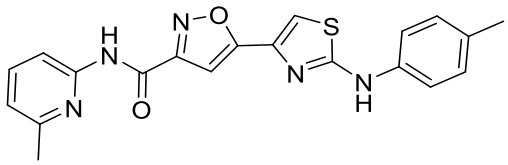

Starting from **3a** (50 mg, 0.17 mmol) and 6-methyl-2-aminopyridine, the title compound was obtained as a pale yellow powder following the **general method A** (yield: 19 mg, 30%). ^{1}H-NMR (400 MHz, DMSO-d_6) δ: 10.69 (s, 1H), 10.39 (s, 1H), 7.97 (d, *J*=8.0 Hz, 1H), 7.78-7.80 (m, 1H), 7.66 (s, 1H), 7.59 (d, *J*=8.4 Hz, 2H), 7.32 (s, 1H), 7.18 (d, J=8.4 Hz, 2H), 7.11 (d, *J*=7.6 Hz, 1H), 2.47 (s, 3H), 2.28 (s, 3H); ^{13}C-NMR (101MHz, DMSO-d_6) δ: 166.9, 164.9, 159.6, 158.0, 157.4, 150.6, 139.2, 138.8, 138.4, 131.2, 130.0, 120.4, 117.8, 112.2, 110.1, 100.6, 24.1, 20.9. HR-MS analysis: calculated for $C_{20}H_{17}N_5O_2S$: 391.11; found: 392.11644 [M+H$^+$].

5-(2-((3,5-difluorophenyl)amino)thiazol-4-yl)-N-(pyridin-2-yl)isoxazole-3-carboxamide (29)

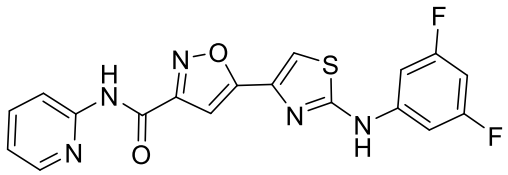

Starting from **3c** (40 mg, 0.12 mmol) and 2-aminopyridine, the title compound was obtained as a white powder following the **general method A** (yield: 8 mg, 17%). ^{1}H-

NMR (400 MHz, DMSO-d_6) δ: 10.94 (1H, s), 10.87 (1H, s), 8.44 (1H, ddd, *J*=1.0, 1.9, 4.8 Hz), 8.15 (1H, d, *J*=8.3 Hz), 7.91 (1H, ddd, *J*=1.9, 7.4, 8.3 Hz), 7.83 (1H, s), 7.44 (2H, dd, *J*=2.3, 9.6 Hz), 7.39 (1H, s), 7.25 (1H, ddd, *J*=1.0, 4.8, 7.4 Hz), 6.84 (1H, tt, *J*=2.3, 9.6 Hz); ^{13}C-NMR (101MHz, DMSO-d_6) δ: 167.1, 164.1, 163.4 (dd, *J*=15.6, 243.1), 159.8, 157.5, 150.7, 146.6, 143.1 (t, *J*=14.2), 138.4, 138.3, 121.3, 116.2, 111.8, 100.9, 100.6 (d, *J*=29.2), 97.0 (d, *J*=24.9). HR-MS analysis: calculated for $C_{18}H_{11}F_2N_5O_2S$: 399.06; found: 400.06818 [M+H$^+$].

5-(2-((3,5-difluorophenyl)amino)thiazol-4-yl)-N-phenylisoxazole-3-carboxamide (30)

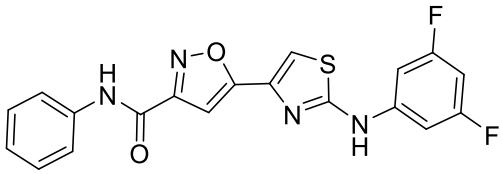

Starting from **3c** (40 mg, 0.12 mmol) and aniline, the title compound was obtained as a white powder following the **general method A** (yield: 30 mg, 63%). ^{1}H-NMR (400 MHz, DMSO-d_6) δ: 10.94 (1H, s), 10.76 (1H, s), 7.84 (1H, s), 7.81 (2H, dd, *J*=1.1, 8.7 Hz), 7.44 (2H, dd, *J*=2.3, 9.6 Hz), 7.42 - 7.37 (2H, m), 7.25 (1H, s), 7.17 (1H, tt, *J*=1.1, 7.4 Hz), 6.83 (1H, tt, *J*=2.3, 9.6 Hz); ^{13}C-NMR (101MHz, DMSO-d_6) δ: 166.5, 164.0, 163.3 (dd, *J*=15.8, 243.0), 160.1, 157.5, 143.3 (t, *J*=14.0), 138.5, 138.3, 129.2, 125.0, 121.1, 111.8, 101.0, 100.5 (d, *J*=29.6), 97.1 (d, *J*=25.0). HR-MS analysis: calculated for $C_{19}H_{12}F_2N_4O_2S$: 398.06; found: 399.07071 [M+H$^+$].

5-(2-((3,5-dimethylphenyl)amino)thiazol-4-yl)-N-(pyridin-2-yl)isoxazole-3-carboxamide (31)

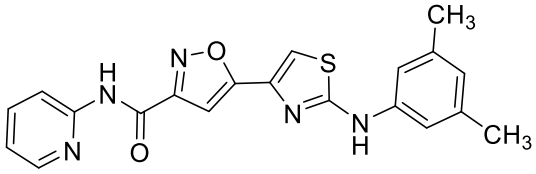

Starting from **3d** (50 mg, 0.16 mmol) and 2-aminopyridine, the title compound was obtained as a white powder following the **general method A** (yield: 15 mg, 18%). ^{1}H-NMR (400 MHz, DMSO-d_6) δ: 10.83 (1H, s), 10.36 (1H, s), 8.43 (1H, ddd, *J*=0.8, 1.9, 4.9 Hz), 8.14 (1H, d, *J*=7.9 Hz), 7.91 (1H, dt, *J*=1.9, 7.9 Hz), 7.69 (1H, s), 7.30 (2H, s), 7.27 -

7.23 (2H, m), 6.67 (1H, s), 2.30 (6H, s); ^{13}C-NMR (101MHz, DMSO-d_6) δ: 167.2, 165.0, 160.2, 157.6, 150.5, 147.1, 141.1, 140.8, 138.6, 121.4, 121.0, 118.8, 116.0, 110.2, 100.7, 21.7. HR-MS analysis: calculated for $C_{20}H_{17}N_5O_2S$: 391.11; found: 392.11823 [M+H$^+$].

5-(2-((3,5-dimethylphenyl)amino)thiazol-4-yl)-N-phenylisoxazole-3-carboxamide (32)

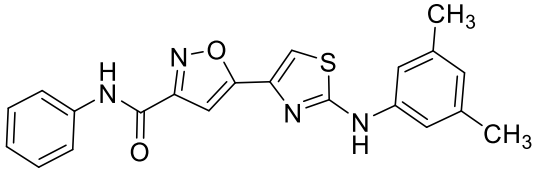

Starting from **3d** (40 mg, 0.13 mmol) and aniline, the title compound was obtained as a white powder following the **general method A** (yield: 32 mg, 65%). ^{1}H-NMR (400 MHz, DMSO-d_6) δ: 10.75 (1H, s), 10.36 (1H, s), 7.81 (2H, d, *J*=7.9 Hz), 7.70 (1H, s), 7.39 (2H, t, *J*=7.9 Hz), 7.29 (2H, s), 7.18 - 7.14 (2H, m), 6.68 (1H, s), 2.29 (6H, s); ^{13}C-NMR (101MHz, DMSO-d_6) δ: 166.8, 165.0, 160.1, 157.6, 141.1, 138.6, 138.5, 138.3, 129.2, 124.9, 124.1, 121.0, 115.6, 110.2, 100.7, 21.7. HR-MS analysis: calculated for $C_{21}H_{18}N_4O_2S$: 390.12; found: 391.12115 [M+H$^+$].

***N*-phenyl-5-(2-(*p*-tolylamino)oxazol-4-yl)isoxazole-3-carboxamide (33)**

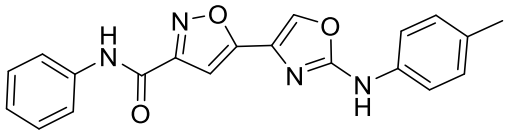

Starting from **3f** (42 mg, 0.15 mmol) and aniline, the title compound was obtained as a white powder following the **general method A** (yield: 30 mg, 57%). ^{1}H-NMR (400 MHz, DMSO-d_6) δ: 10.73 (1H, s), 10.35 (1H, s), 8.44 (1H, s), 7.81 (2H, d, *J*=8.6 Hz), 7.56 (2H, d, *J*=8.5 Hz), 7.39 (2H, t, *J*=7.9 Hz), 7.19 - 7.14 (4H, m), 2.28 (3H, s); ^{13}C-NMR (101MHz, DMSO-d_6) δ: 164.8, 159.9, 158.1, 157.4, 138.5, 136.9, 132.5, 131.0, 129.9, 129.2, 128.6, 124.9, 121.1, 117.4, 101.0, 20.8. HR-MS analysis: calculated for $C_{20}H_{16}N_4O_3$: 360.12; found: 361.13019 [M+H$^+$].

***N*-(pyridin-2-yl)-5-(2-(*p*-tolylamino)oxazol-4-yl)isoxazole-3-carboxamide (34)**

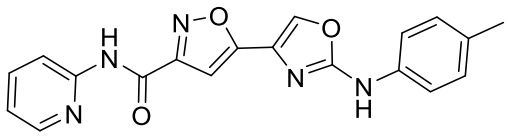

Starting from **3f** (70 mg, 0.24 mmol) and 2-aminopyridine, the title compound was obtained as a white powder following the **general method A** (yield: 15 mg, 17%). ^{1}H-NMR (400 MHz, DMSO-d_6) δ: 10.85 (1H, s), 10.36 (1H, s), 8.45 - 8.42 (2H, m), 8.14 (1H, d, *J*=8.3 Hz), 7.90 (1H, dt, *J*=1.8, 7.7 Hz), 7.56 (2H, d, *J*=8.4 Hz), 7.31 (1H, s), 7.24 (1H, ddd, *J*=0.9, 4.9, 7.7 Hz), 7.17 (2H, d, *J*=8.4 Hz), 2.28 (3H, s); ^{13}C-NMR (101MHz, DMSO-d_6) δ: 164.9, 159.4, 158.1, 157.9, 151.3, 148.8, 138.9, 136.9, 132.5, 131.0, 129.9, 128.6, 121.1, 117.4, 115.4, 100.9, 20.8. HR-MS analysis: calculated for $C_{19}H_{15}N_5O_3$: 361.12; found: 361.12918 [M+H$^+$].

***N*-(2-hydroxyphenyl)-5-(2-(*p*-tolylamino)thiazol-4-yl)isoxazole-3-carboxamide (35)**

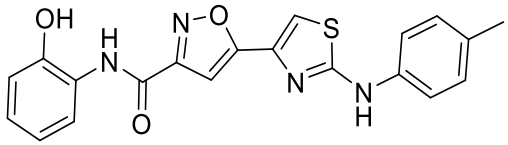

Compound **3a** (30 mg, 0.10 mmol, 1 eq.) and 2-aminophenol were reacted following the **general method B**. The crude was purified by flash column chromatography eluting from 0% to 0.5% v/v MeOH in DCM and the desired compound was obtained as a white powder (yield: 8 mg, 20%). ^{1}H-NMR (400 MHz, DMSO-d_6) δ: 10.40 (1H, s), 10.17 (1H, s), 9.51 (1H, s), 7.97 (1H, d, *J*=8.1 Hz), 7.70 (1H, s), 7.59-7.57 (2H, m), 7.20-7.17 (3H, m), 7.07-6.85 (3H, m), 2.28 (3H, s). ^{13}C-NMR (101MHz, DMSO-d_6) δ: 167.5, 165.1, 159.8, 156.8, 148.5, 138.8, 138.4, 131.4, 130.1, 126.1,125.6, 122.5, 119.8, 118.0, 115.9, 110.4, 100.6, 20.9. HR-MS analysis: calculated for: $C_{20}H_{16}N_4O_3S$: 392.09; found: 393.10159.

***N*-(3-hydroxyphenyl)-5-(2-(*p*-tolylamino)thiazol-4-yl)isoxazole-3-carboxamide (36)**

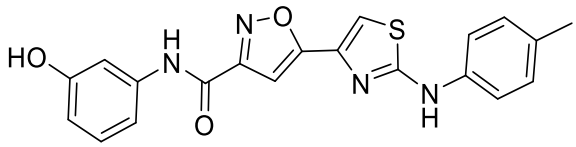

Compound **3a** (30 mg, 0.10 mmol) and 3-aminophenol were reacted following the **general method B**. The crude was purified by flash column chromatography eluting from 0% to 0.5% v/v MeOH in DCM and the desired compound was obtained as a white powder (yield: 11 mg, 28%). ^{1}H-NMR (400 MHz, DMSO-d_6) δ: 10.59 (1H, s), 10.40 (1H, s), 9.51 (1H, s), 7.67 (1H, s), 7.59 (2H, d, *J*=8.0 Hz), 7.38 (1H, s), 7.22 - 7.13 (5H, m), 6.57 (1H, d, *J*=8.0 Hz), 2.27 (3H, s); ^{13}C-NMR (101MHz, DMSO-d_6) δ: 166.9, 165.0, 160.2, 158.1, 157.5, 139.6, 138.8, 138.4, 131.3, 130.1, 130.0, 118.0, 112.1, 111.9, 110.1, 108.2, 100.9, 20.9. HR-MS analysis: calculated for $C_{20}H_{16}N_4O_3S$: 392.09; found: 393.10159.

***N*-(4-hydroxyphenyl)-5-(2-(*p*-tolylamino)thiazol-4-yl)isoxazole-3-carboxamide (37)**

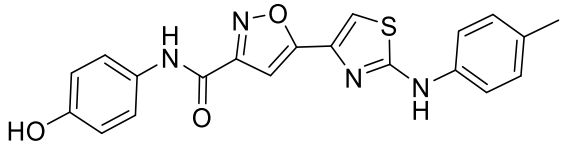

Compound **3a** (30 mg, 0.10 mmol) and 4-aminophenol were reacted following the **general method B**. The crude was purified by flash column chromatography eluting from 0% to 0.5% v/v MeOH in DCM and the desired compound was obtained as a white powder (yield: 4 mg, 10%). ^{1}H-NMR (400 MHz, DMSO-d_6) δ: 10.50 (1H, s), 10.40 (1H, s), 9.38 (1H, s), 7.66 (1H, s), 7.59-7.56 (4H,m), 7.18 (2H, d, *J*=8.4 Hz), 7.15 (1H, s), 6.77 (2H, d, *J*=8.0 Hz), 2.28 (3H, s); ^{13}C-NMR (101MHz, DMSO-d_6) δ: 166.8, 165.0, 160.2, 157.0, 154.8, 138.8, 138.4, 131.3, 130.0, 122.9, 117.9, 115.6, 109.9, 100.7, 20.9 . HR-MS analysis: calculated for: $C_{20}H_{16}N_4O_3S$: 392.09; found: 393.10159.

5-(2-((3-hydroxy-4-methylphenyl)amino)thiazol-4-yl)-N-phenylisoxazole-3-carboxamide (38)

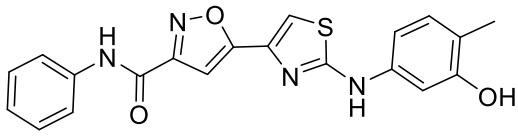

Compound **3e** (24 mg, 0.08 mmol) and aniline were reacted following the **general method B**. The crude was purified by flash column chromatography eluting from 0% to 0.5% v/v MeOH in DCM and the desired compound was obtained as a white powder (yield: 10 mg, 34%). ^{1}H-NMR (400 MHz, DMSO-d_6) δ: 10.80 (1H, s), 10.30 (1H, s), 9.46

(1H, s), 7.82 (2H, d, *J*=8.0 Hz), 7.65 (1H, s), 7.45 (1H, d, *J*=2.0 Hz), 7.39 (2H, t, *J*=8.0 Hz), 7.26 (1H, s), 7.17 (1H, m), 7.00 (1H, d, *J*=8.1 Hz), 6.84 (1H, dd, *J*=2.0, 8.1 Hz), 2.08 (3H, s); ^{13}C-NMR (101MHz, DMSO-d_6) δ: 167.2, 165.0, 160.2, 157.6, 150.5,147.1, 141.1, 140.8, 138.6, 121.4, 121.0, 118.8, 116.0, 110.2, 100.7, 21.7. HR-MS analysis: calculated for: $C_{20}H_{16}N_4O_3S$: 392.09; found: 393.10083.

ethyl 5-acetylisoxazole-3-carboxylate (39)

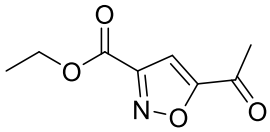

The title compound was synthesized as previously reported.[1] Analytical data matched those reported in literature.

5-acetyl-N-(pyridin-2-yl)isoxazole-3-carboxamide (40)

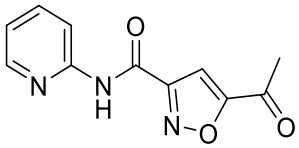

To a solution of compound **39** (350 mg, 1.91 mmol, 1 eq) in absolute EtOH (3 mL), NaOH (pellets) was added (91.5 mg, 3.82 mmol, 2 eq). The reaction was stirred at room temperature for 30 minutes, then the mixture was acidified to pH=1 with 1N aq. HCl. The mixture was extracted with EtOAc (3 x 20 mL) and the organic layers were collected, dried over Na_2SO_4 and evaporated under reduced pressure. The crude obtained was immediately dissolved in dry DMF (3,5 mL) under argon atmosphere. Then, HATU (726 mg, 1.91 mmol, 1 eq) was added and the mixture was left to stir for 10 minutes. 2-aminopyridine (180 mg, 1.91 mmol, 1 eq) and TEA (400 µL, 2.87 mmol, 1.5 eq) were added and the reaction mixture was left to stir at room temperature for 2 h. Then, brine (20 mL) was added and the mixture was extracted with EtOAc (3 x 20 mL). Organic layers were collected, washed with brine (1 x 20 mL), dried over Na_2SO_4 and purified by Combiflash® eluting from 10% to 20% v/v EtOAc in petroleum ether. The title compound was obtained as a white powder (yield: 294 mg, 67%). ^{1}H-NMR (400 MHz, DMSO-d_6) δ: 11.09 (1H, s), 8.43 (1H, ddd, *J*=0.9, 1.9, 4.9 Hz), 8.12 (1H, d, *J*=8.3 Hz), 7.91

(1H, ddd, *J*=1.9, 7.4, 8.3 Hz), 7.87 (1H, s), 7.25 (1H, ddd, *J*=0.9, 4.9, 7.4 Hz), 2.63 (3H, s); ^{13}C-NMR (101MHz, DMSO-d_6) δ: 186.6, 167.1, 159.9, 157.5, 151.2, 148.8, 139.0, 121.2, 115.4, 108.8, 28.0.

5-acetyl-N-phenylisoxazole-3-carboxamide (41)

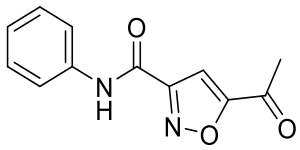

To a solution of compound **39** (472 mg, 2.60 mmol, 1 eq) in absolute EtOH (4 mL), NaOH (pellets) was added (123 mg, 5.15 mmol, 2 eq). The reaction was stirred at room temperature for 30 minutes, then the mixture was acidified to pH=1 with 1N aq. HCl. The aqueous phase was extracted with EtOAc (3 x 20 mL) and the organic layers were collected, dried over Na_2SO_4 and evaporated under reduced pressure. The crude obtained was immediately dissolved in dry DMF (8 mL) under argon atmosphere. Then, HATU (980 mg, 2.58 mmol, 1 eq) was added and the mixture was left to stir for 10 minutes. After this time, aniline (240 mg, 2.58 mmol, 1 eq) and TEA (540 µL, 3.86 mmol, 1.5 eq) were added and the reaction mixture was left to stir at room temperature for 2 h. Then, brine was added and the mixture was extracted with EtOAc (3 x 20 mL). Organic layers were collected, washed with brine (1 x 20 mL), dried over Na_2SO_4 and purified by Combiflash® eluting from 10% to 30% v/v EtOAc in petroleum ether. The title compound was obtained as a white powder (yield: 451 mg, 76%). ^{1}H-NMR (400 MHz, DMSO-d_6) δ: 10.86 (1H, s), 7.80-7.77 (3H, m), 7.39 (2H, t, *J*=7.6), 7.17 (1H, t, *J*=7.6), 2.64 (3H, s); ^{13}C-NMR (101MHz, DMSO-d_6) δ: 186.7, 167.1, 159.7, 151.2, 138.3, 129.3, 125.1, 121.1, 109.0, 28.1.

5-(2-bromoacetyl)-N-(pyridin-2-yl)isoxazole-3-carboxamide (42)

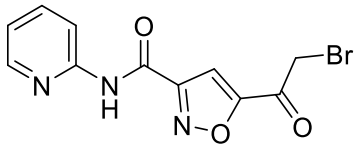

Starting from compound **40** (190 mg, 0.82 mmol, 1 eq), the title compound was obtained as pale yellow powder following the **general method F** (yield: 178 mg, 70%). ^{1}H-NMR (400 MHz, DMSO-d_6) δ: 11.16 (1H, s), 8.44 (1H, ddd, *J*=0.9, 1.9, 4.9 Hz), 8.12 (1H, d, *J*=8.3 Hz), 7.99 (1H, s), 7.91 (1H, ddd, *J*=1.9, 7.4, 8.3 Hz), 7.26 (1H, ddd, *J*=0.9, 4.9, 7.4 Hz), 4.90 (2H, s); ^{13}C-NMR (101MHz, DMSO-d_6) δ: 180.6, 164.7, 159.9, 157.3, 151.2, 148.8, 139.0, 121.3, 115.5, 109.9, 34.1.

5-(2-bromoacetyl)-*N*-phenylisoxazole-3-carboxamide (43)

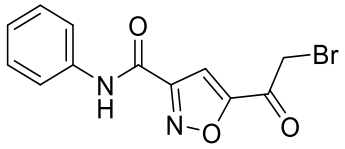

Starting from compound **41** (128 mg, 0.56 mmol, 1 eq) the title compound was obtained as pale yellow powder following the **general method F** (yield: 140 mg, 81%). ^{1}H-NMR (400 MHz, DMSO) δ: 10.93 (1H, s), 7.91 (1H, s), 7.79 (2H, d, *J*=7.8 Hz), 7.39 (2H, t, *J*=7.8 Hz), 7.16-7.18 (1H, m), 4.91 (2H, s). ^{13}C-NMR (101MHz, DMSO-d_6) δ: 180.6, 164.7, 159.9, 151.2, 138.7, 129.8, 125.1, 121.6, 109.9, 34.1.

***N*-(pyridin-2-yl)-5-(2-(*p*-tolylamino)thiazol-4-yl)isoxazole-3-carboxamide (UPAR-453)**

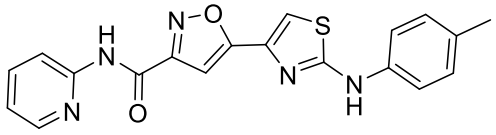

Compound **41** (40 mg, 0.13 mmol, 1 eq) and *p*-tolylthiourea (**a**) were reacted following the **general method D**. The crude was purified by filtration on a silica gel pad eluting with a mixture of 30% v/v EtOAc in hexane and the title compound was obtained as a white powder (yield: 36 mg, 75%). Analytical data matched those reported in literature.[1]

5-(2-((3-hydroxy-4-methylphenyl)amino)thiazol-4-yl)-N-(pyridin-2-yl)isoxazole-3-carboxamide (42e)

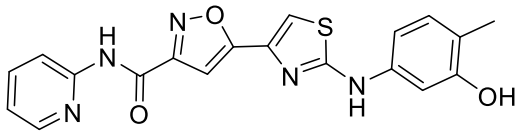

Compound **42** (12 mg, 0.039 mmol) and 3-hydroxy-4-methylphenylthiourea (**e**) were reacted following the **general method E**. After completion, the volatiles were evaporated under reduced pressure and the crude obtained was purified by flash column chromatography eluting from 20% to 40% v/v EtOAc in petroleum ether. The desired compound was obtained as a pale yellow powder (yield: 7 mg, 46%). ^{1}H-NMR (400 MHz, DMSO-d_6) δ: 10.82 (1H, s), 10.30 (1H, s), 9.44 (1H, s), 8.43 (1H, d, *J*=4.5 Hz), 8.14 (1H, d, *J*=8.4 Hz), 7.94 - 7.88 (1H, m), 7.66 (1H, s), 7.42 (1H, d, *J*=1.8 Hz), 7.33 (1H, s), 7.26 - 7.23 (1H, m), 7.00 (1H, d, *J*=8.4 Hz), 6.88 (1H, dd, *J*=1.8, 8.3 Hz), 2.08 (3H, s); ^{13}C-NMR (101MHz, DMSO-d_6) δ: 167.1, 159.6, 158.2, 156.1, 151.3, 148.8, 139.8, 139.0, 138.3, 131.1, 121.2, 117.8, 115.3, 109.9, 108.5, 104.7, 100.8, 16.0. HR-MS analysis: calculated for: $C_{19}H_{15}N_5O_3S$: 393.09; found: 394.09664.

5-(2-((4-(hydroxymethyl)phenyl)amino)thiazol-4-yl)-N-(pyridin-2-yl)isoxazole-3-carboxamide (42h)

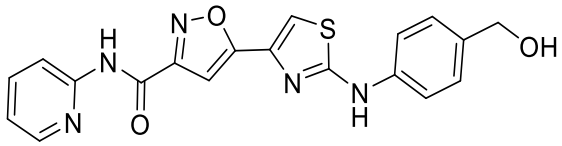

Compound **42** (15 mg, 0.05 mmol) and the thiourea **h** were reacted following the **general method E**. After the completion, as indicated by TLC, the mixture was dried to obtain the O-protected derivative. The crude was dissolved in DMF (0,5 mL) at 0 °C under nitrogen atmosphere, then TBAF on silica gel (0.10 mmol, 2 eq) was added and the mixture was left to stir for 3h. After this time, the reaction was quenched with water and the mixture extracted with EtOAc (3 x 10 mL). Organic layers were collected and dried over Na_2SO_4. The crude was dissolved in Et_2O and the title compound was allowed to precipitate overnight at -20°C (yield: 9 mg, 48%, pale yellow powder). ^{1}H-NMR (600

MHz, DMSO-d_6) δ: 10.78 (s, 1H), 10.41 (s, 1H), 8.39 (ddd, *J*= 4.8, 1.9, 0.9 Hz, 1H), 8.10 (d, *J*=8.3 Hz, 1H), 7.86 (ddd, *J*=8.3, 7.4, 1.9 Hz, 1H), 7.64 (s, 1H), 7.61 (d, *J*=8.3 Hz, 2H), 7.30 – 7.24 (m, 3H), 7.20 (ddd, *J*=7.4, 4.8, 0.9 Hz, 1H), 5.05 (t, *J*=5.7 Hz, 1H), 4.41 (d, *J*=5.7 Hz, 2H). ^{13}C-NMR (150 MHz, DMSO-d_6) δ: 167.0, 164.7, 159.5, 158.2, 151.4, 148.8, 139.7, 139.0, 138.4, 136.5, 128.0, 127.9, 117.5, 115.3, 110.4, 100.9, 63.2. HR-MS analysis: calculated for: $C_{19}H_{15}N_5O_3S$: 393.09; found: 394.09684.

5-(2-((4-(hydroxymethyl)phenyl)amino)thiazol-4-yl)-N-phenylisoxazole-3-carboxamide (43h)

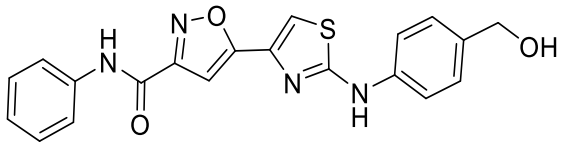

Compound **43** (22 mg, 0.07 mmol, 1eq) and the thiourea **h** were reacted following the **general method E**. After the reaction completion, as indicated by TLC, the mixture was dried to obtain the O-protected derivative. The crude was dissolved in DMF (0,5 mL) at 0 °C under nitrogen atmosphere. Then TBAF on silica gel (0.14 mmol, 2 eq) was added and the mixture was left to stir for 3h. After this time, the reaction was quenched with water and the mixture extracted with EtOAc (3 x 10 mL). Organic layers were collected and dried over Na_2SO_4 and purified by flash column chromatography eluting from 20% to 30 % EtOAc in petroleum ether. The title compound was obtained as a pale yellow powder (yield: 9 mg, 32%). ^{1}H-NMR (300 MHz, DMSO-d_6) δ: 10.76 (1H, s), 10.47 (1H, s), 7.81 (2H, d, *J*=7.9 Hz), 7.69 (1H, s), 7.64 (2H, d, *J*=8.5 Hz), 7.39 (2H, t, *J*=7.9 Hz), 7.31 (2H, d, *J*=8.5 Hz), 7.21 (1H, s), 7.19-7.14 (1H, m), 5.10 (1H, t, *J*=5.7 Hz), 4.46 (2H, d, *J*=5.7 Hz); ^{13}C-NMR (75 MHz, DMSO-d_6) δ: 166.9, 165.0, 160.1, 157.6, 139.9, 138.5, 138.3, 136.5, 129.3, 128.0, 125.0, 121.1, 117.6, 110.3, 100.9, 63.2. HR-MS analysis: calculated for $C_{20}H_{16}N_4O_3S$: 393.10; found: 393.10241.

5-(2-((2-hydroxy-4-methylphenyl)amino)thiazol-4-yl)-N-(pyridin-2-yl)isoxazole-3-carboxamide (42i)

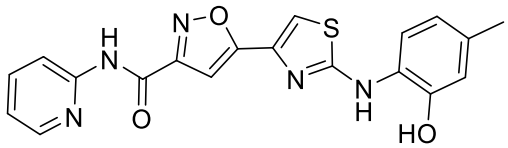

Compound **42** (7 mg, 0.02 mmol) and 1-(2-hydroxy-4-methylphenyl)thiourea (**i**) were reacted following the **general method E**. After reaction completion, the volatiles were evaporated under reduced pressure and the title compound was obtained as a pale yellow powder after recrystallization from EtOH (yield: 4 mg, 45%). ^{1}H-NMR (400 MHz, DMSO-d_6) δ: 10.90 (1H, s), 9.61 (1H, s), 8.43 (1H, d, *J*=4.8 Hz), 8.14 (1H, d, *J*=8.4 Hz), 8.02 (1H, d, *J*=8.0 Hz), 7.93 (1H, dt, *J*=1.7, 8.0 Hz), 7.59 (1H, s), 7.29 - 7.26 (1H, m), 7.25 (1H, s), 6.72 (1H, s), 6.67 (1H, d, *J*=8.4 Hz), 2.22 (3H, s); ^{13}C-NMR (101 MHz, DMSO-d_6) δ: 167.2, 166.5, 159.5, 158.2, 151.2, 148.4, 147.7, 139.3, 138.0, 133.1, 126.6, 121.2, 120.9, 120.2, 116.3, 115.5, 110.4, 100.4, 21.1; HR-MS analysis: calculated for $C_{19}H_{15}N_5O_3S$: 393.09; found: 394.09755.

5-(2-(phenylamino)thiazol-4-yl)-*N*-(pyridin-2-yl)isoxazole-3-carboxamide (42l)

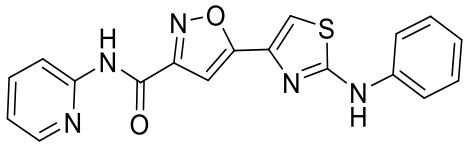

Compound **42** (30 mg, 0.10 mmol, 1 eq) and phenylthiourea (**l**) were reacted following the **general method D**. The title compound precipitated in the reaction mixture and it was obtained as a yellow powder after filtration (yield:18 mg, 51%).^{1}H-NMR (300 MHz, DMSO-d_6) δ: 11.02 (1H, s), 10.52 (1H, s), 8.47 - 8.43 (1H, m), 8.14 (1H, d, *J*=8.5 Hz), 8.01 - 7.94 (1H, m), 7.75 - 7.71 (3H, m), 7.41 - 7.35 (3H, m), 7.30 (1H, ddd, *J*=0.9, 5.0, 7.4 Hz), 7.01 (1H, t, *J*=7.4 Hz); ^{13}C-NMR (150 MHz, DMSO-d_6) δ: 167.2, 164.8, 159.4, 158.4, 150.6, 147.1, 141.3, 140.8, 138.3, 129.6, 122.3, 121.4, 117.7, 116.0, 110.7, 100.9. HR-MS analysis: calculated for $C_{18}H_{13}N_5O_2S$: 363.08; found: 364.08705 [M+H$^+$].

***N*-phenyl-5-(2-(phenylamino)thiazol-4-yl)isoxazole-3-carboxamide (43l)**

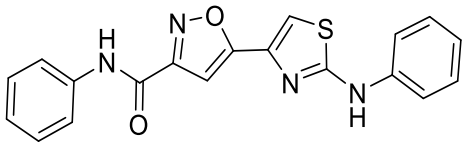

Compound **43** (30 mg, 0.10 mmol, 1 eq) and phenylthiourea (**l**) were reacted following the **general method D**. The title compound precipitated in the reaction mixture and it was obtained as a pale yellow powder after filtration (yield: 9.7 mg, 25%). ^{1}H-NMR (600 MHz, DMSO-d_6) δ: 10.69 (s, 1H), 10.46 (s, 1H), 7.77 (d, *J*=7.6 Hz, 2H), 7.70 – 7.65 (m, 3H), 7.39 – 7.31 (m, 4H), 7.18 (s, 1H), 7.12 (t, *J*= 7.4 Hz, 1H), 6.97 (t, *J*=7.4 Hz, 1H). ^{13}C-NMR (150 MHz, DMSO-d_6) δ: 166.9, 164.8, 160.1, 157.6, 141.2, 138.5, 129.6, 129.2, 124.9, 122.3, 121.1, 117.7, 110.4, 100.8; HR-MS analysis: calculated for $C_{19}H_{14}N_4O_2S$: 362.08; found: 363.09152 [M+H$^+$].

***N*-(pyridin-2-yl)-5-(2-((4-(trifluoromethyl)phenyl)amino)thiazol-4-yl)isoxazole-3-carboxamide (42m)**

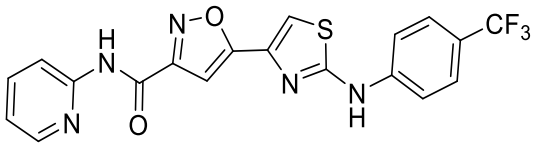

Compound **42** (20 mg, 0.06 mmol, 1 eq) and the *p*-(trifluoromethyl)thiourea (**m**) were reacted following the **general method D**. The title compound precipitated in the reaction mixture and it was obtained as an orange powder after filtration (yield: 14.7, 52%). ^{1}H-NMR (300 MHz, DMSO-d_6) δ: 10.97 (1H, s), 10.94 (1H, s), 8.45 (1H, ddd, *J*=0.9, 1.9, 4.9 Hz), 8.16-8.13 (1H, m), 8.00 - 7.92 (3H, m), 7.83 (1H, s), 7.72 (2H, d, *J*=8.5 Hz), 7.41 (1H, s), 7.29 (1H, ddd, *J*=0.9, 4.9, 7.4 Hz); ^{13}C-NMR (150 MHz, DMSO-d_6) δ: 166.9, 164.1, 159.6, 158.3, 151.0, 148.1, 144.5, 139.8, 138.4, 126.9, 124.2, 121.3, 117.5, 115.7, 111.8, 101.1. HR-MS analysis: calculated for $C_{19}H_{12}F_3N_5O_2S$: 431.07; found: 432.07455 [M+H$^+$].

***N*-phenyl-5-(2-((4-(trifluoromethyl)phenyl)amino)thiazol-4-yl)isoxazole-3-carboxamide (43m)**

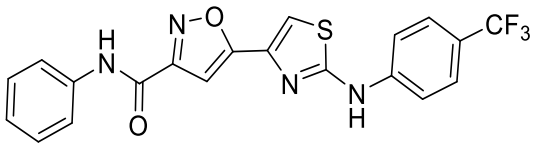

Compound **43** (30 mg, 0.10 mmol, 1 eq) and the *p*-(trifluoromethyl)thiourea (**m**) were reacted following the **general method D**. The title compound precipitated in the reaction mixture and it was obtained as a yellow powder after filtration. (yield: 6.9, 17%). ^{1}H-NMR (300 MHz, DMSO-d_6) δ: 10.94 (1H, s), 10.77 (1H, s), 7.94 (2H, d, *J*=8.6 Hz), 7.84 - 7.78 (3H, m), 7.73 (2H, d, *J*=8.6 Hz), 7.40 (2H, t, *J*=7.9 Hz), 7.30 (1H, s), 7.20 - 7.14 (1H, m);); ^{13}C-NMR (150 MHz, DMSO-d_6) δ: 166.9, 164.1, 159.6, 158.3, 144.5, 138.4, 138.2, 129.5, 126.9, 125.2, 124.2, 121.2, 117.5, 111.8, 101.1. HR-MS analysis: calculated for $C_{20}H_{13}F_3N_4O_2S$: 430.07; found: 431.07932 [M+H$^+$].

***N*-(pyridin-2-yl)-5-(2-((3,4,5-trichlorophenyl)amino)thiazol-4-yl)isoxazole-3-carboxamide (42n)**

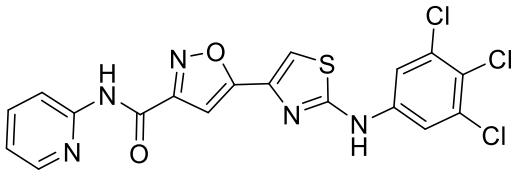

Compound **42** (30 mg, 0.10 mmol, 1 eq) and the 3,4,5-trichlorothiourea (**n**) were reacted following the **general method D**. The title compound precipitated in the reaction mixture and it was obtained as a yellow powder after filtration (yield: 27.7 mg, 61%). ^{1}H-NMR (600 MHz, DMSO-d_6) δ: 11.06 (s, 1H), 10.98 (s, 1H), 8.43 – 8.38 (m, 1H), 8.11 – 8.04 (m, 1H), 7.99 – 7.93 (m, 3H), 7.81 (s, 1H), 7.27 (ddd, *J*=7.4, 5.0, 1.1 Hz, 1H), 7.24 (s, 1H). ^{13}C-NMR (150 MHz, DMSO-d_6) δ: 166.7, 163.7, 159.5, 158.3, 150.8, 147.7, 140.9, 140.2, 138.2, 133.6, 121.8, 121.4, 117.6, 115.8, 112.4, 100.9. HR-MS analysis: calculated for $C_{18}H_{10}Cl_3N_5O_2S$: 464.96; found: 467.96700 [M+H$^+$].

***N*-phenyl-5-(2-((3,4,5-trichlorophenyl)amino)thiazol-4-yl)isoxazole-3-carboxamide (43n)**

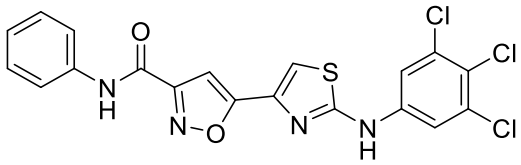

Compound **43** (30 mg, 0.10 mmol, 1 eq) and the 3,4,5-trichlorothiourea (**n**) were reacted following the **general method D**. The title compound precipitated in the reaction mixture and it was obtained as a yellow powder after filtration (yield: 27.7 mg, 61%). ^{1}H-NMR (600 MHz, DMSO-d_6) δ: 10.92 (s, 1H), 10.72 (s, 1H), 7.94 (s, 2H), 7.82 (s, 1H), 7.77 (d, *J* =8.0 Hz, 1H), 7.34 (t, *J*=8.0 Hz, 2H), 7.15-7.09 (m, 2H). ^{13}C-NMR (150 MHz, DMSO-d_6) δ: 166.5, 163.8, 160.2, 157.6, 140.9, 138.6, 138.3, 133.6, 129.3, 125.0, 121.8, 121.2, 117.6, 112.3, 101.0. HR-MS analysis: calculated for $C_{19}H_{11}Cl_3N_4O_2S$: 463.97; found: 466.96710 [M+H$^+$].

5-(2-aminothiazol-4-yl)-*N*-(pyridin-2-yl)isoxazole-3-carboxamide (42o)

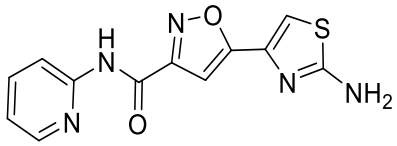

Compound **42** (30 mg, 0.10 mmol, 1 eq) and thiourea (**o**) were reacted following the **general method D**. The title compound precipitated in the reaction mixture and it was obtained as a yellow powder after filtration (yield: 19.6 mg, 70%). ^{1}H-NMR (300 MHz, DMSO-d_6) δ: 11.05 (1H, s), 8.45 (1H, dd, *J*=1.1, 5.2 Hz), 8.13 - 8.08 (1H, m), 8.02-7.96 (1H, m), 7.43 (1H, s), 7.31 (1H, ddd, *J*=1.1, 5.2, 7.4 Hz), 7.11 (1H, s); ^{13}C-NMR (150 MHz, DMSO-d_6) δ: 170.0, 166.8, 159.3, 158.5, 150.4, 146.8, 141.0, 136.8, 121.4, 116.1, 109.6, 100.5. HR-MS analysis: calculated for $C_{12}H_9N_5O_2S$: 287.05; found: 288.05539 [M+H$^+$].

5-(2-aminothiazol-4-yl)-*N*-phenylisoxazole-3-carboxamide (43o)

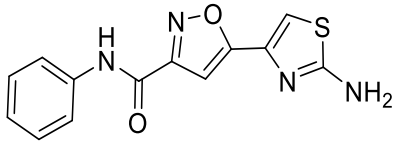

Compound **43** (30 mg, 0.10 mmol, 1 eq) and thiourea (**o**) were reacted following the **general method D**. The title compound precipitated in the reaction mixture and it was obtained as a yellow powder after filtration (yield: 9.7 mg, 35%). ^{1}H-NMR (300 MHz, DMSO-d_6) δ: 10.72 (1H, s), 7.80 (2H, dd, *J*=1.1, 8.6 Hz), 7.43 (1H, s), 7.40-7.35 (2H, m), 7.15 (1H, tt, *J*=1.1, 7.4 Hz), 7.02 (1H, s); ^{13}C-NMR (150 MHz, DMSO-d_6) δ: 170.0, 166.8, 159.3, 150.4, 141.0, 138.5, 129.3, 125.2, 121.1, 109.6, 100.5. HR-MS analysis: calculated for $C_{13}H_{10}N_4O_2S$: 286.05; found: 287.06023 [M+H$^+$].

Ethyl 5-(2-((2-bromo-5-hydroxy-4-methylphenyl)amino)thiazol-4-yl)isoxazole-3-carboxylate (44)

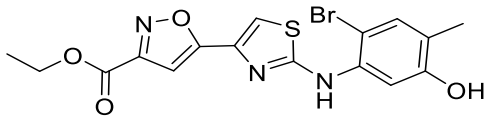

Compound **1** (809 mg, 3.09 mmol) and the thiourea **e** (380 mg, 3.09 mmol) were reacted following the **general method D**. The title compound was collected as a yellow powder by filtration after precipitating in the reaction mixture (yield: 393 mg, 30%). ^{1}H-NMR (400 MHz, DMSO-d_6) δ: 9.84 (s, 1H), 9.63 (s, 1H), 7.73 (s, 1H), 7.70 (s, 1H), 7.33 (s, 1H), 7.18 (s, 1H), 4.40 (q, *J*=7.1 Hz, 2H), 2.10 (s, 3H), 1.35 (t, *J*=7.1 Hz, 3H). HR-MS analysis: calculated for $C_{16}H_{14}BrN_3O_4S$: 424.27; found: 425.99440 [M+H]$^+$.

5-(2-((4-(ethoxymethyl)phenyl)amino)thiazol-4-yl)-*N*-(pyridin-2-yl)isoxazole-3-carboxamide (45)

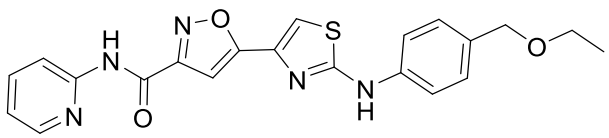

Compound **42** (15 mg, 0.05 mmol) and the thiourea **h** were reacted following the **general method E**. After cooling, the title compound precipitated in the reaction mixture and it was obtained as a pale yellow powder after filtration (yield: 6 mg, 29%). ^{1}H-NMR (600 MHz, DMSO-d_6) δ: 10.78 (s, 1H), 10.41 (s, 1H), 8.39 (ddd, *J*= 4.8, 1.9, 0.9 Hz, 1H), 8.10 (d, *J*=8.3 Hz, 1H), 7.87 (ddd, *J*=8.4, 7.4, 2.0 Hz, 1H), 7.64 (s, 1H), 7.61 (d, *J*=8.4 Hz, 2H), 7.30 – 7.24 (m, 3H), 7.20 (ddd, *J*=7.4, 4.8, 0.9 Hz, 1H), 4.43 (s, 2H), 4.05 (2H, q, *J*=6.9 Hz), 2.32 (3H, s). MS analysis: found: 422.13.

2.5.2 Analytical chemistry

Chemicals and reagents. Human liver microsomes (HLM, pooled fraction derived from 200 male and female donors) were purchased from Xenotech, LLC (Cambridge, Kansas City, USA). 85% v/v formic acid was provided by ACEF Spa (Piacenza, Italy); HPLC-grade acetonitrile (ACN) and dimethylsulfoxide (DMSO) were supplied by Sigma Aldrich (Milan, Italy) and VWR Chemicals (Radnor, Pennsylvania, USA), respectively. Ultra-pure Millipore water (Darmstadt, Germany) was employed for HPLC mobile phase and sample preparations.

Metabolic Stability in Human Liver Microsomes (HLM). Metabolic stability assays on parent compounds **UPAR-452** and **UPAR-453** and on metabolically protected derivatives **42l-o** and **43l-o** were conducted in the presence of pooled human liver microsomes (HLM). Briefly, a solution of enzymatic co-factors containing glucose-6-phosphate (10 mM), $NADP^+$ (2 mM), $MgCl_2$ (5 mM) and glucose-6-phosphate-dehydrogenase (0.4 U/mL) was prepared in 100 mM phosphate buffered saline (PBS) pH 7.4. HLM suspension (i.e. 15 µL; final protein concentration = 1 mg/mL) was added to 60 µL of co-factors mix and 222 µL of PBS buffer. Samples were pre-incubated under continuous stirring at 37 °C for 5 min, then 3 µL of DMSO stock solution of each test compound (final compound concentration = 1 µM; final DMSO concentration: 1% v/v) were added to start the reaction. Sample aliquots were collected at different time points (t = 0, 15, 30, 45, 60 min), enzymatic reactions were quenched by the addition of a double volume of acetonitrile (ACN) containing a structure analogue as internal standard (IS) (100 nM), samples were centrifuged (16000 g, 10 min, 4 °C) and the supernatant was directly analysed by HPLC-Multiple Reaction Monitoring (MRM)-MS for the percentage of test compound remaining over time. In vitro half-life ($t_{1/2}$) and intrinsic clearance (CL_{int}) in liver subcellular fractions were calculated by the following equations: Elimination rate constant (k) = -slope; Half-life ($t_{1/2}$) min = ln2/k. Microsoft Excel (Microsoft Corp., 2010, USA) was employed for data analysis. GraphPad Prism v. 6.01 (GraphPad, USA) was employed for plotting graphs. Intrinsic Clearance values

(CL_{int}) were calculated as follows: CL_{int} (µL/min/mg protein) = (Volume of incubation · ln2)/(mg protein in the incubation · $t_{1/2}$).

Phase I metabolite ID profiling. For profiling phase I metabolites in HLM, initial concentration of test compounds **UPAR-452** and **UPAR-453** in HLM incubates was increased to 100 µM. Aliquots of the incubates were collected at the beginning of incubation time and after 180 min, quenched by ACN addition, centrifuged and analysed by HR-MS by means of a LTQ-Orbitrap mass spectrometer (Thermo, USA).

In HLM spiking experiments, in which the HPLC retention times (RT) of hydroxylated metabolites of **UPAR-452** and **UPAR-453** were compared to those of corresponding synthetic standards, 10 mL of HLM incubates were diluted with either 90 mL of ACN (vehicle) or with a 250 nM solution of each synthetic standard dissolved in the same vehicle. After centrifugation, samples were analysed in HPLC-MS/MS.

HPLC-MRM-MS analysis. For the analysis of metabolic stability of UPAR-452, UPAR-453 and metabolically protected derivatives **42l-o** and **43l-o** in HLM, HPLC-MRM-MS traces were acquired both in positive (ESI^+) and in negative (ESI^-) ion mode. An Accela UHPLC system (Thermo, USA), equipped with a Synergy Fusion C18 80 Å RP-column (2.0 x 100 mm, 4 µm; Phenomenex, USA) was employed for HPLC-MRM-MS analysis. Mobile phases were: A: ACN and B: ultra-pure water respectively, both containing 0.1% v/v formic acid. The following general gradient was applied for the elution: 5%A between 0 and 1 min; linear gradient to 100%A from 1 to 6 min; 100%A between 6 and 10 min returning to 5%A in 2 min with a 3-min reconditioning time. Total run time: 15 min. The flow rate was maintained at 0.35 mL/min and injection volume was 10 µL. A TSQ Quantum Access Max Triple Quadrupole mass spectrometer (Thermo, USA), equipped with a heated electrospray (H-ESI) ion source, was employed for compound detection in stability assays. All analyses were performed by setting ion source voltage at 3500 V, Collision Induced Dissociation (CID) voltage at 12 V and capillary temperature at 270 °C. Nitrogen served both as sheath and auxiliary gas at 15 psi and 35 psi, respectively; argon with a pressure of 1.5 mtorr was employed as collision gas.

Xcalibur software version 2.2 (Thermo, USA) was employed for both data acquisition and processing.

Tube lens voltages (TL) and collision energies (CE) for each parent-product ion transition were optimized by Flow Injection Analysis (FIA) of 10 mM solutions of each compound dissolved in MeOH. **UPAR-452**: *m/z* = 377.09 $[M+H]^+ \rightarrow$ *m/z* = 235.00, 258.06, 189.04 (TL = 104 V; CE = 13, 15, 32 eV, respectively); **UPAR-453**: *m/z* = 378.10 $[M+H]^+ \rightarrow$ *m/z* = 257.97, 234.97, 121.03 (TL = 74 V; CE = 17, 18, 24 eV); **42l**: *m/z* = 364.09 $[M+H]^+ \rightarrow$ *m/z* = 221.02, 244.02, 121.10 (TL = 72 V; CE = 15, 18, 23 eV); **42m**: *m/z* = 432.09 $[M+H]^+ \rightarrow$ *m/z* = 412.10, 291.96, 121.09 (TL = 94 V; CE = 19, 24, 28 eV); **42n**: *m/z* = 465.98 $[M+H]^+ \rightarrow$ *m/z* = 322.89, 121.06, 345.87 (TL = 83 V; CE = 13, 21, 23 eV); **42o**: *m/z* = 288.06 $[M+H]^+ \rightarrow$ *m/z* = 168.04, 121.11, 78.19 (TL = 65 V; CE = 16, 20, 35 eV); **43l**: *m/z* = 363.09 $[M+H]^+ \rightarrow$ *m/z* = 220.99, 244.02, 175.03 (TL = 86 V; CE = 12, 14, 32 eV); **43m**: *m/z* = 429.03 $[M-H]^- \rightarrow$ *m/z* = 309.93, 282.96, 184.98 (TL = 81 V; CE = 22, 26, 37 eV); **43n**: *m/z* = 462.93 $[M-H]^- \rightarrow$ *m/z* = 343.88, 316.82, 218.84 (TL = 78 V; CE = 22, 25, 39 eV); **43o**: *m/z* = 287.1 $[M+H]^+ \rightarrow$ *m/z* = 145.05, 168.01, 127.05 (TL = 73 V; CE = 11, 11, 22 eV).

In HLM spiking experiments, a longer HPLC gradient was employed to discriminate between the Retention Times of the hydroxylated derivatives in ortho and meta-positions to the methyl group of the toluene ring. Chosen mobile phases were: A: ACN and B: ultra-pure water respectively, both containing 0.1% v/v formic acid. HPLC gradient conditions were: 5%A between 0 and 1 min; linear gradient to 100%A from 1 to 120 min, returning to 5%A in 2 min with a 3-min reconditioning time. Total run time: 125 min. The flow rate was kept at 0.35 mL/min and injection volume was 10 µL. TSQ Quantum Access Max mass spectrometer acquired both in MRM and in product ion mode. For MRM acquisition mode, the following parent-product ion transitions were optimized by FIA and employed for M1 and M2 metabolites derived from **UPAR-452** and **UPAR-453**: **$M1_{UPAR-452}$:** m/z = 393.09 $[M+H]^+ \rightarrow$ *m/z* = 256.01, 233.00, 116.10 (TL = 124 V; CE = 16, 20, 39 eV). **$M2_{UPAR-452}$:** *m/z* = 393.06 $[M+H]^+ \rightarrow$ *m/z* = 250.98, 273.96, 204.95 (TL = 106 V; CE = 11, 15, 32 eV); **$M1_{UPAR-453}$:** *m/z* = 394.08 $[M+H]^+ \rightarrow$ *m/z* = 376.07,

255.97, 121.02 (TL = 90 V; CE = 15, 20, 23 eV); **M2$_{UPAR-453}$:** *m/z* = 394.07 $[M+H]^+$→ *m/z* = 250.97, 274.00, 121.07 (TL = 90 V; CE = 18, 19, 23 eV); **42i**: *m/z* = 394.075 $[M+H]^+$→ *m/z* = 274.01, 121.13, 205.00 (TL = 77 V; CE = 19, 24, 28 eV).

In product ion mode, MS/MS spectra were acquired in the m/z = 100-400 amu range and CE was set at 30 V. Parent mass was set at m/z = 377.1 (**UPAR-452**), 393.1 (M1-M2), and at m/z = 378.1 (**UPAR-453**) and 394.1 (M1-M2).

HR-MS analysis. For the determination of high-resolution mass values of parent compounds UPAR-452 and UPAR-453 and of corresponding synthetic metabolite standards M1 and M2, 10 µM solutions of test compounds in MeOH were directly infused into a LTQ-Orbitrap high-resolution mass spectrometer (Thermo, USA), interfaced with a heated electrospray (H-ESI) ion source. Analysis was performed in Full Scan mode (m/z = 150-1500 amu) and in positive electrospray (ESI+). Capillary temperature was set at 275 °C, sheath gas flow rate at 8.03 (arbitrary unit). Source parameters were as follows: source voltage: 3.51 kV, capillary voltage: 13 V and tube lens voltage: 100 V with an ion injection time of 250 ms. For tandem mass analysis, Collision-induced dissociation (CID) value was set at 30 or 35 V and an isolation width of 1 m/z and an ion injection time of 1000 ms were employed.

For the HR-MS analysis of HLM incubates of UPAR-452 and UPAR-453, a Dionex HPLC (Thermo, USA) was coupled with the LTQ-Orbitrap mass analyzer (Thermo, USA). An AERIS Peptide 3.6um XB-C18 150x2.10mm column equipped with a SecurityGuard ULTRA cartridge (Phenomenex, USA), thermostated at 35°C, was employed for compound separation. Mobile phases A and B were ACN and ultra-pure water both added with 0.2% v/v formic acid. The following elution gradient was applied: 10%A between 0 and 5 min; to 95%A between 5 and 36 min; to 96%A between 36 and 40 min; back to 10%A at 41 min with a 9-min reconditioning time. Total run time was 50 min. Flow rate was set at 0.2 mL/min and injection volume was 10 µL. Analysis was first performed in Full Scan mode (*m/z* = 150-1500 amu), both in ESI^+ and ESI^-. Capillary temperature was set at 275 °C, sheath, auxiliary and sweep gas pressures were 20, 5 and 5 psi, respectively. Source parameters in ESI^+ employed a source voltage of 3000 V,

a capillary voltage of 13 V and a tube lens voltage of 85 V. For ESI^- they were 2500 V, 35 V and -110 V, respectively. Resolution was set at 15000 (at m/z = 400). For tandem mass analysis, the first and second most intense ions of the parent list were acquired if having a minimum signal of 10000 in data dependent scan, an isolation window of 1 m/z in collision-induced dissociation (CID) and a collision energy of 30-35 V. Xcalibur software version 2.07 (Thermo, USA) was employed for both data acquisition and processing.

Reactivity with glutathione. 2 mL of 2 mM stock solution of test compounds **UPAR-452**, **UPAR-453**, **33**, **34** in DMSO were added to 198 mL of freshly-prepared 2 mM glutathione (GSH) solution (GSH : compound molar ratio 100:1) in 10 mM Phosphate Buffered Saline (PBS) buffer pH 7.4, adjusted to 0.15M ionic strength by KCl addition. The formation of the corresponding GSH-conjugate was measured after 24 h of incubation at 37 °C by HPLC-MS acquiring in full scan mode (m/z = 100-800 amu) and in positive electrospray (ESI^+) extracting the single and double-charged ions corresponding to the GSH-conjugates of each compound. For UPAR-452-GSH conjugate: $[M+2H]^{2+}$ = 341.6 and $[M+H]^+$ = 682.2; For UPAR-453-GSH conjugate: $[M+2H]^{2+}$ = 342.9 and $[M+H]^+$ = 683.1; For UPAR-752-GSH conjugate: $[M+2H]^{2+}$ = 333.6 and $[M+H]^+$ = 666.2; For UPAR-753-GSH conjugate: $[M+2H]^{2+}$ = 333.9 and $[M+H]^+$ = 667.2. An Accela UHPLC system (Thermo, USA), equipped with a Synergy Fusion C18 80 Å RP-column (2.0 x 100 mm, 4 µm; Phenomenex, USA) was employed for HPLC-MS analysis. Mobile phases were: A: ACN and B: ultra-pure water respectively, both containing 0.1% v/v formic acid. The following gradient was applied for the elution: start with 20%A; linear gradient to 95%A in 12 min; 95%A between 12 and 16 min returning to 20%A in 1 min with a 3-min reconditioning time. Total run time: 20 min.

Determination of Kinetic Solubility. Kinetic solubility for compounds **UPAR-452**, **UPAR-453**, **33**, **34** was determined starting from freshly prepared 10 mM DMSO stock solutions. In a 96-well plate, 2 mL of stock solution were added to 198 mL of (i) water or (ii) 10 mM PBS buffer pH 7.4, adjusted to 0.15M ionic strength by KCl addition. The plate was stirred (250 rpm, 4 h, room temperature). At the end of the incubation time, the precipitated compound was separated by centrifugation (1000g, 3 min, 20°C) and

an aliquot of the supernatant was diluted 1:100 with MeOH and injected in the HPLC-MS/MS system for quantification. Calibration curves for each compound were built in MeOH. HPLC-MS/MS analytical method was the same reported for HLM stability assays.

2.5.3 Biology

Determination of the MIC for the SAR and SMR studies. MIC were determined following a previously reported method.[19] Two independent *M. tuberculosis* cultures were grown approximately to mid-log phase, then diluted to a final OD_{600}=0.0005 and used to determine MIC_{90} in microtiter. Streptomycin was used as control. Concentrations assayed were: 20-10-5-2.5-1.25-0.6-0.3-0.15 ug/ml, 0 as control. After an incubation of 7 days at 37°C, resazurin was added at a final concentration of 0.0025%. After 1 day of incubation, plates were read (Ex 544 nm, Em 590 nm, Floroskan ThermoScientific).

Cytotoxicity assay and IC_{50} determination:

Cell culture. THP-I cells were grown in suspension in RPMI 1640 culture media (Euroclone, Italy) supplemented with Sodium Pyruvate 100mM (1%; Life Technologies, USA), Gentamicin 10mg/ml (0,5%; Sigma Aldrich, USA), 2-Mercaptoethanol 50mM (0,1%; Life Technologies, USA), Glucose (0,25% g/ml) and Fetal Bovine Serum (FBS, Euroclone, Italy) at 10%. When in confluent state, cells were counted and plated at density of 500000 cells/well in 24-well plates (Sarstedt, Germany) in the presence of 50 ng/mL phorbol 12-miristate 13-acetate (PMA; Sigma Aldrich, USA) and then incubated at 37°C, 5% CO_2 for 72 h to allow the differentiation into macrophages.

Cytotoxicity assay (MTT assay). MTT assay has been used to assess the cytotoxicity of synthetized compounds upon THP-derived macrophages by evaluating the ability of mitochondrial succinate dehydrogenase to catalyse the enzymatic reduction of yellow water soluble 3-[4,5-dimethylthiazole-2-yl]-2,5-diphenyltetrazolium bromide (MTT; Sigma Aldrich, USA) to insoluble purple formazan, an index of cellular viability.

Differentiated macrophages were treated with different concentrations of synthetized compounds at increasing concentrations (1 µM, 10 µM, 50 µM and 100 µM, in double)

dissolved in RPMI 1640 supplemented with 1% FBS for 72 hours. Afterwards, cells were incubated with a solution of 1mg/ml of MTT dissolved in RPMI 1640, supplemented with 5% FBS, at 37ºC, 5% CO_2 for 2 hours in dark. The solution was then removed and intracellular formazan was solubilized by adding 0,2 mL DMSO per well and shaking the plates for 10 minutes. Subsequently, absorbance was measured on a cellular lysate aliquot (0,15 mL) using a Spark® Tecan fluorimeter recording the absorbance of each sample at 570 nm.

Statistical analysis . Statistical analysis were performed using GraphPad Prism software version 7.0 (GraphPad Software Inc., La Jolla, CA). Results were expressed as % cell viability at each concentration compared to viability of non-treated cells (100% viability). IC_{50} values for each tested compound were calculated by interpolating the % viability obtained at each concentration through a non-linear regression analysis.

Investigation of the mechanism of action:

Broth microdilution assay/microplate alamar blue assay (MABA) minimum inhibitory concentration 90 (MIC_{90}) for the various compounds tested, was determined as described.[20] Briefly, a pre-culture of *M. tuberculosis* H37RvMa was prepared from a glycerol stock and grown for 4 days followed by a sub-culture grown to an OD_{600} 0.6-0.8 (logarithmic phase) in filter-sterilized 7H9 media supplemented with either 10% ADC, 0.2% glycerol and 0.25% Tween 80 (20% in H2O) or 0.4% glucose, 0.03% casitone, 0.2% glycerol and 0.25% tween-80 (20% in H_2O). The media was added to 96 microtitre well plates followed by addition of the drugs which were then serially diluted. Finally the culture (diluted x 1000) was added to the wells. The controls included media only and the solvent used to dissolve the drugs at a concentration corresponding to that of the working solutions of the drugs. Rifampicin (RIF) was used as a reference drug. Incubation was carried out at 37°C with no shaking for 7 days then resazurin dye was added to the plates. Further incubation was carried out for 24 h in the same conditions.

Cross-resistance activity: Broth microdilution assay/mycobacterium alamar blue assay (MABA). Briefly, a pre-culture of *M. tuberculosis* [H_{37}Rv (Ma) and resistant mutants; linezolid resistant (LZD-R) strains (*rplC*; t460c, *rrl*; g2270t),

spectinomycin resistant SPEC-R) strain (*rrs*; g1379t) fusidic acid resistant strain (*fus1;* g1384t, strains] and rifampicin resistant strain (*rpoB*; S531L) were prepared from a glycerol stock and grown for 4 days (OD_{600} 0.8) followed by a subculture grown to an OD_{600} 0.6-0.8 (exponential phase) in filter-sterilized 7H9 media, supplemented with 0.4% w/v glucose, 0.03% w/v casitone, 0.2% v/v glycerol and 0.25% v/v tween-80 (20% in H_2O). The media was added to 96 microtiter well plates followed by addition of the drugs which were then serially diluted. *M. tuberculosis* culture (diluted x 500) was then added to the wells containing the drugs at different concentrations. The controls consisted media and the solvent that used to dissolve the drugs at a concentration corresponding to that of the working solutions of the drugs. Isoniazid (INH) was used as a reference drug. The plates were incubated at 37^{o}C with no shaking for 7 days followed by addition of resazurin dye. Further incubation at 37^{o}C for 24h was done and at the 8th day MIC_{90} was recorded.

2.6 References

(1) Azzali, E.; Machado, D.; Kaushik, A.; Vacondio, F.; Flisi, S.; Cabassi, C. S.; Lamichhane, G.; Viveiros, M.; Costantino, G.; Pieroni, M. Substituted N-Phenyl-5-(2-(Phenylamino)Thiazol-4-Yl)Isoxazole-3-Carboxamides Are Valuable Antitubercular Candidates That Evade Innate Efflux Machinery. *J. Med. Chem.* **2017**, *60* (16), 7108–7122.

(2) Baell, J. B.; Holloway, G. A. New Substructure Filters for Removal of Pan Assay Interference Compounds (PAINS) from Screening Libraries and for Their Exclusion in Bioassays. *J. Med. Chem.* **2010**, *53* (7), 2719–2740.

(3) Baell, J. B.; Nissink, J. W. M. Seven Year Itch: Pan-Assay Interference Compounds (PAINS) in 2017—Utility and Limitations. *ACS Chem. Biol.* **2018**, *13* (1), 36–44.

(4) Glaser, J.; Holzgrabe, U. Focus on PAINS: False Friends in the Quest for Selective Anti-Protozoal Lead Structures from Nature? *MedChemComm* **2016**, *7* (2), 214–223.

(5) Devine, S. M.; Mulcair, M. D.; Debono, C. O.; Leung, E. W. W.; Nissink, J. W. M.; Lim, S. S.; Chandrashekaran, I. R.; Vazirani, M.; Mohanty, B.; Simpson, J. S.; et al. Promiscuous 2-Aminothiazoles (PrATs): A Frequent Hitting Scaffold. *J. Med. Chem.* **2015**, *58* (3), 1205–1214.

(6) Burger, A. Isosterism and Bioisosterism in Drug Design. *Prog. Drug Res. Fortschritte Arzneimittelforschung Progres Rech. Pharm.* **1991**, *37*, 287–371.

(7) Kilbourn, M. R. Thiophenes as Phenyl Bio-Isosteres: Application in Radiopharmaceutical Design--I. Dopamine Uptake Antagonists. *Int. J. Rad. Appl. Instrum. B* **1989**, *16* (7), 681–686.

(8) Wermuth, C.; Aldous, D.; Raboisson, P.; Rognan, D. The Practice of Medicinal Chemistry - 4th Edition, **2015**, Academic Press.

(9) Machado, D.; Girardini, M.; Viveiros, M.; Pieroni, M. Challenging the Drug-Likeness Dogma for New Drug Discovery in Tuberculosis. *Front. Microbiol.* **2018**, *9*, 1367.

(10) Haake, Paul.; Miller, W. B. A Comparison of Thiazoles and Oxazoles. *J. Am. Chem. Soc.* **1963**, *85* (24), 4044–4045.

(11) Jin, Z. Imidazole, Oxazole and Thiazole Alkaloids. *Nat. Prod. Rep.* **2006**, *23* (3), 464–496.

(12) Mathew, B.; Hobrath, J. V.; Connelly, M. C.; Guy, R. K.; Reynolds, R. C. Oxazole and Thiazole Analogs of Sulindac for Cancer Prevention. *Future Med. Chem.* **2018**, *10* (7), 743–753.

(13) Lilienkampf, A.; Pieroni, M.; Wan, B.; Wang, Y.; Franzblau, S. G.; Kozikowski, A. P. Rational Design of 5-Phenyl-3-Isoxazolecarboxylic Acid Ethyl Esters as Growth Inhibitors of Mycobacterium Tuberculosis. a Potent and Selective Series for Further Drug Development. *J. Med. Chem.* **2010**, *53* (2), 678–688.

(14) Lilienkampf, A.; Pieroni, M.; Franzblau, S. G.; Bishai, W. R.; Kozikowski, A. P. Derivatives of 3-Isoxazolecarboxylic Acid Esters: A Potent and Selective Compound Class against Replicating and Nonreplicating Mycobacterium Tuberculosis. *Curr. Top. Med. Chem.* **2012**, *12* (7), 729–734.

(15) Hay, M. P.; Turcotte, S.; Flanagan, J. U.; Bonnet, M.; Chan, D. A.; Sutphin, P. D.; Nguyen, P.; Giaccia, A. J.; Denny, W. A. 4-Pyridylanilinothiazoles That Selectively Target von Hippel−Lindau Deficient Renal Cell Carcinoma Cells by Inducing Autophagic Cell Death. *J. Med. Chem.* **2010**, *53* (2), 787–797.

(16) Vogt, D.; Weber, J.; Ihlefeld, K.; Brüggerhoff, A.; Proschak, E.; Stark, H. Design, Synthesis and Evaluation of 2-Aminothiazole Derivatives as Sphingosine Kinase Inhibitors. *Bioorg. Med. Chem.* **2014**, *22* (19), 5354–5367.

(17) PATENT UY37728 (A), **2019**

(18) Azzali, E. Toward Innovative Therapeutics for the Eradication of Mycobacterial, **2016**, PhD Thesis, University of Parma.

(19) Palomino, J.-C.; Martin, A.; Camacho, M.; Guerra, H.; Swings, J.; Portaels, F. Resazurin Microtiter Assay Plate: Simple and Inexpensive Method for Detection of Drug Resistance in Mycobacterium Tuberculosis. *Antimicrob. Agents Chemother.* **2002**, *46* (8), 2720–2722.

(20) Collins, L.; Franzblau, S. G. Microplate Alamar Blue Assay versus BACTEC 460 System for High-Throughput Screening of Compounds against Mycobacterium Tuberculosis and Mycobacterium Avium. *Antimicrob. Agents Chemother.* **1997**, *41* (5), 1004–1009.

3. Inhibition of efflux systems through bacterial energetic shutdown

3.1 Introduction

Bacterial efflux pumps have recently emerged as a valuable target in TB drug discovery. Since efflux pumps (EP) require an energetic source, any compound able to interfere with bacterial energy production is able not only to weaken the bacteria but also to interfere with the efflux systems, thereby increasing the intracellular concentration of co-administered drugs. In recent years many drugs, mainly repurposed, have been tested as efflux pumps inhibitors, showing good results both in vitro and in vivo.[1] The phenothiazines thioridazine (TZ) and chlorpromazine (CPZ) have been reported to have efflux inhibitory activity. They exert their activity by blocking the calcium channels that inhibit the NDH-2 enzyme, causing dissipation of the membrane potential.[2,3] Promising results were obtained with TZ both in a murine model against MDR-TB and in patients with XDR-TB in combination with antitubercular drugs.[4]

Verapamil (VP) is known as the most potent inhibitor of EP in *M. tuberculosis,* acting as potent calcium channel blockers.[5] Despite its excellent activity as efflux inhibitor, its use as adjuvant is not recommended due to the toxicity derived from the blockage of these channels. VP was proved to inhibit the efflux of several structurally unrelated compounds, seemingly extruded by both ATP-dependent and Proton Motive Force (PMF) driven EPs. Numerous studies have demonstrated that it is able to reverse resistance to various antitubercular drugs and, when used in combination, to enhance the activity of molecules known to be EP substrates.[6–9] More importantly, inhibition of EPs in *M. tuberculosis* by VP was found to reduce drug tolerance inside the macrophages and in zebrafish granuloma-like lesions.

In the research group where I have conducted this PhD research, different attempts to synthesize thioridazine analogues, verapamil analogues as well as hybrid structures were carried out.[10] During a screening of an in-house chemical library to identify novel antitubercular chemotypes, compound **UPAR-174** was found to have a moderate

antitubercular activity (MIC=16 μg/mL). **UPAR-174** has a planar, tricyclic chemical structure containing a sulphur atom, which recalls, to a little extent, the general structure of a phenothiazine. Moreover, it has a relatively high lipophilicity (ClogP= 6.35), a feature that is known to confer affinity to the mycobacterial cell wall.[5] All the above considerations prompted us to evaluate the activity of **UPAR-174** as EP inhibitor, and we were pleased to noticed that it showed promising activity in an ethidium bromide efflux inhibition assay (Figure 1A).[11] Evaluation of the intracellular accumulation of a fluorescent well-known EP substrate such as ethidium bromide is a standard assay to preliminary assess the activity of a potential EPI.[11,12] After this encouraging result, the inhibitory profile of **UPAR-174** was further defined by: (i) the evaluation of its synergistic activity with currently used antitubercular first-line and second-line drugs; (ii) the evaluation of its intracellular synergistic effect with INH and RIF on human macrophages infected with *M. tuberculosis*, (iii) the evaluation of its impact on bacterial energetics, in particular dissipation of the proton motive force (PMF) and synthesis of ATP. When tested in combination with first-line and second-line antitubercular drugs on susceptible, single-drug resistant, MDR and XDR *M. tuberculosis,* **UPAR-174** showed different interesting properties: not only it was able to potentiate the antitubercular activity of most of the drug currently used in tuberculosis treatment, but it also showed the ability to restore the susceptibility to drug treatment of MDR and XDR mycobacterial strains. Moreover, a synergistic effect of **UPAR-174** with RIF and INH was also observed in *M. tuberculosis* infected human macrophages*,* an experimental condition that mimics the most what actually occurs inside the lung of the patients. When tested at its MIC (16 μg/mL) on human macrophages infected with M. *tuberculosis* in combination with sublethal concentration of RIF or INH, it showed a synergistic affect with INH and, to a lesser extent, also with rifampicin (Figure 1C), without killing the macrophages. The ability of **UPAR-174** to dissipate the membrane potential (Figure 1B) without damaging the membrane integrity and the observation of the decreased ATP cellular levels provided preliminary insights about its mechanism of efflux inhibition.

Figure 1.

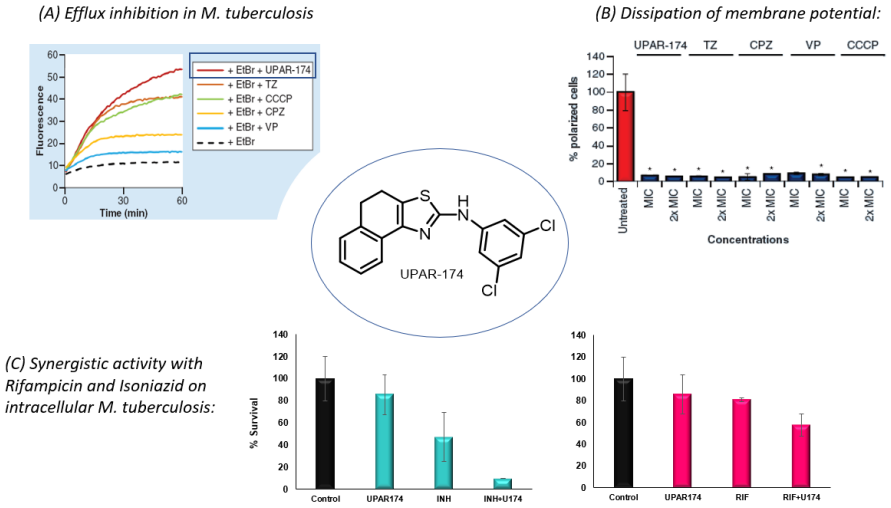

Figure 1. *(A) Efflux inhibition by UPAR-174 on M. tuberculosis in comparison with known EPI; EtBr was tested at 1 µM, inhibitors were tested at 18 µM. (B) Dissipation of the membrane potential by UPAR-174 in comparison with known EPI; Compound tested at MIC and 2X MIC. Dissipation of membrane potential was calculated using BacLight membrane kit after 30 min exposure;*p < 0.01 . (C) synergistic activity of UPAR-174 with INH and RIF in intramacrophageal M. tuberculosis. INH and RIF were used at ½ of their MIC (0.05 and 0.5 µg/mL, respectively), being inactive. Macrophage viability was determined after 3 days of treatment with compound UPAR-174 administered at 16 µg/mL. Above these concentrations, macrophage viability is reduced below 90%.*

Despite its intriguing activity as EPI by virtue of its capability to disrupt the PMF, its cytotoxicity (IC_{50} = 37 µg/mL) did not allowed to evaluate **UPAR-174** at optimal concentrations, especially in intracellular infection, and was particularly disadvantageous for the future development of this molecule as antitubercular chemotype.

In this chapter, a parallel study of Structure-Activity and Structure-Toxicity-Relationships was carried out to provide insights about the chemical features responsible for the toxicity and identify a potent and non-cytotoxic efflux pump inhibitor *via* a Ligand-Based Drug Design approach.

3.2 Results and discussion

A systematic medicinal chemistry approach was carried out with the ultimate aim of selecting a hit compound with a promising activity and an improved toxic profile. For this investigation, a panel of 15 derivatives was rationally designed to cover a reasonably wide chemical space (Chart 1). The biological evaluation of the compounds allowed to obtain insights about the relationships between structure, activity and toxicity, and to obtain a valuable hit for further development with high inhibitory activity and scarce cytotoxicity.

Chart 1

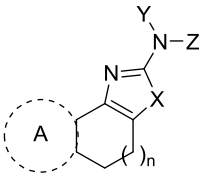

Cmpd.	A	*n*	X	Y	Z
UPAR-174	Ph	1	S	3,5-dichlorophenyl	H
3	Ph	1	O	H	H
4	Ph	1	O	3,5-dichlorophenyl	H
5	Ph	1	S	H	H
6	Ph	1	S	3,5-dichlorosulfonyl	H
7	Ph	1	S	3,5-dichlorobenzoyl	H
8	Ph	1	S	Phenyl	H
10	Ph	1	S	cyclohexyl	H
11	Ph	0	S	3,5-dichlorophenyl	H
12	Ph	1	S	3,5-dichlorophenyl	benzyl
13	Ph	1	S	3,5-dichlorophenyl	methyl
14	Ph	1	S	3,5-dichlorophenyl	2-(1-methylpiperidin-2-yl)ethyl
16	-	1	S	H	H
17	-	1	S	phenyl	H
18	-	1	S	3,5-dichlorophenyl	H
19	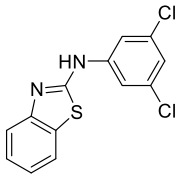				

For the design of the derivatives, the parent compound **UPAR-174** was ideally divided, pivoting on the central amine function, into three regions which were variously modified (R_1 green, R_2 light blue and R_3 orange, Figure 2).

Figure 2

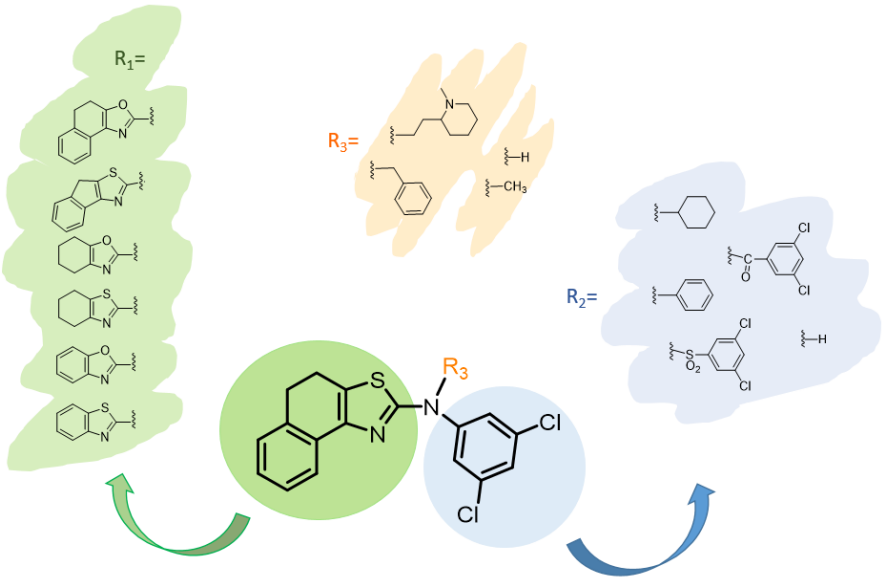

Figure 2. *Rational design of UPAR-174 derivatives*

Various modifications were made on the tricyclic core R_1, from the isosteric[13–15] replacement of the sulfur with the oxygen (compound **4**) to the shrinkage of tetraline to indane (compound **11**). Since we hypothesized that the bulky and lipophilic tricyclic core of **UPAR-174** could play a role in the cytotoxicity, also different bicyclic structures, totally or partially aromatic, were as well explored at R_1. To investigate the contribution of the region R_2 to both activity and toxicity, the 3,5-dichlorobenzyl ring was removed (compound **5**) or replaced with benzene (compound **8**) or cyclohexane (compound **10**). In addition, the 3,5-dichlorobenzyl moiety was attached to the central amine either through an amide (compound **7**) or sulfonamide (compound **6**) linker. The central secondary amine group of **UPAR-174** gives also the possibility to introduce a third substituent (R_3), represented in this study by either a small methyl group or bulkier substituents such as phenyl or 2-ethyl-1-methylpiperidine. In particular, the 2-ethyl-1-

methylpiperidine moiety was introduced at this position in order to mimic somehow the structure of thioridazine, that contains a protonatable nitrogen which seems to be important for the activity.[10]

The derivatives were evaluated to test their ability to inhibit the efflux. The first screening was performed on *M. smegmatis*, a non-pathogenic mycobacterium which allows a faster and safer evaluation of the set of compounds synthesized. Cytotoxicity was assessed on THP-derived macrophages using the MTT method.[16] Prior to evaluate the efflux inhibition, the MICs values (Table 1) were calculated and, although none of the compounds was expected to show "*cidal*" activity, interestingly compound **14** exhibited an MIC of 4 μg/mL. Similarly to **UPAR-174**, efflux inhibition was evaluated as the ability to promote the intracellular retention of ethidium bromide at a non-bactericidal concentration (18 μM) and indicated as Relative Final Fluorescence (RFF; see section Materials and methods). From this preliminary screening, some interesting considerations about the SAR can be delineated. As hypothesized, compounds **16-18** showed low cytotoxicity (IC_{50} > 100 μM), although this kind of modification led to the complete loss of anti-efflux properties, highlighting the crucial role of the R_1 moiety for this series of EPIs. Compound **19**, analogue of **18** with an aromatic bicycle at R_1, was found to be toxic and showed only moderate ability to retain ethidium bromide inside the cell. Compound **3**, **5**, **8** and **10** showed significant improvement in the toxic profile, but also in this case the novel structures negatively impacted on efflux inhibition, suggesting that also the 3,5-dichlorophenyl group of **UPAR-174** play an important role in both activity and toxicity. In particular, this moiety might be important by virtue of its lipophilicity that warrant membrane interaction and affinity. The R_3 substituted compounds **12** and **13** resulted inactive as efflux inhibitors, while **14**, bearing a 2-(1-methylpiperidin-2-yl)ethyl motif as in the case of thioridazine, showed a profile comparable with the parent compound both for inhibition of efflux and toxicity. The sulfonamide **7** showed no activity, while the amide **6**, despite a reasonable activity, was found to be the most cytotoxic compound of the series. The isosteric replacement of thiazole with an oxazole (compound **4**) seemed beneficial for the activity but not for

the toxicity, while compound **11**, where the tetraline structure is shrunk to an indane, was found to be particularly encouraging. Indeed, **11** showed to be a potent (RFF=2.25±0.11) and non-cytotoxic (IC_{50}=93.4) efflux pumps inhibitor on *M. smegmatis*. As in the case of **UPAR-174**, we refined the biological profile of **11** also toward *M. tuberculosis*, confirming **11** as a valuable chemical tool in the fighting of tubercular infections. Interestingly, compound **11** showed an MIC of 64 µg/mL. The absence of bactericidal activity on *M. tuberculosis* observed for compound **11** is a desirable feature for EPIs, which are intended to act as adjuvant compounds.

Table 1

Compound	Smeg mc² 155		Mtb M37Rv		IC_{50} (µM)
	MIC (µg/mL)	RFF [a]	MIC (µg/mL)	RFF	
UPAR-174	64	1.92 ± 0.04	16	3.29 ± 0.39	33.8
3	64	0.11 ± 0.04	- [b]	-	>100
4	64	2.30 ± 0.02	-	-	13.2
5	64	0.44 ± 0.02	-	-	>100
6	64	1.47 ± 0.16	-	-	<12.0
7	64	0.29 ± 0.03	-	-	92.6
8	64	0.03 ± 0.01	-	-	80.8
10	64	-0.05 ± 0.01	-	-	89.2
11	64	2.25 ± 0.11	64	3.01 ± 0.25	93.4
12	128	0.11± 0.01	-	-	>100
13	64	0.46 ± 0.04	-	-	>100
14	4	1.73 ± 0.00	-	-	35.0
16	64	0.15 ± 0.02	-	-	>100
17	64	-0.04 ± 0.02	-	-	>100
18	64	0.15 ± 0.00	-	-	>100
19	64	0.43 ± 0.08	-	-	16.2
TZ	15	1.95 ± 0.02	15	0.82 ± 0.08	-
VP	800	0.01 ± 0.01	256	1.19 ± 0.02	-

Table 1. *Intracellular retention of ethidium bromide on M. smegmatis and M. tuberculosis and cytotoxicity on THP-derived macrophages of the panel of compound synthesized.* [a] *RFF= relative final fluorescence ;* [b] *= not determined*

3.3 Chemistry

The majority of the target compounds (**3**, **5**, **8**, **10**, **11**, **16-18** and **UPAR-174**) were synthetized in a range of variable yields by employing an established *Hantzsch protocol*, refluxing the appropriate α-bromoketone with an equimolar amount of thiourea (or 10 equivalents of urea in case of compound **3**) in absolute ethanol (Scheme 1 and Scheme 2). Suitable α-bromoketones were synthesized as reported,[17,18] while the thioureas and urea used were purchased with the exception of the 1-cyclohexylthiourea **9**, which was obtained as reported.[19]

Scheme 1 *(a,b)*

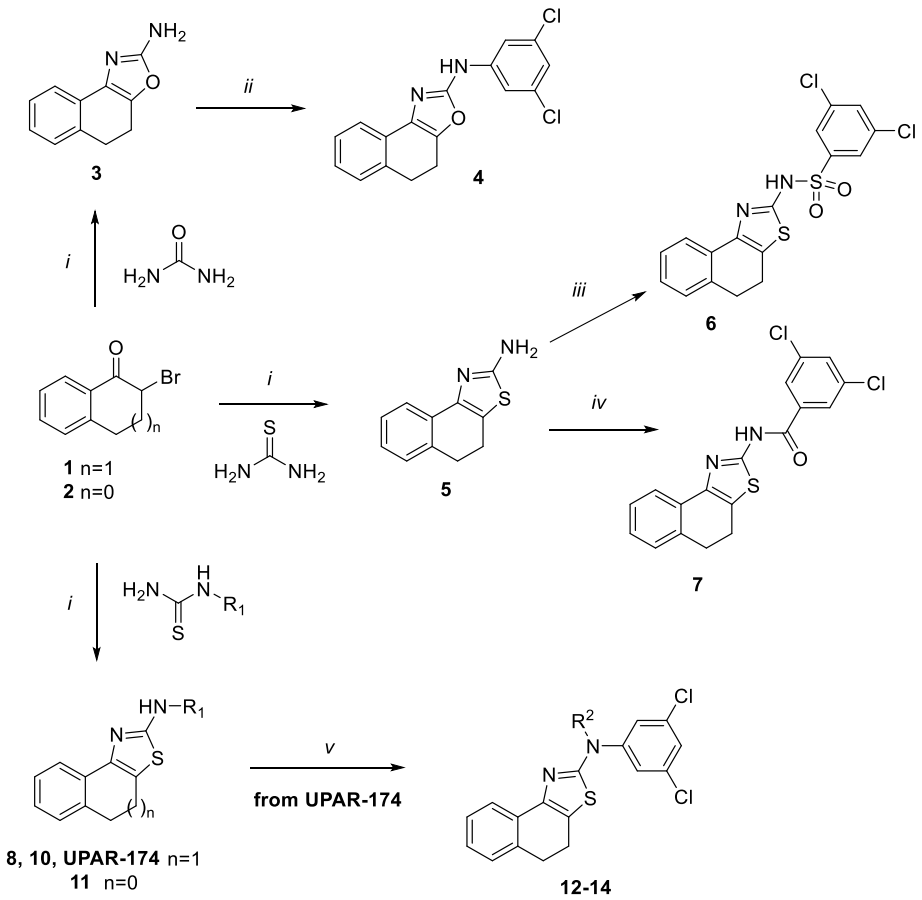

Scheme 1. *a Reagents and conditions* : *i)* absolute ethanol, 70 °C, 2-4 h, yield: 19-50%; *ii)* NaO*t*Bu, dry *tert*-butanol, dry toluene, r.t., 15 min; then, X-Phos Pd G2, MW: 130 °C, 15 minutes, yield: 18%; *iii)* 3,5-dichlorobenzenesulfonyl chloride in pyridine, 0 °C to 60 °C, overnight, yield: 13%; *iv)* 3,5-dichlorobenzoic acid, TBTU, EDC·HCl, dry DMF, 10 min; then compound **5** and TEA, r.t., 4h, yield: 27%; *v)* NaH, dry DMF, 0°C, 15 min; then the suitable halide, r.t., 6-18 h, yield: 25-80%. *b* for complete structures, see Chart 1.

Scheme 2 *(a,b)*

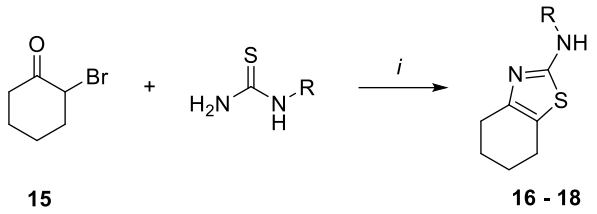

Scheme 2. *a Reagents and conditions*: *i)* absolute ethanol, 70 °C, 10-18 h, yield: 12-95%. *b* for complete structures, see Chart 1.

Compounds **4** (Scheme 1) and **19** (Scheme 3) were conveniently obtained by employing a Buchwald-Hartwig cross coupling protocol. The reaction was carried out in a microwave reactor, reacting the proper amine and the suitable aryl halide at 130°C for 15 minutes in *tert*-butanol and dry toluene and using NaO*t*Bu as base and X-Phos Pd G2 as catalyst. Compounds **12** - **14** where prepared via a nucleophilic substitution stirring compound **UPAR-174** and NaH in dry DMF for 15 minutes before adding the suitable aryl halide (Scheme 1). The synthesis of compound **7** (Scheme 1) was accomplished by activating 3,5-dichlorobenzoic acid in dry DMF with TBTU and EDC·HCl before adding compound **5** and TEA. Compound **6** was synthesized reacting compound **5** and 3,5-dichlorobenzenesulfonyl chloride in pyridine from 0°C to 65°C (Scheme 1).

Scheme 3 *a*

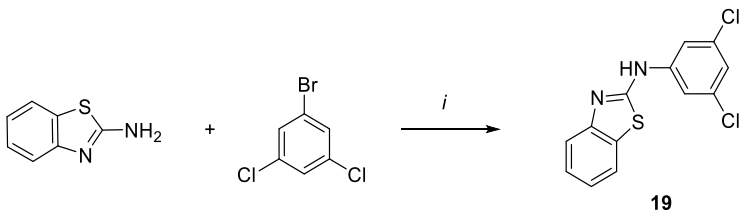

Scheme 3. *a Reagents and conditions* : *i)* NaO*t*Bu, dry *tert*-butanol, dry toluene, X-Phos Pd G2, MW: 130 °C, 15 minutes, yield: 10%.

3.4 Conclusions

Since the multiple role of EP in the drug tolerance and resistance, their inhibition is emerging as a new and attractive adjuvant strategy in the antibiotic field. Starting from **UPAR-174**, a potent but quite cytotoxic efflux pump inhibitor of *M. tuberculosis*, a Ligand Based Drug Design approach was used to define a set of Structure-Activity and Structure-Toxicity Relationships, to be then combined to deliver an improved hit compound. The two main results of this investigation were the understanding of the characteristics ensuring a promising efflux pump inhibitory activity and the disclosure of an encouraging derivative (compound **11**, Figure 3), with activity comparable to **UPAR-174** but with improved toxic profile.

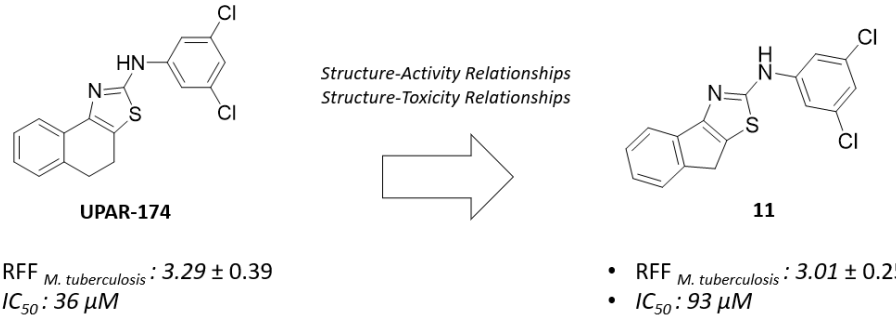

Figure 3. *Optimization of compound UPAR-174 to compound 11*

In addition, although further studies are needed in order to better characterize the biological properties of compound **11**, the fact that this new EPI chemotype has proved its efficacy also toward *M. smegmatis* strains suggests that this class of compounds is a valuable adjuvant tool not only for *M. tuberculosis*, but also for other Nontubercular infections in which EPs play a crucial role in resistance and tolerance.

3.5 Material and methods

All the reagents were purchased from Sigma-Aldrich and Alfa-Aesar at reagent purity and, unless otherwise noted, were used without any further purification. Dry solvents used in the reactions were purchased from Sigma Aldrich. Reactions were monitored by thin layer chromatography on silica gel-coated aluminum foils (silica gel on Al foils, SUPELCO Analytical, Sigma-Aldrich) at both 254 and 365 nm wavelengths. Where indicated, intermediates and final products were purified through silica gel flash column chromatography (silica gel, 0.040-0.063 mm), using appropriate solvent mixtures. ^{1}H-NMR and ^{13}C-NMR spectra were recorded on BRUKER AVANCE spectrometers (^{1}H at 300 or 400 MHz and ^{13}C at 75 or 101 MHz respectively), using residual solvents as internal standards in all cases. ^{1}H-NMR spectra are reported in this order: δ ppm (multiplicity, number of protons). Standard abbreviation indicating the multiplicity was used as follows: s = singlet, d = doublet, dd = doublet of doublets, t = triplet, q = quadruplet, m = multiplet and br = broad signal. HPLC/MS experiments were performed with HPLC: Agilent 1100 series, equipped with a Waters Symmetry C18, 3.5 µm, 4.6 mm x 75 mm column and MS: Applied Biosystem/MDS SCIEX, with API 150EX ion source. HR-MS experiments were performed with LTQ ORBITRAP XL THERMO.
All compounds were tested as 95–100% purity samples (by HPLC/MS).

3.5.1 Synthetic chemistry

General method A: Hantzsch synthesis. The suitable α-bromoketone (1 eq) and the proper thiourea (1 eq), were solubilized in absolute ethanol (4 mL/mmol) and reacted at 70 °C until consumption of the starting materials as indicated by TLC (30% v/v ethyl acetate in petroleum ether). After cooling, the desired compound was collected by filtration when precipitated in the reaction mixture. When the precipitation of the desired compound was not observed, reaction mixture was evaporated under reduced pressure, partitioned between water (5 mL) and EtOAc (5 mL), extracted with EtOAc (20 mL x3) and purified by flash column chromatography. Purification conditions, yields and analytical data are reported below.

General method B: nucleophilic substitution. UPAR-174 (1 eq) was added to a suspension of NaH (2 eq) in dry DMF (10 ml/mmol) at 0 °C. After stirring for 15 minutes, the suitable halide (1.3 eq) was added and the reaction was stirred at room temperature until the complete consumption of the starting material, as indicated by TLC (1% v/v ethyl acetate in hexane). Then water was carefully added and the mixture was extracted with ethyl acetate (3 x 10 mL). Organic layers were collected, dried over Na_2SO_4, and purified by flash column chromatography.

General method C: Buchwald-Hartwig cross coupling . The proper amine (1 eq), the suitable aryl halide (0.5 eq) and NaO*t*Bu (1 eq) were dissolved in a mixture of *tert*-Butanol (0.5 mL/mmol) and dry toluene (2.5 mL/mmol). Reaction mixture was stirred under nitrogen atmosphere for 15 minutes. Then, a catalytic amount of X-Phos Pd G2 (0.1 eq) was added and the reaction mixture was irradiated with microwaves at 130 °C for 15 minutes. After this time the TLC showed the complete consumption of the starting materials. The mixture was quenched with H_2O, extracted with ethyl acetate (3 x 10 mL) and purified by flash column chromatography. Purification conditions, yields and analytical data are reported below.

***N*-(3,5-dichlorophenyl)-4,5-dihydronaphtho[1,2-d]thiazol-2-amine (UPAR-174)**

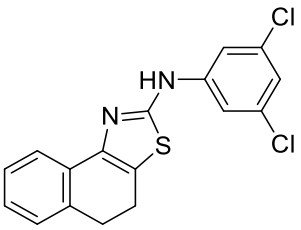

The title compound was synthesized as previously reported.[20] Analytica data matched those reported.

2-bromo-3,4-dihydronaphthalen-1(2H)-one (1)

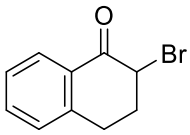

Compound **1** was synthesized as previously reported.[17] Analytical data matched those reported.

2-bromo-2,3-dihydro-1H-inden-1-one (2)

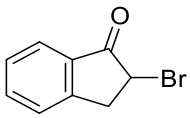

Compound **1** was synthesized as previously reported.[17] Analytical data matched those reported.

4,5-dihydronaphtho[1,2-d]oxazol-2-amine (3)

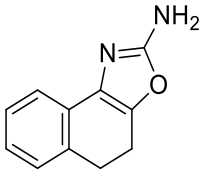

Compound **1** (500 mg, 2.22 mmol, 1 eq) and urea (1.33 g, 22.21 mmol, 10 eq) were solubilized in absolute ethanol (8 mL) and reacted at 70 °C until consumption of the starting materials as indicated by TLC (30% v/v ethyl acetate in petroleum ether). After the complete consumption of the starting material, water was added to the mixture and it was extracted with ethyl acetate (3 x 10 mL). The organic layers were collected, washed with brine (1 x 10 mL) and dried over Na_2SO_4. The solvent was removed under vacuum and the crude material was purified by silica gel flash column chromatography column eluting from 15% to 30% v/v petroleum ether in ethyl acetate. The title compound was obtained as a light brown powder. Yield 21%. ^{1}H-NMR (300 MHz, DMSO-d_6) δ: 7.26 (1H, d, *J*=7.4 Hz), 7.21 - 7.13 (2H, m), 7.10 - 7.03 (1H, m), 3.04 (2H, t, *J*=8.1 Hz), 2.81 (2H, t, *J*=8.1 Hz); ^{13}C-NMR (101 MHz, DMSO-d_6) δ: 161.6, 140.4, 133.5, 132.9,

131.0, 128.2, 127.0, 126.1, 120.4, 28.8, 20.4; HR-MS analysis: calculated for $C_{11}H_{10}N_2O$: 186.08; found: 187.08682 $[M+H]^+$.

***N*-(3,5-dichlorophenyl)-4,5-dihydronaphtho[1,2-d]oxazol-2-amine (4)**

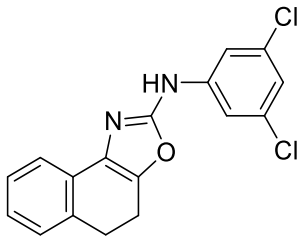

Compound **3** (80 mg, 0.43 mmol, 1 eq) and 1-bromo-3,5-dichlorobenzene were reacted following the **general method C**. The crude was purified by flash column chromatography eluting with 2% v/v ethyl acetate in hexane and the title compound was obtained as a yellow powder. Yield 18%. ^{1}H-NMR (400 MHz, $CDCl_3$) δ: 7.58 (1H, d, *J*=7.9 Hz), 7.49-7.48 (2H, m), 7.28 - 7.23 (1H, m), 7.20 - 7.13 (2H, m), 7.02 - 7.00 (1H, m), 3.17 (2H, t, *J*=8.2 Hz), 2.96 (2H, t, *J*=8.2 Hz); ^{13}C-NMR (101 MHz, DMSO-d_6) δ: 161.6, 145.6, 140.4, 133.9, 132.1, 131.0, 128.2, 126.1, 120.4, 124.2, 122.7, 28.8, 21.2; HR-MS analysis: calculated for $C_{17}H_{12}Cl_2N_2O$: 330.03; found: 331.03093 $[M+H]^+$.

4,5-dihydronaphtho[1,2-d]thiazol-2-amine (5)

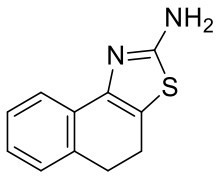

Compound **1** (110 mg, 0.49 mmol, 1 eq) and thiourea were reacted following the **general method A**. After cooling, the title compound was collected by filtration as white powder. Yield = 47%. ^{1}H-NMR (300 MHz, DMSO-d_6) δ: 8.87 (2H, bs), 7.58 - 7.53 (1H, m), 7.36 - 7.24 (3H, m), 3.04 - 2.96 (2H, m), 2.86 - 2.78 (2H, m); ^{13}C-NMR (101 MHz, DMSO-d_6) δ: 169.6, 134.9, 128.9, 128.8, 127.4, 126.3, 122.1, 175.5, 28.2, 21.2. HR-MS analysis: calculated for $C_{11}H_{10}N_2S$: 202.06; found: 203.06375 $[M+H]^+$.

Synthesis of 3,5-dichloro-*N*-(4,5-dihydronaphtho[1,2-d]thiazol-2-yl)benzenesulfonamide (6)

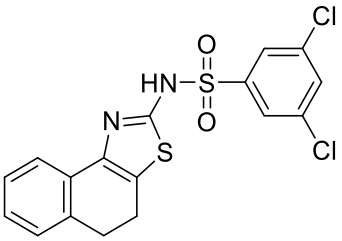

A solution of 3,5-dichlorobenzenesulfonyl chloride (73 mg, 0.30 mmol, 1.5 eq) in anhydrous pyridine (1 mL) was added dropwise to a suspension of compound **5** (40 mg, 0.20 mmol, 1 eq) in dry pyridine (1 mL) at 0 °C (ice bath). After stirring at 60 °C overnight, the reaction mixture was cooled down at room temperature, then water was added and the mixture extracted with ethyl acetate (3 x 10 mL). The organic layers were collected, washed with brine, dried over Na_2SO_4, and purified by column chromatography eluting with 20% v/v MeOH in DCM. The title compound was obtained as a brown powder. Yield = 13%. ^{1}H-NMR (300 MHz, DMSO-d_6) δ: 12.71 (bs, 1H), 7.95-7.84 (m, 2H), 7.81-7.77 (m, 2H), 7.68-7.47 (m, 3H), 2.97 (t, *J*=7.9 Hz, 2H), 2.78 (t, *J*=7.9 Hz, 2H); ^{13}C-NMR (101 MHz, DMSO-d_6) δ: 168.2, 148.7, 142.8, 135.4, 135.0, 132.2, 128.8, 128.7, 127.4, 124.8, 121.9, 118.6, 28.2, 21.4; HR-MS analysis: calculated for $C_{17}H_{12}Cl_2N_2O_2S_2$: 409.97; found: 410.97900 $[M+H]^+$.

3,5-dichloro-*N*-(4,5-dihydronaphtho[1,2-d]thiazol-2-yl)benzamide (7)

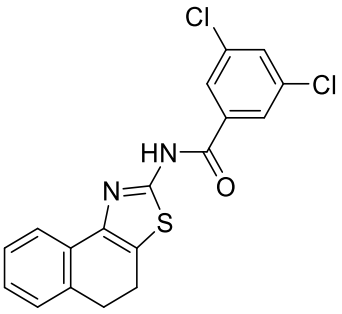

O-(Benzotriazol-1-yl)-*N,N,N',N'*-tetramethyluronium tetrafluoroborate (TBTU, 55 mg, 0.17 mmol, 1eq) and *N*-(3-Dimethylaminopropyl)-*N'*-ethylcarbodiimide hydrochloride

(EDC·HCl) (27 mg, 0.17 mmol, 1 eq) were added to a solution of 3,5-dichlorobenzoic acid (33 mg, 0.17 mmol, 1 eq) in dry DMF (0.5 mL). The reaction mixture was stirred at room temperature under nitrogen atmosphere for 15 minutes, then triethylamine (26 mg, 0.26 mmol) and compound **5** (35 mg, 0.17 mmol) were added and the mixture was stirred at room temperature until the complete consumption of the starting material, as indicated by TLC (10% v/v ethyl acetate in petroleum ether). Reaction was taken up with water (10 mL) and the mixture was extracted with ethyl acetate (3 x 10 mL). The organic layers were collected, washed with brine, dried over Na_2SO_4 and purified by flash column chromatography eluting with 3% v/v ethyl acetate in petroleum ether. The title compound was obtained as a light yellow powder. Yield = 27 %. ^{1}H-NMR (400 MHz, DMSO-d_6) δ: 12.91 (1H, s), 8.16-8.14 (2H, m), 7.90 (1H, s), 7.73 (1H, d, *J*=7.8 Hz), 7.33 - 7.19 (3H, m), 3.05 - 2.94 (4H, m); ^{13}C-NMR (101 MHz, DMSO-d_6) δ: 165.8, 163.4, 148.8, 135.3, 134.9, 132.2, 128.5, 127.6, 127.5, 127.4, 125.1, 122.5, 28.7, 21.2. HR-MS analysis: calculated for $C_{18}H_{12}Cl_2N_2OS$: 374.00; found: 375.01193 $[M+H]^+$.

***N*-phenyl-4,5-dihydronaphtho[1,2-d]thiazol-2-amine (8)**

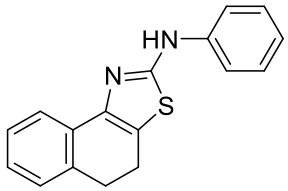

Compound **1** (135 mg, 0.60 mmol, 1eq) and phenylthiourea were reacted following the **general method A**. After precipitating in the reaction mixture, the title compound was collected by filtration as a white powder. Yield = 31%. ^{1}H-NMR (300 MHz, DMSO-d_6) δ: 10.21 (1H, s), 7.76 - 7.70 (3H, m), 7.38 - 7.15 (5H, m), 6.96 (1H, t, *J*=7.5 Hz), 3.03 - 2.96 (2H, m), 2.92 - 2.85 (2H, m); ^{13}C-NMR (101 MHz, DMSO-d_6) δ: 162.1, 141.7, 134.7, 133.7, 131.6, 129.4, 128.3, 127.3, 127.1, 122.8, 121.6, 119.3, 117.4, 28.7, 21.3. HR-MS analysis: calculated for $C_{17}H_{14}N_2S$: 278.09; found: 279.09505 $[M+H]^+$.

1-cyclohexylthiourea (9)

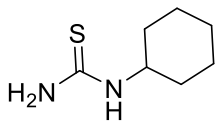

Compound **9** was synthesized as previously reported.[19] Analytical data matched those reported.

***N*-cyclohexyl-4,5-dihydronaphtho[1,2-d]thiazol-2-amine (10)**

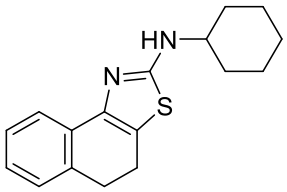

Compound **1** (130 mg, 0.58 mmol, 1 eq) and compound **9** were reacted following the **general method A**. After precipitating in the reaction mixture, the title compound was collected by filtration as white powder. Yield = 50 %. ^{1}H-NMR (300 MHz, DMSO-d_6) δ: 9.20 (s, 1H), 7.67 (m, 1H), 7.34-7.22 (m, 3H), 2.98 (m, 2H), 2.79 (m, 2H), 1.99 (m, 2H), 1.74 (s, 2H), 1.61 (m, 1H), 1.39-1.33 (m, 5H).^{13}C-NMR (101 MHz, DMSO-d_6) δ: 167.2, 135.0, 128.7, 128.5, 127.2, 122.8, 117.1, 54.9, 32.2, 28.4, 25.3, 24.6, 21.4. HR-MS analysis: calculated for $C_{17}H_{20}N_2S$: 284.13; found: 285.14228 $[M+H]^+$.

***N*-(3,5-dichlorophenyl)-8H-indeno[1,2-d]thiazol-2-amine (compound 11)**

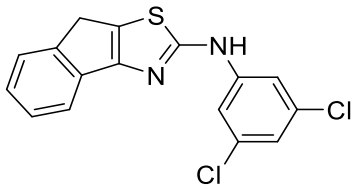

Compound **2** (500 mg, 0.24 mmol, 1eq) and 3,5-dichlorophenyltiourea were reacted following the **general method A**. After precipitating in the reaction mixture, the title compound was collected by filtration as white powder. Yield = 19%. ^{1}H-NMR (300 MHz, DMSO-d_6) δ: 10.80 (1H, s), 7.82 (2H, d, *J*=1.9 Hz), 7.59 - 7.52 (2H, m), 7.36 (1H, dt, *J*=1.1, 7.4 Hz), 7.23 (1H, dt, *J*=1.1, 7.1 Hz), 7.14 (1H, t, *J*=1.9 Hz), 3.85 (2H, s); ^{13}C-NMR (101 MHz, DMSO-d_6) δ: 166.9, 156.5, 145.8, 143.6, 137.5, 134.8, 127.3, 126.4, 125.4, 125.1,120.5, 118.3, 115.4, 32.9. HR-MS analysis: calculated for $C_{16}H_{10}Cl_2N_2S$: 331.99; found: 333.00140 $[M+H]^+$.

***N*-benzyl-N-(3,5-dichlorophenyl)-4,5-dihydronaphtho[1,2-d]thiazol-2-amine (12)**

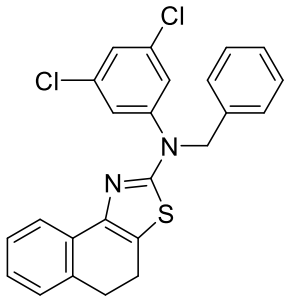

UPAR-174 (40 mg, 0.12 mmol, 1 eq) and benzyl bromide were reacted following the **general method B**. The title compound was obtained as a yellow oil after flash column chromatography eluting with 0.5% v/v ethyl acetate in hexane. Yield = 80%. ^{1}H-NMR (400 MHz, DMSO-d_6) δ: 7.64 (2H, d, *J*=1.7 Hz), 7.63 - 7.59 (1H, m), 7.41 (1H, t, *J*=1.7 Hz), 7.37 - 7.15 (8H, m), 5.31 (2H, s), 3.01 - 2.95 (2H, m), 2.89 - 2.83 (2H, m); ^{13}C-NMR (101 MHz, DMSO-d_6) δ: 166.3, 164.9, 145.4, 137.3, 135.0, 134.8, 131.4, 129.3, 129.1, 128.9, 129.3, 127.8, 127.7, 127.4, 127.3, 125.0, 122.8, 122.7, 121.5, 55.8, 28.6, 21.4. HR-MS analysis: calculated for $C_{24}H_{18}Cl_2N_2S$ 436.06; found 437.06364 $[M+H]^+$.

***N*-(3,5-dichlorophenyl)-*N*-methyl-4,5-dihydronaphtho[1,2-d]thiazol-2-amine (13)**

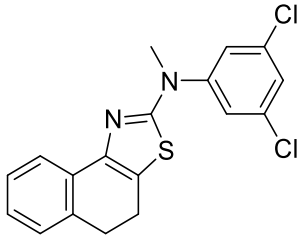

UPAR-174 (30 mg, 0.0864 mmol, 1 eq) and methyl iodide were reacted following the **general method B**. The title compound was obtained as white semisolid after flash column chromatography eluting with 0.5% v/v ethyl acetate in hexane. Yield= 60%. ^{1}H-NMR (400 MHz, $CDCl_3$) δ: 7.82 (1H, d, *J*=7.6 Hz), 7.42 (2H, d, *J*=1.8 Hz), 7.32 - 7.27 (1H, m), 7.22 - 7.18 (2H, m), 7.17 (1H, t, *J*=1.8 Hz), 3.58 (3H, s), 3.09 - 3.04 (2H, m), 2.94 - 2.89 (2H, m); ^{13}C-NMR (101 MHz, DMSO-d_6) δ:166.2, 147.8, 145.6, 134.9, 131.5, 128.4, 127.4, 127.3, 124.2, 122.7, 121.6, 121.3, 40.5, 28.6, 21.4. HR-MS analysis: calculated for $C_{18}H_{14}Cl_2N_2S$: 360.03; found: 361.03270 $[M+H]^+$.

***N*-(3,5-dichlorophenyl)-*N*-(2-(1-methylpiperidin-2-yl)ethyl)-4,5-dihydronaphtho[1,2-d]thiazol-2-amine (14)**

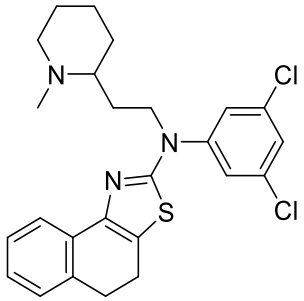

UPAR-174 (30 mg, 0.09 mmol, 1 eq) and 2(2-chloroethyl)-1-methylpiperidine hydrochloride were reacted following the **general method B**. The title compound was obtained as a brown oil after flash column chromatography eluting from 2% to 4% v/v MeOH in DCM. Yield= 33%. ^{1}H-NMR (400 MHz, $CDCl_3$) δ: 7.76 (1H, d, *J*=7.6 Hz), 7.36 (2H, d, *J*=1.8 Hz), 7.30 - 7.25 (1H, m), 7.23 (1H, t, *J*=1.8 Hz), 7.21 - 7.17 (2H, m), 4.09 (2H, t, *J*=7.6 Hz), 3.08 - 3.02 (2H, m), 2.90 - 2.85 (2H, m), 2.42 (3H, s), 2.28 - 2.19 (2H, m), 2.13 - 1.97 (2H, m), 1.87 - 1.79 (2H, m), 1.71 - 1.53 (4H, m), 1.40 - 1.26 (2H, m); ^{13}C-NMR (101 MHz, DMSO-d_6) δ: 166.2, 147.2, 145.4, 135.5, 135.3, 134.8, 131.6, 128.3, 127.3, 125.9, 124.1, 122.6, 120.5, 61.2, 56.3, 49.6, 29.9, 28.7, 25.0, 23.9, 21.4. HR-MS analysis: calculated for $C_{25}H_{27}Cl_2N_3S$: 471.13; found: 472.13748 $[M+H]^+$.

2-bromocyclohexan-1-one (15)

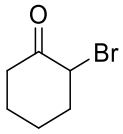

The title compound was synthesized as previously reported. Analytical data matched those reported in literature.[18]

4,5,6,7-tetrahydrobenzo[d]thiazol-2-amine (16)

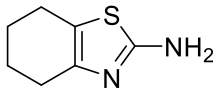

The title compound was synthesized as previously reported. Analytical data matched those reported.[21]

***N*-phenyl-4,5,6,7-tetrahydrobenzo[d]thiazol-2-amine (17)**

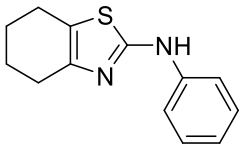

The title compound was synthesized as previously reported. Analytical data matched those reported.[22]

***N*-(3,5-dichlorophenyl)-4,5,6,7-tetrahydrobenzo[d]thiazol-2-amine (18)**

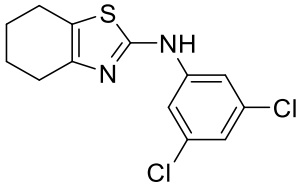

Compound **15** (50 mg, 0.28 mmol, 1 eq) and 3,5-dichlorophenyltiourea were reacted following the **general method A**. After precipitating in the reaction mixture, the title compound was collected by filtration as white powder. Yield = 12%. ^{1}H-NMR (400 MHz, DMSO-d_6) δ: 10.45 (1H, s), 7.67 (2H, d, *J*=1.8 Hz), 7.08 (1H, t, *J*=1.8 Hz), 2.62 - 2.56 (4H, m), 1.79 - 1.76 (4H, m); ^{13}C-NMR (101 MHz, DMSO-d_6) δ: 160.0, 145.6, 143.7, 134.7, 120.2, 118.4, 115.2, 31.2, 26.8, 23.4, 23.0, 22.8. HR-MS analysis: calculated for $C_{13}H_{12}Cl_2N_2S$: 298.01; found: 299.01727 $[M+H]^+$.

***N*-(3,5-dichlorophenyl)benzo[d]thiazol-2-amine (19)**

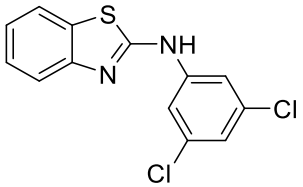

2-aminobenzothiazole (80 mg, 0.53 mmol, 1 eq) and 1-bromo-3,5-dichlorobenzene were reacted following the **general method C**. The title compound was obtained as a white powder after flash column chromatography eluting with 5% v/v ethyl acetate in hexane. Yield = 10 %. ^{1}H-NMR (300 MHz, DMSO-d_6) δ: 9.77 (1H, s), 7.67 - 7.58 (2H, m), 7.46 (1H, t, *J*=1.9 Hz), 7.30 (1H, dd, *J*=1.4, 7.6 Hz), 7.20 (1H, dt, *J*=1.4, 7.6 Hz), 7.01 (2H, d, *J*=1.9 Hz); ^{13}C-NMR (101 MHz, DMSO-d_6) δ: 141.7, 141.0, 138.5, 135.2, 133.2, 126.1, 125.1, 124.7, 116.7, 112.1. HR-MS analysis: calculated for $C_{13}H_8Cl_2N_2S$: 293.98; found: 294.98605 $[M+H]^+$.

3.5.2 Biology

Strains. *M. smegmatis* mc^2 155 and *M. tuberculosis* H37Rv ATCC27294^T reference strains belong to the culture collection maintained at the Laboratório de Micobactérias, Instituto de Higiene e Medicina Tropical, Universidade Nova de Lisboa, Lisboa, Portugal.

Determination of minimum inhibitory concentrations (MIC) using TEMA. The MIC of compounds and EtBr was determined by a TEMA as previously described.[23,24] The strains were grown in MB7H9 supplemented with 10% OADC, at 37 °C until an OD_{600} of 0.8. The inoculum was adjusted to a final cell density of approximately $5x10^5$ CFU/mL. Aliquots of 100 µL were transferred to each well of the plate that contained 100 µL of each compound at concentrations prepared from two-fold serial dilutions in MB7H9/OADC medium. Growth controls with no compound and a sterility control were included in each plate. The plates were sealed in plastic bags and incubated at 37 °C for 7 days and one more day at room temperature, after the addition of the metabolic indicator MTT (10 µL of 1:1 MTT/Tween 80). Since MTT stains viable cells in black, the MIC was defined as the lowest concentration of compound that totally inhibited bacterial growth indicated by the absence of a black precipitate. The assays were carried out at least in duplicate (biological replicates) and the final value was given as the result of two concordant values.

Measurement of EtBr efflux inhibitory activity. The capacity of the compounds to inhibit EtBr efflux was performed by a semi-automated fluorometric method using a Rotor-Gene 3000 thermocycler (Corbett Research, Australia).[6,25] Briefly, the strains were grown in MB7H9 containing 10% OADC and 0.05% Tween 80. Cultures were incubated at 37 °C until an OD_{600} of 0.8. After, the cells were centrifuged at 3500 rpm, during 3 min, room temperature. The supernatant was discarded, the pellet washed, resuspended in PBS, and centrifuged as before. After, the washed cells were resuspended in PBS and the OD_{600} adjusted to 0.8. To determine the lowest concentration of EtBr that causes accumulation, 50 µL of the bacterial suspension was added to 0.2 mL tubes containing different concentrations of EtBr that ranged from

0.125 to 5 µg/mL. The final OD_{600} of the bacterial suspension in the assay was 0.4. The assays were conducted at 37 °C in a Rotor-Gene 3000, and the fluorescence of EtBr was measured (530/585 nm) at the end of each cycle of 60 s, for 60 min. After determining the higher concentration of EtBr that do not cause accumulation, the effect of the compounds on the accumulation of EtBr was evaluated. In order to compare the activity of all compounds these were tested at the same molar concentration, 18 µM, a non-toxic concentration that not interfere with the viability of the bacteria.[11] Therefore, these assays were performed as described above with each compound at 18 µM, EtBr at the higher concentration that do not cause accumulation (determined for each strain), at 37 °C and with glucose. To better evaluate the effect of the inhibitors in the accumulation of EtBr, for each assay we determined the relative final fluorescence (RFF) at the last time point (min 60) of the assay in comparison with the control condition using the formula RFF = $(RF_{treated\text{-}RFnon\text{-}treated})/(RF_{non\text{-}treated})$.[12] High RFF values indicated that cells accumulate more EtBr under the condition used than those of the control (non-treated cells). Negative RFF values indicated that treated cells accumulated less EtBr than those of the control condition. Each assay was performed in triplicate (biological replicates) and the results presented correspond to the average of three independent assays (± SD).

Cytotoxicity assay and IC_{50} determination

Cell culture. THP-I cells were grown in suspension in RPMI 1640 culture media (Euroclone, Italy) supplemented with Sodium Pyruvate 100mM (1%; Life Technologies, USA), Gentamicin 10mg/ml (0.5%; Sigma Aldrich, USA), 2-Mercaptoethanol 50mM (0.1%; Life Technologies, USA), Glucose (0,25% g/ml) and Fetal Bovine Serum (FBS, Euroclone, Italy) at 10%. When in confluent state, cells were counted and plated at density of 500000 cells/well in 24-well plates (Sarstedt, Germany) in the presence of 50 ng/mL phorbol 12-miristate 13-acetate (PMA; Sigma Aldrich, USA) and then incubated at 37^{o}C, 5% CO_2 for 72 h to allow the differentiation into macrophages.

Cytotoxicity assay (MTT assay). MTT assay was used to assess the cytotoxicity of synthetized compounds upon THP-derived macrophages by evaluating the ability of mitochondrial succinate dehydrogenase to catalyze the enzymatic reduction of yellow water soluble 3-[4,5-dimethylthiazole-2-yl]-2,5-diphenyltetrazolium bromide (MTT; Sigma Aldrich, USA) to insoluble purple formazan, an index of cellular viability.

Differentiated macrophages were treated with different concentrations of synthetized compounds at increasing concentrations (1 µM, 10 µM, 50 µM and 100 µM, in triple (biological replicates)) dissolved in RPMI 1640 supplemented with 1% FBS for 72 hours. Afterwards, cells were incubated with a solution of 1mg/ml of MTT dissolved in RPMI 1640, supplemented with 5% FBS, at 37°C, 5% CO_2 for 2 hours in dark. The solution was then removed, and intracellular formazan was solubilized by adding 0.2 mL DMSO per well and shaking the plates for 10 minutes. Subsequently, absorbance was measured on a cellular lysate aliquot (0,15 mL) using a Spark® Tecan fluorimeter recording the absorbance of each sample at 570 nm.

Statistical analysis. Statistical analysis were performed using GraphPad Prism software version 7.0 (GraphPad Software Inc., La Jolla, CA). Results were expressed as % cell viability at each concentration compared to viability of non-treated cells (100% viability). IC_{50} values for each tested compound were calculated by interpolating the % viability obtained at each concentration through a non-linear regression analysis.

3.6 References

(1) Li, G.; Zhang, J.; Li, C.; Guo, Q.; Jiang, Y.; Wei, J.; Qiu, Y.; Zhao, X.; Zhao, L.; Lu, J.; Wan, K. Antimycobacterial Activity of Five Efflux Pump Inhibitors against Mycobacterium Tuberculosis Clinical Isolates. *J. Antibiot. (Tokyo)* **2016**, *69* (3), 173–175.

(2) Warman, A. J.; Rito, T. S.; Fisher, N. E.; Moss, D. M.; Berry, N. G.; O'Neill, P. M.; Ward, S. A.; Biagini, G. A. Antitubercular Pharmacodynamics of Phenothiazines. *J. Antimicrob. Chemother.* **2013**, *68* (4), 869–880.

(3) Weinstein, E. A.; Yano, T.; Li, L.-S.; Avarbock, D.; Avarbock, A.; Helm, D.; McColm, A. A.; Duncan, K.; Lonsdale, J. T.; Rubin, H. Inhibitors of Type II NADH:Menaquinone Oxidoreductase Represent a Class of Antitubercular Drugs. *Proc. Natl. Acad. Sci. U. S. A.* **2005**, *102* (12), 4548–4553.

(4) Abbate, E.; Vescovo, M.; Natiello, M.; Cufré, M.; García, A.; Gonzalez Montaner, P.; Ambroggi, M.; Ritacco, V.; van Soolingen, D. Successful Alternative Treatment of Extensively Drug-Resistant Tuberculosis in Argentina with a Combination of Linezolid, Moxifloxacin and Thioridazine. *J. Antimicrob. Chemother.* **2012**, *67* (2), 473–477.

(5) Machado, D.; Girardini, M.; Viveiros, M.; Pieroni, M. Challenging the Drug-Likeness Dogma for New Drug Discovery in Tuberculosis. *Front. Microbiol.* **2018**, *9*, 1367.

(6) Machado, D.; Couto, I.; Perdigão, J.; Rodrigues, L.; Portugal, I.; Baptista, P.; Veigas, B.; Amaral, L.; Viveiros, M. Contribution of Efflux to the Emergence of Isoniazid and Multidrug Resistance in Mycobacterium Tuberculosis. *PLOS ONE* **2012**, *7* (4), e34538.

(7) Adams, K. N.; Szumowski, J. D.; Ramakrishnan, L. Verapamil, and Its Metabolite Norverapamil, Inhibit Macrophage-Induced, Bacterial Efflux Pump-Mediated Tolerance to Multiple Anti-Tubercular Drugs. *J. Infect. Dis.* **2014**, *210* (3), 456–466.

(8) Singh, K.; Kumar, M.; Pavadai, E.; Naran, K.; Warner, D. F.; Ruminski, P. G.; Chibale, K. Synthesis of New Verapamil Analogues and Their Evaluation in Combination with Rifampicin against Mycobacterium Tuberculosis and Molecular Docking Studies in the Binding Site of Efflux Protein Rv1258c. *Bioorg. Med. Chem. Lett.* **2014**, *24* (14), 2985–2990.

(9) Gupta, S.; Cohen, K. A.; Winglee, K.; Maiga, M.; Diarra, B.; Bishai, W. R. Efflux Inhibition with Verapamil Potentiates Bedaquiline in Mycobacterium Tuberculosis. *Antimicrob. Agents Chemother.* **2014**, *58* (1), 574–576.

(10) Pieroni, M.; Machado, D.; Azzali, E.; Santos Costa, S.; Couto, I.; Costantino, G.; Viveiros, M. Rational Design and Synthesis of Thioridazine Analogues as Enhancers of the Antituberculosis Therapy. *J. Med. Chem.* **2015**, *58* (15), 5842–5853.

(11) Machado, D.; Azzali, E.; Couto, I.; Costantino, G.; Pieroni, M.; Viveiros, M. Adjuvant Therapies against Tuberculosis: Discovery of a 2-Aminothiazole Targeting Mycobacterium Tuberculosis Energetics. *Future Microbiol.* **2018**, *13* (12), 1383–1402.

(12) Machado, L.; Spengler, G.; Evaristo, M.; Handzlik, J.; Molnár, J.; Viveiros, M.; Kiec-Kononowicz, K.; Amaral, L. Biological Activity of Twenty-Three Hydantoin Derivatives on Intrinsic Efflux Pump System of Salmonella Enterica Serovar Enteritidis NCTC 13349. *Vivo Athens Greece* **2011**, *25* (5), 769–772.

(13) Haake, Paul.; Miller, W. B. A Comparison of Thiazoles and Oxazoles. *J. Am. Chem. Soc.* **1963**, *85* (24), 4044–4045. https://doi.org/10.1021/ja00907a039.

(14) Jin, Z. Imidazole, Oxazole and Thiazole Alkaloids. *Nat. Prod. Rep.* **2006**, *23* (3), 464–496.

(15) Mathew, B.; Hobrath, J. V.; Connelly, M. C.; Guy, R. K.; Reynolds, R. C. Oxazole and Thiazole Analogs of Sulindac for Cancer Prevention. *Future Med. Chem.* **2018**, *10* (7), 743–753.

(16) Kumar, P.; Nagarajan, A.; Uchil, P. D. Analysis of Cell Viability by the MTT Assay. *Cold Spring Harb. Protoc.* **2018**, *2018* (6).

(17) Prokopowicz, M.; Młynarz, P.; Kafarski, P. Synthesis of Phosphonate Derivatives of 2,3-Dihydroindene. *Tetrahedron Lett.* **2009**, *50* (52), 7314–7317.

(18) Zhang, G.-B.; Wang, F.-X.; Du, J.-Y.; Qu, H.; Ma, X.-Y.; Wei, M.-X.; Wang, C.-T.; Li, Q.; Fan, C.-A. Toward the Total Synthesis of Palhinine A: Expedient Assembly of Multifunctionalized Isotwistane Ring System with Contiguous Quaternary Stereocenters. *Org. Lett.* **2012**, *14* (14), 3696–3699.

(19) Grosjean, S.; Triki, S.; Meslin, J.-C.; Julienne, K.; Deniaud, D. Synthesis of Nitrogen Bicyclic Scaffolds: Pyrimido[1,2-a]Pyrimidine-2,6-Diones. *Tetrahedron* **2010**, *66* (52), 9912–9924.

(20) Pieroni, M.; Wan, B.; Cho, S.; Franzblau, S. G.; Costantino, G. Design, Synthesis and Investigation on the Structure–Activity Relationships of N-Substituted 2-Aminothiazole Derivatives as Antitubercular Agents. *Eur. J. Med. Chem.* **2014**, *72*, 26–34.

(21) Annadurai, S.; Martinez, R.; Canney, D. J.; Eidem, T.; Dunman, P. M.; Abou-Gharbia, M. Design and Synthesis of 2-Aminothiazole Based Antimicrobials Targeting MRSA. *Bioorg. Med. Chem. Lett.* **2012**, *22* (24), 7719–7725.

(22) Zhang, B.; Shi, L. CuBr2 Mediated Synthesis of 2-Aminothiazoles from Dithiocarbamic Acid Salts and Ketones. *Phosphorus Sulfur Silicon Relat. Elem.* **2019**, *194* (12), 1134–1139.

(23) Caviedes, L.; Delgado, J.; Gilman, R. H. Tetrazolium Microplate Assay as a Rapid and Inexpensive Colorimetric Method for Determination of Antibiotic Susceptibility of Mycobacterium Tuberculosis. *J. Clin. Microbiol.* **2002**, *40* (5), 1873–1874.

(24) Coelho, T.; Machado, D.; Couto, I.; Maschmann, R.; Ramos, D.; von Groll, A.; Rossetti, M. L.; Silva, P. A.; Viveiros, M. Enhancement of Antibiotic Activity by Efflux Inhibitors against Multidrug Resistant Mycobacterium Tuberculosis Clinical Isolates from Brazil. *Front. Microbiol.* **2015**, *6*, 330.

(25) Viveiros, M.; Rodrigues, L.; Martins, M.; Couto, I.; Spengler, G.; Martins, A.; Amaral, L. Evaluation of Efflux Activity of Bacteria by a Semi-Automated Fluorometric System. *Methods Mol. Biol. Clifton NJ* **2010**, *642*, 159–172.

4. Exploring the inhibition of Proteasome accessory factor A (PafA) as innovative antitubercular drug target

Another part of my PhD thesis has regarded the development of a biochemical platform for the screening of inhibitors of Proteasome accessory factor A (PafA), that represents a key enzyme in the intracellular protein degradation of *M. tuberculosis*. To this purpose, during my PhD program, I have spent a short period at the University of Piemonte Orientale in Novara, to gain insights on the expression and purification of mycobacterial proteins.

4.1 Introduction

The increasing emergence of resistant *M. tuberculosis* has prompted researches to investigate novel molecular targets, toward which resistance has not yet developed. The antitubercular first-line and second-line drugs cover different molecular targets, mainly involved in two processes: the protein synthesis and biosynthesis of molecular components of the cell wall.[1] Besides these pathways, other targets were found to be essential for *M. tuberculosis,* thus potentially interesting for the development of inhibitors.

A promising antibacterial drug target/pathway should possess the following characteristics:

- It should be involved in essential process for the bacterial survival or virulence
- It should be present in bacteria but not in the host, in order to allow the development of selective inhibitors, avoiding the toxic effect derived from the interaction with its human counterpart.
- In addition, it should be ideally present only in a single bacterial species in order to prevent the horizontal transfer of resistance genes.

In the past few years, several studies have focused their attention on the role of bacterial proteasome and, in general, of intracellular protein degradation system of *M. tuberculosis*, suggesting its implication in bacterial virulence and survival.[2–5] This intracellular proteolytic machinery is constituted by the proteasome and the signalling

pathway responsible for tagging the target protein which is supposed to undergo proteasomal degradation.[6] Although the functional similarity with the eukaryotic ubiquitin-proteasome system (see Chapter 4), post-translational modification of the target protein in prokaryotic cells occurs *via* a chemically distinct pathway.[7] This process consists in a covalent attachment of a peptide of 64 amino acids to the ε-amino group of a lysine on the target protein.[8] For its functional analogy to ubiquitin, its eukaryotic counterpart, this peptide was called Prokaryotic ubiquitin-like protein (Pup), even if it does not share any sequence analogy to ubiquitin except for the di-glycine motif near the carboxyl terminus.[4] Briefly, Pup is encoded as a 64 amino acid peptide ending with a C-terminal glutamine. The enzyme Deaminase of Pup (Dop) catalyses the conversion of the C-terminal glutamine into glutamate and it is responsible for the activation of the Pup into PupE. In fact, the C- terminal glutamate γ-carboxylate represents the functional group needed for covalent linkage of PupE with the ε-amino groups of a lysine on the target protein.[9] In contrast to ubiquitination, which employs a cascade of enzymes, the attachment of Pup (pupylation) is promoted only by the proteasome accessory factor A (PafA), an ATP dependent enzyme.[10]

Figure 1.

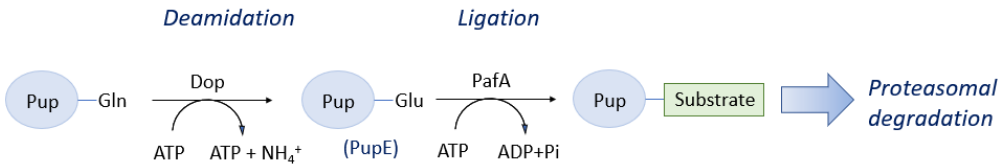

Figure 1. *Pup-proteasome system (PPS)*

Once pupylated, the target protein is recognized by the proteasome and degraded. While in all eukaryotes protein degradation requires ubiquitin-proteasome system, in bacterial kingdom Pup tagging and proteasome are conserved only in species belonging to the phyla Actinobacteria, among which *M. tuberculosis*, and in the Gram-negative genus Nitrospira.[11–13] Other bacterial species rely on smaller and less complex proteases for protein degradation.[14] Many pupylation substrates of *M. tuberculosis* has

been identified, among those the enzymes 3-methyl-2-oxobuthanoate hydroxymethyl transferase (PanB), inositol-1-phosphate synthetase (Ino1) and the malonyl CoA-acyl carrier protein transacylase (FabD), as well as the enzyme PafA itself.[15]

Although the Pup-proteasome system (PPS) is, as yet, not fully understood, it has proved to be essential for both virulence and persistence of *M. tuberculosis* inside the host.[2,9,16,17] In a murine tubercular infection model, deletion of PafA significantly increased the survival of the infected mice.[17] Moreover, the PPS system was found to be involved in the resistance of *M. tuberculosis* to nitric oxide (NO), a bactericidal molecule synthesized by macrophages as first defence against tubercular invasion. In fact, a recent screening of over 10,000 mycobacterial transposon mutants for the identification of molecular mechanism linked to NO sensitivity, allowed to identify 12 mutants, among which five had insertions in proteasome-associated genes.[2] In addition, a more recent study proved that the pupylation is also involved in iron homeostasis.[3]

Protein catabolism regulated by PPS might play a crucial role upon nitrogen starvation, a characteristic of the granuloma-like lesions, where many *Mycobacterial* species have the peculiar ability to survive.[18,19] In fact, a study on *M. smegmatis*, proved that the PPS system is upregulated during nitrogen starvation, suggesting that, under nutrient limitation, mycobacterial survival depends on the proteasome-mediated amino acid recycling.[5]

Darwin and co-workers[20] demonstrated that the N-terminally truncated PupE (31-64) was sufficient for the pupylation in *M. tuberculosis* and a subsequent study by Smirnov and co-workers[21] further refined the minimum recognition motif to the C-terminal sequence 39-64. In 2013, the crystal structure of the complex between *Corynebacterium glutamicum* PafA and the truncated PupE (38-64) confirmed the hypothesis that only the C-terminal region of the PupE was involved in the binding and provided insights about their interaction.[22] Since the binding pocket of PafA for PupE is highly conserved throughout the species, and since PupE of *C. glutamicum* shows high identity to that of *M. tuberculosis* at the C-terminal,[22,23] the hints provided by this

seminal study could be extended to the PupE-PafA interaction in *M. tuberculosis*. The crystal structure showed that the intrinsically disordered protein Pup folds into the enzyme in two α-helixes called Helix 1 (S38-L47) and Helix 2 (A51-Y58), separated by a linker (E48–N50). The interactions between the Pup and PafA are highlighted in Figure 2.

Figure 2.

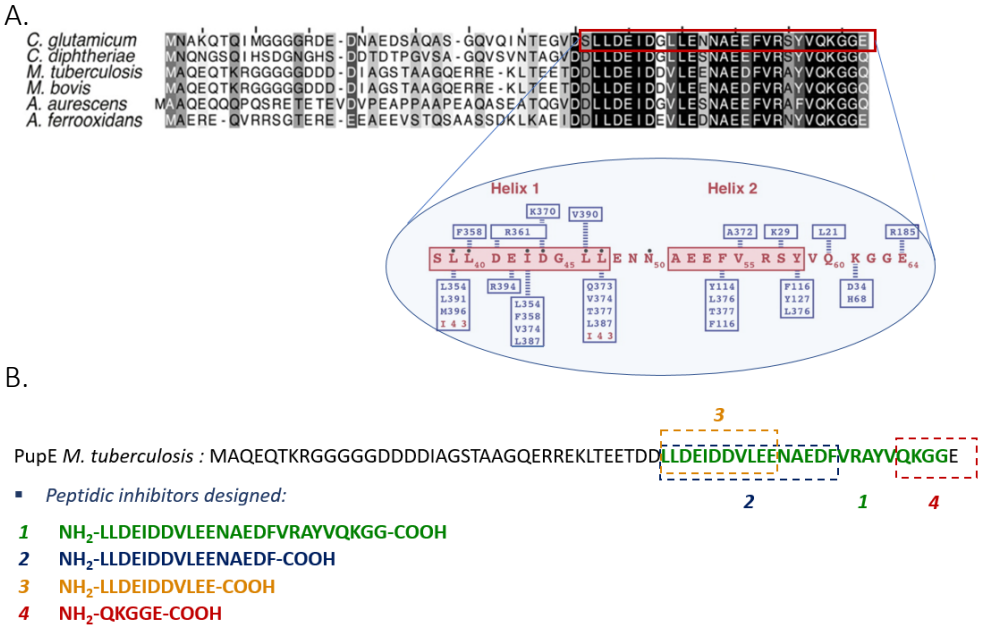

Figure 2. *(A) Alignment of Pups from different actinobacteria. In the blue cycle the sequence of C. glutamicum Pup (red) is showed with H1 and H2 outlined as red boxes. PafA–Pup interactions are indicated with dashed lines. PafA residues are colored blue and Pup residues red.*[22] *(B) The sequence of the M. tuberculosis Pup and the sequences of the peptid designed as inhibitors.*

Starting from these premises, in this chapter the possibility to interfere with PafA/PupE interaction was investigated, with the aim to pave the way for the future development of PafA competitive inhibitors.

4.2 Results and discussion

To study the possibility to interfere with Pup-PafA interaction *in vitro*, we first set up a biochemical assay involving: (i) the enzyme PafA, (ii) the activated form of the Pup with a glutamate at C-terminal (PupE) and (iii) the enzyme PanB, as substrate of pupylation. The *M. tuberculosis* enzymes PafA and PanB were expressed in *E. coli* and purified according to an optimized protocol described in the section "Materials and Methods", while the peptide PupE was purchased. The activity of PafA was evaluated *via* a coupled assay in presence of PK/LDH (pyruvate kinase/lactate dehydrogenase) enzymes (Figure 3). In this assay, the ADP generated from the pupylation reaction by PafA is used by the PK/LDH enzymes to oxidize NADH to NAD^+. Since NADH, but not NAD^+, absorbs energy at a wavelength of 340 nm, its conversion into NAD^+ results in a decreasing absorbance at 340 nm, which is proportional to the ATP consumed by PafA in the pupylation reaction. The reaction was carried out with ATP (500 µM), phosphoenolpyruvate (PEP, 2 mM), PK/LDH enzymes, NADH (150 µM), PupE (4 µM), PanB (2 µM) and PafA, in a reaction buffer containing Mg^{2+} as cofactor: this allowed to assess that the expressed and purified PafA was functional (see Materials and Methods).

Figure 3.

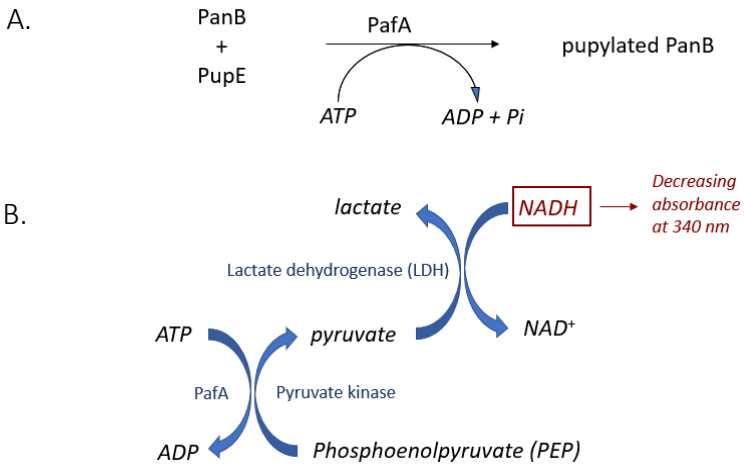

Figure 3. *(A) Schematic representation of the pupylation reaction catalysed by PafA; (B) The ADP generated by PafA is used by the PK/LDH enzymes to oxidize NADH to NAD+ (decreasing abs. at 340 nm).*

Then, the K_M of ATP for PafA was calculated using the same coupled assay described above, in presence of six concentrations of ATP on a microplate reader. The K_M obtained (4.89 ± 1.04 μM, Figure 4) was found to be comparable to that derived from the experiment based on radiolabelled ATP recently reported (8.7 ± 3.7 μM),[24] confirming this assay as a reliable way to evaluate *in vitro* pupylation reaction. Moreover, the assay herein presented is also safer, as it does not require radiolabelled molecules, and cheaper compared to that reported in literature. This assay may then serve as a valuable biochemical platform for the evaluation of potential PafA inhibitors.

Chart 1.

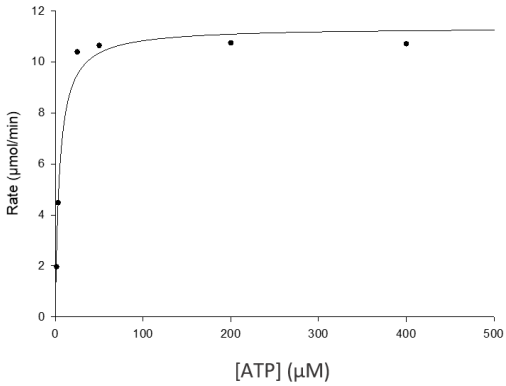

	Value	±Std Error	95% Conf. Interval
Vmax	11.3533	0.4276	10.1661 to 12.5405
K_M	4.8925	1.0351	2.0185 to 7.7664

Chart 1. Determination of the K_M of PafA for the ATP

Starting from the sequence of the PuPE and considering the interaction between PupE and PafA described above, four Pup segments (Chart 1) were synthesized and their ability to interfere with pupylation was evaluated. Peptide **1** represents the sequence 39-64 of Pup, containing the two helixes, the linker sequence and the disordered C-terminal region apart from the terminal glutamate, removed in order to avoid the transfer of this Pup segments to PanB. **2** (39-54) contains the Helix 1 residues and half of the Helix 2 until the phenylalanine 54, involved in many key interactions with PafA. Compound **3** (39-49) contains all the key residues of the Helix 1. For comparative purpose, also **4** (60-64) containing the C-terminal disordered region was tested even if the crystal suggested a marginal role in the interaction.

The peptide synthesized were tested using the PK/LDH couple assay described before. The assay was performed using the similar conditions to the that above described. The peptidic inhibitors **1**,**3** and **4** were tested at 50 µM, while **2** could only be tested at 25 µM, as solubility issues occurred at higher concentrations.

Chart 2.

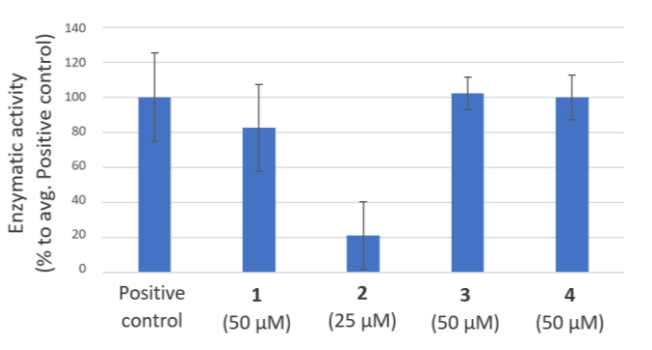

Chart 2. *Enzymatic activity of PafA in presence of compounds 1-4. Activity was calculated as % to average positive control (no inhibitor).*

No significant inhibition of pupylation was observed in presence of compounds **1**, **3** and **4** (Chart 2), while compound **2**, which is a segment of **1**, surprisingly provided an encouraging inhibition, especially considering that it was tested at a lower concentration. Although further studies are needed to explain the reason of such a counterintuitive activity, it might be speculated that the number of amino acids composing the peptides may play a role in their structural conformation, that, in turn, affects the interaction of key amino acids with the target binding site.

4.3 Conclusions

In this study a reliable biochemical platform for the screening of pupylation inhibitors was set up. Preliminary investigations on the inhibitory properties of some Pup fragments were carried out and a promising inhibitory sequence of 16 amino acids was identified. Although deeper studies are necessary, these findings might be useful both for the synthesis of valuable chemical tools to investigate protein degradation in *M. tuberculosis*, and for the preparation of potential inhibitors of this important catabolic pathway.

4.4 Materials and methods

All chemical reagents were purchased from Sigma Aldrich or Novabiochem and used without any further purification. PupE peptide was purchased from Gentaur. Single spectrophotometric analysis were performed at 340 nM using VARIAN-CARY 50 BIO UV/VISIBLE spectrophotometer. Multiplate analysis were performed at 340 nM using TECAN SUNRISE spectrophotometer.

All compounds were tested as 95–100% purity samples (by UPLC/MS).

4.4.1 Synthetic chemistry

The synthesis of the peptides **1-3** was carried out using Fmoc-Solid Phase Peptide Synthesis (SPPS) on Wang resins preloaded with the C-terminal amino acids using an automatic synthesizer (Sirio 1, Biotage). Amino acid couplings were performed in presence of 5 eq. of amino acid, 10 eq. of DIEA and 4.7 eq. of HBTU to the initial loading of the resin. Fmoc-deprotection was achieved by treatment of the resin with 40 % (w/v) piperidine. After completion of peptide synthesis, the peptide-resins were dried under vacuum; cleavage of the peptides from the resins was achieved by treatment with a mixture of TFA, TIS and water (95: 2.5: 2.5) for 2 h at room temperature. The resins were removed by filtration and washed with TFA. The combined filtrates were then dried under N_2 flux. Cold ethyl ether (5 °C) was added to the residues to precipitate the unprotected peptides. The products obtained were characterized by RP-UPLC-ESI-MS.

The synthesis of the peptide **4** was carried out using Fmoc-SPPS on Wang resin preloaded with the C-terminal amino acid in a solid phase reaction vessel following a double coupling scheme. *Resin swelling*: Fmoc-Glu(O*tBu*) Wang resin (loading: 0.70 mmol/g, 40 mg, 0.028 mmol, 1 eq.) was swollen in a solid phase reaction vessel with dry DMF (3 mL) under mechanical stirring; after 40 min the solvent was drained and the resin was washed with DCM (2 × 3 mL) and DMF. *Peptide coupling*: a preformed solution of the suitable Fmoc-protected amino acid (0.042 mmol, 1.5 eq.) in dry DMF (3 mL) was treated with HATU (0.056 mmol, 2 eq.), HOAt (0.056 mmol, 2 eq.), and 2,4,6-collidine (0.056 mmol, 2 eq.) and stirred for 10 min before adding to the resin. The

mixture was shaken at room temperature for 2 h. The solution was drained and the resin was washed with DMF (2 ×) and DCM (2 ×). A double coupling was performed with fresh reagents and stirred for additional 2 h to ensure the reaction completion. Fmoc-deprotection: The resin was treated with 20% v/v piperidine in DMF (3 mL) and the mixture was stirred for 30 min. The solution was drained and the resin was washed with DMF (3 mL × 2), iPrOH, (3 mL × 2), DCM (3 mL × 2). *Resin cleavage:* resin cleavage was achieved by treatment with a mixture of TFA, TIS and water (95: 2.5: 2.5) for 2 h at room temperature. After this time, the solution was collected and the resin was washed several times with DCM. The combined solutions were then dried under N_2 flux. Cold ethyl ether (5 °C) was added to the residues to precipitate the unprotected peptides.

Characterization of the compounds:

The peptides obtained were characterized by RP-UPLC-ESI-MS, using ACQUITY UPLC® Peptide BEH C18 Column, 300 Å, 1.7 µm, 2.1 mm X 150 mm. Solvent A: 0.1% v/v formic acid in H_2O; Solvent B: 0.1% v/v formic acid in CH_3CN; Gradient: 0 min: 100% A; 7 min: 100% A; 47 min: 53.5 % A.

- Compound **1**:

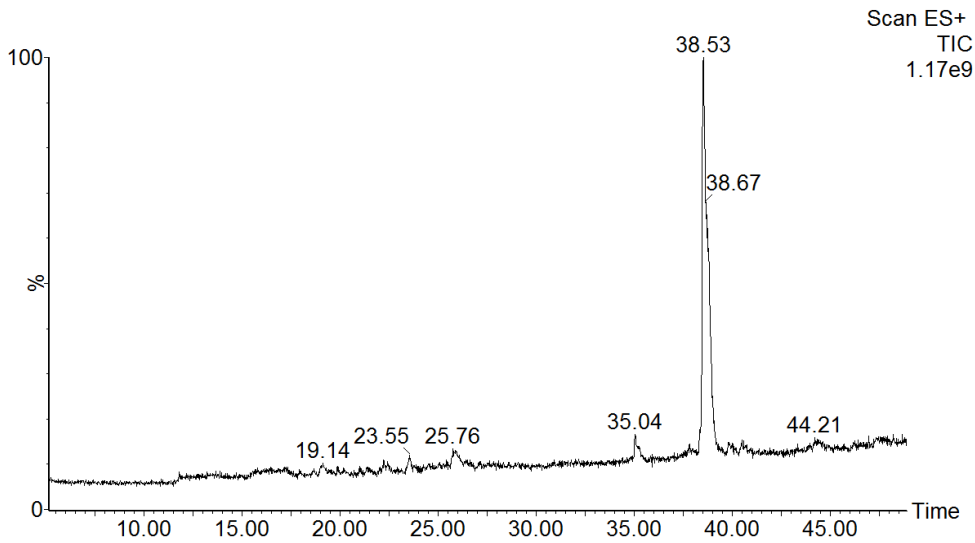

r.t. 38.461 min

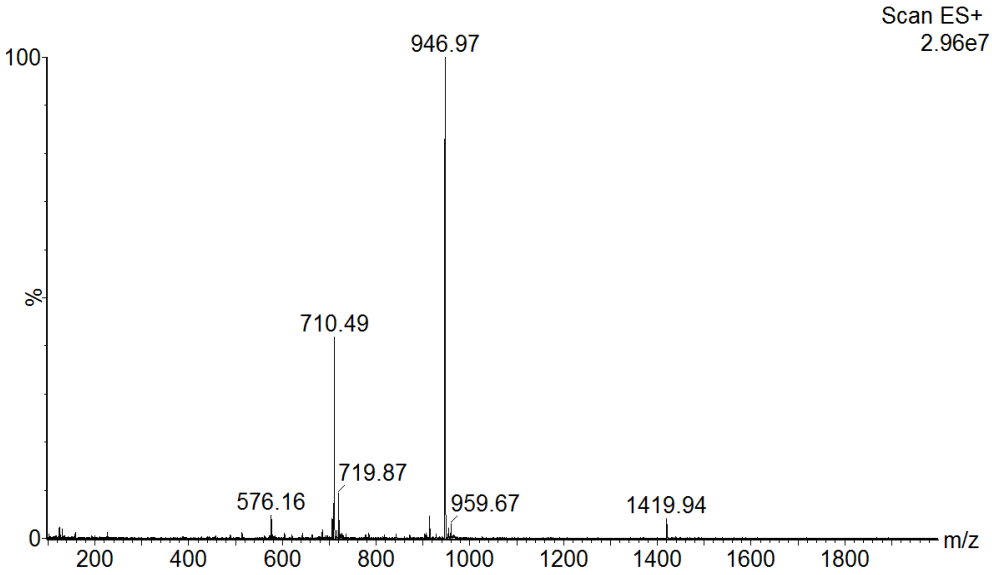

- Compound **2**:

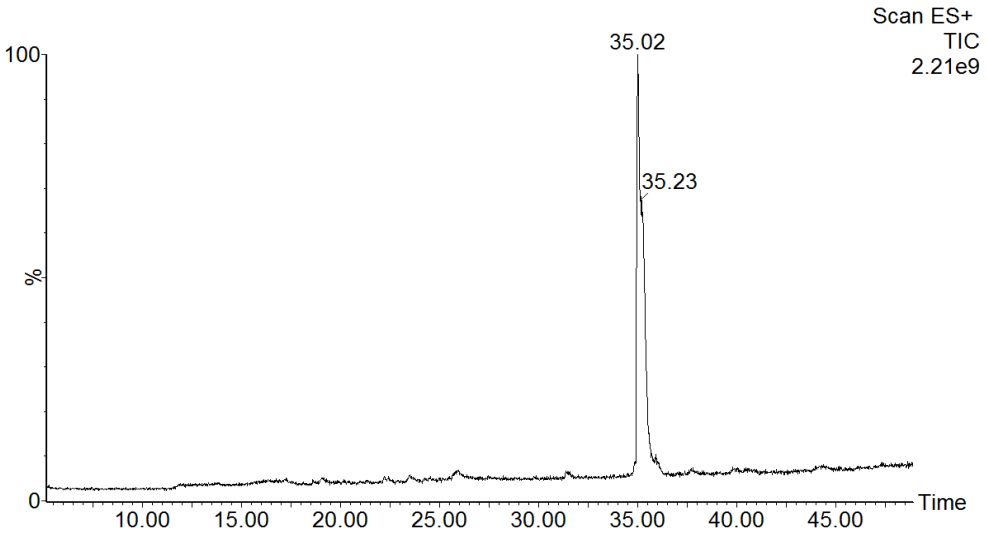

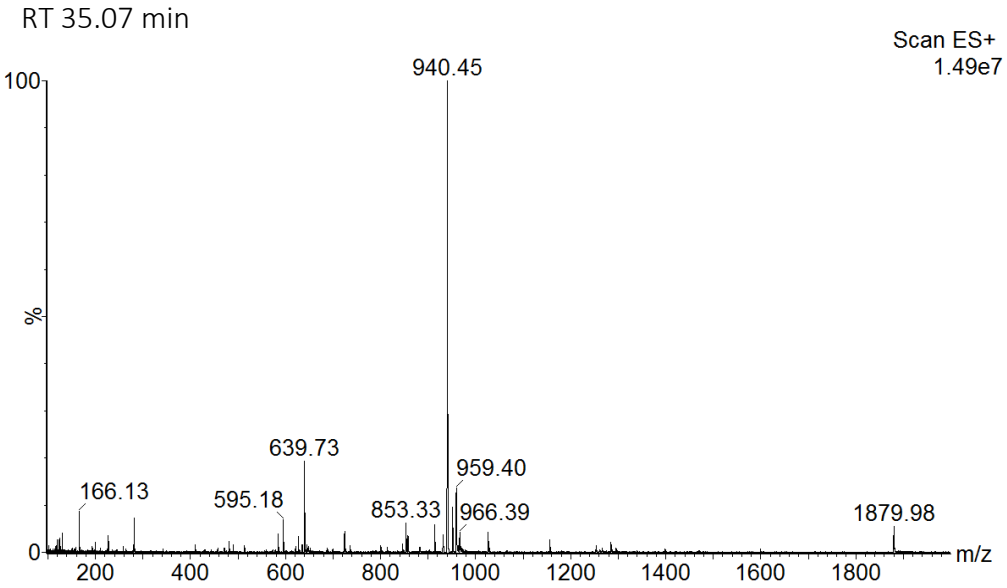
RT 35.07 min
Scan ES+
1.49e7
940.45
100
%
639.73
959.40
166.13
595.18
853.33
966.39
1879.98
0
200
400
600
800
1000
1200
1400
1600
1800
m/z

- Compound **3**:

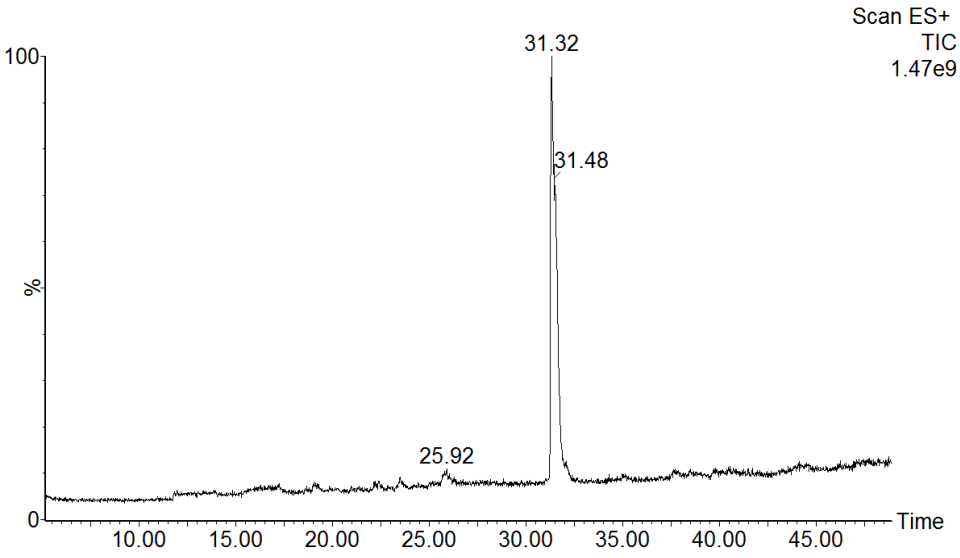
Scan ES+
TIC
1.47e9
31.32
100
31.48
%
25.92
0
10.00
15.00
20.00
25.00
30.00
35.00
40.00
45.00
Time

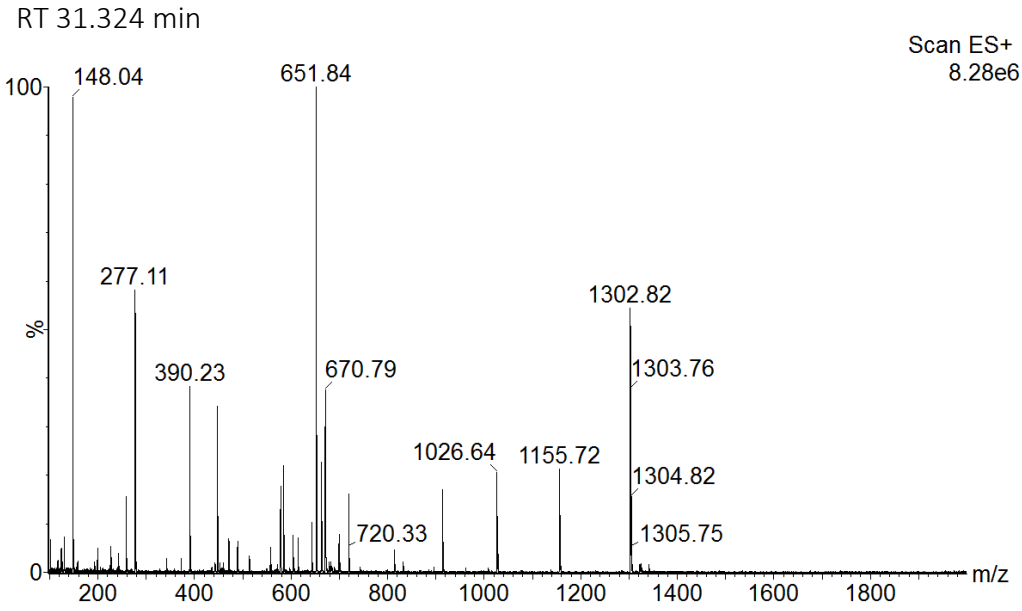
RT 31.324 min
Scan ES+
8.28e6
100
%
0
148.04
651.84
277.11
1302.82
390.23
670.79
1303.76
1026.64
1155.72
1304.82
720.33
1305.75
200
400
600
800
1000
1200
1400
1600
1800
m/z

- Compound **4**:

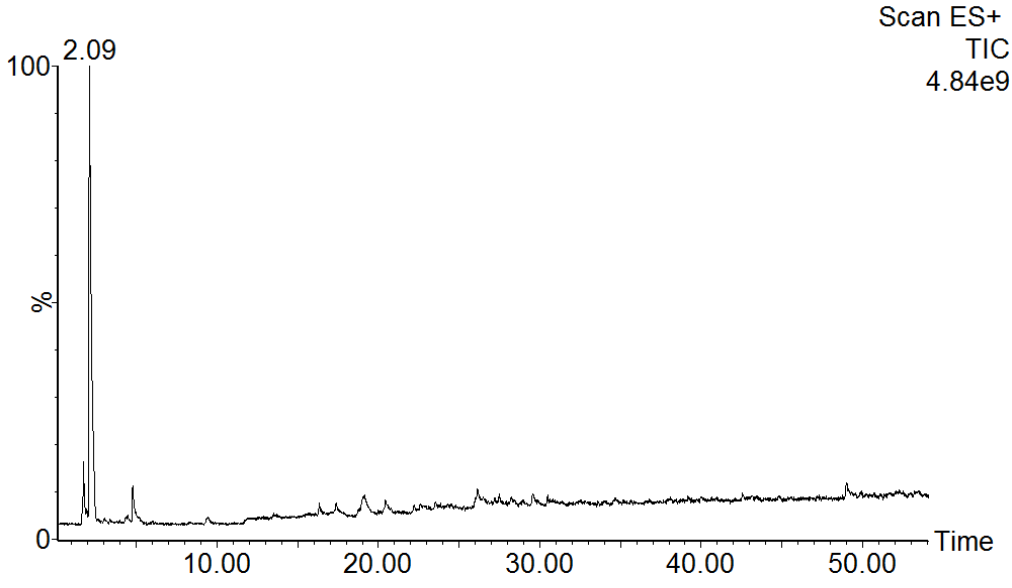
Scan ES+
TIC
4.84e9
100
2.09
%
0
10.00
20.00
30.00
40.00
50.00
Time

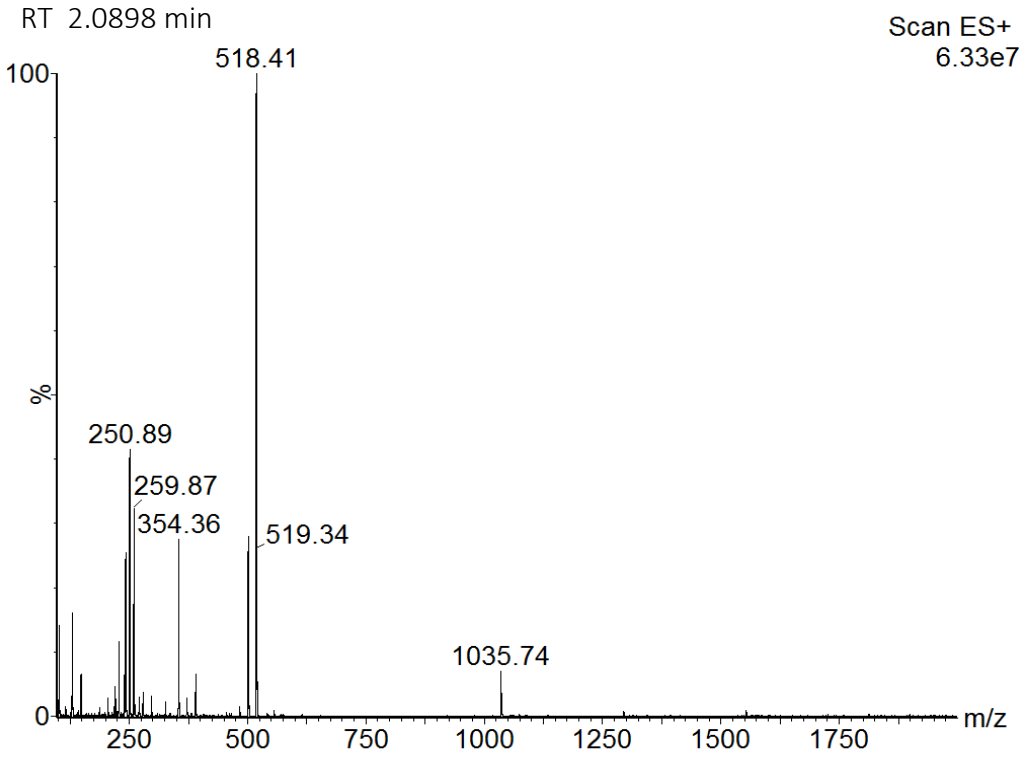

4.4.2 Biology

Proteins expression and purification

***Mtb* PanB.** *E. coli* BL21(DE3) cells were freshly transformed with pET16B_*Mt*PanB plasmid supplied by Genescript. Cells were grown in ZYP5052 auto-inducing media for 3 h at 37 °C before switching the cell culture temperature at 17 °C for an overnight growth. Cells were harvested by centrifugation at 8000 rpm, 4 °C for 30 min. The cell pellet was washed with PBS and then resuspended in the lysis buffer (8 mL for 1g of pellet) consisting of 50 mM Tris-HCl pH= 7.4, 300mM NaCl, 1mM β-mercaptoethanol and 10% v/v glycerol, proteases inibitors and benzonases were added (protease inhibitors 200µL each 40 mL, benzonase 1 µL each 80 mL). Cells were lysed by ten sonication cycles at 60 W of amplitude for 1 min on ice alternated with 30 sec of pause. The insoluble cellular debris was cleared by centrifugation at 16000 rpm at 4 °C for 40 min, followed by clarification. The filtrate containing the His_6-tagged protein was

loaded over 8 mL His-Pur™ Ni-NTA resin pre-equilibrated with the lysis buffer containing 20 mM imidazole. The column was washed with the lysis buffer containing 50 mM imidazole and the protein of interest was eluted with the lysis buffer with 300 mM imidazole. Elution fraction 5 and 6 were collected and dialyzed in the lysis buffer to remove the imidazole and the purity was assessed by 12% SDS Page.

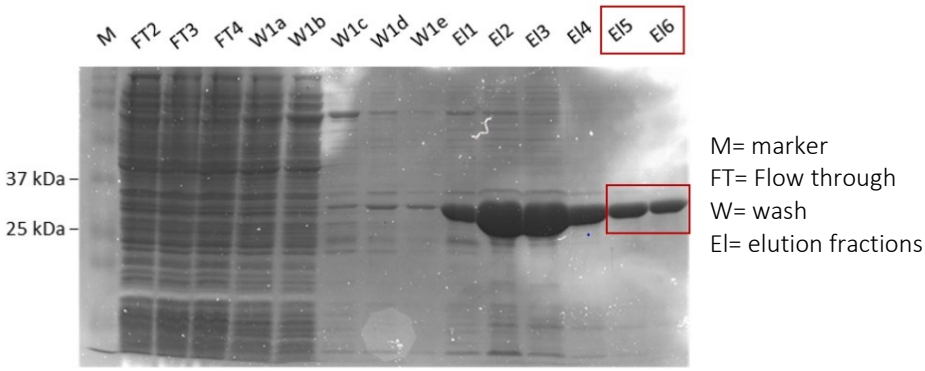

***Mtb* PafA.** *E. coli* BL21(DE3) cells were freshly transformed with pET22b_*Mt*PafA plasmid supplied by Genescript, that allow us to express the recombinant protein bearing a C-terminal His-tag. Cells were grown in 2XTY media until they reached OD_{600}= 0,6. The protein expression was induced by adding IPTG at the final concentration of 0.2 mM. The induced culture was grown for 15h hours at 16 °C. Cells were harvested by centrifugation at 8000 rpm, 4 °C for 30 min. The cell pellet was washed with PBS and then resuspended in the lysis buffer consisting of 50 mM Tris-HCl pH= 7.4, 300mM NaCl, 1mM β-mercaptoethanol and 10% v/v glycerol, proteases inhibitors and benzonases were added (protease inhibitors 200 µL each 40 mL, benzonase 1 µL each 80 mL). Cells were lysed by ten sonication cycles at 60 W of amplitude for 1 min on ice alternated with 30 sec of pause. The insoluble cellular debris was cleared by centrifugation at 16000 rpm at 4 °C for 40 min, followed by clarification. The filtrate containing the His_6-tagged protein was loaded over 4 mL His-Pur™ Ni-NTA resin pre-equilibrated with lysis buffer containing 20 mM imidazole. The column was washed with the lysis buffer containing 50 mM imidazole and the protein eluted with 300 mM imidazole. The

elution fractions 3 and 4 were dialyzed in the lysis buffer to remove the imidazole and the purity was assessed by 12% SDS Page.

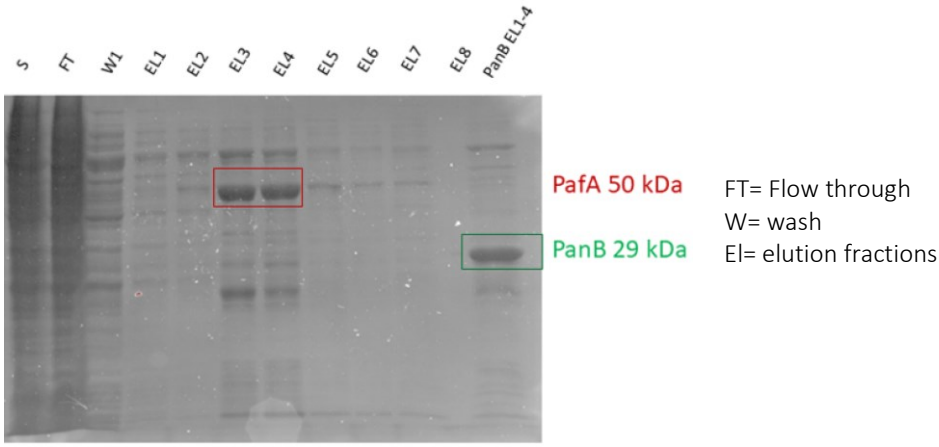

Spectrophotometric assay for the evaluation of PafA activity

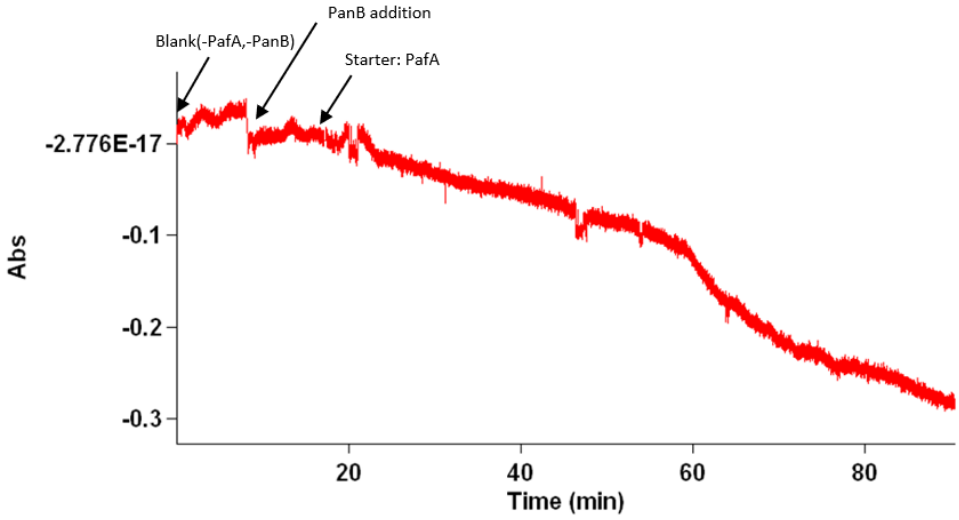

Single kinetic assays were performed with the following concentrations: ATP 1mM; PEP 2 mM; PK/LDH Sigma Aldrich (2.8 µL in 200 µL); NADH 150 µM; PuP 4 µM; PanB 2 µM; PafA (starter) 1 µM; Reaction buffer: 50 mM Tris-HCl pH= 7.4, 300mM NaCl, 20 mM $MgCl_2$, 1mM β-mercaptoethanol and 10% v/v glycerol.

Calculation of the K_M. Reaction mixture: PEP 2 mM; PK/LDH Sigma Aldrich (2.8 µL in 200 µL); NADH 150 µM; PuP 4 µM; PanB 2 µM; PafA (starter) 1 µM and six concentrations of ATP (400, 200, 50, 25, 6.25, 1.55 µM). Reaction buffer: 50 mM Tris-

HCl pH= 7.4, 300mM NaCl, 20 mM $MgCl_2$, 1mM β-mercaptoethanol and 10% v/v glycerol.

Multiplate spectrophotometric assay for the evaluation of PafA activity. Multiplate kinetic assays were performed in triplicate with the following concentrations: ATP 0.5 mM; PEP 2 mM; PK/LDH Sigma Aldrich (2.8 µL in 200 µL); NADH 150 µM; PuP 4 µM; PanB 2 µM; inhibitors (tested at 50 µM with the exception of compound 2 which was tested at 25 µM); PafA (starter) 1 µM; Reaction buffer: 50 mM Tris-HCl pH= 7.4, 300mM NaCl, 20 mM $MgCl_2$, 1mM β-mercaptoethanol and 10% v/v glycerol. Assays were performed in triplicate. The rate of the reaction expressed in OD/min (λ=340 nm) was used to calculate the percentage of activity of the protein incubated with the inhibitor peptides vs control.

4.5 References

(1) Bahuguna, A.; Rawat, D. S. An Overview of New Antitubercular Drugs, Drug Candidates, and Their Targets. *Med. Res. Rev. 0* (0).

(2) Darwin, K. H.; Ehrt, S.; Gutierrez-Ramos, J.-C.; Weich, N.; Nathan, C. F. The Proteasome of Mycobacterium Tuberculosis Is Required for Resistance to Nitric Oxide. *Science* **2003**, *302* (5652), 1963–1966.

(3) Küberl, A.; Polen, T.; Bott, M. The Pupylation Machinery Is Involved in Iron Homeostasis by Targeting the Iron Storage Protein Ferritin. *Proc. Natl. Acad. Sci. U. S. A.* **2016**, *113* (17), 4806–4811.

(4) Barandun, J.; Delley, C. L.; Weber-Ban, E. The Pupylation Pathway and Its Role in Mycobacteria. *BMC Biol.* **2012**, *10*, 95.

(5) Elharar, Y.; Roth, Z.; Hermelin, I.; Moon, A.; Peretz, G.; Shenkerman, Y.; Vishkautzan, M.; Khalaila, I.; Gur, E. Survival of Mycobacteria Depends on Proteasome-Mediated Amino Acid Recycling under Nutrient Limitation. *EMBO J.* **2014**, *33* (16), 1802–1814.

(6) Samanovic, M. I.; Li, H.; Darwin, K. H. The Pup-Proteasome System of Mycobacterium Tuberculosis. *Subcell. Biochem.* **2013**, *66*, 267–295.

(7) Striebel, F.; Imkamp, F.; Sutter, M.; Steiner, M.; Mamedov, A.; Weber-Ban, E. Bacterial Ubiquitin-like Modifier Pup Is Deamidated and Conjugated to Substrates by Distinct but Homologous Enzymes. *Nat. Struct. Mol. Biol.* **2009**, *16* (6), 647–651.

(8) Pearce, M. J.; Mintseris, J.; Ferreyra, J.; Gygi, S. P.; Darwin, K. H. Ubiquitin-like Protein Involved in the Proteasome Pathway of Mycobacterium Tuberculosis. *Science* **2008**, *322* (5904), 1104–1107.

(9) Cerda-Maira, F. A.; Pearce, M. J.; Fuortes, M.; Bishai, W. R.; Hubbard, S. R.; Darwin, K. H. Molecular Analysis of the Prokaryotic Ubiquitin-like Protein (Pup) Conjugation Pathway in Mycobacterium Tuberculosis. *Mol. Microbiol.* **2010**, *77* (5), 1123–1135.

(10) Kerscher, O.; Felberbaum, R.; Hochstrasser M. Modification of Proteins by Ubiquitin and Ubiquitin-Like Proteins. *Annu. Rev. Cell. Dev. Biol.*, **2006**, 22, 159–180.

(11) Lupas, A.; Zühl, F.; Tamura, T.; Wolf, S.; Nagy, I.; De Mot, R.; Baumeister, W. Eubacterial Proteasomes. *Mol. Biol. Rep.* **1997**, *24* (1–2), 125–131.

(12) De Mot, R. Actinomycete-like Proteasomes in a Gram-Negative Bacterium. *Trends Microbiol.* **2007**, *15* (8), 335–338.

(13) Valas, R. E.; Bourne, P. E. Rethinking Proteasome Evolution: Two Novel Bacterial Proteasomes. *J. Mol. Evol.* **2008**, *66* (5), 494–504.

(14) Gur, E.; Biran, D.; Ron, E. Z. Regulated Proteolysis in Gram-Negative Bacteria--How and When? *Nat. Rev. Microbiol.* **2011**, *9* (12), 839–848.

(15) Zhang, S.; Burns-Huang, K. E.; Janssen, G. V.; Li, H.; Ovaa, H.; Hedstrom, L.; Darwin, K. H. Mycobacterium Tuberculosis Proteasome Accessory Factor A (PafA) Can Transfer Prokaryotic Ubiquitin-Like Protein (Pup) between Substrates. *mBio* **2017**, *8* (1).

(16) Darwin, K. H. Prokaryotic Ubiquitin-like Protein (Pup), Proteasomes and Pathogenesis. *Nat. Rev. Microbiol.* **2009**, *7* (7), 485–491.

(17) Gandotra, S.; Lebron, M. B.; Ehrt, S. The Mycobacterium Tuberculosis Proteasome Active Site Threonine Is Essential for Persistence Yet Dispensable for Replication and Resistance to Nitric Oxide. *PLOS Pathog.* **2010**, *6* (8), e1001040.

(18) Ndlovu, H.; Marakalala, M. J. Granulomas and Inflammation: Host-Directed Therapies for Tuberculosis. *Front. Immunol.* **2016**, *7*.

(19) Awuh, J. A.; Flo, T. H. Molecular Basis of Mycobacterial Survival in Macrophages. *Cell. Mol. Life Sci. CMLS* **2017**, *74* (9), 1625–1648.

(20) Burns, K. E.; Pearce, M. J.; Darwin, K. H. Prokaryotic Ubiquitin-Like Protein Provides a Two-Part Degron to Mycobacterium Proteasome Substrates. *J. Bacteriol.* **2010**, *192* (11), 2933–2935.

(21) Smirnov, D.; Dhall, A.; Sivanesam, K.; Sharar, R. J.; Chatterjee, C. Fluorescent Probes Reveal a Minimal Ligase Recognition Motif in the Prokaryotic Ubiquitin-like Protein from Mycobac-Terium Tuberculosis. *J. Am. Chem. Soc.* **2013**, *135* (8), 2887–2890.

(22) Barandun, J.; Delley, C. L.; Ban, N.; Weber-Ban, E. Crystal Structure of the Complex between Prokaryotic Ubiquitin-like Protein and Its Ligase PafA. *J. Am. Chem. Soc.* **2013**, *135* (18), 6794–6797.

(23) Iyer, L. M.; Burroughs, A.; Aravind, L. Unraveling the Biochemistry and Provenance of Pupylation: A Prokaryotic Analog of Ubiquitination. *Biol. Direct* **2008**, *3*, 45.

(24) Guth, E.; Thommen, M.; Weber-Ban, E. Mycobacterial Ubiquitin-like Protein Ligase PafA Follows a Two-Step Reaction Pathway with a Phosphorylated Pup Intermediate. *J. Biol. Chem.* **2011**, *286* (6), 4412–4419.

5. Hijacking E3 ligases against each other using PROTACs

As part of my PhD program, I spent 10 months at the University of Dundee, working on the synthesis and the biological evaluation of Proteolysis Targeting Chimeras (PROTACs) directed against E3 ligases. Part of the work presented in this chapter has been recently published.[1] Compound **14a** and compounds reported in the section 5.2.2 are covered by a patent application (patent number WO 2018/189554).

5.1 Introduction

The Ubiquitin Proteasome System (UPS) is a complex pathway which plays a crucial role in many process of the eukaryotic cells, including homeostasis.[2,3] It controls the protein degradation and turnover, via the sequential action of the enzymes E1, E2 and E3 and the activity of a highly sophisticated protease complex, called proteasome.[4,5] Based on their function, the enzymes E1, E2 and E3 are also called respectively ubiquitin activating enzymes, ubiquitin conjugating enzymes and ubiquitin ligases. As a result of the activation of this pathway, the substrate protein is covalently modified with a polyubiquitin chain which works as a molecular tag for the recognition and subsequent degradation by the proteasome (Figure 1, A). The cascade begins with the chemical activation of ubiquitin, a protein of 76 amino acids, via a thioester bond between the C-terminal glycine residue of ubiquitin and a conserved cysteine residue of the enzyme E1. Then, ubiquitin is transferred to an E2-conjugating enzyme and finally an E3 ligase catalyses the transfer of ubiquitin from the E2-ubiquitin complex to the substrate protein, via an isopeptide bond between the ε-amino group of a substrate lysine residue and the C-terminal glycine residue of ubiquitin.[6] Protein ubiquitination is a reversible process as the substrate-ubiquitin as well as the ubiquitin-ubiquitin amide bonds can be hydrolysed by protease enzymes called deubiquitinases (DUBs).[7] The process becomes irreversible when the ubiquitinated protein reaches the proteasome leading, in most cases, to a complete, rapid, and sustained degradation of such proteins. In such manner, the UPS regulates the level and function of many proteins that are essential for the adaptation to new physiologic conditions.

The human genome encodes for two E1-activating enzymes, 37 E2-conjugating enzymes and over 600 E3 ubiquitin ligases.[8] E3 ubiquitin ligases are the most heterogeneous class of enzymes as they are responsible for substrate specificity.[9] Based on their structure and their mechanism of action they are classified in three main families: the homologous with E6-associated protein C-terminus domain family (HECT), the RING-between-RING domain family (RBR) and the RING domain family (RING).[10]

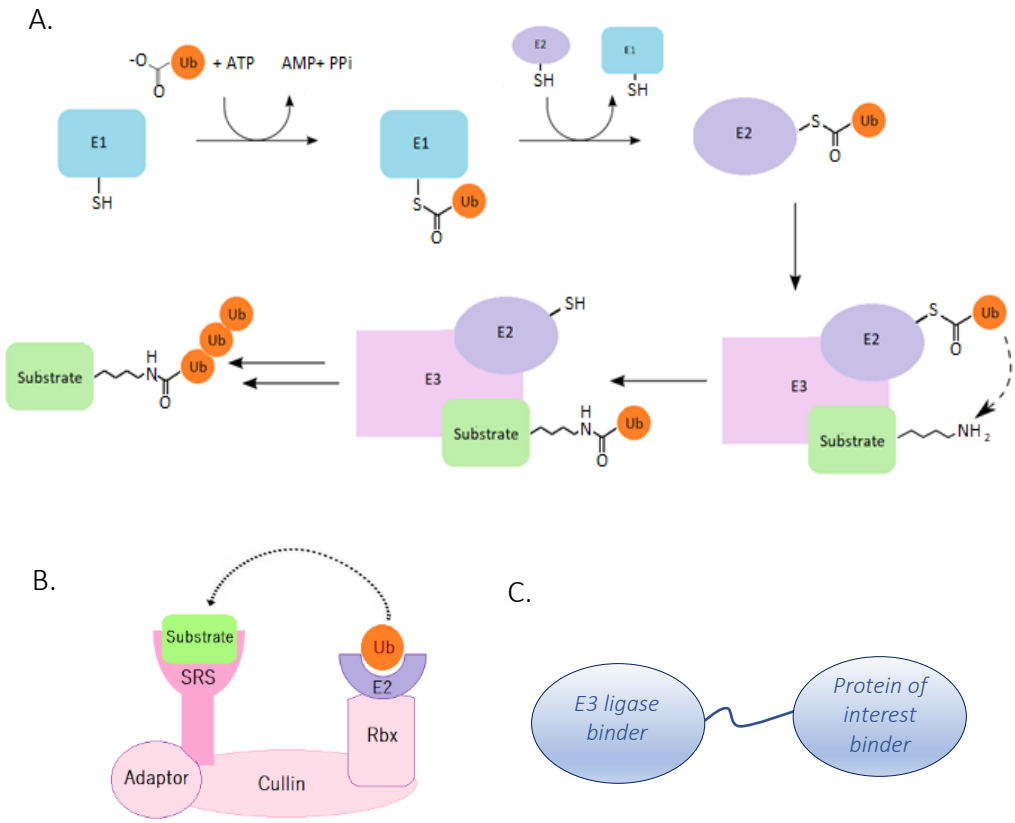

Figure 1. *A) The ubiquitination pathway; B) The transfer of ubiquitin to a substrate protein, catalyzed by a Cullin Ring E3 ligases; C) Schematic representation of a PROTAC molecule.*

The RING domain ligases are the most abundant types of E3 ligases. They are characterized by the presence of a RING or U-Box domain, responsible both for the binding of the ubiquitin-E2 conjugate and for the stimulation of the following ubiquitin transfer to the protein substrate.[11] Among those, the Cullin RING Ligases (CRLs) are a family of multi-component enzymes characterized by a central Cullin subunit (Figure 1,

B). The Cullin subunit binds the RING box protein at the C-terminus and the substrate recognition subunit (SRS), via adaptor subunit(s) at the N-terminus.[12] Von Hippel-Lindau protein (VHL) and cereblon (CRBN) function as SRSs of two ubiquitously expressed and biologically relevant E3 ligases with the homonymous name.

The von Hippel–Lindau (VHL) E3 ligase consists of the substrate recognition subunit VHL (also called pVHL), elongins B and C as adaptor complex, cullin 2, and ring box protein 1 (Rbx1).[13] Two major splicing variants of the pVHL are documented: a 19 kDa isoform (pVHL19) and a 30 kDa isoform (pVHL30). Both isoforms are functional and their primary substrate is the hydroxylated form of the hypoxia-inducible factor 1α (HIF-1α), a transcription factor involved in the response to low oxygen intracellular levels and implicated in the upregulation of various genes, such as the vascular endothelial growth factor (VEGF), the glucose transporter (GLU1) and erythropoietin. In normoxia, the VHL E3 ligase recognizes the hydroxylated HIF-1α and targets it for the degradation by proteasome, while during hypoxia HIF-1α can no longer be recognized by VHL, as it is be no longer hydroxylated. This because the hydroxylation is catalysed by the prolyl hydroxylase domain (PHD) enzymes, requiring oxygens for their function. Thus, during oxygen limitation HIF-1α binds to the HIF-1β and the complex translocates into the nucleus where it can bind the hypoxia-response elements (HRE) on DNA, activating the transcription of hypoxia responsive genes.[14,15] The discoveries that elucidated the mechanism of the VHL-HIF pathways were awarded the Nobel Prize in Physiology and Medicine in October 2019.[16]

The CRBN E3 ligase consists of a substrate recognition subunit called CRBN, a damage specific DNA binding protein (DDB1), Cullin 4, and ring box protein 1 (Rbx1).[17] Several studies suggests that CRBN binds to large-conductance calcium- and voltage-activated potassium (BK_{Ca}) channels, having a key role in their regulation.[18] CRBN can also bind immunomodulatory drugs (IMiDs), such as thalidomide, lenalidomide and pomalidomide and plays an important role in cancer cell biology and in the energy metabolism.[19,20] Recent findings revealed that CRBN deficient mice are resistant to

various stress condition such as high-fat diet, ischemia/reperfusion injuries, endoplasmic reticulum stress and alcohol-associated liver damage.[21]

In recent years, the interest of the scientific community for VHL and CRBN E3 ligases has considerably increased not only for their implication in physiological and pathological processes as targets in their own right, but also for the potential to be hijacked by an innovative approach based the Proteolysis Targeting Chimeras (PROTACs).[15,21–25] A PROTAC is a two-headed molecule capable of inducing selective intracellular proteolysis of a target protein by hijacking the UPS. It comprises an E3-ligase ligand and moiety able to bind a specific protein of interest, linked together via a flexible linker (Figure 1C). By binding the E3 ligase and the protein of interest simultaneously, PROTACs can catalyse the intracellular proximity-induced ubiquitination of the protein and, this way, targeting the protein for the proteasomal degradation. Via a sub-stoichiometric catalytic mode of action, which does not require full occupancy of the target-binding site and involves turnover of multiple target molecules by a single PROTAC molecule, PROTACs are able to induce a rapid, profound and sustained degradation of the target protein, also modulating challenging and non-traditional drug targets.[23,26] Using the PROTAC technology, the degradation of many target proteins has been successfully achieved, such as in the case of BET proteins Brd2, Brd3, Brd4, Brd7 and Brd9[27–32] and protein kinases[33,34], among the others.[33,35] Recently in the research group headed by Professor Ciulli, it was hypothesized that the E3 ligases themselves might be hijacked against one another inducing E3 ligase degradation. In 2017 the first small molecule dimerizers of the VHL E3 ligase were disclosed, with the most promising compound being CM11.[36] This was the first example of E3-ligase targeting PROTACs, which not only represent powerful tools for the investigation the biology of the E3 ligases, but they may also have a possible therapeutic role. For example, it was hypothesized that the PROTAC-induced degradation of the von Hippel-Lindau ligase (VHL), an E3-ligase known to recognize the hydroxylated form of HIF-1α, could provide therapeutic benefits in anaemia, ischemia and ischemia-reperfusion injuries by preventing HIF degradation and inducing HIF transcriptional activity, hence

triggering a potentially beneficial hypoxic response.[15] This type of PROTAC in which the same E3 ligase is targeted at either end was called "Homo-PROTAC", while the PROTACs hijacking two different E3 ligases will be called in this chapter "Hetero-PROTAC". Applying the same idea on CRBN E3 ligase, also the first example of CRBN-CRBN Homo-PROTAC was published while the study presented herein was ongoing.[37]

5.2 Results and Discussion [a]

*[a] Not all the compounds presented in this section were synthesized by me: compounds **25c**, **26d**, **CMP85** and **CMP86** were received as gifts from Dr. Chiara Maniaci, **28i** was received as a gift from Dr. Andrea Testa.*

In this section, the possibility of promoting the degradation of the two most popular E3 ligases, VHL and CRBN, using the PROTACs was investigated according to three different approaches, which will be presented in three separate sections:

- design, synthesis and biological evaluation of VHL-CRBN Hetero-PROTACs (Section 5.2.1)
- optimization of the VHL-HomoPROTAC CM11 (Section 5.2.2)
- design, synthesis and biological evaluation of CRBN Hetero-PROTACs (Section 5.2.3)

In all cases, the design of the PROTACs began with the careful choice of the VHL and CRBN binders. As VHL ligands, compound **1**[38] was selected on the basis of being one of the most potent VHL ligands described, bearing a convenient amine group available for derivatization. Compound **2** and **3** represent two variants of a potent VHL binder previously reported,[39] respectively with a phenol and a thiol group, recently reported as convenient derivatization points for the linker attachment in PROTACs.[29,32] As CRBN binder pomalidomide (Figure 2) was chosen because of its greater cellular stability compared to other ImIds[40] and it was synthesized in two variants: (i) the fluorine derivative **4** , a suitable substrate for a nucleophilic aromatic substitution, and (ii) compound **5**, bearing an ethylenediamine spacer to provide a synthetically convenient attachment point for amide conjugation with a linker.

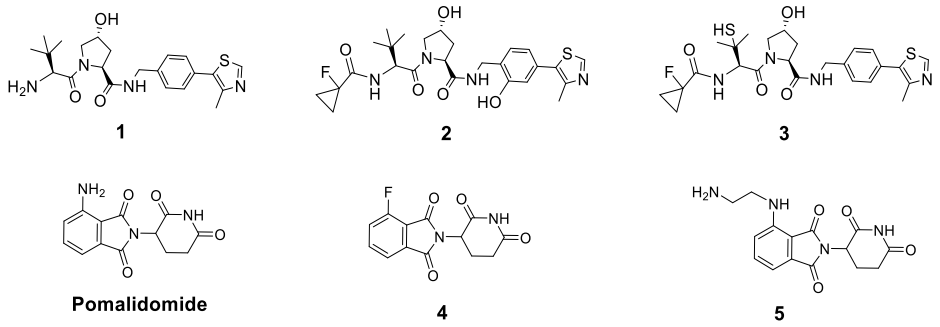

Figure 2. *Structure of three VHL binder **1**,**2**,**3** and two CRBN ligands **4** and **5**, derived from pomalidomide*

5.2.1 VHL-CRBN Hetero- PROTACs

5.2.1.1 Design of compounds

Using compound **1-3** as VHL binders and compound **5** as CRBN ligand, different VHL-CRBN Hetero-PROTACs were explored (Figure 3).

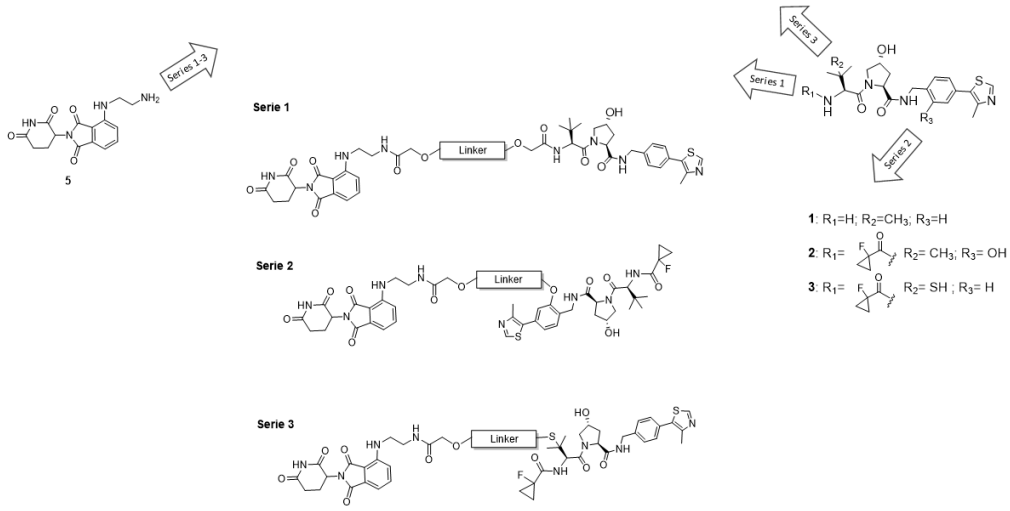

Figure 3. *Graphical representation of the three series of compounds*

The design was mainly focused on the linker, which in PROTACs does not only work as chemical connector of the two binding units but it also has an impact on the ability of the PROTAC molecule to form the key ternary complex constituted by the E3 ligase, the PROTAC and the target protein. The properties of the ternary complex then impact on the promotion of target ubiquitination and subsequent degradation of the target protein.[41,42] It is known that even small changes in both length and physicochemical

nature of the linker (e.g. alkylic versus PEG), affects the degradation activity and selectivity in often unpredictable ways.[43–45] Therefore, in this study, different linkers were explored, focusing on varying lengths and ratio between carbon and oxygen atoms with the goal to obtain a panel of compounds with different derivatizations, linker length and chemical properties. Compounds synthesized can be classified in three different series based on the derivatization point on the VHL ligand, while compound **5** was used as CRBN binder in all cases.

The amine of **1** represented a convenient attachment point for the design and synthesis of the first series of compounds in which, using dicarboxylic spacer, compound **1** and **5** could be successfully linked. Using this strategy compounds **14a-e** were designed and synthesized. Compounds **14a-e** are reported in the Chart 1 with the molecules **CMP85** and **CMP86** (gifts from Dr. Chiara Maniaci).

Chart 1

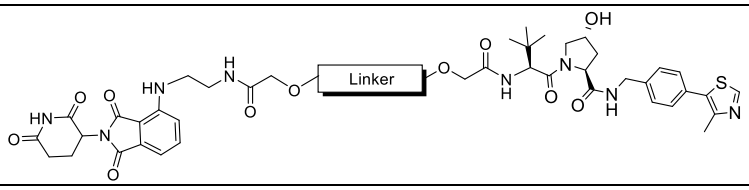

Cmpd.	Linker	*N° of oxygens in the linker*	Linker length (number of atoms)
CMP85	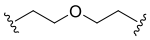	1	5
CMP86	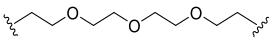	3	11
14a	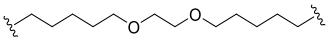	2	14
14b	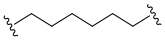	0	6
14c	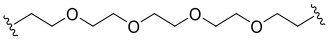	4	14
14d	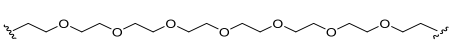	7	23
14e	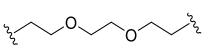	2	8

For the second and third series, compounds **2** and **3** were respectively selected as VHL binder. Compound **2** was derivatized on the phenol ring while compound **3** was

derivatized on the thiol group. In either case bifunctional linker were needed, giving the different nature of the attachment points on the VHL and CRBN ligands. At this purpose, three linkers bearing a free carboxylic acid at one end, available for the coupling reaction with the amino group of **5,** and a leaving group at the other end, available for a nucleophilic substitution with the phenol **2** or the thiol **3**, were synthesized and incorporated in both series. Also in this case, the linkers were designed in order to cover different length and chemical properties and three final PROTACs for each series were synthesized (see Chart 2 and Chart 3).

Chart 2

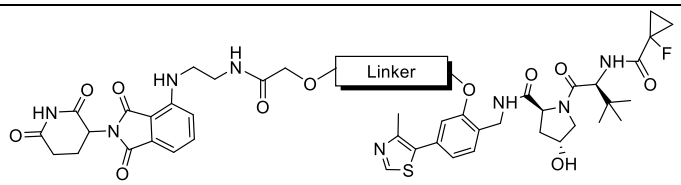

Cmpd.	Linker	N° of oxygens in the linker	Linker length (number of atoms)
18a	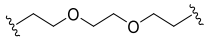	2	8
18b	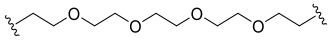	4	14
18c	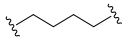	0	4

Chart 3

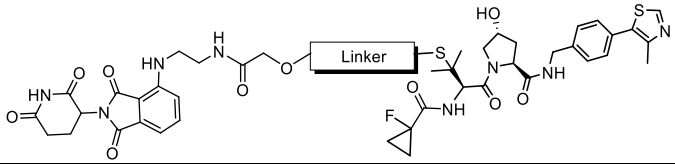

Cmpd.	Linker	N° of oxygens in the linker	Linker length (number of atoms)
22a	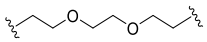	2	8
22b	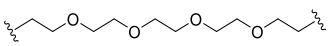	4	14
22c	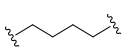	0	4

5.2.1.2 Evaluation of PROTACs cellular activity [b]

[b] *Western blots, time-dependent and concentration-dependent experiments showed in this section were performed by Dr. Scott Hughes*

To profile the degradation activity of the three series of PROTACs synthesized, VHL and CBRN protein levels were quantified by Western Blot analysis after treating Hela cells with 1 µM and 10 nM compounds. **CM11**[36] and **CC15a**[37] were used as positive controls for VHL and CRBN degradation, respectively (Figure 4). Testing two concentrations is important for this type of molecules in order to avoid false negative potentially due to the "hook-effect", which occurs when molecules preferentially forms 1:1 complex with the target protein, acting as inhibitors over degraders.

Figure 4

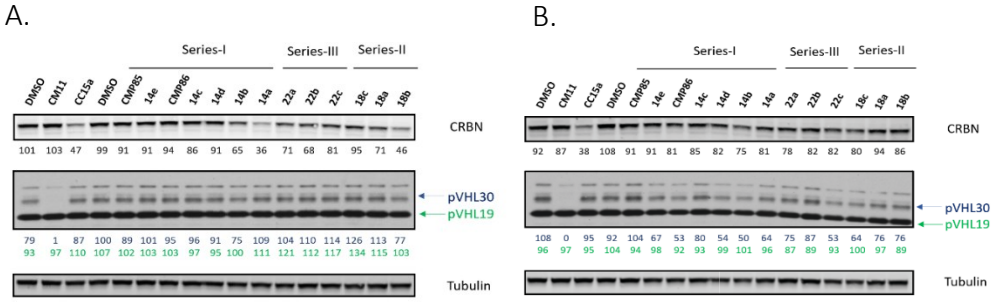

Figure 4. *Screening of VHL-CRBN hetero-PROTACs. Western blot analysis of CRBN and VHL levels following 4 h treatment of HeLa cells with 1 µM compound (A) and 10 nM compound (B). Values reported below each lane indicate protein abundance relative to the average 0.1% DMSO vehicle.*

Interestingly, the screening in HeLa cells at 1 µM revealed that the degradation of CRBN was observed with a few compounds, while no significant degradation of VHL was noticed with any of the compounds tested. The most potent CRBN degrader was found to be compound **14a** (36% residual protein level), following by compound **18b** which induced the degradation of CRBN to a lower extent (46% residual protein level). At the concentration of 10 nM no remarkable CRBN degradation was observed. All compounds induced less CRBN degradation at this concentration compared to 1 µM as expected, making it unlikely that the results obtained at 1 µM might be considered as false negatives due to a hook effect. Interestingly, for few compounds (compounds **14b**, **14d** and **CMP86**) an encouraging VHL degradation was observed (up to 50%),

suggesting that, depending on the concentration used, this class of compounds can induce preferentially the degradation of one E3 ligase over the other.

Figure 5

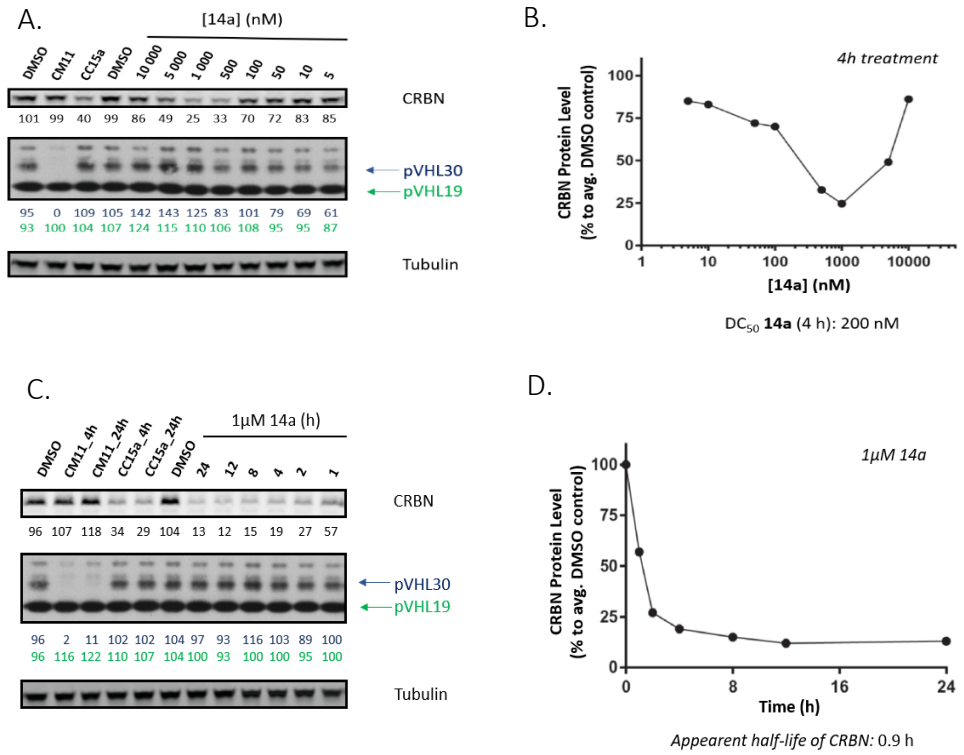

Figure 5. *(A) Western blot analysis of CRBN and VHL levels following 4 h treatment of HeLa cells with the indicated concentrations of **14a**. (B) Quantification of CRBN levels following concentration-dependent assessment. (C) Western blot analysis of CRBN and VHL levels following treatment of HeLa cells with 1 µM **14a** for the indicated time points. (D) Quantification of CRBN levels following time-dependent assessment. Values reported below each lane indicate protein abundance relative to the average 0.1% DMSO vehicle.*

Giving these interesting results, compound **14a** was further characterized by concentration- and time-dependent assays performed in both HeLa and HEK293 cells. For the concentration dependent assay, Hela cells were incubated for 4 h with eight different concentrations of compound **14a,** from 5 nM to 10 µM. The assay revealed that compound **14a** degraded CRBN with a DC_{50} of 200 nM, reaching the maximal degradation of 75%. The decreasing degradation observed above 1 µM could be attributed to the "hook effect", characteristic of bivalent molecules. A similar

degradation profile was observed in HEK293. Interestingly, some concentration-dependent degradation of pVHL30 was noticed in the range of 5-50 nM when compound **14a** was tested in HeLa as suggested from the first screening, while this effect was not observed in Hek293. The time-dependent assays in HeLa (Figure 5, A-B) suggests that **14a** is able to induce a rapid degradation of CRBN, with >50% protein depleted already after only 1 h and with the maximal degradation (>80% CRBN depleted) reached after 8 h. In Hek293 the **14a**-induced degradation of CRBN was faster, with >80% protein degraded after 1 h, and 98% depletion achieved in 8 h (Figure 6, A-B).

Figure 6

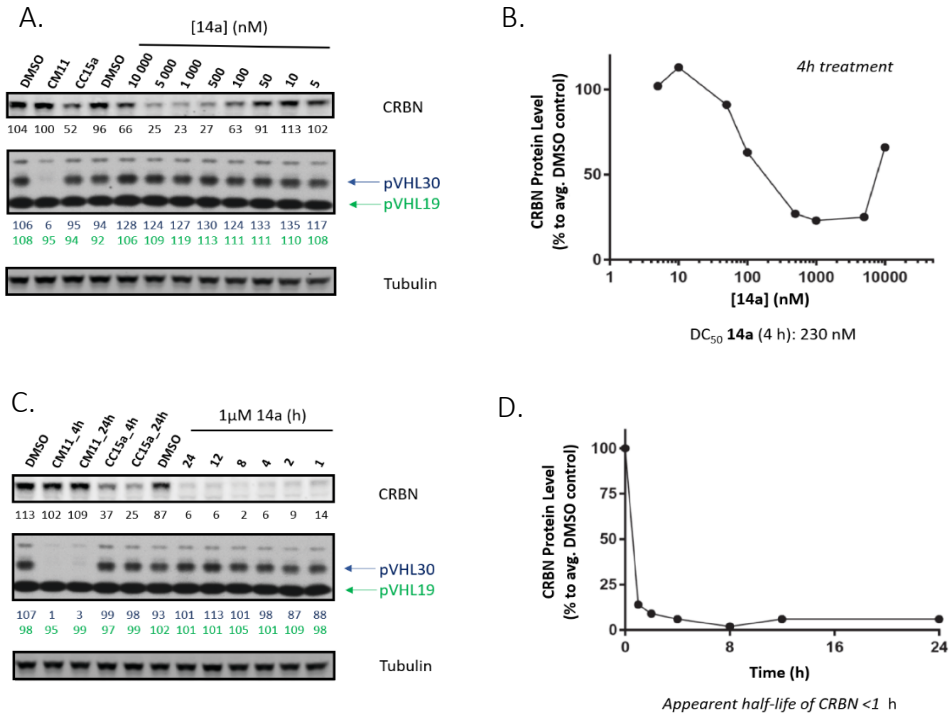

Figure 6. *(A) Western blot analysis of CRBN and VHL levels following 4 h treatment of Hek293 cells with the indicated concentrations of **14a**. (B) Quantification of CRBN levels following concentration-dependent assessment. (C) Western blot analysis of CRBN and VHL levels following treatment of HeLa cells with 1 µM **14a** for the indicated time points. (D) Quantification of CRBN levels following time-dependent assessment. Values reported below each lane indicate protein abundance relative to the average 0.1% DMSO vehicle.*

5.2.1.3 Conclusions

A number of VHL-CRBN PROTACs were described, providing a proof of principle for dimerizing two different E3 ligases as a novel approach to induce one ligase to degrade the other one. Interestingly, preferential degradation of CRBN was observed for the synthesized compounds, resulting in CRBN ligase 'winning' over VHL. Moreover, a partial VHL degradation was observed at lower concentrations, suggesting that depending on the concentration being used this class of compounds could preferentially induce the depletion of one ligase over the other. Compound **14a** was identified as the most promising of the series as it was able to induce potent, rapid and profound degradation of CRBN.

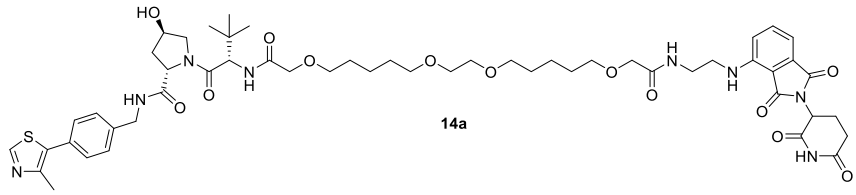

Figure 7. *The VHL-CRBN Hetero-PROTAC 14a*

This type of PROTACs could be helpful to reveal new mechanism for proximity-mediated hijacking between different E3 ligases. Although the outcome of their activity might be unpredictable, they might also work as precious tools to unravel innovative ways of chemical intervention on E3 ligases themselves, with both biological and therapeutic benefits.

5.2.2 CM11 optimization

5.2.2.1 Design of compounds

CM11 was found to be a promising VHL degrader in the first VHL Homo-PROTAC investigation. However, it was able to promote only the degradation of pVHL30 isoform while no significant degradation was observed for pVHL19. Although the biological characterization of CM11 was crucial as it gave insight about the optimal linker length needed to promote a rapid and consistent pVHL30 degradation, only peg-based linkers were explored, leaving the space for further investigations. We hypothesized that, with

the modulation of some linker parameters, i.e. length and number and distribution of oxygen atoms, it would have been possible to synthesize compounds able to engage also the pVHL19 isoform. With this aim, seven PROTACs were designed and synthesized to further elaborate the peg-based structure and introducing slight modifications on the linker (**28a-g**, Chart 4). Moreover, a different attachment points on one of the two VHL binders was also explored (compound **28h**). The impact of the introduction of a small group like fluorine on the hydroxyproline core of the VHL binding units was also investigated (compound **28i**).

Chart 4

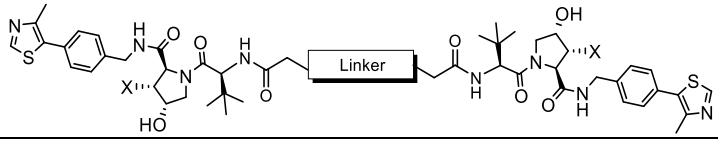

Cmpd.	Linker	X	N° oxygens in the linker	Linker length (number of atoms)
CM11	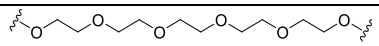	H	6	16
28a	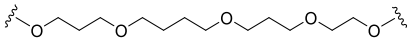	H	5	17
28b	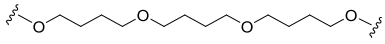	H	4	16
28c	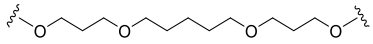	H	4	15
28d	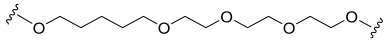	H	5	16
28e	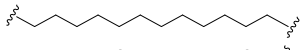	H	0	12
28f	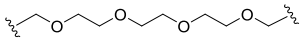	H	4	12
28g	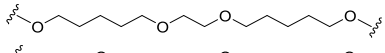	H	4	16
28i	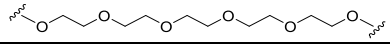	F	6	16
28h	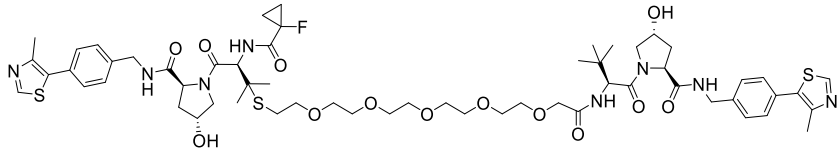			

5.2.2.2 Evaluation of PROTACs cellular activity

To profile the degradation activity of the PROTACs synthesized, VHL protein levels were quantified by Western Blot analysis following a 4 h treatment with 1 µM and 10 nM compounds in HeLa cells (Figure 8, A-B). Compounds **CM11** and **CMP98** were also tested respectively as positive and negative controls.[36]

Figure 8

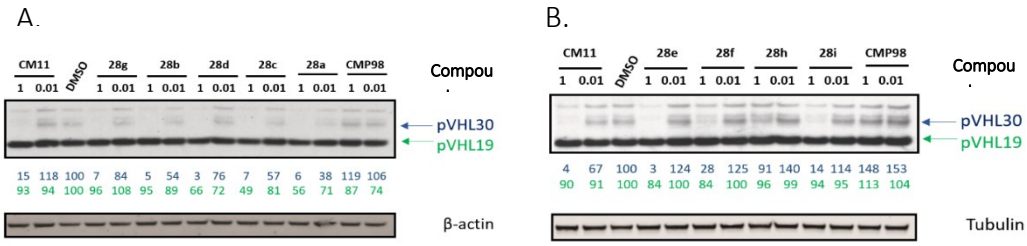

Figure 8. A, B) *Screening of VHL Homo-PROTACs. Western blot analysis of VHL levels following 4 h treatment of HeLa cells with 1 µM and 10 nM compound. Values reported below each lane indicate protein abundance relative to the 0.1% DMSO vehicle.*

A consistent degradation of pVHL30 was observed for the majority of compounds with compounds **28 a-d** and compound **28g** showing the most promising results (Figure 8, A). Interestingly, these compounds, characterized by linkers designed to escape the peg-motif and with a length varying between 15 and 17 atoms, showed to be more potent than the hit compound CM11. For three of these PROTACs, **28a**, **28c** and **28d**, also a partial degradation of pVHL19 could be observed with 1 µM compounds, with respectively 56%, 49% and 66% residual protein level. **28f**, with a significant shorter linker, promoted the degradation of pVHL30 (28% residual protein level) only at 1 µM, without effecting pVHL19. However, it is interesting to notice an improvement of the degradation of pVHL30 for its alkyl counterpart **28e**, suggesting that reducing the oxygens/carbons ratio in PROTAC's linker could represent a valuable strategy for improving the potency. The introduction of the fluorine in the hydroxyproline ring on VHL mojety (**28i**) seems to negatively impact on the VHL degradation. No significant degradation was observed for compound **28h**.

The five more promising compounds (**28a-d, 28g**) were tested in HEK93 cells, following the same protocol reported above, i.e. 4 h treatment with 1 µM and 10 nM compounds (Figure 9). Interestingly in HEK cells, all the compounds tested seemed able to affect both pVHL30 and pVHL19 isoforms. Analogously to what observed in HeLa cells, compounds **28a**, **28c** and **28d** were found to be the most potent molecules, even if in this case compounds **28c** seemed slightly more potent than the other two compounds in degrading the two VHL isoforms.

Figure 9

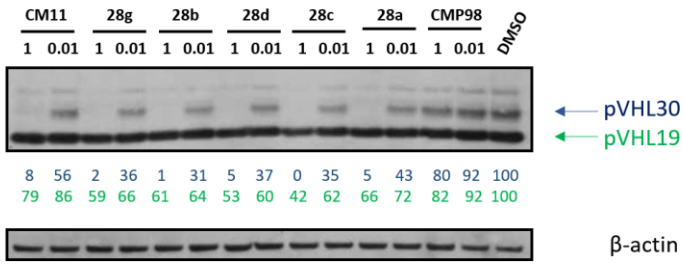

Figure 9. *Evaluation of **28a-d** and **28g** VHL Homo-PROTACs. Western blot analysis of VHL levels following 4 h treatment of HeK293 cells with 1 µM and 10 nM compound. Values reported below each lane indicate protein abundance relative to the 0.1% DMSO vehicle.*

5.2.2.3 Conclusions

In this study, the hit compound CM11 was optimized through the rational modification of the linker in order to evaluate its impact on the ability of PROTACs to promote the degradation of the two functional isoforms of VHL. Interestingly, this approach allowed to synthesize a panel of promising compounds more potent than CM11 in degrading pVHL30 and able to affect the pVHL19 levels. Among those, compound **28c** was identified as the most promising molecule.

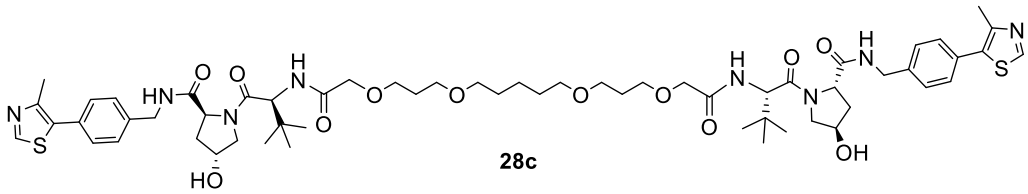

Figure 10. *The VHL-VHL Homo-PROTAC 28c*

This study demonstrates that even if, at the current state, peg-based linkers represent the first choice for the linkage of two functional units in PROTACs, mainly for their synthetic accessibility, they could not always be the most effective option. Further investigations are needed to define whether the correlation between the carbon/oxygen ratio in the linker and the increasing potency of PROTACs depends on an enhanced penetration in the cells or if structural aspects are involved.

5.2.3 CRBN Homo-PROTACs

Following a similar approach to those above reported, in this paragraph the possibility to degrade CRBN E3 ligase using Homo-PROTACS was investigated. While this study was being prepared a study by Steinebach and co-authors reporting CRBN Homo-PROTACs was published with compound **CC15a** as most active degrader, providing insights about the optimal linker length.[37] However the present study represents a unique investigation on CRBN Homo-PROTACs for the variability of the chemical structure presented, allowing to obtain potent CRBN degraders.

5.2.3.1 Design of compounds

Analogously to the studies reported in the two previous sections of this chapter, a modular approach was followed in the design and synthesis of the compounds starting from the two functional units. As CRBN binder either molecule **4** or **5** were used and, again, the attention was focused on the linker with the aim of obtaining an heterogenous class of potential CRBN degraders. The variability of the linkers in this class of compounds is remarkable, moving from peg-based linkers of various length, to more aliphatic structures, even including rings and aromatic cycles (Chart 5).

Chart 5

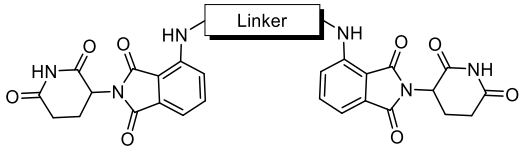

Compound	Linker
29a	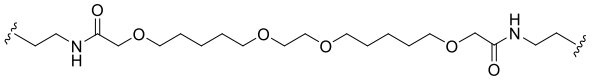
29b	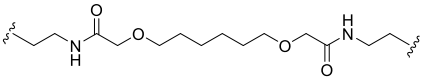
29c	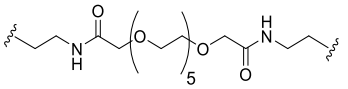
29d	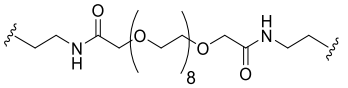
29e	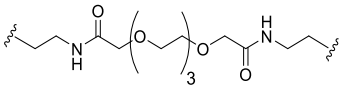
29f	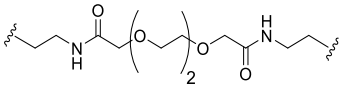
29g	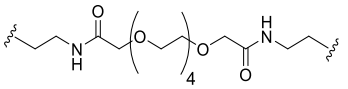
30a	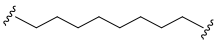
30b	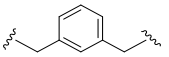
30c	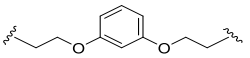
30d	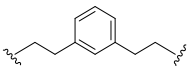
30e	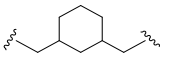

5.2.3.2 Evaluation of PROTACs cellular activity

To profile the degradation activity of the PROTACs synthesized, CRBN protein levels were quantified by Western Blot analysis following a 4 h treatment with 1 µM and 10 nM compounds in HeLa cells (Figure 11).

Figure 11

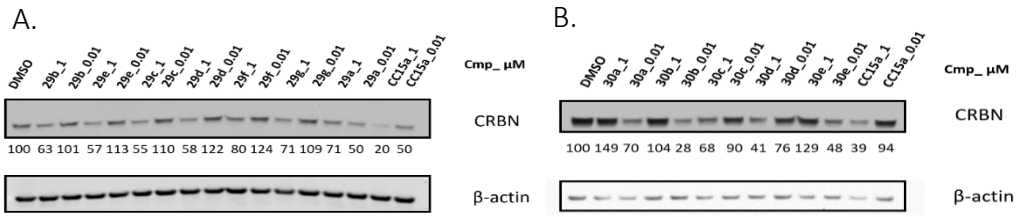

Figure 11. *Evaluation of **29a-g** (A) and **30 a-e** (B) CRBN Homo-PROTACs. Western blot analysis of VHL levels following 4 h treatment of Hela cells with 1 µM and 10 nM compound. Values reported below each lane indicate protein abundance relative to the 0.1% DMSO vehicle.*

Interestingly, all compounds seemed to affect the CRBN levels. Compounds **29b-g**, characterized by an ethylene diamine spacer attached to the pomalidomide unit and two amide function in the linker, seemed to promote the CRBN degradation only at 1 µM to a maximal residual protein level of 55% for compound **29c** (Figure 9, A). Compounds **30c** and **30d** showed a comparable potency with 68% and 41% respectively of CRBN residual level with 1 µM compound and no significant degradation observed with 10 nM compound. More interesting results were obtained in the case of compounds **29a**, **30a**, **30b** and **30e**, which were seen to remarkably induce the degradation of CRBN already at 10 nM (with respectively 50%, 70%, 29% and 48% residual protein levels). However, interestingly, instead of being more active at the higher compound concentration of 1 µM, much less degradation was observed instead (residual protein levels of 71%, 149%, 104% and 129%, respectively). The loss of activity with 1 µM of these compounds could be referred to the "hook-effect", when at high concentration compounds preferentially behave like inhibitors over degraders, because the binary 1:1 complexes saturate and ultimately out-compete formation of the ternary 2:1 complexes[46] This suggests that these three compounds may be potent

CRBN degraders, active perhaps at much lower concentration of the tested 10 nM. However further investigations, such as the concentration dependency assay are needed to further characterize those promising compounds.

5.2.3.3 Conclusions

In this study, different CRBN Homo-PROTACS were synthesized and their activity evaluated. Modulating the length and nature of the linker (i.e. aliphatic, partially aromatic, containing or not heteroatoms) a panel of 12 compounds was synthesized and evaluated, suggesting compounds **29a**,**30a**, **30b** and **30e** as potent CRBN degraders that "hook" at 1 μM concentration, warranting further investigations to completely characterized their degradation activity. This approach can be considered a powerful tool to investigate the mechanism of CRBN degradation mediated by Homo-PROTACs, potentially with both biological and therapeutic benefits.

5.3 Chemistry

All the final compounds were synthesized following a modular approach, consisting in the synthesis of the CRBN or VHL binding units, the synthesis of the linkers and the linkage of these three units to give the desired PROTACs. The symmetric linkers **12a-e** (Scheme1) were efficently obtained in two steps from the corrisponding diols, commercially available **10b-e** or synthesized starting from compound **8** as in the case of **10a** (SI Scheme 1). The first step was carried out reacting **10a-e** with an excess of *tert*-butyl bromoacetate, in a biphasic nucleophilic substitution reaction, using NaOH as base and TBABr as phase transfer catalyst. The di *tert*-butyl esters obtained **11a-e** were then deprotected to give the final symmetric dicarboxylic linkers, **12a-e**.

Scheme 1

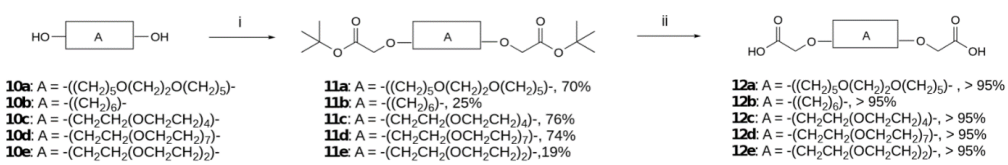

Scheme 1: *Synthesis of linkers **12a-e**. i) Tert-butyl bromoacetate, TBABr, NaOH 37%, DCM, r.t, overnight; ii) 1:1 TFA/DCM, r.t, 1 h.*

Compounds **12a-e** (scheme 2), were activated with 1.1 eq. *N*-hydroxysuccinimide (NHS) and 1.2 eq. *N*,*N*'-dicycloesilcarbodiimide (DCC), in order to promote the formation of the mono *N*-hydroxysuccinamide ester derivatives. Then, the NHS esters were reacted in excess (again to minimize the formation of 2:1 conjugates) with the CRBN ligand **5**. This strategy allowed to obtain the desired 1:1 adducts **13a-e**, characterized by the CRBN ligand **5** attached at one end of the linker, as major products. However, in most cases 2:1 adducts (**29b-e**), were also observed as minor products and they were isolated as CRBN Homo-PROTACs. Reacting the carboxylic acids **13a-e**, with compound **1** in presence of COMU and DIPEA in DMF, the final compounds **14a-e** were obtained (Scheme 2).

The asymmetric linkers **16a** and **16b** (Scheme 3) were synthesized from the previously reported compounds **15a** and **15b** respectively.[44] For VHL-CRBN PROTACs derivatized on the phenol (**18 a-c**), the linkers previously synthesized, **16a-b**, or commercially available, **16c**, were reacted overnight with compound **2** (Scheme 3), via a nucleophilic substitution in DMF at 70°C, using K_2CO_3 as base. The esters **17a-c** obtained were then hydrolysed, in acidic conditions with 50% TFA in DCM for the *tert*-butyl esters **17a-b** or using LiOH in a mixture of water and methanol for the methyl ester **17c**. Reacting the three carboxylic acids obtained with the amine **5**, gave the final compounds **18a-c**.

Scheme 2

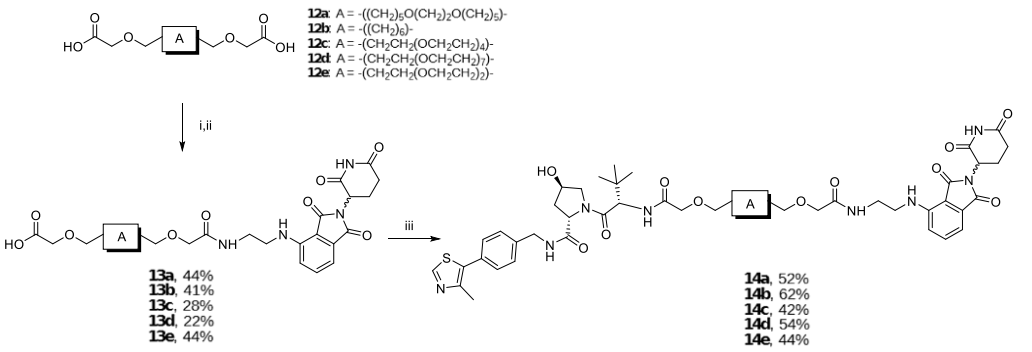

Scheme 2. *Synthesis of PROTACs **14a-e**. Reagents and conditions: i) NHS, DCC, DCM, r.t, overnight; ii) **5**, DIPEA, DMF, r.t; iii) **1**, COMU, DIPEA, DMF.*

Scheme 3

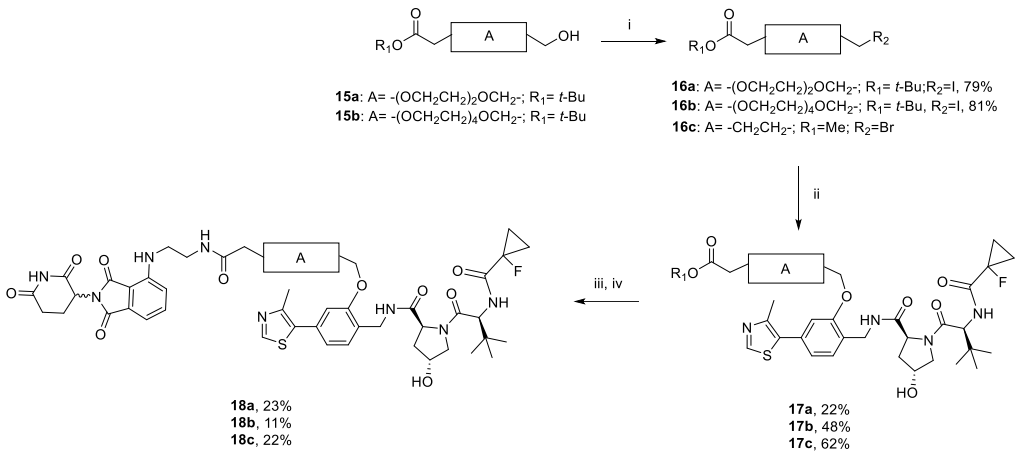

Scheme 3. *Synthesis of PROTACs **18a-c**. Reagents and conditions: i) Iodine, triphenylphosphine, imidazole, DCM, 0°C; ii) **2**, K_2CO_3, DMF, 70°C, overnight, iii) for tert-butyl deprotection: 1:1 TFA/DCM; for the methyl deprotection: LiOH in water/THF, 2 h, r.t; iv) COMU, **5**, DIPEA, DMF, r.t.*

Compounds **22a-c** were synthesized applying a synthetic strategy similar to that reported above for compounds **18a-c**. The linkers **16a-c** were reacted via a nucleophilic substitution with compound **3**, synthesized in two steps from the previously reported **19**.[29] The reaction was carried out in DMF at room temperature using DBU as base. Again, the *tert*-butyl esters **21a-b** were hydrolysed in acidic condition with 50% TFA in DCM, while methyl ester **21c** was hydrolysed with LiOH in a mixture of water and methanol. The coupling reaction between the carboxylic acids obtained and compound **5**, gave the final PROTACs **22a-c**.

Scheme 4

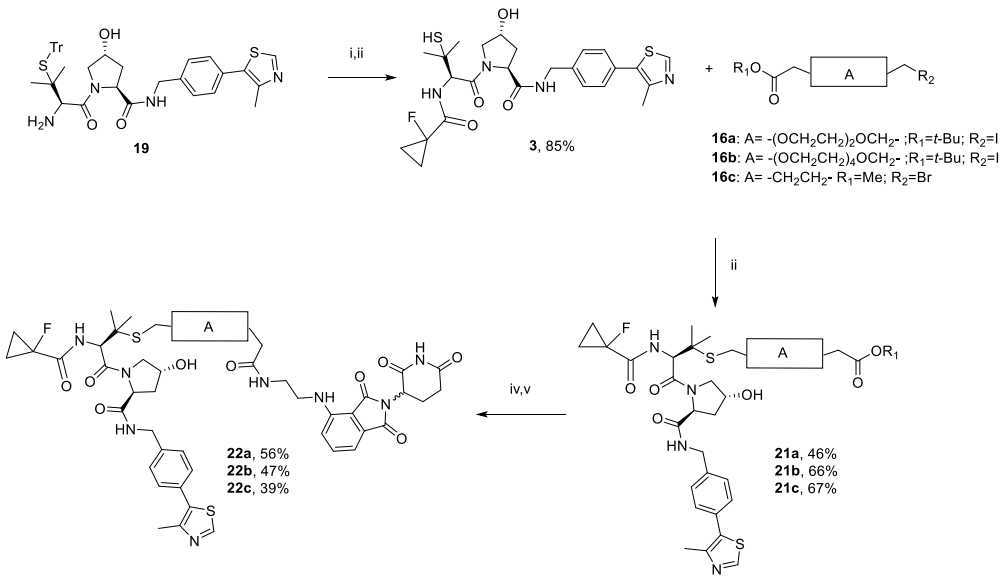

Scheme 4. *Synthesis of PROTACs **22a-c**. Reagents and conditions: i) 1-fluorocyclopropane-1-carboxylic acid, HATU, HOAt, DIPEA, DMF, r.t., 30 min; ii) TIPS, TFA, DCM, r.t., 2h; iii) DBU, DMF, 0°C to r.t, 4 h; iv) For tert-butyl deprotection: 1:1 TFA/DCM; for the methyl deprotection: LiOH in water/THF 2h, r.t; v) COMU, **5**, DIPEA in DMF, r.t.*

The linkers **27a-c** (Scheme 5) were obtained in two steps from the corresponding diols **25a-c**. The synthesis of compound **25b** has been previously reported.[47] Compound **25a** was synthesized in two steps from the previously reported **23**[44] (SI Scheme 2) and compound **25c** derived from the hydroboration/oxidation of **S1**[48] (SI Scheme 3). The dicarboxylic acids **27a-c** were activated with COMU and reacted with 2.1 equivalents of the amine **1**. This synthetic strategy allowed to obtained compound **28a-c** in good yields (Scheme 5). Final compounds **28d-f**, **28g** and **28i** (Scheme 6) were obtained following the same protocol from the corresponding dicarboxylic linkers (**27d-f**, **12a**, **12c**). The synthesis of **27d** was successfully achieved by reacting compound **S2** and **S3** via a nucleophilic substitution, followed by the hydrogenation of the debenzylated product obtained, and the formation of the di *tert*-butyl esters. **27f** was synthesized from the commercially available triethylene glycol in two steps: the diol was first reacted with *tert*-butyl acrylate in a biphasic reaction with DCM and 50% $NaOH_{aq.}$ and then deprotected using 50% TFA in DCM (SI Scheme 5). The hexadecanedioic acid linker **27e** is commercially available. Compound **28h** was synthesized from compound **21b**,

hydrolysing the *tert*-butyl ester in 50% TFA in DCM and then reacting the carboxylic acid derivate with the amine **1** (Scheme 7).

Scheme 5

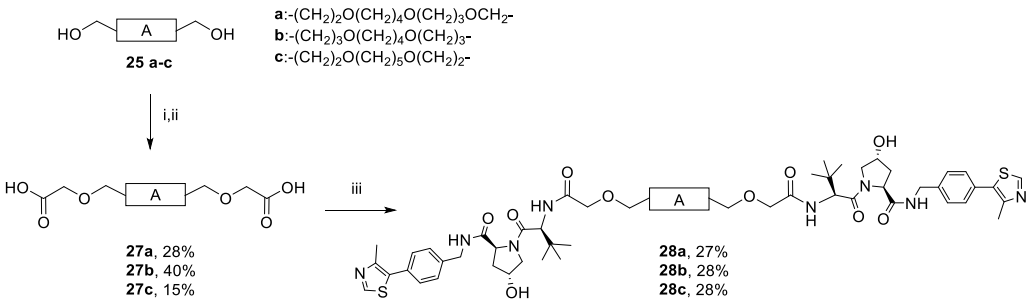

Scheme 5. *i) tert-butyl bromoacetate, TBABr, NaOH 37%, DCM, r.t, overnight; ii) 50% TFA in DCM, r.t, 1 h, quantitative; iii) COMU, DIPEA (5 eq.) in DMF dry, r.t. After 10 min:* ***1****, DIPEA, r.t., 2h.*

Scheme 6

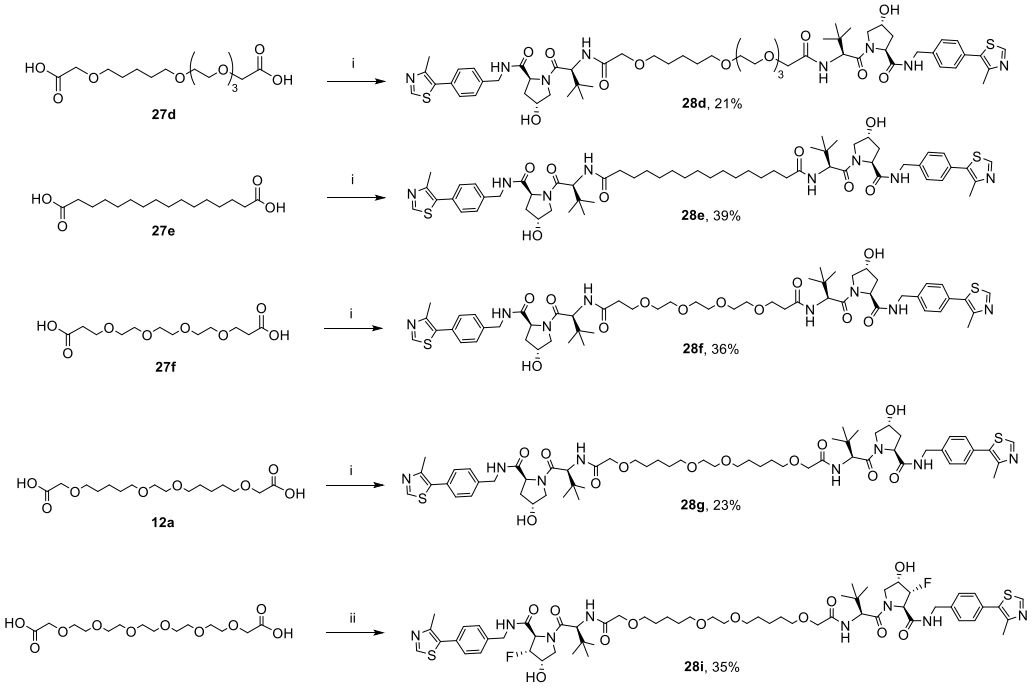

Scheme 6. *i) COMU, DIPEA (5 eq.),* ***1*** *(2.1 eq.), DMF dry, 2h; ii) COMU, DIPEA (5 eq.),* ***S5*** *(2.1 eq.), DMF dry, 2h.*

Scheme 7

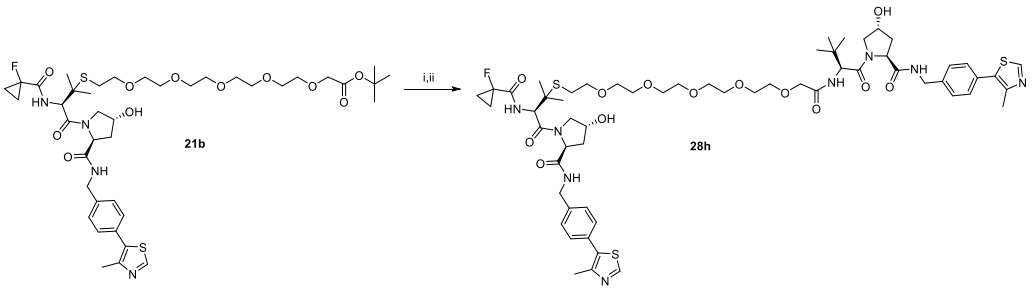

Scheme 7. *i) 50% TFA in DCM, r.t, 1 h, quantitative; ii) COMU, DIPEA (5 eq.),* ***1*** *(2.1 eq.), DMF dry, 2h, 42%.*

The final CRBN-CRBN Homo-PROTACs **29f-g** were obtained in good yields after the reaction among the dicarboxylic acids **12f-g**, previously synthesized in one step from **6** and **7**, and 2.1 equivalents of the amine **5**, with COMU and DIPEA in dry DMF. Analogously compound **29a** was obtained from **12a**. The PROTACs **30a-e** were obtained reacting overnight the CRBN ligand **4** with the appropriate commercially available diamine linkers via a nucleophilic aromatic substitution in DMSO, using DIPEA as base.

Scheme 8

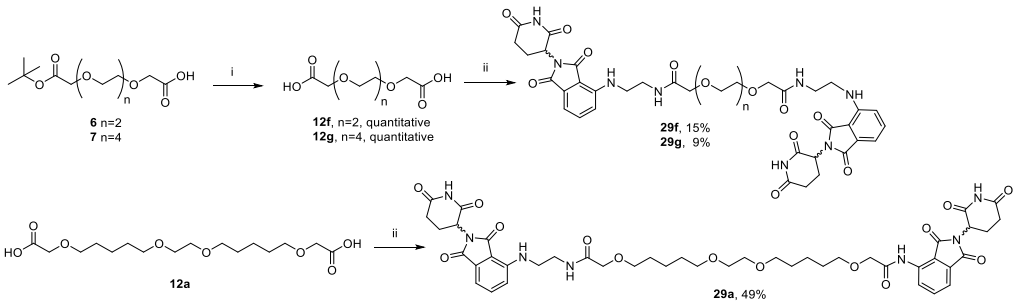

Scheme 8. *i) 50% TFA in DCM, r.t, 1 h, quantitative; ii) COMU, DIPEA (5 eq.),* ***1*** *(2.1 eq.), DMF dry, 2h.*

Scheme 9

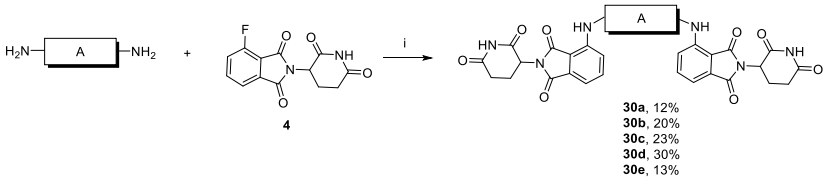

Schema 9. *Synthesis of compounds* ***31 a-e****. Conditions: i) DIPEA, DMSO, 90°C, overnight. For complete structures see Chart 5.*

5.4 Materials and methods

5.4.1 Synthetic chemistry

Commercially available chemicals were purchased from Apollo Scientific, Sigma-Aldrich, Fluorochem, or Manchester Organics and used without any further purification. Compounds **1**,[38] **2**,[32] **4**,[49] **5**,[32] **CMP85** e **CMP86**[50] were prepared as previously reported. The synthesis of compounds **S1-S5** is described in the Appendix B. All reactions were carried out using anhydrous solvents. Analytical thin-layer chromatography (TLC) was performed on precoated TLC plates (layer 0.20 mm silica gel 60 with fluorescent indicator (UV 254: Merck)). The TLC plates were air-dried and revealed under UV lamp (254/365 nm). Flash column chromatography was performed using prepacked silica gel cartridges (230–400 mesh, 40–63 mm; SiliCycle) using a Teledyne ISCO Combiflash Companion or Combiflash Retrieve using the solvent mixtures stated for each synthesis as mobile phase. Preparative HPLC was performed on a Gilson preparative HPLC with a Waters X-Bridge C18 column (100 mm x 19 mm; 5 µm particle size, flow rate 25 ml/min). Liquid chromatography–mass spectrometry (LC–MS) analyses were performed with either an Agilent HPLC 1100 series connected to a Bruker Daltonics MicroTOF or an Agilent Technologies 1200 series HPLC connected to an Agilent Technologies 6130 quadrupole spectrometer. For LC-MS the analytical column used was a Waters X-bridge C18 column (50 mm × 2.1 mm × 3.5 mm particle size); flow rate, 0.5 mL/min with a mobile phase of water/MeCN + 0.01% NH4OH or water/MeCN + 0.01% HCOOH; 95/5 water/MeCN was initially held for 0.5 min followed by a linear gradient from 95/5 to 5/95 water/MeCN over 3.5 min which was then held for 2 min. The purity of all the compounds was evaluated using the analytical LC–MS system described before, and purity was >95%. ^{1}H NMR and ^{13}C NMR spectra were recorded on a Bruker Avance II 500 spectrometer (^{1}H at 500.1 MHz, ^{13}C at 125.8 MHz) or on a Bruker DPX-400 spectrometer (^{1}H at 400.1 MHz, ^{13}C at 101 MHz).

Chemical shifts (δ) are expressed in ppm reported using residual solvent as the internal reference in all cases. Signal splitting patterns are described as singlet (s), doublet (d),

triplet (t), multiplet (m), or a combination thereof. Coupling constants (*J*) are quoted to the nearest 0.1 Hz.

General method A: to a solution of diol (1 eq.) in DCM (4 mL per mmol), *tert*-butyl bromoacetate (8 eq.), TBABr (1.1 eq.) and 37% w/w aqueous NaOH (4 mL per mmol) were added. The biphasic reaction was vigorously stirred at room temperature overnight. The organic phase was separated from the aqueous layer and then the aqueous phase was extracted with DCM (x3). Organic layers were collected, dried over $MgSO_4$ and evaporated under reduced pressure. The crude was purified by flash chromatography.

General Method B: a solution of the starting material in a 50% v/v TFA in DCM (6 mL per mmol) was stirred at r.t. for 2 h. Then, the reaction mixture was concentrated under reduced pressure and the crude was freeze-dried to obtain the desired product.

General method C: potassium *tert*-butoxide (1 eq.) was added to polyethylene glycol (8 eq.) in anhydrous THF (0.2 mL/mmol) at 0 °C. The resulting mixture was stirred at 60 °C for 0.5 h, then it was cooled to r.t. A solution of tert-butyl-bromoacetate (1.0 eq.) in anhydrous THF (0.1 mL/mmol) was added to the reaction mixture at r.t. The resulting mixture was stirred at r.t. for 24 h. The reaction was quenched with brine and the aqueous phase was extracted with ethyl acetate. The combined organic phase was evaporated to dryness. The crude material was purified by column chromatography (from 0 to 8% of methanol in dichloromethane) to afford the desired compound.

General method D: iodine (1.3 eq.) was added to triphenylphosphine (1.3 eq.) and imidazole (1.3 eq.) in DCM (7 mL/mmol) at 0 °C. The resulting mixture was stirred at r.t. for 5 min, then was cooled to 0 °C. A solution of alcohol (1.0 eq.) in dichloromethane (3 mL/mmol) was added to the reaction mixture at 0 °C and the resulting mixture was stirred at r.t. for 3 h. The reaction was quenched with saturated NaHCO3 solution and saturated Na_2SO_3 solution and the aqueous phase was extracted with ethyl acetate. The combined organic phase was evaporated to dryness. The crude material was purified by column chromatography (from 20 to 75% of ethyl acetate in heptane) to afford the desired compound.

General method E: the dicarboxylic acid linker (1 eq.) and *N*-hydroxysuccinimide (1.1 eq.) were dissolved in dry DCM (~10 mL per mmol). *N*,*N*'-dicyclohexylcarbodiimide (1.2 eq.) was added and the reaction was left to stir overnight. The dicyclohexylurea was filtered off, the solution was evaporated and the residue dissolved in dry DMF. Compound **5** (0.5 eq.) and DIPEA (3 eq.) were added and the reaction mixture was left to stir at room temperature for 2 h. Then it was quenched with ice, dried under high vacuum and purified by HPLC using a gradient from 10% to 80% v/v acetonitrile with 0.01% v/v aqueous solution of formic acid over 15 min to yield the desired compound.

General method F: to a solution of carboxylic compound (1 eq.) in dry DMF (~ 50 mL per mmol), COMU (1 eq.), compound **1** (1.1 eq.) and DIPEA (3 eq.) were added. Reaction mixture was left to stir for 1 h and monitored by LC-MS. When completed, ice was added to quench the reaction, the volatiles were evaporated under high vacuum and the residue purified by HPLC with a gradient from 5% to 90% v/v acetonitrile with 0.01% v/v aqueous solution of formic acid over 15 min to yield the desired compound.

General method G: to a solution of **3** (1 eq.) and the linker (1.1 eq.) in dry DMF (~ 14 mL per mmol), DBU (1.1 eq.) was added at 0 °C under a nitrogen atmosphere. Reaction mixture was stirred at r.t. for 4 h. Reaction was quenched with a 5% v/v aqueous solution of citric acid and the solvent was evaporated under high vacuum. The crude was purified by HPLC using a gradient from 5% to 90% v/v acetonitrile with 0.01% v/v aqueous solution of formic acid over 15 min to yield the desired compound.

General method H: to a solution of the carboxylic compound (1 eq.) in DMF dry (~ 100 mL per mmol), COMU (1 eq.), compound **5** (1.1 eq.) and DIPEA (3 eq.) were added. The reaction mixture was left to stir for 1 h and monitored by LC-MS. Then, ice was added to quench the reaction, the volatiles were evaporated under high vacuum and the residue purified by HPLC using a gradient from 5% to 90% v/v acetonitrile with 0.01% v/v aqueous solution of formic acid over 15 min to yield the desired compound.

General method I: compound **2** (1 eq.), K_2CO_3 (3 eq.) and the halogenated linker (1.5 eq.) was dissolved in DMF (~ 50 mL per mmol) and heated at 70 °C overnight. Reaction mixture was taken up with water and extracted with DCM (x3). Organic layers were

collected, dried over $MgSO_4$, evaporated under reduced pressure and purified by HPLC using a gradient from 5% to 95% v/v acetonitrile with 0.01% v/v aqueous solution of formic acid over 10 min to yield the desired compound.

General method L:

A solution of the benzylated starting material in absolute EtOH (0.05 M) was flown in an H-cube machine at a rate of 1 mL/min, H_2 10 atm, 70 °C. Solvent was evaporated under reduced pressure and the product was obtained in quantitative yield.

General method M:

The dicarboxylic acid linker (1 eq.) was dissolved in dry DMF. Then COMU (2 eq.) and DIPEA (5 eq.) and the appropriate amine (2.1 eq.) were added. The mixture was stirred at r.t. until no presence of the starting material was detected by LC-MS. Ice was added and the volatiles were evaporated under reduced pressure to give the crude which was purified by HPLC using a gradient of 20% to 70% v/v acetonitrile in 0.1% v/v aqueous solution of formic acid to yield the final compound.

General method N:

A solution of compound **4** (2 eq.), the appropriate diamine (1 eq.) and DIPEA (4 eq.) in DMSO (10 mL per mmol) was heated at 90°C and stirred overnight. Then the mixture was cooled to room temperature and neutralized with a 5% aqueous solution of citric acid. Brine was added and the mixture was extracted with DCM (x4). Organic layers were collected, dried over $MgSO_4$ and purified by HPLC using a gradient of 5% to 95% v/v acetonitrile in 0.1% v/v aqueous solution of formic acid to yield the final compound.

(2S,4R)-1-((R)-2-(1-fluorocyclopropane-1-carboxamido)-3-mercapto-3-methylbutanoyl)4-hydroxy-N-(4-(4-methylthiazol-5-yl)benzyl)pyrrolidine-2-carboxamide (3)

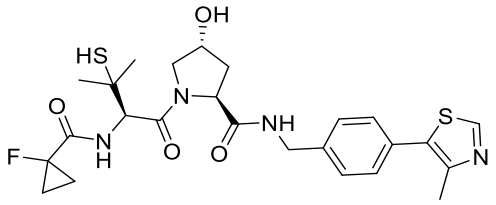

To a solution of compound **19** (0.04 mmol), HATU (16 mg, 0.04 mmol), HOAT (5.71 mg, 0.04 mmol) 1-fluorocyclopropane-1-carboxylic acid (4.3 mg, 0.04 mmol) in DMF (1 mL), DIPEA (25 µL, 0.14 mmol) was added. The reaction mixture was stirred at room temperature for 30 min, then water (1 mL) was added and the resulting mixture was extracted with DCM (3 x 5 mL). After drying the organic phase over $MgSO_4$ and the solvent was removed under reduced pressure to afford the title compound (28.3 mg, 85% yield) which was used without further purification.^{1}H-NMR (400 MHz, $CDCl_3$) δ 8.71 (s, 1H), 7.54 - 7.51 (m, 6H), 7.34 - 7.31 (m, 3H), 7.25 - 7.19 (m, 12H), 4.69 - 4.64 (m, 1H), 4.38 - 4.36 (m, 1H), 4.32 - 4.19 (m, 2H), 3.66 (d, *J*=4.0 Hz, 1H), 3.50 (d, *J*=11.6 Hz, 1H), 3.26 (dd, *J*=4.0, 11.6 Hz, 1H), 3.09 (d, *J*=5.9 Hz, 1H), 2.41 - 2.33 (m, 1H), 2.14 - 2.07 (m, 1H), 1.38 - 1.21 (m, 7H), 0.97 (s, 3H). ^{19}F-NMR: -197.41. MS analysis: calculated for $C_{44}H_{45}FN_4O_4S_2$: 776.3; observed: 777.3 $[M+H]^+$. The trityl protected compound (0.04 mmol) was dissolved in 1.8 mL of DCM. TIPS (0.1 mL) and TFA (0.1 mL) were added, and the mixture was left to react at room temperature for 2 h. HPLC analysis showed complete conversion of the starting material. Volatiles were removed and the crude was dissolved in MeOH, filtered and purified by preparative HPLC and freeze-dried to give pure deprotected compound as white solid (16 mg, 79% yield). ^{1}H-NMR (500 MHz, $CDCl_3$) δ: 8.72 (s, 1H), 7.44 (brs, 1H), 7.39 (d, *J*=9.4 Hz, 2H), 7.36 (d, *J*=7.8 Hz, 2H), 7.15 (br. s, 1H), 4.71 (t, *J*=7.9 Hz, 1H), 4.64 (d, *J*=8.5 Hz, 1H), 4.60 - 4.55 (m, 2H), 4.36 (dd, *J*=5.3, 14.8 Hz, 1H), 4.15 - 4.12 (m, 1H), 3.74 (dd, *J*=3.5, 11.3 Hz, 1H), 2.70 (s, 1H), 2.60 (s, 1H), 2.53 - 2.46 (m, 4H), 2.20 - 2.13 (m, 1H), 1.39 - 1.30 (m, 10H). 19F-NMR: -197. 80. ^{13}C NMR (101 MHz, $CDCl_3$): 169.7 (d, ^2J = 20.7 Hz), 169.4, 169.2, 169.5, 147.3, 137.0, 130.0, 128.7, 127.2, 77.05 (d, 1*J*= 232.0 Hz), 69.1, 57.9, 56.6, 55.5, 45.0, 42.3, 35.3, 29.5,

27.7, 14.9, 13.0 (d, ^2J = 10.6 Hz), 12.8 (d, ^2J = 10.5 Hz). MS analysis: calculated for $C_{25}H_{31}FN_4O_4S_2$: 534.2; observed: 535.2 $[M+H]^+$.

13,13-dimethyl-11-oxo-3,6,9,12-tetraoxatetradecanoic acid (6)

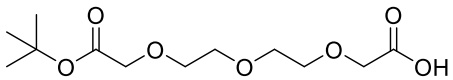

The title compound was synthesized as previously reported. Analytical data matched those reported.[50]

19,19-dimethyl-17-oxo-3,6,9,12,15,18-hexaoxaicosanoic acid (7)

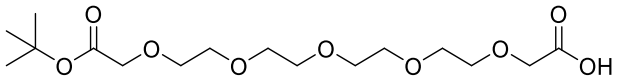

The title compound was synthesized as previously reported. Analytical data matched those reported.[36]

5-(Benzyloxy)pentyl 4-methylbenzenesulfonate (8)

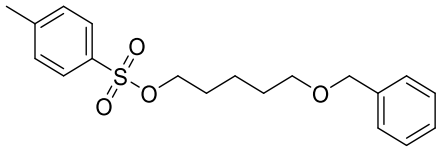

Compound **8** was prepared as previously reported. Analytical data matched those previously reported.[51]

1,18-diphenyl-2,8,11,17-tetraoxaoctadecane (9)

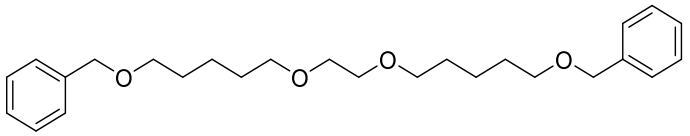

A solution of ethylene glycol (178 mg, 160 µL, 2.87 mmol, 1 eq.) and DMF dry (24.5 mL) was chilled to 0°C. NaH 60% dispersion in mineral oil (459 mg, 11.5 mmol, 4 eq.) was added and the mixture was left to stir for 1 h at room temperature. Then, compound 8 (2.0 g, 5.74 mmol, 2 eq.) was added and the mixture was stirred at 50°C overnight. After reaction completion, NH_4Cl (saturated solution) was added to pH=7, the mixture was dried under reduced pressure and partitioned between water and DCM. The aqueous phase was extracted with DCM (x2) and the organic layers were collected, dried over $MgSO_4$ and purified by flash chromatography eluting from 0% to 30% v/v ethyl acetate in heptane to yield the desired product (700 mg, yield: 79%).^{1}H-NMR (400 MHz, $CDCl_3$)

δ: 7.35 - 7.23 (m, 10H), 4.47 (s, 4H), 3.54 (s, 4H), 3.45 (t, *J*=6.5 Hz, 4H), 3.44 (t, *J*=6.5 Hz, 4H), 1.66 - 1.54 (m, 8H), 1.44 - 1.36 (m, 4H).

5,5'-(ethane-1,2-diylbis(oxy))bis(pentan-1-ol) (10a)

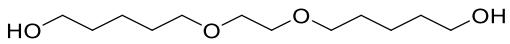

Compound **9** (500 mg, 1.21 mmol) was dissolved in EtOH (15 mL) in a dried round bottom flask under nitrogen atmosphere. Pd/C was added and the flask was evacuated and backfield with argon. The flask was evacuated again before a hydrogen balloon was connected to the reaction mixture. The reaction mixture was stirred for 6h, filtered on celite and dried under reduced pressure. The product was obtained in quantitative yield without any further purification (268 mg). ^{1}H-NMR (500 MHz, $CDCl_3$) δ: 3.45 (t, *J*=6.6 Hz, 4H), 3.43 (s, 4H), 3.34 (t, *J*=6.6 Hz, 4H), 1.50 - 1.40 (m, 8H), 1.31 - 1.21 (m, 4H);^{13}C-NMR (101 MHz, $CDCl_3$) δ: 71.2, 70.0, 62.1, 32.3, 29.2, 22.3.

Di-*tert*-butyl 3,9,12,18-tetraoxaicosanedioate (11a)

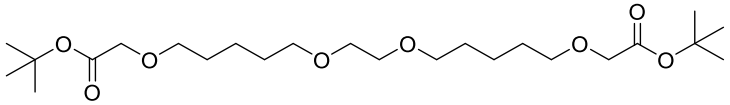

Starting from compound **10a** (118 mg, 0.50 mmol), *tert*-butyl bromoacetate (786 mg, 4.00 mmol, 8 eq.), TBABr (184 mg, 0.55 mmol, 1.1 eq.) and following the **general method A**, the title compound was obtained (168 mg, yield 70%), after flash chromatography eluting from 0% to 50% v/v ethyl acetate in heptane. ^{1}H-NMR (500 MHz, $CDCl_3$) δ: 3.87 (s, 4H), 3.49 (s, 4H), 3.44 (t, *J*=6.7 Hz, 4H), 3.39 (t, *J*=6.7 Hz, 4H), 1.61 - 1.50 (m, 8H), 1.41 (s, 18H), 1.39 - 1.31 (m, 4H).

3,9,12,18-tetraoxaicosanedioic acid (12a)

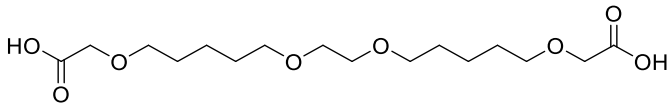

Starting from compound **11a** (83 mg, 0.17 mmol) and following the **general method B** compound **12a** was obtained in quantitative yield (64 mg). ^{1}H-NMR (500 MHz, $CDCl_3$) δ: 8.06 (s, 2H), 4.09 (s, 4H), 3.59 (s, 4H), 3.56 (t, *J*=6.5 Hz, 4H), 3.49 (t, *J*=6.5 Hz, 4H), 1.66 - 1.58 (m, 8H), 1.47 - 1.41 (m, 4H); ^{13}C-NMR (101 MHz, $CDCl_3$) δ: 174.4, 72.0, 71.4, 70.1, 67.9, 29.2, 29.1, 22.6.

1-((2-(2,6-dioxopiperidin-3-yl)-1,3-dioxoisoindolin-4-yl)amino)-4-oxo-6,12,15,21tetraoxa-3-azatricosan-23-oic acid (13a)

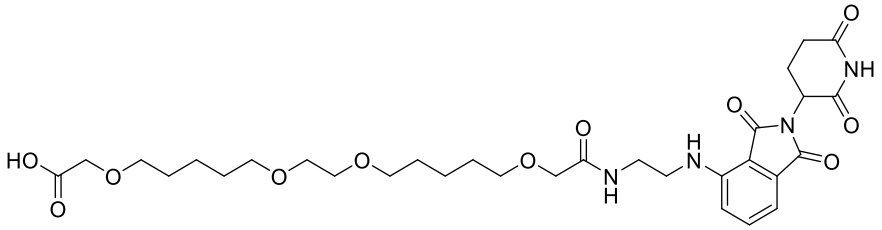

Starting from compound **12a** (36 mg, 0.10 mmol,1 eq) and following the **general method E**, the title compound was obtained (14 mg, yield: 44%). ^{1}H-NMR (500 MHz, $CDCl_3$) δ: 7.48 (dd, *J*=7.2, 8.8 Hz, 1H), 7.09 (d, *J*=7.2 Hz, 1H), 6.98 (d, *J*=8.8 Hz, 1H), 4.93 - 4.89 (m, 1H), 4.04 (s, 2H), 3.93 (s, 2H), 3.55 - 3.41 (m, 16H), 2.88 - 2.66 (m, 3H), 2.13 - 2.06 (m, 1H), 1.64 - 1.52 (m, 8H), 1.46 - 1.32 (m, 4H); ^{13}C-NMR (126 MHz, $CDCl_3$) δ: 172.4, 171.7, 171.4, 169.5, 168.8, 167.7, 146.9, 136.4, 132.7, 116.9, 112.1, 110.7, 71.9, 71.3, 71.2, 70.3, 70.2, 68.1, 49.1, 42.3, 38.6, 31.6, 29.4, 29.3, 22.9, 22.7. MS analysis: calculated for $C_{31}H_{44}N_4O_{11}$: 648.301; observed: 649.0 $[M+H]^+$

N^1-(2-((2-(2,6-dioxopiperidin-3-yl)-1,3-dioxoisoindolin-4-yl)amino)ethyl)-N^{20}-((S)-1((2S,4R)-4-hydroxy-2-((4-(4-methylthiazol-5-yl)benzyl)carbamoyl)pyrrolidin-1-yl)-3,3dimethyl-1-oxobutan-2-yl)-3,9,12,18-tetraoxaicosanediamide (14a)

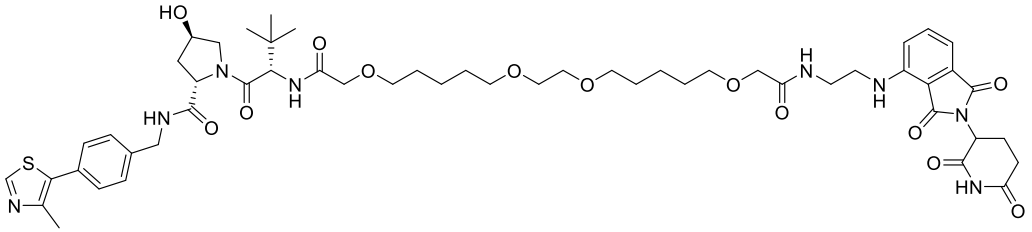

Starting from compound **13a** (14 mg, 0.02 mmol, 1 eq.) and following the **general method F**, the title compound was obtained (12 mg, yield: 52%). ^{1}H-NMR (400 MHz, MeOD) δ: 9.00 (s, 1H), 7.56-7.52 (m, 1H), 7.48-7.41 (m, 4H), 7.14 (d, *J*=8.5 Hz, 1H), 7.05 (d, *J*=7.5 Hz, 1H), 5.05 (dd, *J*=5.2, 12.7 Hz, 1H), 4.70 (d, *J*=10.3 Hz, 1H), 4.60 - 4.50 (m, 3H), 4.36 (d, *J*=16.0 Hz, 1H), 3.96 (d, *J*=6.9 Hz, 2H), 3.91 - 3.78 (m, 4H), 3.47 (m, 16H), 2.90 - 2.64 (m, 3H), 2.48 (s, 3H), 2.26 - 2.21 (m, 1H), 2.12 - 2.05 (m, 2H), 1.68 - 1.33 (m, 12H), 1.03 (s, 9H); ^{13}C-NMR (101 MHz, MeOD) δ: 174.5, 174.2, 173.4, 172.0, 171.9, 171.6, 171.4, 170.5, 169.1, 153.1, 148.2, 148.0, 140.4, 137.1, 133.8, 133.7, 131.0, 130.3, 129.4, 128.9, 118.0, 112.0, 111.3, 72.7, 72.6, 72.0, 71.0, 70.8, 70.6, 66.8, 60.7, 58.0, 57.9, 43.6, 42.6, 39.3, 38.8, 37.1, 32.1, 30.3, 30.1, 26.8, 23.7, 23.6, 15.5, 15.3. HR-MS analysis: calculated for $C_{53}H_{72}N_8O_{13}S$: 1060.4942; observed: 1061.5065 $[M+H]^+$.

Di-*tert*-butyl 2,2'-(hexane-1,6-diylbis(oxy))diacetate (11b)

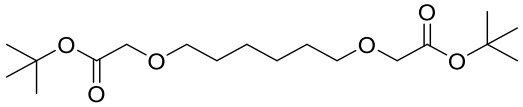

Starting from the commercially available 1,6-hexandiol (250 mg, 2.2 mmol), *tert*-butyl bromoacetate (3.3 g, 17.6 mmol, 8 eq.), TBABr (750 mg, 2.4 mmol, 1.1 eq.) and following the **general method A** the titled compound was obtained (185 mg, yield 25%), after flash chromatography eluting from 0% to 10% v/v ethyl acetate in heptane.^{1}H-NMR (400 MHz, $CDCl_3$) δ: 3.92 (s, 4H), 3.49 (t, *J*=6.6 Hz, 4H), 1.64 - 1.56 (m, 4H), 1.46 (s, 18H), 1.41 - 1.34 (m, 4H).

2,2'-(hexane-1,6-diylbis(ox))diacetic acid (12b)

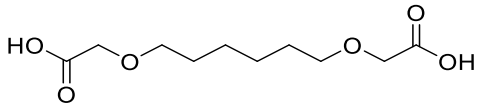

Starting from compound **11b** (185 mg, 0.53 mmol) and following the **general method B** compound **12b** was obtained in quantitative yield (125 mg). ^{1}H-NMR (400 MHz, DMSO-d_6) δ: 12.49 (s, 2H), 3.97 (s, 4H), 3.43 (t, *J*=6.6 Hz, 4H), 1.55 - 1.47 (m, 4H), 1.34 - 1.28 (m, 4H);^{13}C-NMR (101 MHz, DMSO-d_6) δ 171.6, 70.4, 67.4, 29.0, 25.3.

2-((6-(2-((2-(2,6-dioxopiperidin-3-yl)-1,3-dioxoisoindolin-4-yl)amino)ethyl)amino)-2oxoethoxy)hexyl)oxy)acetic acid (13b)

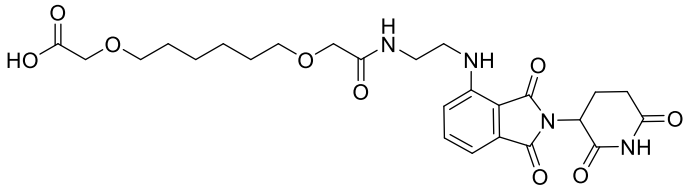

To a solution of compound **12b** (15.0 mg, 0.06 mmol, 1 eq.) and following the **general method E**, the title compound was obtained (7 mg, yield: 41%). ^{1}H-NMR (400 MHz, MeOD) δ: 7.56 (dd, *J*=7.1, 8.6 Hz, 1H), 7.15 (d, *J*=8.6 Hz, 1H), 7.07 (d, *J*=7.1 Hz, 1H), 5.05 (dd, *J*=5.5, 12.5 Hz, 1H), 4.02 (s, 2H), 3.90 (s, 2H), 3.52 - 3.45 (m, 8H), 2.91 - 2.67 (m, 3H), 2.15 - 2.08 (m, 1H), 1.63 - 1.55 (m, 4H), 1.38 - 1.34 (m, 4H); ^{13}C-NMR (126 MHz, MeOD) δ: 174.6, 174.1, 173.5, 171.5, 170.6, 169.3, 148.2, 137.2, 134.0, 118.1, 112.1, 111.5, 72.8, 72.6, 70.9, 68.7, 42.7, 39.4, 32.2, 30.4, 26.8, 23.8. MS analysis: calculated for $C_{25}H_{32}N_4O_9$: 532.22; observed: 533.3 $[M+H]^+$.

(2S,4R)-1-((2S)-2-(tert-butyl)-18-((2-(2,6-dioxopiperidin-3-yl)-1,3-dioxoisoindolin-4yl)amino)-4,15-dioxo-6,13-dioxa-3,16-diazaoctadecanoyl)-4-hydroxy-N-(4-(4methylthiazol-5-yl)benzyl)pyrrolidine-2-carboxamide (14b)

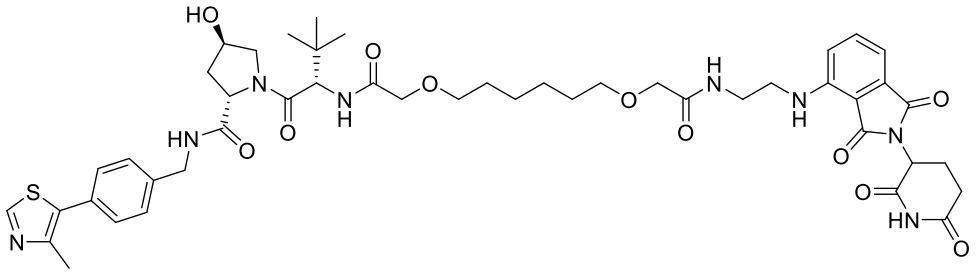

Starting from compound **13b** (7 mg, 0.01 mmol, 1 eq) and following the **general method F**, the title compound was obtained (7.7 mg, yield: 62%). ^{1}H-NMR (400 MHz, MeOD) δ: 8.99 (s, 1H), 7.56 -7.49 (m, 1H), 7.44 (dd, *J*=7.9, 21.3 Hz, 4H), 7.11 (d, *J*=8.9 Hz, 1H), 7.05 (d, *J*=7.0 Hz, 1H), 5.04 (dd, *J*=5.6, 12.6 Hz, 1H), 4.71-4.68 (m, 1H), 4.61 - 4.33 (m, 4H), 3.95 (d, *J*=6.3 Hz, 2H), 3.91 - 3.78 (m, 4H), 3.54 - 3.42 (m, 8H), 2.85 - 2.63 (m, 3H), 2.48 (s, 3H), 2.26 - 2.21 (m, 1H), 2.10 - 2.07 (m, 2H), 1.63 - 1.56 (m, 4H), 1.40 - 1.31 (m, 4H), 1.03 (s, 9H).^{13}C-NMR (101 MHz, MeOD) δ: 174.4, 174.1, 173.3, 171.8, 171.5, 171.3, 170.4, 169.0, 153.0, 148.0, 140.3, 137.0, 133.8, 130.9, 130.2, 128.9, 117.9, 112.0, 111.2, 72.7, 72.5, 70.9, 70.7, 70.5, 60.6, 57.9, 57.8, 43.5, 42.5, 39.2, 38.7, 37.0, 32.0, 30.3, 30.2, 26.7, 26.6, 23.6, 15.2. HR-MS analysis: calculated for $C_{47}H_{60}N_8O_{11}S$: 944.410; observed: 945.4270 $[M+H]^+$.

Di-*tert*-butyl 3,6,9,12,15,18-hexaoxaicosanedioate (11c)

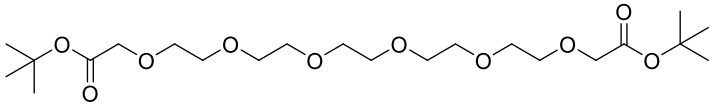

Starting from the commercially available pentaethylene glycol **10c** (201 mg, 0.84 mmol), *tert*-butyl bromoacetate (1.318 g, 6.7 mmol, 8 eq.), TBABr (308 mg, 0. 92 mmol, 1.1 eq.) and following the **general method A** the title compound was obtained (300 mg, yield 76%), after flash chromatography eluting from 0% to 20% v/v methanol in dichloromethane. Analytical data matched those previously reported.[52]

3,6,9,12,15,18-hexaoxaicosanedioic acid (12c)

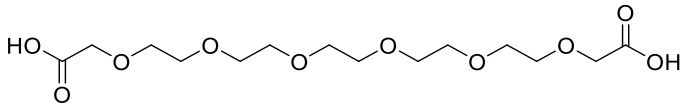

Starting from compound **11c** (300 mg, 0.64 mmol) and following the **general method B** compound **12c** was obtained in quantitative yield (226 mg). Analytical data matched those previously reported.[52]

1-((2-(2,6-dioxopiperidin-3-yl)-1,3-dioxoisoindolin-4-yl)amino)-4-oxo-6,9,12,15,18,21-hexaoxa-3-azatricosan-23-oic acid (13c)

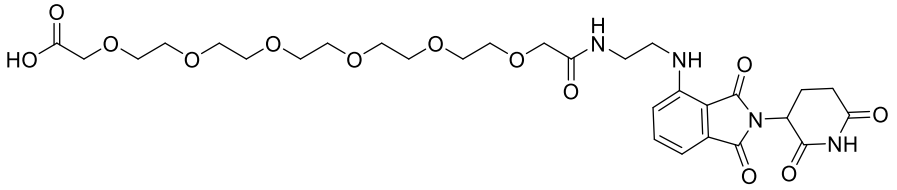

Starting from compound **12c** (23 mg, 0.07 mmol, 1 eq.) and following the **general method E**, the title compound was obtained (5.9 mg, 28%). ^{1}H-NMR (400 MHz, $CDCl_3$) δ: 7.49 (t, *J*=7.8 Hz, 1H), 7.08 (d, *J*=6.8 Hz, 1H), 7.03 (d, *J*=8.4 Hz, 1H), 4.93 - 4.86 (m, 1H), 4.10 (s, 2H), 3.97 (s, 2H), 3.72 - 3.45 (m, 24H), 2.89 - 2.65 (m, 3H), 2.13 - 2.07 (m, 1H); ^{13}C-NMR (126 MHz, $CDCl_3$) δ:172.5, 171.4, 171.3, 169.4, 168.7, 167.8, 147.0, 136.4, 132.7, 117.0, 111.9, 110.5, 71.0, 70.5, 70.4, 70.3, 70.2, 69.4, 49.1, 42.0, 38.5, 31.6, 22.9. MS analysis: calculated for $C_{29}H_{40}N_4O_{13}$: 652.259 observed: 653.3 $[M+H]^+$.

***N*^{1}-(2-((2-(2,6-dioxopiperidin-3-yl)-1,3-dioxoisoindolin-4-yl)amino)ethyl)-*N*^{20}-((S)-1((2S,4R)-4-hydroxy-2-((4-(4-methylthiazol-5-yl)benzyl)carbamoyl)pyrrolidin-1-yl)-3,3dimethyl-1-oxobutan-2-yl)-3,6,9,12,15,18-hexaoxaicosanediamide (14c)**

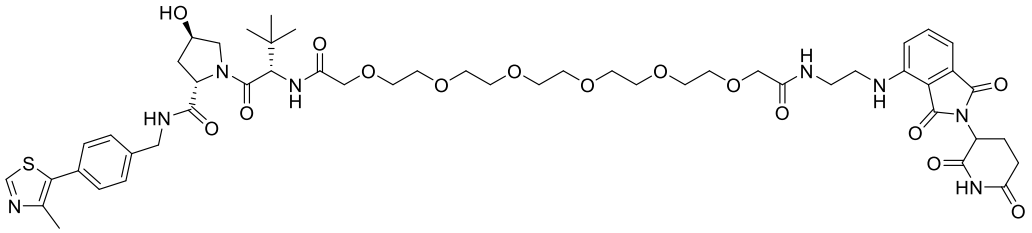

Starting from compound **13c** (5.9 mg, 0.01 mmol, 1 eq.) and following the **general method F**, the title compound was obtained (4 mg, yield: 42%). ^{1}H-NMR (400 MHz, MeOD) δ: 8.86 (s, 1H), 7.55 (dd, *J*=7.1, 8.5 Hz, 1H), 7.44 (dd, *J*=8.2, 18.7 Hz, 4H), 7.14 (d, *J*=8.5 Hz, 1H), 7.05 (d, *J*=7.1 Hz, 1H), 5.04 (dd, *J*=5.6, 12.8 Hz, 1H), 4.70 (s, 1H), 4.61 - 4.48 (m, 3H), 4.35 (d, *J*=14.2 Hz, 1H), 4.03 (d, *J*=4.4 Hz, 2H), 3.95 (s, 2H), 3.90 - 3.77 (m,

2H), 3.71 - 3.58 (m, 20H), 3.52 - 3.49 (m, 4H), 2.89 - 2.65 (m, 3H), 2.47(s, 3H), 2.26 - 2.18 (m, 1H), 2.14 - 2.05 (m, 2H), 1.04 (s, 9H).^{13}C-NMR (101 MHz, MeOD) δ 174.7, 174.4, 173.6, 172.1, 171.7, 171.5, 170.6, 169.3, 152.8, 149.1, 148.2, 140.3, 137.3, 134.0, 133.4, 131.6, 130.4, 129.0, 118.2, 112.1, 111.5, 72.3, 72.0, 71.7, 71.6, 71.5, 71.3, 71.1, 60.8, 58.2, 58.1, 43.8, 42.5, 39.4, 38.9, 37.1, 32.2, 27.0, 23.8, 15.9. HR-MS analysis: calculated for $C_{51}H_{68}N_8O_{15}S$: 1064.452; observed: 1082.4790 $[M+NH_4]^+$.

Di-*tert*-butyl 3,6,9,12,15,18,21,24,27-nonaoxanonacosanedioate (11d)

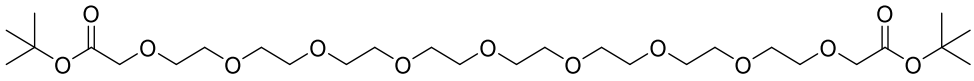

Starting from commercially available octaethylene glycol **10d**, (200 mg, 0.54 mmol) *tert*-butyl bromoacetate (842 mg, 4.32 mmol, 8 eq.), TBABr (191 mg, 0.59 mmol, 1.1 eq.) and following the **general method A**, the title compound was obtained (240 mg, yield 74%), after flash chromatography eluting from 0% to 20% v/v methanol in dichloromethane.^{1}H-NMR (400 MHz, $CDCl_3$) δ: 4.02 (s, 4H), 3.73 - 3.64 (m, 32H), 1.48 (s, 18H);^{13}C-NMR (101 MHz, $CDCl_3$) δ: 169.7, 81.5, 70.8, 70.7, 69.2, 28.2.

3,6,9,12,15,18,21,24,27-nonaoxanonacosanedioic acid (12d)

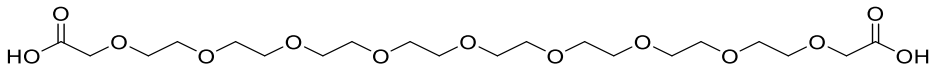

Starting from compound **11d** (100 mg, 0.17 mmol) and following the **general method B** compound **12d** was obtained in quantitative yield (80 mg). ^{1}H-NMR (400 MHz, D_2O) δ: 4.32 (4H, s), 3.87 - 3.78 (32H, m).

1-((2-(2,6-dioxopiperidin-3-yl)-1,3-dioxoisoindolin-4-yl)amino)-4-oxo-6,9,12,15,18,21,24,27,30-nonaoxa-3-azadotriacontan-32-oic acid (13d)

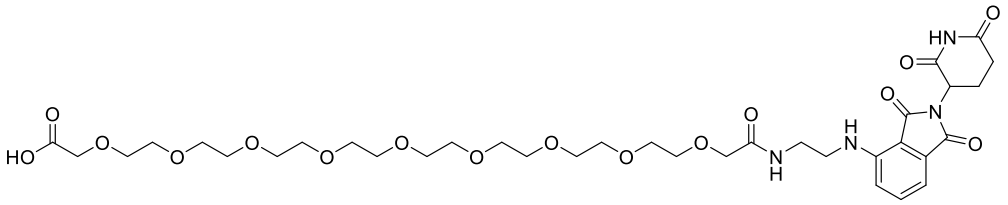

Starting from compound **12d** (48.6 mg, 0.10 mmol, 1 eq.) and following the **general method E**, the title compound was obtained (8.5 mg, yield: 22%). ^{1}H-NMR (500 MHz, $CDCl_3$) δ: 7.49 (dd, *J*=7.2, 8.5 Hz, 1H), 7.08 (d, *J*=7.1 Hz, 1H), 7.02 (d, *J*=8.6 Hz, 1H), 4.89 (dd, *J*=5.5, 12.3 Hz, 1H), 4.12 (s, 2H), 3.98 (s, 2H), 3.72 - 3.48 (m, 36H), 2.89 - 2.69 (m, 3H), 2.12 - 2.08 (m, 1H); ^{13}C-NMR (126 MHz, $CDCl_3$) δ: 172.1, 171.4, 169.4, 168.6, 167.7, 147.0, 136.4, 132.7, 117.0, 111.9, 110.5, 71.1, 70.8, 70.7, 70.6, 70.5, 70.4, 70.2, 69.3, 49.1, 42.1, 38.6, 31.6, 22.9. MS analysis: calculated for $C_{35}H_{52}N_4O_{16}$: 784.3; observed: 784.8 $[M+H]^+$.

N^1-(2-((2-(2,6-dioxopiperidin-3-yl)-1,3-dioxoisoindolin-4-yl)amino)ethyl)-N^{29}-((S)-1((2S,4R)-4-hydroxy-2-((4-(4-methylthiazol-5-yl)benzyl)carbamoyl)pyrrolidin-1-yl)-3,3dimethyl-1-oxobutan-2-yl)-3,6,9,12,15,18,21,24,27-nonaoxanonacosanediamide (14d)

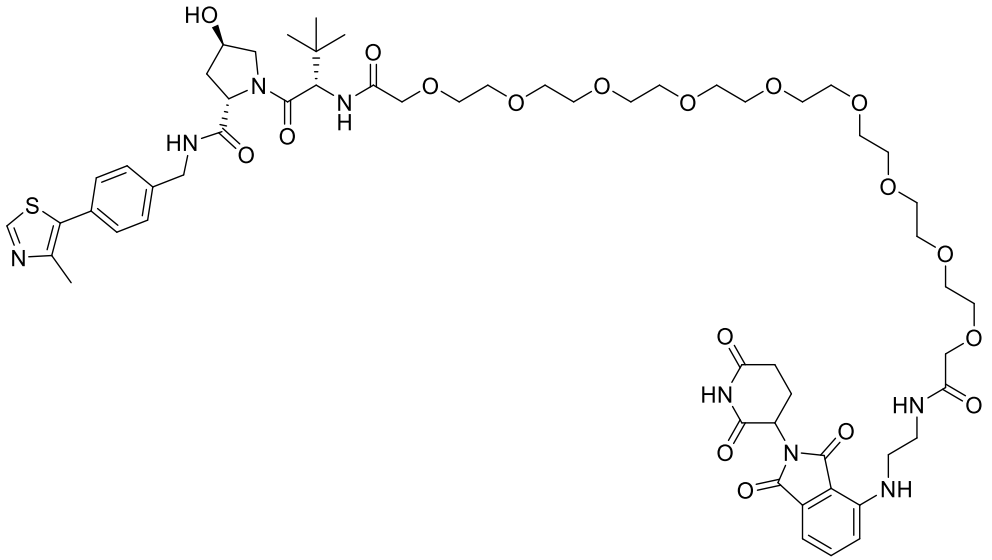

Starting from compound **13d** (8.5 mg, 0.01 mmol, 1 eq.) and following the **general method F**, the title compound was obtained (7.0 mg, yield: 54%). ^{1}H-NMR (500 MHz, MeOD) δ: 8.87 (s, 1H), 7.55 (dd, *J*=7.1, 8.6 Hz, 1H), 7.44 (dd, J=8.5, 22.4 Hz, 4H), 7.15 (d,

J=8.5 Hz, 1H), 7.06 (d, *J*=7.1 Hz, 1H), 5.04 (dd, J=5.0, 12.4 Hz, 1H), 4.70 (d, *J*=9.4 Hz, 1H), 4.60 - 4.50 (m, 3H), 4.36 (dd, *J*=5.0, 15.8 Hz, 1H), 4.04 (d, *J*=6.1 Hz, 2H), 3.96 (s, 2H), 3.89 - 3.79 (m, 2H), 3.71 - 3.51 (m, 36H), 2.88 - 2.66 (m, 3H), 2.47 (s, 3H), 2.24 - 2.20 (m, 1H), 2.12 - 2.07 (m, 2H), 1.04 (s, 9H);^{13}C-NMR (126 MHz, MeOD) δ: 174.6, 174.3, 173.5, 172.1, 171.7, 171.4, 170.6, 169.2, 152.8, 149.1, 148.2, 140.3, 137.3, 134.0, 133.4, 131.5, 130.5, 130.4, 129.5, 129.0, 118.2, 112.1, 111.5, 72.3, 72.0, 71.6, 71.5, 71.4, 71.3, 71.1, 71.0, 60.8, 58.1, 43.7, 42.5, 39.4, 38.9, 37.1, 32.2, 27.0, 23.8, 15.8. HR-MS analysis: calculated for $C_{57}H_{80}N_8O_{18}S$: 1196.531; observed: 1214. 6375 $[M+NH_4]^+$.

3,6,9,12-tetraoxatetradecanedioic acid (12e)

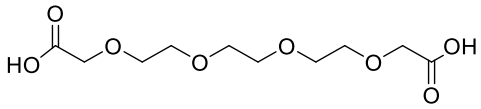

The title compound was synthesized as previously reported.[36] Analytical data matched those reported.

1-((2-(2,6-dioxopiperidin-3-yl)-1,3-dioxoisoindolin-4-yl)amino)-4-oxo-6,9,12,15-tetraoxa3-azaheptadecan-17-oic acid (13e)

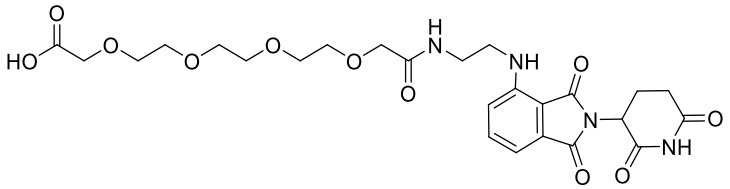

Starting from compound **12e** (26.6 mg, 0.10 mmol, 1 eq.) and following the **general method E**, the title compound was obtained (12.5 mg, 44%). ^{1}H-NMR (400 MHz, $CDCl_3$) δ: 7.47 (dd, *J*=7.2, 8.5 Hz, 1H), 7.06 (d, *J*=7.2 Hz, 1H), 7.01 (d, *J*=8.5 Hz, 1H), 4.90 (dd, *J*=5.6, 11.7 Hz, 1H), 4.08 (s, 2H), 3.99 (s, 2H), 3.72 - 3.47 (m, 16H), 2.87 - 2.70 (m, 3H), 2.13 - 2.05 (m, 1H); ^{13}C-NMR (126 MHz, $CDCl_3$) δ: 172.6, 171.7, 171.4, 169.5, 169.0, 167.7, 147.0, 136.4, 132.6, 117.1, 111.9, 110.4, 71.1, 71.0, 70.5, 70.3, 69.0, 49.1, 42.1, 38.5, 31.6, 22.9. MS analysis: calculated for $C_{25}H_{32}N_4O_{11}$: 564.21 observed: 565.3 $[M+H]^+$.

N^1-(2-((2-(2,6-dioxopiperidin-3-yl)-1,3-dioxoisoindolin-4-yl)amino)ethyl)-N^{14}-((S)-1((2S,4R)-4-hydroxy-2-((4-(4-methylthiazol-5-yl)benzyl)carbamoyl)pyrrolidin-1-yl)-3,3dimethyl-1-oxobutan-2-yl)-3,6,9,12-tetraoxatetradecanediamide (14e)

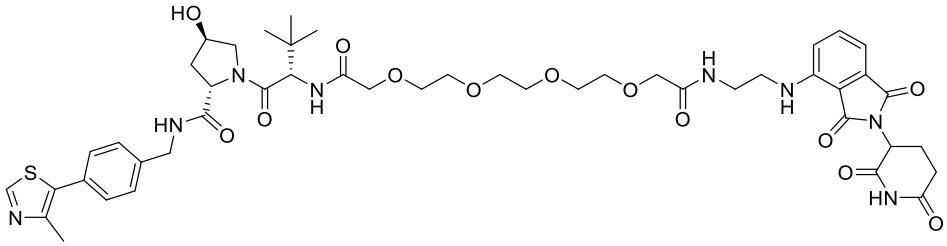

Starting from compound **13e** (12.5 mg, 0.02 mmol, 1 eq.) and following the **general method F**, the title compound was obtained (9.5 mg, yield: 44%). ^{1}H-NMR (400 MHz, MeOD) δ: 8.87 (s, 1H), 7.54 (dd, *J*=7.1, 8.4 Hz, 1H), 7.42 (dd, *J*=8.3, 20.1 Hz, 4H), 7.12 (d, *J*=8.3 Hz, 1H), 7.04 (d, J=7.1 Hz, 1H), 5.03 (dd, J=5.5, 12.6 Hz, 1H), 4.70 (d, *J*=7.1 Hz, 1H), 4.61 - 4.48 (m, 3H), 4.35 (d, *J*=15.3 Hz, 1H), 4.03 (d, *J*=3.2 Hz, 2H), 3.94 (s, 2H), 3.88 - 3.78 (m, 2H), 3.70 - 3.49 (m, 16H), 2.89 - 2.66 (m, 3H), 2.46 (s, 3H), 2.25 - 2.20 (m, 1H), 2.13 - 2.06 (m, 2H), 1.03 (s, 9H). ^{13}C-NMR (101 MHz, MeOD) δ: 174.7, 174.4, 173.6, 172.0, 171.7, 171.5, 170.6, 169.3, 152.8, 149.0, 148.2, 140.3, 137.3, 134.0, 133.4, 131.5, 130.4, 129.0, 112.2,111.5, 72.2, 72.0, 71.5, 71.4, 71.3, 71.1, 60.8, 58.1, 43.8, 42.5, 39.5, 38.9, 37.1, 32.2, 27.0, 23.8, 15.8. HR-MS analysis: calculated for $C_{47}H_{60}N_8O_{13}S$: 976.400; observed: 977.4179 $[M+H]^+$.

***Tert*-butyl 2-(2-(2-(2-hydroxyethoxy)ethoxy)ethoxy)acetate (15a)**

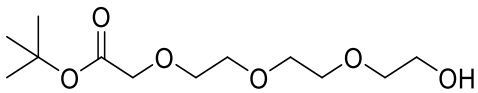

Starting from triethylene glycol (6.9 g, 45.9 mmol) and following the **general method C**, the title compound was obtained (540 mg, yield: 40%). Analytical data matched with those previously reported.[44]

***Tert*-butyl 2-(2-(2-(2-iodoethoxy)ethoxy)ethoxy)acetate (16a)**

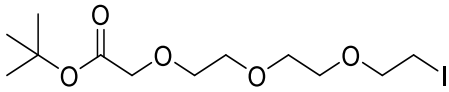

Starting from compound **15a** (350 mg, 1.33 mmol) and following the **general method D**, the title compound was obtained (yield: 414 mg, 79%). ^{1}H-NMR (400 MHz, $CDCl_3$) δ: 4.06 (s, 2H), 3.81 - 3.70 (m, 10H), 3.28 (t, *J*=6.9 Hz, 2H), 1.50 (s, 9H). ^{13}C-NMR (101 MHz, $CDCl_3$) δ: 169.7, 81.6, 72.0, 70.7, 70.6, 70.2, 69.1, 69.0, 28.1.

***Tert*-butyl-2-(2-(2-(2-(2-(((2S,4R)-1-((S)-2-(1-fluorocyclopropane-1-carboxamido)-3,3dimethylbutanoyl)-4-hydroxypyrrolidine-2-carboxamido)methyl)-5-(4-methylthiazol-5yl)phenoxy)ethoxy)ethoxy)ethoxy)acetate (17a)**

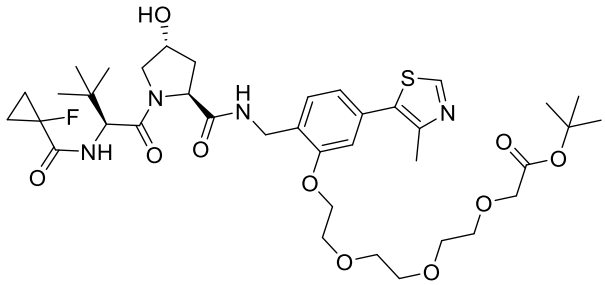

Starting from compound **3** (40 mg, 0.08 mmol, 1 eq.), **16a** (42 mg, 0.11 mmol, 1.5 eq.) and K_2CO_3 (31 mg, 0.22, 3 eq.), and following the **general method I**, the titled compound was obtained (yield: 13 mg, 22%). ^{1}H-NMR (500 MHz, $CDCl_3$) δ: 8.66 (s, 1H), 7.00 (dd, *J*=3.4, 8.9 Hz, 1H), 6.95 (dd, *J*=1.6, 7.6 Hz, 1H), 6.88 (d, *J*=1.6 Hz, 1H), 4.65 (t, *J*=8.0 Hz, 1H), 4.53 - 4.44 (m, 4H), 4.24 - 4.14 (m, 2H), 4.00 - 3.59 (m, 14H), 2.50 (s, 3H), 2.42 - 2.36 (m, 1H), 2.13 - 2.08 (m, 1H), 1.44 (s, 9H), 1.32 - 1.22 (m, 4H), 0.94 (s, 9H); ^{13}C-NMR (126 MHz, $CDCl_3$) δ: 170.8, 170.7, 170.1 (d, ^{2}J=20.4 Hz), 169.8, 157.0, 150.4, 148.7, 132.5, 131.9, 130.0, 127.1, 122.2, 113.0, 81.8, 79.5, 70.9, 70.7, 70.4, 69.8, 69.2, 68.1, 58.8, 57.6, 56.7, 39.3, 36.6, 35.7, 28.3, 26.5, 16.3, 13.8 (d, ^{2}J=5.2 Hz), 13.7 (d, ^{2}J=5.2 Hz). MS analysis: calculated for $C_{38}H_{55}FN_4O_{10}S$: 778.362; observed: 780.7 $[M+H]^+$.

(2S,4R)-*N*-(2-((1-((2-(2,6-dioxopiperidin-3-yl)-1,3-dioxoisoindolin-4-yl)amino)-4-oxo6,9,12-trioxa-3-azatetradecan-14-yl)oxy)-4-(4-methylthiazol-5-yl)benzyl)-1-((S)-2-(1fluorocyclopropane-1-carboxamido)-3,3-dimethylbutanoyl)-4-hydroxypyrrolidine-2carboxamide (18a)

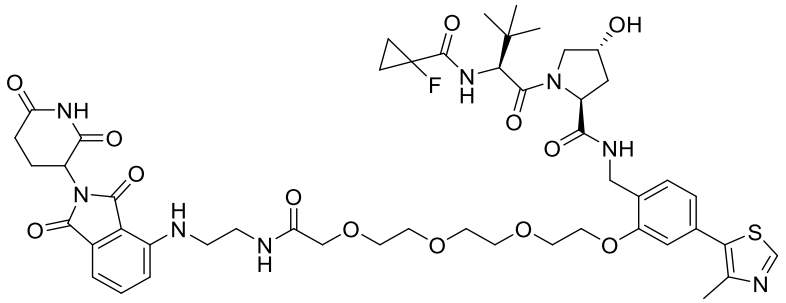

Starting from compound **17a** (13 mg, 0.0167 mmol) and following the **general method B** the deprotected carboxylic acid derivative was obtained in quantitative yield (12 mg). Starting from the crude carboxylic acid (0.0166 mmol, 1 eq.) and following the **general method H**, the desired compound was obtained (yield: 4 mg, 23%). ^{1}H-NMR (500 MHz, $CDCl_3$) δ: 8.65 (s, 1H), 7.47 - 7.43 (m, 1H), 7.32 - 7.29 (m, 1H), 7.06 (dd, *J*=2.4, 7.2 Hz, 1H), 6.99 - 6.94 (m, 2H), 6.88 - 6.86 (m, 1H), 4.90 - 4.79 (m, 1H), 4.65 - 4.59 (m, 1H), 4.56 (t, *J*=9.0 Hz, 1H), 4.49 - 4.39 (m, 3H), 4.22 - 4.11 (m, 2H), 3.96 - 3.43 (m, 18H), 2.84 - 2.61 (m, 3H), 2.50 (d, *J*=2.7 Hz, 3H), 2.38 - 2.30 (m, 1H), 2.14 - 2.04 (m, 2H), 1.37 - 1.18 (m, 4H), 0.96 (d, *J*=1.8 Hz, 9H);^{13}C-NMR (126 MHz, $CDCl_3$) δ: 171.3, 171.1, 171.0, 170.9, 170.3 170.1, 169.5, 169.0, 168.8, 167.7, 156.8, 150.4, 148.7, 146.9, 136.3, 132.7, 132.5, 131.8, 130.0, 129.8, 127.1, 127.0, 122.3, 122.2, 116.9, 113.0, 112.9, 112.0, 110.5, 79.6, 71.0, 70.8, 70.7, 70.5, 70.3, 70.2, 69.8, 68.1, 59.0, 58.9, 57.6, 56.8, 49.1, 49.1, 42.1, 39.2, 39.2, 38.7, 38.7, 36.8, 35.7, 35.6, 31.6, 26.5, 23.0, 22.9, 16.3, 13.9 (d, ^{2}J=10.0 Hz),13.8 (d, ^{2}J=10.0 Hz). HR-MS analysis: calculated for $C_{49}H_{61}FN_8O_{13}S$: 1020.406; observed: 1021.4480 $[M+H]^+$.

***Tert*-butyl 17-hydroxy-3,6,9,12,15-pentaoxaheptadecanoate (15b)**

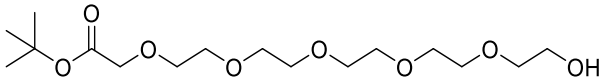

Starting from pentaethylene glycol (7.32 g, 31 mmol) and following the **general method C**, the title compound was obtained (yield: 600 mg, 44%). Analytical data matched with those previously reported.[44]

***Tert*-butyl 17-iodo-3,6,9,12,15-pentaoxaheptadecanoate (16b)**

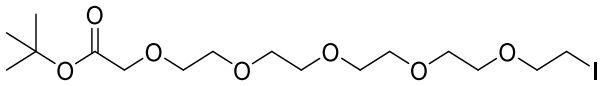

Starting from compound **15b** (400 mg, 1.14 mmol) and following the **general method D**, the title compound was obtained (yield: 402 mg, 81%). ^{1}H-NMR (500 MHz, $CDCl_3$) δ: 4.05 (s, 2H), 3.81 - 3.69 (m, 18H), 3.29 (t, *J*=6.9 Hz, 2H), 1.50 (s, 9H). ^{13}C-NMR (126 MHz, $CDCl_3$) δ: 169.7, 81.5, 72.0, 70.8, 70.7, 70.7, 70.6, 70.3, 69.1, 28.1.

***Tert*-butyl 17-(2-(((2S,4R)-1-((S)-2-(1-fluorocyclopropane-1-carboxamido)-3,3-dimethylbutanoyl)-4-hydroxypyrrolidine-2-carboxamido)methyl)-5-(4-methylthiazol-5-yl)phenoxy)-3,6,9,12,15-pentaoxaheptadecanoate (17b)**

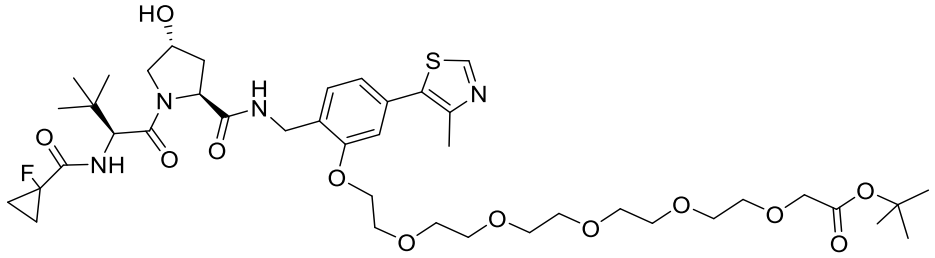

Starting from compound **3** (40 mg, 0.075 mmol, 1 eq.), **16b** (42 mg, 0.09 mmol, 1.2 eq.) and K_2CO_3 (31 mg, 0.22, 3 eq.), and following the **general method I**, the titled compound was obtained (yield: 29 mg, 48%). ^{1}H-NMR (500 MHz, $CDCl_3$) δ: 8.64 (s, 1H), 7.02 (dd, *J*=3.6, 8.8 Hz, 1H), 6.94 (dd, *J*=1.6, 7.7 Hz, 1H), 6.87 (d, *J*=1.4 Hz, 1H), 4.63 (t, *J*=8.1 Hz, 1H), 4.54 - 4.42 (m, 4H), 4.22 - 4.12 (m, 2H), 3.97 (s, 2H), 3.93 - 3.83 (m, 3H), 3.75 - 3.60 (m, 17H), 2.49 (s, 3H), 2.39 - 2.33 (m, 1H), 2.10 - 2.06 (m, 1H), 1.43 (s, 9H), 1.31 - 1.20 (m, 4H), 0.93 (s, 9H); ^{13}C-NMR (101 MHz, $CDCl_3$) δ: 170.8, 170.7, 170.0 (d, ^{2}J=20.3 Hz), 169.8, 157.0, 150.4, 148.6, 132.4, 131.8, 129.9, 127.1, 122.1, 113.0, 81.7, 79.5, 70.9, 70.7, 70.3, 69.8, 69.2, 68.1, 58.8, 57.5, 56.7, 39.2, 36.6, 35.8, 28.2, 26.5, 16.2, 13.7 (t, ^{2}J=9.6 Hz). MS analysis: calculated for $C_{42}H_{63}FN_4O_{12}S$: 866.5; observed: 867.7 $[M+H]^+$.

(2S,4R)-N-(2-((1-((2-(2,6-dioxopiperidin-3-yl)-1,3-dioxoisoindolin-4-yl)amino)-4-oxo6,9,12,15,18-pentaoxa-3-azaicosan-20-yl)oxy)-4-(4-methylthiazol-5-yl)benzyl)-1-((S)-2(1-fluorocyclopropane-1-carboxamido)-3,3-dimethylbutanoyl)-4-hydroxypyrrolidine-2carboxamide (18b)

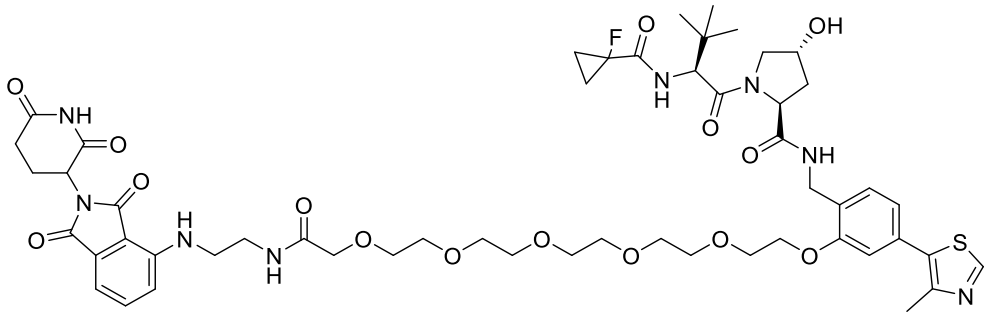

Starting from compound **17b** (29 mg, 0.03 mmol) and following the **general method B** the deprotected carboxylic acid derivative was obtained in quantitative yield (27 mg). Starting from the crude carboxylic acid (27 mg, 0.03, 1 eq.) and following the **general method H**, the desired compound was obtained (yield: 4.2 mg, 11%). ^{1}H-NMR (500 MHz, $CDCl_3$) δ: 8.65 (s, 1H), 7.47 (t, *J*=7.6 Hz, 1H), 7.31 (d, *J*=7.6 Hz, 1H), 7.07 (dd, *J*=1.4, 7.0 Hz, 1H), 7.00 (dd, *J*=1.4, 8.5 Hz, 1H), 6.94 (d, *J*=7.6 Hz, 1H), 6.87 (d, *J*=1.5 Hz, 1H), 4.90 - 4.82 (m, 1H), 4.63 (dt, *J*=3.2, 7.8 Hz, 1H), 4.55 (d, *J*=9.1 Hz, 1H), 4.50 - 4.42 (m, 3H), 4.21 - 4.10 (m, 2H), 3.95 (s, 2H), 3.95 - 3.43 (m, 24H), 2.92 - 2.62 (m, 3H), 2.50 (s, 3H), 2.39 - 2.31 (m, 1H), 2.15 - 2.04 (m, 2H), 1.35 - 1.18 (m, 4H), 0.94 (d, *J*=1.8 Hz, 9H). ^{13}C-NMR (500 MHz, $CDCl_3$) δ: 171.4, 171.3, 171.2, 170.9, 170.8, 170.1(d,2J=20.5 Hz), 169.5, 168.8, 168.7, 167.7, 157.0, 150.4, 148.7, 147.0, 136.3, 132.7, 132.4, 131.8, 130.1, 127.1, 122.2, 117.0, 113.0, 111.9, 110.5, 79.3, 71.1, 70.9, 70.7, 70.6, 70.5, 70.5, 70.2, 69.8, 68.2, 58.9, 57.6, 56.8, 49.1, 42.1, 39.2, 38.6, 36.8, 35.7, 31.6, 26.5, 22.9, 16.3, 13.8 (d,^{2}J=10.2 Hz), 13.7 (d,^{2}J=10.2 Hz) HR-MS analysis: calculated for $C_{53}H_{69}FN_8O_{15}S$: 1109.2342; observed: 1110.4625 $[M+H]^+$.

Methyl-5-(2-(((2S,4R)-1-((S)-2-(1-fluorocyclopropane-1-carboxamido)-3,3dimethylbutanoyl)-4-hydroxypyrrolidine-2-carboxamido)methyl)-5-(4-methylthiazol-5yl)phenoxy)pentanoate (17c)

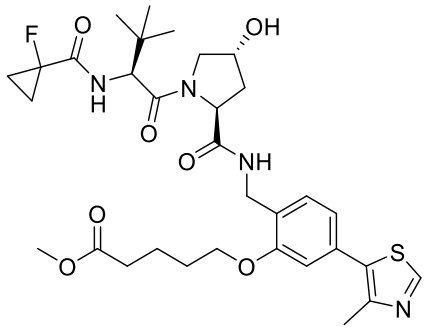

Starting from compound **3** (40 mg, 0.08 mmol, 1 eq.), methyl 5-bromobutanoate **16c** (21 mg, 0.11 mmol, 1.5 eq.) and K_2CO_3 (31 mg, 0.22 mmol, 3 eq.), and following the **general method I**, the titled compound was obtained (yield: 30 mg, 62%). ^{1}H-NMR (500 MHz, $CDCl_3$) δ: 8.66 (s, 1H), 7.03 (dd, *J*=3.5, 8.8 Hz, 1H), 6.92 (dd, *J*=1.5, 7.7 Hz, 1H), 6.82 (d, *J*=1.5 Hz, 1H), 4.69 (t, *J*=7.8 Hz, 1H), 4.54 - 4.45 (m, 3H), 4.38 (dd, *J*=5.5, 14.9 Hz, 1H), 4.05 - 3.96 (m, 2H), 3.96 - 3.91 (m, 1H), 3.64 (s, 3H), 3.61 (dd, *J*=4.2, 11.2 Hz, 1H), 2.52 - 2.45 (m, 4H), 2.40 (t, *J*=6.8 Hz, 2H), 2.09 - 2.04 (m, 1H), 1.91 - 1.78 (m, 4H), 1.33 - 1.24 (m, 4H), 0.91 (s, 9H); ^{13}C-NMR (101 MHz, $CDCl_3$) δ: 173.9, 171.0, 170.3 (d, ^2J=20.5 Hz), 170.2, 156.8, 150.4, 148.6, 132.4, 131.9, 129.7, 126.4, 121.7, 112.1, 79.5, 70.3, 67.7, 58.6, 57.5, 56.6, 51.7, 38.9, 36.0, 35.5, 33.7, 28.8, 26.4, 21.8, 16.2, 13.8 (d,^2J=3.7 Hz), 13.7 (d, ^2J=3.7 Hz). MS analysis: calculated for $C_{32}H_{43}FN_4O_7S$: 646.2; observed: 647.7 $[M+H]^+$.

(2S,4R)-*N*-(2-((5-((2-((2-(2,6-dioxopiperidin-3-yl)-1,3-dioxoisoindolin-4yl)amino)ethyl)amino)-5-oxopentyl)oxy)-4-(4-methylthiazol-5-yl)benzyl)-1-((S)-2-(1fluorocyclopropane-1-carboxamido)-3,3-dimethylbutanoyl)-4-hydroxypyrrolidine-2carboxamide (18c)

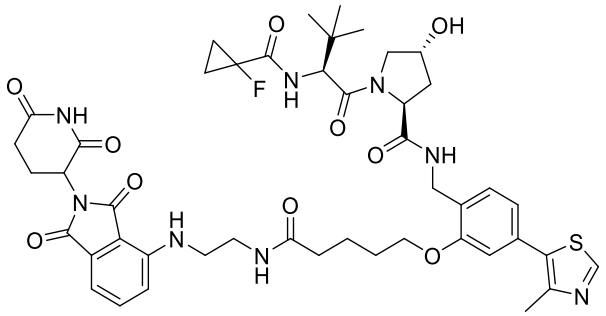

Compound **17c** (30 mg, 0.05 mmol, 1 eq.) was dissolved in a mixture of THF (2 mL) and water (0.50 mL). Then LiOH was added (2.2 mg, 0.09 mmol, 2 eq.) and the mixture was stirred at room temperature for 2 h. A solution of HCl 4N in dioxane was added to pH <6 and the mixture was evaporated to dryness to yield the deprotected carboxylic acid derivative (25 mg, yield: quantitative). Starting from the crude carboxylic acid (0.02 mmol, 1 eq.) and following the **general method H**, the desired compound was obtained (yield: 5 mg, 22%). ^{1}H-NMR (500 MHz, $CDCl_3$) δ: 8.66 (s, 1H), 7.47 (t, *J*=7.9 Hz, 1H), 7.29 (dd, *J*=2.2, 7.7 Hz, 1H), 7.07 (d, *J*=7.2 Hz, 1H), 6.97 (dd, *J*=3.1, 8.6 Hz, 1H), 6.95 - 6.94 (m, 1H), 6.85 - 6.83 (m, 1H), 4.90 - 4.80 (m, 1H), 4.68 (ddd, *J*=7.7, 7.7, 1.9 Hz, 1H), 4.55 - 4.45 (m, 3H), 4.38 - 4.30 (m, 1H), 4.05 - 3.93 (m, 3H), 3.60 (qd, *J*=1.9, 11.2 Hz, 1H), 3.47 - 3.36 (m, 4H), 2.85 - 2.60 (m, 3H), 2.50 (s, 3H), 2.47 - 2.40 (m, 1H), 2.34 - 2.25 (m, 2H), 2.11 - 2.02 (m, 2H), 1.90 - 1.81 (m, 4H), 1.36 - 1.17 (m, 4H), 0.90 (d, *J*=3.1 Hz, 9H); ^{13}C-NMR (126 MHz, $CDCl_3$) δ: 173.9, 171.4, 171.2, 170.5, 170.4, 170.3, 169.7, 169.6, 169.0, 168.9, 167.6, 156.9, 150.4, 148.7, 147.0, 136.4, 132.7, 131.8, 130.2, 130.1, 126.2, 121.8, 121.8, 117.0, 112.3, 112.1, 79.4, 70.3, 67.9, 58.8, 57.7, 56.8, 56.7, 49.2, 49.1, 42.3, 39.3, 39.2, 39.1, 36.4, 36.1, 35.5, 31.6, 28.8, 28.7, 26.5, 22.9, 16.3, 13.9 (d, ^{2}J=3.7 Hz), 13.8 (d, ^{2}J=3.7 Hz). HR-MS analysis: calculated for $C_{46}H_{55}FN_8O_{10}S$: 930.375; observed: 931.3823 $[M+H]^+$.

(2S,4R)-1-((R)-2-amino-3-methyl-3-(tritylthio)butanoyl)-4-hydroxy-N-(4-(4-methylthiazol-5-yl)benzyl)pyrrolidine-2-carboxamide (19)

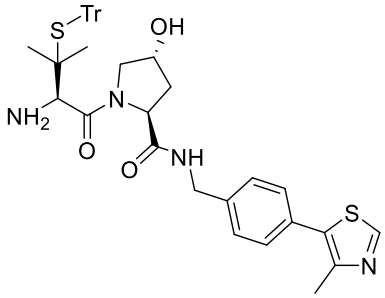

The title compound was synthesized as previously reported.[29] Analytical data matched those reported.

***Tert*-butyl(R)-1-(1-fluorocyclopropyl)-3-((2S,4R)-4-hydroxy-2-((4-(4-methylthiazol-5yl)benzyl)carbamoyl)pyrrolidine-1-carbonyl)-4,4-dimethyl-1-oxo-8,11,14-trioxa-5-thia2-azahexadecan-16-oate (21a)**

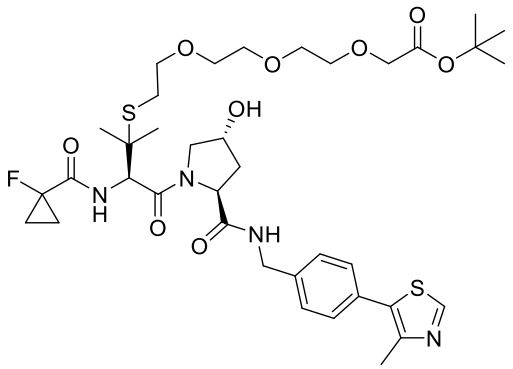

Starting from compound **3** (20 mg, 0.04 mmol, 1 eq.), **16a** (15 mg, 0.04 mmol, 1.1 eq.) and DBU (6,3 µL, 0.04, 1.1 eq.), and following the **general method G**, compound **21a** was obtained (yield: 15 mg, 46%). ^{1}H-NMR (400 MHz, $CDCl_3$) δ: 8.64 (s, 1H), 7.33 (dd, *J*=8.2, 14.2 Hz, 4H), 4.78 (d, *J*=8.2 Hz, 1H), 4.74 (t, *J*=7.6 Hz, 1H), 4.53 - 4.49 (m, 1H), 4.42 (ddt, *J*=6.0, 13.9, 13.2 Hz, 2H), 3.96 (s, 2H), 3.96 - 3.91 (m, 1H), 3.81 (dd, *J*=4.2, 11.1 Hz, 1H), 3.68 - 3.43 (m, 10H), 2.79 - 2.64 (m, 2H), 2.49 (s, 3H), 2.44 - 2.36 (m, 1H), 2.23 - 2.15 (m, 1H), 1.44 (s, 9H), 1.35 - 1.24 (m, 10H); ^{13}C-NMR (101 MHz, $CDCl_3$) δ: 170.8, 170.2 (d, ^{2}J=20.7 Hz), 169.8, 169.6, 150.2, 148.5, 138.1, 131.6, 131.0, 129.5, 128.3, 128.2, 81.7, 79.3, 77.3, 77.0, 76.7, 70.7, 70.5, 70.5, 70.4, 70.2, 69.9, 69.0, 59.1, 56.4, 56.0, 47.9, 43.0, 36.8, 28.4, 28.1, 25.8, 25.1, 16.1, 13.9 (d, ^{2}J=4.8 Hz),13.8 (d, ^{2}J=4.8 Hz). MS analysis: calculated for $C_{37}H_{53}FN_4O_9S_2$: 780.3; observed: 781.8 $[M+H]^+$.

(2S,4R)-1-((17R)-1-((2-(2,6-dioxopiperidin-3-yl)-1,3-dioxoisoindolin-4-yl)amino)-17-(1fluorocyclopropane-1-carboxamido)-16,16-dimethyl-4-oxo-6,9,12-trioxa-15-thia-3azaoctadecan-18-oyl)-4-hydroxy-N-(4-(4-methylthiazol-5-yl)benzyl)pyrrolidine-2carboxamide (22a)

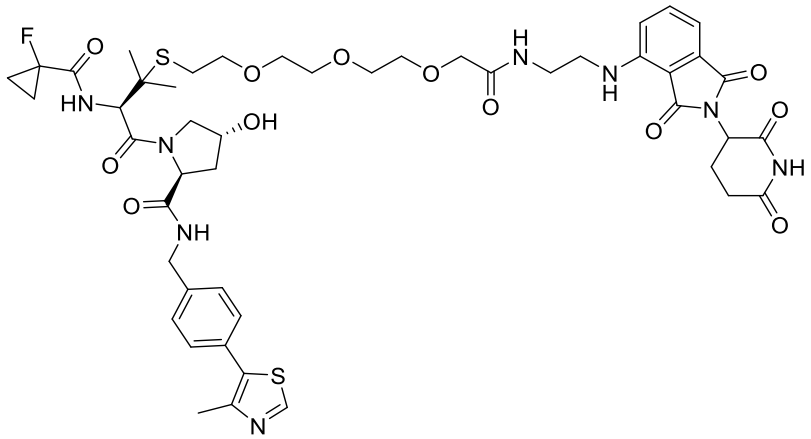

Starting from compound **21a** (15 mg, 0.02 mmol) and following the **general method B** the deprotected carboxylic acid derivative was obtained in quantitative yield (13.9 mg). Starting from the crude carboxylic acid (0.02, 1 eq.) and following the **general method H**, the desired compound was obtained (yield: 11 mg, 56%). ^{1}H-NMR (400 MHz, MeOD) δ: 8.86 (s, 1H), 7.55 (dd, *J*=7.2, 8.5 Hz, 1H), 7.46 - 7.40 (m, 4H), 7.13 (d, *J*=9.0 Hz, 1H), 7.05 (d, *J*=7.5 Hz, 1H), 5.04 (dd, *J*=5.6, 12.8 Hz, 1H), 4.93 (s, 1H), 4.60 (t, *J*=8.4 Hz, 1H), 4.54 - 4.35 (m, 3H), 3.95 (s, 2H), 3.88 (d, *J*=3.1 Hz, 2H), 3.59 - 3.45 (m, 14H), 2.89 - 2.65 (m, 5H), 2.47 (s, 3H), 2.28 - 2.23 (m, 1H), 2.14 - 2.06 (m, 2H), 1.42 - 1.25 (m, 10H); ^{13}C-NMR (101 MHz, MeOD) δ: 174.6, 174.0, 173.5, 171.6, 171.5 (d, ^{2}J= 21.2 Hz) 171.4, 170.8, 170.6, 169.3, 152.8, 149.1, 148.2, 140.2, 137.3, 134.0, 133.4, 131.6, 130.4, 129.0, 118.1, 112.2, 111.6, 79.1 (d, ^{1}J= 231.9 Hz), 72.0, 71.7, 71.4, 71.3, 71.1, 71.0, 61.1, 58.1, 57.2, 50.2, 43.7, 42.5, 39.5, 39.0, 32.2, 29.6, 27.0, 25.7, 23.8, 15.9, 14.2, 14.1 (t, ^{2}J= 9.5 Hz). HR-MS analysis: calculated for $C_{48}H_{59}FN_8O_{12}S_2$: 1022.368; observed: 1023.3730 $[M+H]^+$.

***Tert*-butyl(R)-1-(1-fluorocyclopropyl)-3-((2S,4R)-4-hydroxy-2-((4-(4-methylthiazol-5yl)benzyl)carbamoyl)pyrrolidine-1-carbonyl)-4,4-dimethyl-1-oxo-8,11,14,17,20pentaoxa-5-thia-2-azadocosan-22-oate (21b)**

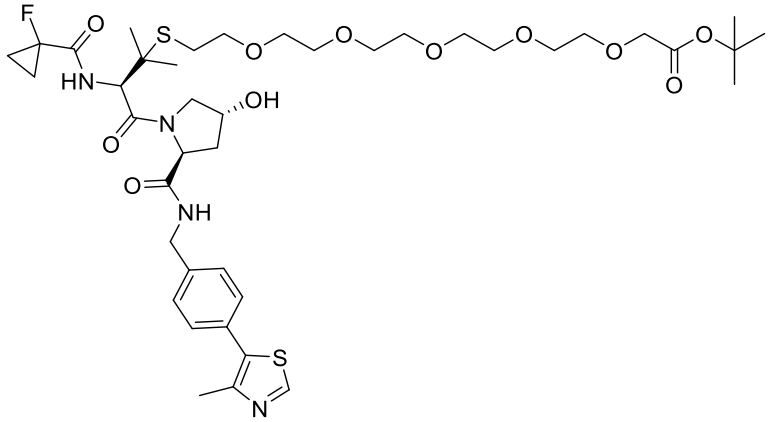

Starting from compound **3** (20 mg, 0.04 mmol, 1 eq.), **16b** (19 mg, 0.04 mmol, 1.1 eq.) and DBU (6,3 µL, 0.04, 1.1 eq.), and following the **general method G**, the titled compound was obtained (yield: 19.4 mg, 66%). ^{1}H-NMR (400 MHz, $CDCl_3$) δ: 8.65 (s, 1H), 7.34 (dd, *J*=8.4, 13.6 Hz, 4H), 4.81 (d, *J*=8.4 Hz, 1H), 4.74 (t, *J*=7.7 Hz, 1H), 4.53 - 4.50 (m, 1H), 4.42 (ddt, *J*=5.8, 15.2, 15.3 Hz, 2H), 3.98 (s, 2H), 3.94 - 3.80 (m, 2H), 3.70 - 3.42 (m, 18H), 2.80 - 2.64 (m, 2H), 2.49 (s, 3H), 2.43 - 2.36 (m, 1H), 2.24 - 2.15 (m, 1H), 1.44 (s, 9H), 1.33 - 1.24 (m, 10H); ^{13}C-NMR (101 MHz, $CDCl_3$) δ: 171.0, 170.3 (d, ^{2}J= 20.5 Hz), 169.9, 169.8, 150.4, 148.6, 138.3, 131.7, 131.1, 129.6, 128.3, 81.7, 79.4, 70.9, 70.7, 70.6, 70.3, 70.0, 69.2, 59.3, 56.5, 56.0, 48.1, 43.2, 37.0, 28.6, 28.3, 25.9, 25.2, 16.2, 14.0 (d, ^{2}J= 2.9 Hz), 13.9 (d, ^{2}J= 2.9 Hz). MS analysis: calculated for $C_{41}H_{61}FN_4O_{11}S_2$: 868.376; observed: 869.3 $[M+H]^+$.

(2S,4R)-1-((17R)-1-((2-(2,6-dioxopiperidin-3-yl)-1,3-dioxoisoindolin-4-yl)amino)-17-(1fluorocyclopropane-1-carboxamido)-16,16-dimethyl-4-oxo-6,9,12-trioxa-15-thia-3azaoctadecan-18-oyl)-4-hydroxy-*N*-(4-(4-methylthiazol-5-yl)benzyl)pyrrolidine-2carboxamide (22b)

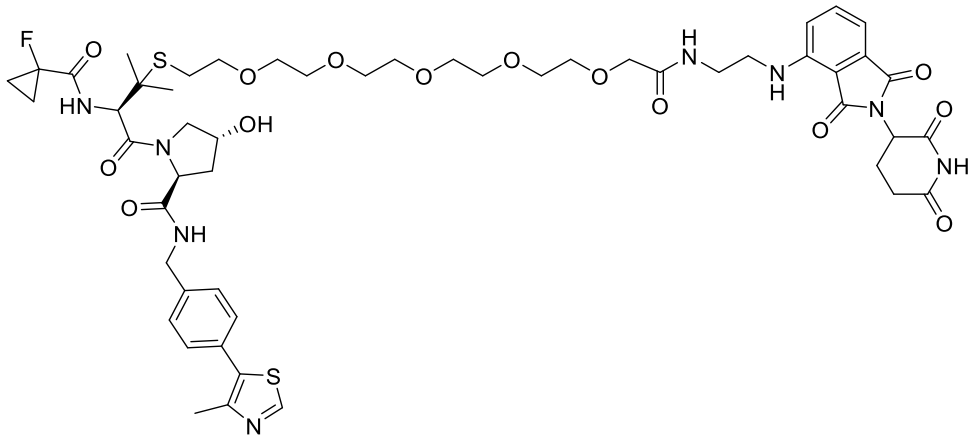

Starting from compound **21b** (19.4 mg, 0.02 mmol) and following the **general method B** the deprotected carboxylic acid derivative was obtained in quantitative yield (17 mg, yield: quantitative). Starting from the crude carboxylic acid (0.01 mmol, 1 eq.) and following the **general method H**, the desired compound was obtained (yield: 7.3 mg, 47%). ^{1}H-NMR (500 MHz, MeOD) δ: 8.86 (s, 1H), 7.55 (dd, *J*=7.2, 8.6 Hz, 1H), 7.44 (dd, *J*=8.6, 11.4 Hz, 4H), 7.14 (d, *J*=8.4 Hz, 1H), 7.05 (d, *J*=7.0 Hz, 1H), 5.04 (dd, *J*=5.4, 12.4 Hz, 1H), 4.94 (s, 1H), 4.61 (t, *J*=8.4 Hz, 1H), 4.52 - 4.37 (m, 3H), 3.96 (s, 2H), 3.92 - 3.86 (m, 2H), 3.57 - 3.47 (m, 22H), 2.88 - 2.66 (m, 5H), 2.48 (s, 3H), 2.28 - 2.24 (m, 1H), 2.14 - 2.07 (m, 2H), 1.42 - 1.27 (m, 10H); ^{13}C-NMR (126 MHz, MeOD) δ: 174.7,174.1, 173.6, 171.5 (d, ^{2}J=19.8 Hz) 171.5, 170.8, 170.6, 169.2, 152.9, 149.1, 148.1, 140.2, 137.3, 134.0, 133.4, 131.6, 130.5, 130.4, 129.6, 129.0, 118.1, 112.1, 111.5, 79.1 (d, ^{1}J=231.2 Hz), 72.0, 71.6, 71.6, 71.5, 71.4, 71.3, 71.1, 71.0, 61.1, 58.1, 57.1, 43.6, 42.5, 39.4, 39.1, 32.2, 29.6, 26.9, 25.7, 23.8, 15.9, 14.2 (d, ^{2}J=7.9 Hz), 14.1 (d, ^{2}J=7.9 Hz). HR-MS analysis: calculated for $C_{52}H_{67}FN_8O_{14}S_2$: 1110.420; observed: 1111.4052 $[M+H]^+$.

Methyl 5-(((R)-3-(1-fluorocyclopropane-1-carboxamido)-4-((2S,4R)-4-hydroxy-2-((4-(4methylthiazol-5-yl)benzyl)carbamoyl)pyrrolidin-1-yl)-2-methyl-4-oxobutan-2yl)thio)pentanoate (21c)

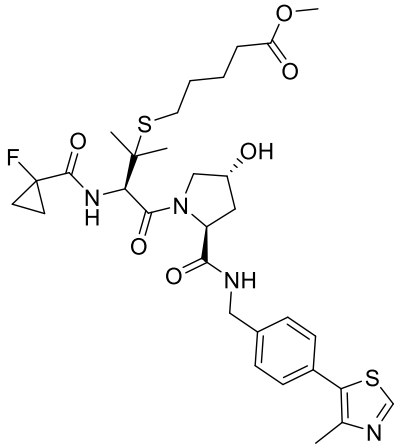

Starting from compound **3** (20 mg, 0.04 mmol, 1 eq.), methyl 5-bromobutanoate **16c** (8 mg, 0.04 mmol, 1.1 eq.) and DBU (6.3 µL, 0.04, 1.1 eq.), and following the **general method G**, compound **21c** was obtained (16.5 mg, yield: 67%). ^{1}H-NMR (400 MHz, $CDCl_3$) δ: 8.65 (s, 1H), 7.33 (dd, *J*=8.0, 16.3 Hz, 4H), 4.76 - 4.71 (m, 2H), 4.50 (t, *J*=6.9 Hz, 1H), 4.42 (d, *J*=6.1 Hz, 2H), 3.97 (d, *J*=11.8 Hz, 1H), 3.74 - 3.69 (m, 1H), 3.62 (s, 3H), 2.54 - 2.37 (m, 6H), 2.24 (t, *J*=7.6 Hz, 2H), 2.21 - 2.16 (m, 1H), 1.67 - 1.58 (m, 2H), 1.52 - 1.42 (m, 2H), 1.32 - 1.24 (m, 10H); ^{13}C-NMR δ: (101 MHz, $CDCl_3$) δ 173.8, 170.9, 170.5 (d, ^{2}J= 20.7 Hz), 170.0, 150.5, 148.6, 138.2, 131.7, 131.1, 129.6, 128.2, 79.4, 70.2, 59.2, 56.7, 56.2, 51.7, 48.1, 43.2, 36.9, 33.6, 28.9, 28.0, 25.8, 25.4, 24.4, 16.1, 14.0 (d, ^{2}J= 3.4 Hz), 13.9 (d, ^{2}J= 3.4 Hz). MS analysis: calculated for $C_{31}H_{41}FN_4O_6S_2$: 648.245; observed: 649.3 $[M+H]^+$.

(2S,4R)-1-((2R)-3-((4-((2-((2-(2,6-dioxopiperidin-3-yl)-1,3-dioxoisoindolin-4yl)amino)ethyl)amino)-4-oxobutyl)thio)-2-(1-fluorocyclopropane-1-carboxamido)-3methylbutanoyl)-4-hydroxy-N-(4-(4-methylthiazol-5-yl)benzyl)pyrrolidine-2carboxamide (22c)

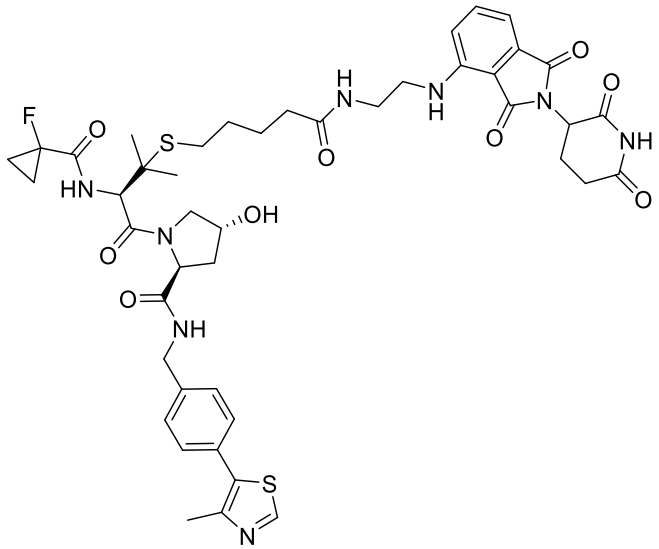

Compound **21c** (16.5 mg, 0.03 mmol, 1 eq.) was dissolved in a mixture of THF (1 mL) and water (0.25 mL). Then LiOH was added (1.2 mg, 0.05 mmol, 2 eq.) and the mixture was stirred at room temperature for 2 h. A solution of HCl 4N in dioxane was added to pH <6 and the mixture was evaporated to dryness to yield the deprotected carboxylic acid derivative (16.1 mg, yield: quantitative). Starting from the crude carboxylic acid and following the **general method H**, the desired compound was obtained (9.2 mg, yield: 39%). ^{1}H-NMR (500 MHz, MeOD) δ: 8.92 (s, 1H), 7.54 (dd, *J*=7.2, 8.5 Hz, 1H), 7.46 - 7.39 (m, 4H), 7.07 (dd, *J*=7.8, 23.5 Hz, 2H), 5.04 (dd, *J*=5.6, 12.9 Hz, 1H), 4.91 (d, *J*=9.2 Hz, 1H), 4.61 (t, *J*=8.3 Hz, 1H), 4.53 - 4.36 (m, 3H), 3.90 - 3.82 (m, 2H), 3.48 - 3.37 (m, 4H), 2.89 - 2.68 (m, 3H), 2.56 (t, *J*=7.4 Hz, 2H), 2.48 (s, 3H), 2.29 - 2.22 (m, 1H), 2.14 - 2.08 (m, 4H), 1.67 - 1.55 (m, 2H), 1.51 - 1.43 (m, 2H), 1.41 - 1.25 (m, 10H); ^{13}C-NMR (126 MHz, MeOD) δ: 176.4, 174.6, 174.1, 171.5, 170.9, 170.6, 169.3, 153.0, 148.7, 148.2, 140.3, 137.2, 134.0, 133.6, 131.4, 130.5, 130.4, 129.5, 129.0, 118.0, 112.1, 111.5, 79.1 (d, 1J= 232.0 Hz) 71.0, 61.1, 58.1, 57.3, 57.2, 43.7, 42.8, 39.8, 39.0, 36.4, 32.2, 30.2, 29.0, 27.1, 26.2, 25.7, 23.8, 15.7, 14.2, 14.1 (dd, ^{2}J=9.1 Hz). HR-MS analysis: calculated for $C_{45}H_{53}FN_8O_9S_2$: 932.336; observed: 933.3263 $[M+H]^+$.

3,3'-(Butane-1,4-diylbis(oxy))bis(propan-1-ol) (23)

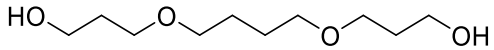

The title compound was prepared as previously reported.[44] Analytical data matched those previously reported.

1-phenyl-2,5,9,14-tetraoxaheptadecan-17-ol (24)

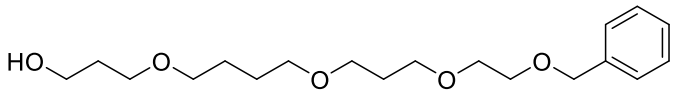

Compound **23** (1.1 g, 5.33 mmol, 3 eq.) was dissolved in toluene (10 mL) and 50% NaOH aq. (5mL). TBABr (590 mg, 1.78 mmol, 1 eq.), a catalytic amount of TBAI and benzyl-2-bromoethyl ether (382 mg, 1.78 mmol, 1 eq.) were added and the reaction mixture was vigorously stirred for 48 h. Organic layer was separated from the aqueous phase and the aqueous phase was extracted with DCM (x3). The crude was purified by flash chromatography eluting from 0% to 5% v/v MeOH in DCM to obtain the product as an oil (yield: 350 mg, 57%). ^{1}H-NMR (400 MHz, $CDCl_3$) δ: 7.33 - 7.22 (m, 5H), 4.55 (s, 2H), 3.74 (dd, *J*=5.7, 11.2 Hz, 2H), 3.59 - 3.55 (m, 6H), 3.53 (t, *J*=6.5 Hz, 2H), 3.47 (t, *J*=6.4 Hz, 2H), 3.44 - 3.37 (m, 4H), 2.44 (t, *J*=5.7 Hz, 1H), 1.87 - 1.76 (m, 4H), 1.61 - 1.57 (m, 4H).

3-(4-(3-(2-Hydroxyethoxy)propoxy)butoxy)propan-1-ol (25a)

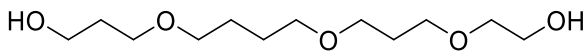

The product was obtained starting from compound **24** (350mg, 1.03 mmol) and following the **general method L**. The conversion was not quantitative, so the product was separated from the starting material by a flash chromatography eluting from 100% DCM to 9:1 v/v DCM/MEOH (yield: 87 mg, 34%). ^{1}H-NMR (400 MHz, $CDCl_3$) δ: 3.66 - 3.60 (m, 4H), 3.51 - 3.38 (m, 8H), 3.38 - 3.31 (m, 4H), 1.79 - 1.69 (m, 4H), 1.57 - 1.50 (m, 4H).

Di-*tert*-butyl-3,6,10,15,19-pentaoxahenicosanedioate (26a)

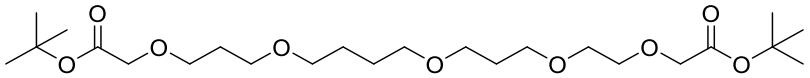

Starting from compound **25a** (87 mg, 0.35 mmol) and following the **general method A**, the title compound was obtained as a pale yellow oil (yield: 47 mg, 28 %).^{1}H-NMR (400 MHz, $CDCl_3$) δ: 3.99 (s, 2H), 3.68 - 3.42 (m, 12H), 3.41 - 3.36 (m, 4H), 1.88 - 1.77 (m, 4H), 1.59 - 1.55 (m, 4H), 1.44 (s, 18H).

3,6,10,15,19-pentaoxahenicosanedioic acid (27a)

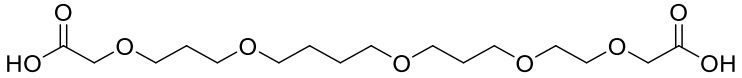

Prepared following the **general method B** starting from compound **26a** (47 mg, 0.10 mmol). The title compound was obtained a colourless oil (yield: 35 mg, quantitative).^{1}H-NMR (500 MHz, $CDCl_3$) δ: 4.14 (s, 2H), 4.07 (s, 2H), 3.73 - 3.69 (m, 2H), 3.65 - 3.59 (m, 4H), 3.59 - 3.53 (m, 4H), 3.49 (t, *J*=6.3 Hz, 2H), 3.47 - 3.40 (m, 4H), 1.89 - 1.81 (m, 4H), 1.62 - 1.57 (m, 4H).^{13}C-NMR (101 MHz, $CDCl_3$) δ: 173.9, 173.7, 71.3, 71.0, 70.8, 70.0, 69.6, 68.7, 68.6, 68.1, 68.0, 67.6, 29.7, 29.5, 26.3, 26.2.

4,4'-(butane-1,4-diylbis(oxy))bis(butan-1-ol) (25b)

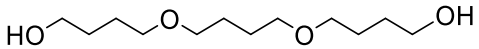

The title compound was prepared as previously reported.[47] Analytical data matched those reported.

Di-*tert*-butyl 3,8,13,18-tetraoxaicosanedioate (26b)

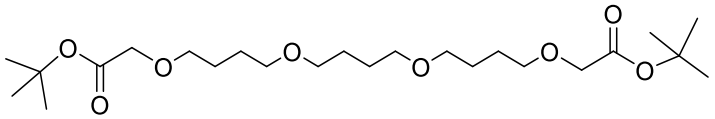

Prepared following the **general method D** from compound **25b** (198 mg, 0.84 mmol). The title compound was obtained as a colourless (yield: 158 mg, 40%). ^{1}H-NMR (400 MHz, $CDCl_3$) δ: 3.87(4H, s), 3.45 (4H, t, *J*=6.1 Hz), 3.38 - 3.30 (8H, m), 1.67 - 1.51 (12H, m), 1.41 (18H, s).

3,8,13,18-tetraoxaicosanedioic acid (27b)

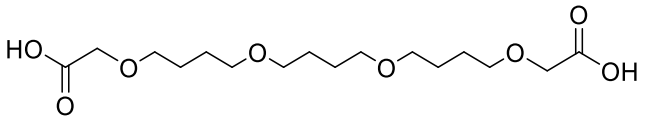

Prepared following the **general method B** starting from compound **26b** (158 mg, 0.34 mmol). The title compound was obtained as a colourless oil (yield: 120 mg, quantitative). ^{1}H-NMR (400 MHz, $CDCl_3$) δ: 8.26 (s, 2H), 4.09 (s, 4H), 3.58 (t, *J*=6.1 Hz, 4H), 3.48 - 3.41 (m, 8H), 1.75 - 1.60 (m, 12H).^{13}C-NMR (101 MHz, $CDCl_3$) δ: 173.1, 71.7, 70.6, 70.4, 67.9, 26.4, 26.3, 26.1.

3,3'-(Pentane-1,5-diylbis(oxy))bis(propan-1-ol) (25c)

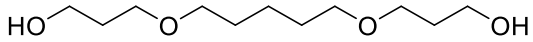

A solution of compound **S1** (500 mg, 2.71 mmol, 1 eq.) in dry THF (4.2 mL) was added dropwise to a solution 0.5 M of 9-Borabicyclo[3.3.1]nonane in THF (993 mg, 16.28 mL, 8.14 mmol, 3eq.) at 0 °C and the resulting solution was stirred at r.t. overnight. The reaction was quenched by MeOH (3.17 mL), 30% w/w aq. NaOH (6.35 mL), 30% v/v aq. H_2O_2 (6.35 mL) and the mixture was left to stir for 2 h. Then it was extracted with ethyl acetate (x3). Organic layers were collected, wash with brine, dried over $MgSO_4$ and evaporated under reduced pressure. The crude was purified by flash chromatography eluting from 0% to 100% ethyl acetate in heptane to yield the desired product as an oil (483 mg, yield: 81%). Analytical data matched those previously reported.[48]

Di-*tert*-butyl-3,7,13,17-tetraoxanonadecanedioate (26c)

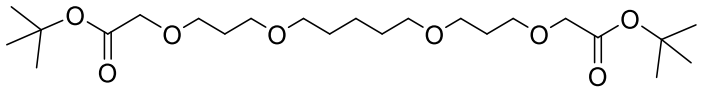

Prepared from compound **25c** (214 mg, 0.97 mmol) following the **general method D**. The desired product was obtained as a pale-yellow oil (yield: 65 mg, 15%).^{1}H-NMR (400 MHz, $CDCl_3$) δ: 3.88 (s, 4H), 3.53 (t, *J*=6.5 Hz, 4H), 3.44 (t, *J*=6.4 Hz, 4H), 3.34 (t, *J*=6.9 Hz, 4H), 1.85 - 1.78 (m, 4H), 1.55 - 1.47 (m, 4H), 1.41 (s, 18H), 1.36 - 1.29 (m, 2H).

3,7,13,17-Tetraoxanonadecanedioic acid (27c)

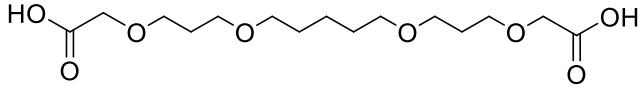

Prepared following the **general method B** starting from compound **26c** (64 mg, 0.14 mmol). The title compound was obtained as an oil (yield: 47.5 mg, quantitative).^{1}H-NMR (400 MHz, $CDCl_3$) δ: 8.11 (s, 2H), 4.06 (s, 4H), 3.64 (t, *J*=5.9 Hz, 4H), 3.54 (t, *J*=5.9 Hz, 4H), 3.42 (t, *J*=6.4 Hz, 4H), 1.88 - 1.81 (m, 4H), 1.60 - 1.52 (m, 4H), 1.36 (dt, *J*=7.6, 11.9 Hz, 2H). ^{13}C-NMR (101 MHz, $CDCl_3$) δ: 173.3, 71.1, 69.6, 68.2, 67.9, 29.4, 29.2, 22.7.

Di-tert-butyl 3,6,9,12,18-pentaoxaicosanedioate (26d)

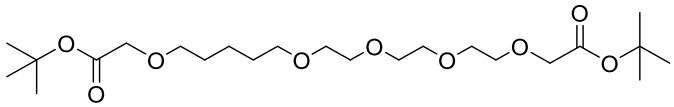

Compound **S4** (265 mg, 0.610 mmol) was reacted following the **general method L**. Solvent was evaporated under reduced pressure and the deprotected compound was obtained as an oil (131 mg) and used without any further purification for the next step. Following the **general method D** from the deprotected compound (131 mg, 0.5544 mmol) in 37% w/w aqueous NaOH (2.2 mL) and DCM (2.2 mL) the title compound was obtained as an oil (yield: 122 mg, 47%).^{1}H-NMR (500 MHz, $CDCl_3$) δ: 4.00 (s, 2H), 3.92 (s, 2H), 3.69 - 3.60 (m, 10H), 3.57 - 3.53 (m, 2H), 3.52 - 3.46 (m, 2H), 3.43 (t, *J*=7.1 Hz, 2H), 1.67 - 1.56 (m, 4H), 1.46 (d, *J*=0.6 Hz, 18H), 1.43 - 1.37 (m, 2H). ^{13}C-NMR (101 MHz, $CDCl_3$) δ: 169.8, 81.5, 81.4, 71.6, 71.3, 70.7, 70.6, 70.1, 69.0, 68.8, 29.5, 29.4, 28.1, 22.6.

3,6,9,12,18-Pentaoxaicosanedioic acid (27d)

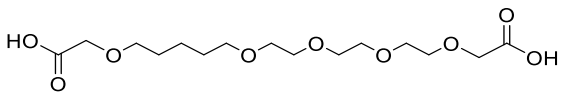

Prepared following the **general method B** starting from compound **26d** (90 mg, 0.19 mmol). The title compound was obtained a colourless oil (yield: 66 mg, quantitative). ^{1}H-NMR (400 MHz, $CDCl_3$) δ: 8.15 (s, 2H), 4.11 (s, 2H), 4.02 (s, 2H), 3.71 - 3.40 (m, 16H), 1.65 - 1.52 (m, 4H), 1.43 - 1.34 (m, 2H); ^{13}C-NMR (101 MHz, $CDCl_3$) δ: 172.8, 71.7, 71.3, 70.6, 70.4, 70.3, 70.1, 69.0, 67.9, 29.1, 29.0, 22.5.

Di-*tert*-butyl-4,7,10,13-tetraoxahexadecanedioate (26f)

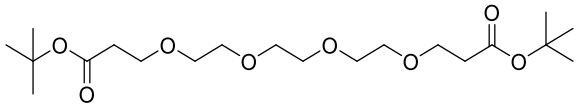

To a solution of triethylenglicole (136 mg, 0.90 mmol, 1 eq.) and *tert*-butyl acrylate (1.19 mL, 8.15 mmol, 9 eq.) in dichloromethane (2.2 mL), TBABr (58 mg, 0.18 mmol, 0.2 eq) was added. Then a 50% v/v aqueous solution of NaOH was added (0.8 mL) and the biphasic reaction was vigorously stirred for 12 h. The organic layer was separated and the aqueous phase was extracted with dichloromethane (x3). The organic layers were collected, died over $MgSO_4$ and purified by flash chromatography eluting from 0% to 10 % v/v methanol in dichloromethane. The title compound was obtained as an oil (yield: 258 mg, 78%). Analytical data matched those previously reported.[53]

4,7,10,13-tetraoxahexadecanedioic acid (27f)

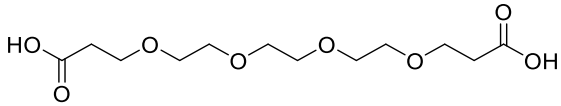

Prepared following the **general method B** starting from compound **26f** (92 mg, 0.23 mmol). The title compound was obtained a colourless oil (yield: 66 mg, quantitative). Analytical data matched those previously reported.[53]

***N*^{1},*N*^{21}-Bis((S)-1-((2S,4R)-4-hydroxy-2-((4-(4-methylthiazol-5-yl)benzyl)carbamoyl)pyrrolidin-1-yl)-3,3-dimethyl-1-oxobutan-2-yl)-3,6,10,15,19-pentaoxahenicosanediamide (28a)**

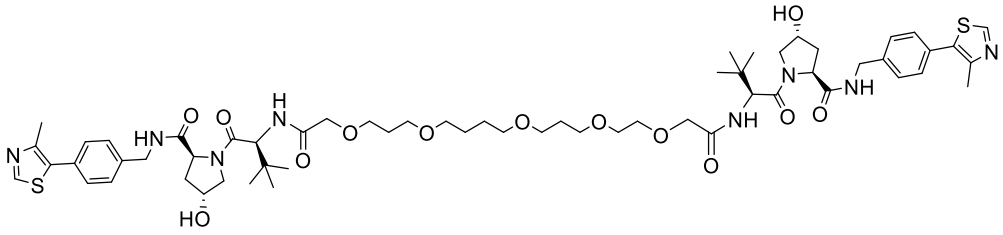

The title compound was prepared accordingly to the **general method M**, starting from compound **1** (20 mg, 0.04 mmol) and compound **27a** (7.5 mg, 0.02 mmol). The title compound was obtained as a white solid (yield: 6.5 mg, 27%).^{1}H-NMR (500 MHz, MeOD) δ: 9.00 (d, *J*=1.1 Hz, 2H), 7.45 (dd, *J*=8.4, 23.1 Hz, 8H), 4.71 - 4.68 (m, 2H), 4.55 (tt, *J*=12.4, 11.9 Hz, 6H), 4.36 (d, *J*=15.5 Hz, 2H), 4.03 (d, *J*=3.6 Hz, 2H), 3.97 (d, *J*=5.9 Hz, 2H), 3.89 - 3.78 (m, 4H), 3.71 - 3.68 (m, 2H), 3.64 - 3.36 (m, 14H), 2.49 (s, 6H), 2.26 -

2.19 (m, 2H), 2.13 - 2.06 (m, 2H), 1.90 - 1.84 (m, 2H), 1.85 - 1.79 (m, 2H), 1.61 - 1.55 (m, 4H), 1.04 (d, *J*=3.4 Hz, 18H).^{13}C-NMR (101 MHz, MeOD) δ: 174.4, 174.3, 172.1, 171.9, 171.8, 171.7, 153.3, 140.6, 131.1, 130.4, 129.0, 72.3, 71.8, 71.2, 71.1, 70.9, 69.9, 69.4, 68.7, 68.4, 60.8, 58.2, 58.1, 58.0, 43.7, 38.9, 37.2, 37.1, 31.1, 31.0, 27.5, 27.0, 15.4. HR-MS: found 1191.6137 $[M+H]^+$.

N^1,N^{20}-Bis((S)-1-((2S,4R)-4-hydroxy-2-((4-(4-methylthiazol-5-yl)benzyl)carbamoyl)pyrrolidin-1-yl)-3,3-dimethyl-1-oxobutan-2-yl)-3,8,13,18-tetraoxaicosanediamide (28b)

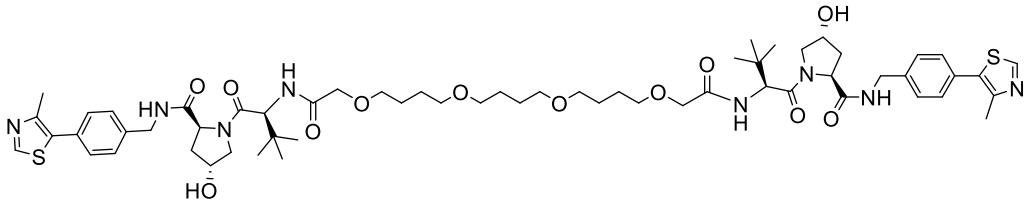

The title compound was prepared accordingly to **general method M**, starting from compound **1** (20 mg, 0.04 mmol) and compound **27b** (7.1 mg, 0.02 mmol). 6.7 mg were obtained (yield: 28%). ^{1}H-NMR (500 MHz, MeOD) δ: 8.77 (s, 2H), 7.34 (dd, *J*=8.3, 23.6 Hz, 8H), 4.59 (d, *J*=12.0 Hz, 2H), 4.50 - 4.40 (m, 6H), 4.26 (dd, *J*=4.9, 15.9 Hz, 2H), 3.86 (dd, *J*=15.3, 23.4 Hz, 4H), 3.77 (d, *J*=11.4 Hz, 2H), 3.70 (dd, J=3.9, 11.1 Hz, 2H), 3.46 (t, *J*=6.0 Hz, 4H), 3.38 - 3.28 (m, 8H), 2.37 (s, 6H), 2.16 - 2.10 (m, 2H), 2.02 - 1.96 (m, 2H), 1.62 - 1.52 (m, 8H), 1.51 - 1.45 (m, 4H), 0.93 (s, 18H).^{13}C-NMR (101 MHz, MeOD) δ: 174.3, 172.1, 172.0, 171.7, 152.8, 149.1, 140.3, 133.4, 131.5, 130.5, 130.4, 129.5, 129.0, 72.7, 71.7, 71.5, 71.1, 70.7, 60.8, 58.1, 58.0, 43.7, 39.0, 37.2, 27.6, 27.5, 27.4, 15.9. HR-MS: found 1175.6623 $[M+H]^+$.

N^1,N^{19}-Bis((S)-1-((2S,4R)-4-hydroxy-2-((4-(4-methylthiazol-5-yl)benzyl)carbamoyl)pyrrolidin-1-yl)-3,3-dimethyl-1-oxobutan-2-yl)-3,7,13,17-tetraoxanonadecanediamide (28c)

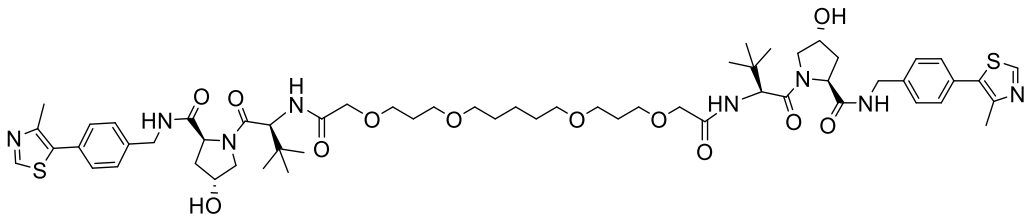

The title compound was prepared accordingly to **general method M**, starting from compound **1** (20 mg, 0.04 mmol) and compound **27c** (6.8 mg, 0.02 mmol). The desired

compound was obtained as a white solid (yield: 6.6 mg, 28%).[1]H-NMR (500 MHz, MeOD) δ: 8.76 (s, 2H), 7.37 - 7.30 (m, 8H), 4.60 (d, *J*=9.4 Hz, 2H), 4.50 - 4.24 (m, 8H), 3.87 (d, *J*=6.5 Hz, 4H), 3.77 (d, *J*=11.2 Hz, 2H), 3.70 (dd, *J*=3.8, 11.5 Hz, 2H), 3.55 - 3.49 (m, 4H), 3.43 (dt, *J*=1.2, 6.2 Hz, 4H), 3.33 - 3.29 (m, 4H), 2.37 (s, 6H), 2.16 - 2.10 (m, 2H), 2.03 - 1.96 (m, 2H), 1.80 - 1.74 (m, 4H), 1.47 - 1.40 (m, 4H), 1.30 - 1.23 (m, 2H), 0.93 (s, 18H). [13]C-NMR (101 MHz, MeOD) δ: 174.3, 171.8, 171.6, 152.8, 149.0, 140.2, 133.4, 131.5, 130.5, 130.3, 129.5, 128.9, 71.9, 71.0, 70.8, 69.8, 68.3, 60.8, 58.1, 57.9, 43.7, 38.9, 37.2, 30.9, 30.5, 26.9, 23.9, 15.8. HR-MS: found 1161.6446 $[M+H]^+$.

N^1,N^{20}-Bis((S)-1-((2S,4R)-4-hydroxy-2-((4-(4-methylthiazol-5-yl)benzyl)carbamoyl)pyrrolidin-1-yl)-3,3-dimethyl-1-oxobutan-2-yl)-3,6,9,12,18-pentaoxaicosanediamide (28d)

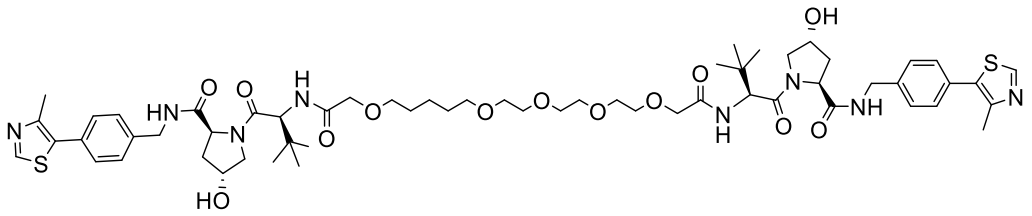

The title compound was prepared accordingly to **general method M**, starting from compound **1** (20 mg, 0.04 mmol) and compound **27d** (7.2 mg, 0.02 mmol). The desired product was obtained as a white solid (yield: 5.0 mg, 21%). [1]H-NMR (500 MHz, MeOD) δ: 8.77 (s, 2H), 7.34 (dd, *J*=7.4, 23.2 Hz, 8H), 4.59 (dd, *J*=2.4, 9.4 Hz, 2H), 4.50 - 4.38 (m, 6H), 4.27 (t, *J*=4.3 Hz, 1H), 4.24 (t, *J*=4.3 Hz, 1H), 3.94 (dd, *J*=15.3, 22.3 Hz, 2H), 3.85 (dd, *J*=15.3, 24.4 Hz, 2H), 3.76 (d, *J*=10.7 Hz, 2H), 3.72 - 3.68 (m, 2H), 3.61 - 3.40 (m, 14H), 3.35 (dt, *J*=1.0, 6.5 Hz, 2H), 2.37 (s, 6H), 2.16 - 2.09 (m, 2H), 2.02 - 1.96 (m, 2H), 1.57 - 1.45 (m, 4H), 1.39 - 1.32 (m, 2H), 0.94 (s, 18H). [13]C-NMR (101 MHz, MeOD) δ: 174.4, 174.3, 172.1, 172.0, 171.7, 152.9, 149.0, 140.3, 133.4, 131.5, 130.5, 130.4, 129.5, 129.0, 72.9, 72.3, 72.2, 71.7, 71.6, 71.5, 71.2, 71.1, 70.7, 60.8, 58.1, 58.0, 43.7, 38.9, 37.2, 37.1, 30.5, 30.4, 27.0, 26.9, 23.8, 15.8. HR-MS: found 1177.6435 $[M+H]^+$.

N^1,N^{16}-bis((S)-1-((2S,4R)-4-hydroxy-2-((4-(4-methylthiazol-5-yl)benzyl)carbamoyl)pyrrolidin-1-yl)-3,3-dimethyl-1-oxobutan-2-yl)hexadecanediamide (28e)

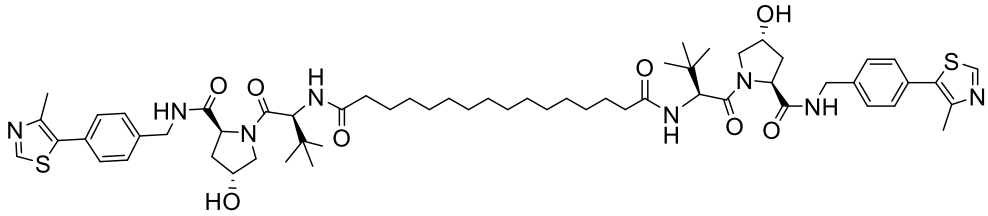

The title compound was prepared accordingly to **general method M**, starting from compound **1** (14.4 mg, 0.03 mmol) and the commercially available hexadecandioic acid **27e** (4.6 mg, 0.02 mmol). The desired product was obtained as a white solid (yield: 7.0 mg, 39%). ^{1}H-NMR (400 MHz, MeOD) δ: 8.76 (s, 2H), 7.33 (dd, *J*=8.5, 20.1 Hz, 8H), 4.56 - 4.40 (m, 8H), 4.25 (d, *J*=15.3 Hz, 2H), 3.82 - 3.68 (m, 4H), 2.37 (s, 6H), 2.28 - 2.07 (m, 8H), 2.03 - 1.96 (m, 2H), 1.54 - 1.48 (m, 4H), 1.27 - 1.16 (m, 18H), 0.94 (s, 18H). ^{13}C-NMR (101 MHz, MeOD) δ: 176.0, 174.4, 172.3, 152.7, 149.0, 140.2, 133.3, 131.5, 130.3, 128.9, 71.0, 60.7, 58.9, 57.9, 43.7, 38.8, 36.6, 36.5, 30.6, 30.5, 30.4, 30.2, 27.0, 26.9, 15.7. HR-MS: found 1111.6166 $[M+H]^+$.

N^1,N^{16}-bis((S)-1-((2S,4R)-4-hydroxy-2-((4-(4-methylthiazol-5-yl)benzyl)carbamoyl)pyrrolidin-1-yl)-3,3-dimethyl-1-oxobutan-2-yl)-4,7,10,13-tetraoxahexadecanediamide (28f)

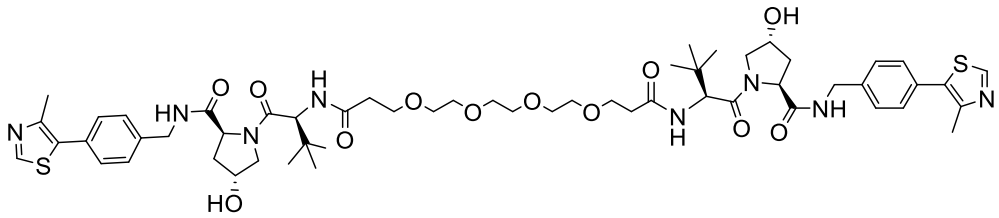

The title compound was prepared accordingly to **general method M**, starting from compound **1** (14.4 mg, 0.03 mmol) and **27f** (4.7 mg, 0.02 mmol). The desired product was obtained as a white solid (yield: 6.5 mg, 36%). ^{1}H-NMR (400 MHz, MeOD) δ: 9.11 (s, 2H), 7.46 (dd, *J*=8.3, 21.6 Hz, 8H), 4.65 (s, 2H), 4.60 - 4.34 (m, 8H), 3.89 - 3.77 (m, 4H), 3.75 - 3.69 (m, 4H), 3.64 - 3.60 (m, 12H), 2.61 - 2.53 (m, 2H), 2.49 (s, 6H), 2.52 - 2.42 (m, 2H), 2.25 - 2.17 (m, 2H), 2.12 - 2.04 (m, 2H), 1.03 (s, 18H); ^{13}C-NMR (101 MHz, MeOD) δ: 174.4, 173.7, 172.1, 153.4, 140.6, 130.4, 129.1, 71.5, 71.4, 71.1, 68.3, 60.8, 58.9, 58.0, 43.7, 38.9, 37.3, 36.7, 27.0, 15.4. HR-MS: found 1119.5165 $[M+H]^+$.

N^1,N^{20}-bis((S)-1-((2S,4R)-4-hydroxy-2-((4-(4-methylthiazol-5-yl)benzyl)carbamoyl)pyrrolidin-1-yl)-3,3-dimethyl-1-oxobutan-2-yl)-3,9,12,18-tetraoxaicosanediamide (28g)

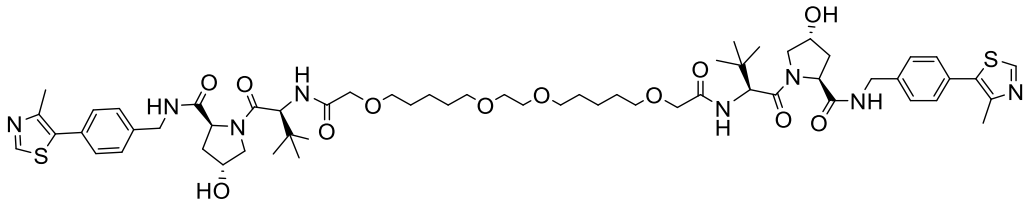

The title compound was prepared accordingly to **general method M**, starting from compound **1** (20 mg, 0.04 mmol) and **27g** (7.5 mg, 0.02 mmol). The desired product was obtained as a white solid (yield: 5.9 mg, 23%). ^{1}H-NMR (400 MHz, MeOD) δ: 8.92 (s, 2H), 7.47-7.40 (m, 8H), 4.68 (d, *J*=9.6, 2H), 4.59-4.49 (m, 6H), 4.35 (dd, *J*= 3.7, 15.6, 2H), 3.96-3.77 (m, 8H), 3.31-3.29 (m, 12H), 2.47 (s, 6H), 2.24-2.19 (m, 2H), 2.11-2.04 (m, 2H), 1.67-1.56 (m, 8H), 1.48-1.42 (m, 4H), 1.02 (s, 18H). ^{13}C-NMR (101 MHz, MeOD) δ: 173.0, 170.6, 170.3, 151.6, 147.4, 139.0, 132.2, 130.0, 129.0, 127.6, 71.5, 70.8, 69.8, 69.7, 69.3, 59.4, 56.7, 56.6, 42.3, 37.6, 35.8, 29.1, 29.0, 25.5, 22.4, 14.3. HR-MS: found 1175.5958 $[M+H]^+$.

(2S,4R)-1-((3R,24S)-24-(tert-butyl)-1-(1-fluorocyclopropyl)-3-((2S,4R)-4-hydroxy-2-((4-(4-methylthiazol-5-yl)benzyl)carbamoyl)pyrrolidine-1-carbonyl)-4,4-dimethyl-1,22-dioxo-8,11,14,17,20-pentaoxa-5-thia-2,23-diazapentacosan-25-oyl)-4-hydroxy-N-(4-(4-methylthiazol-5-yl)benzyl)pyrrolidine-2-carboxamide (28h)

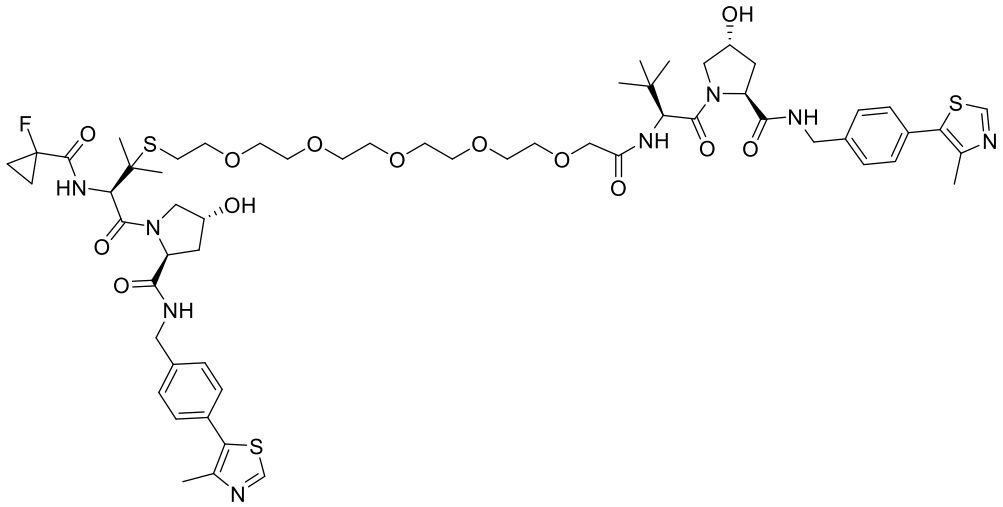

Starting from compound **21b** (8.5 mg, 0.01 mmol) and following the **general method B** the deprotected carboxylic acid derivative was obtained in quantitative yield. The crude carboxylic acid (0.01 mmol, 1 eq.) was dissolved in dry DMF. Then compound **1** (5.5, 0.01 mmol, 1.2 eq.), COMU (4.1 mg, 0.01 mmol, 1 eq.), and DIPEA (5.1 µL, 0.03 mmol, 3 eq.), were added. The mixture was stirred at r.t. until no presence of the starting material was detected by LC-MS. Then ice was added and the volatiles were evaporated under reduced pressure. The crude was purified by HPLC using a gradient of 20% to 70% v/v acetonitrile in 0.1% v/v aqueous solution of formic acid to yield the title compound as a pale yellow solid (yield: 5.1 mg, 42%). ^{1}H-NMR (400 MHz, MeOD) δ: 8.86 (s, 2H), 7.47 - 7.39 (m, 8H), 4.94 (d, *J*=9.1 Hz, 1H), 4.70 (d, *J*=9.1 Hz, 1H), 4.63 - 4.32 (m, 8H), 4.04 (d, *J*=3.8 Hz, 2H), 3.92 - 3.78 (m, 4H), 3.72 - 3.48 (m, 20H), 2.48 (s, 3H), 2.47 (s, 3H), 2.30 - 2.18 (m, 2H), 2.15 - 2.05 (m, 2H), 1.45 - 1.27 (m, 10H), 1.04 (s, 9H). ^{13}C-NMR (101 MHz, MeOD) δ: 174.4, 174.1, 172.1, 171.7, 170.8, 152.9, 149.1, 140.3, 140.2, 133.4, 131.7, 131.6, 130.6, 130.5, 130.4, 129.5, 129.1, 129.0, 80.4, 78.1, 72.4, 71.7, 71.6, 71.6, 71.3, 71.2, 71.1, 71.0, 61.2, 60.9, 58.2, 58.1, 57.2, 43.8, 43.7, 39.1, 39.0, 37.1, 29.6, 27.0, 26.9, 25.8, 15.9, 14.2, 14.2. HR-MS: found 613.2597 $[M+2H]^{+}$.

N^1,N^{20}-Bis((S)-1-((2R,3R,4S)-3-fluoro-4-hydroxy-2-((4-(4-methylthiazol-5-yl)benzyl)carbamoyl)pyrrolidin-1-yl)-3,3-dimethyl-1-oxobutan-2-yl)-3,6,9,12,15,18-hexaoxaicosanediamide (28i)

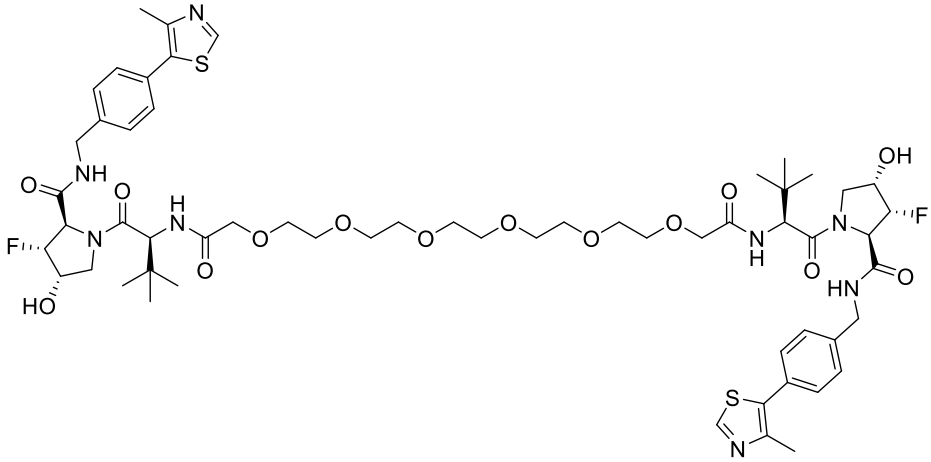

Prepared accordingly to **general method F**, starting from **S5** (16.9 mg, 0.0348 mmol) and **12c** (6.17 mg, 0.0174 mmol). Obtained 7.5 mg (35% yield) as white solid. ^{1}H-NMR (400 MHz, MeOD) 8.89 (s, 2), 7.46 (d, *J*=8.7 Hz, 8H), 4.99 (td, *J*=3.3, 52.9 Hz, 2H), 4.69 (s, 2H), 4.65 (dd, *J*=2.9, 21.3 Hz, 2H), 4.60 - 4.34 (m, 6H), 4.08 - 4.03 (m, 6H), 3.77 - 3.59 (m, 22H), 2.49 (s, 6H), 1.06 (s, 18H).^{19}F-NMR (376.45 MHz, MeOD): -201.87 ,^{13}C-NMR (101 MHz, MeOD) 170.9, 170.5, 169.2, 169.1, 151.5, 147.7, 138.6, 130.2, 129.0, 127.5, 94.0, 92.1, 70.9, 70.2, 70.1, 70.1, 69.6, 69.5, 64.4, 64.1, 56.1, 50.9, 42.4, 35.3, 25.5, 14.4. HR-MS: found 1215.5214 $[M+H]^+$.

2,2'-((oxybis(ethane-2,1-diyl))bis(oxy))diacetic acid (12f)

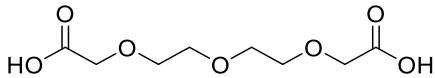

Starting from compound **6** (30 mg, 0.11 mmol) and following the **general method B**, the title compound was obtained as a colourless oil (yield: 23 mg, quantitative). Analytical data matched those reported.[54]

3,6,9,12,15-pentaoxaheptadecanedioic acid (12g)

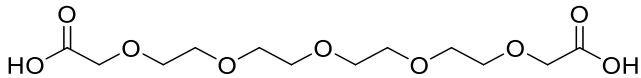

Starting from compound **7** (30 mg, 0.08 mmol) and following the **general method B**, the title compound was obtained as a colourless oil (yield: 24 mg, quantitative). Analytical data matched those reported.[36]

2,2'-((oxybis(ethane-2,1-diyl))bis(oxy))bis(N-(2-((2-(2,6-dioxopiperidin-3-yl)-1,3-dioxoisoindolin-4-yl)amino)ethyl)acetamide) (29f)

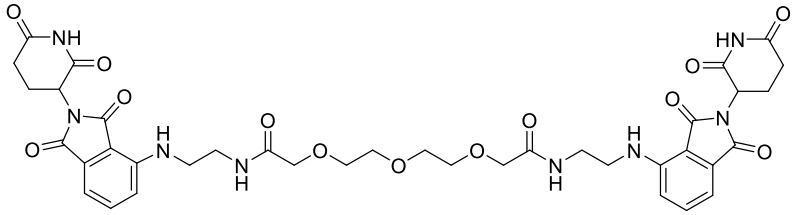

The title compound was prepared accordingly to **general method M**, starting from compound **5** (14.8 mg, 0.04 mmol) and compound **12f** (6.1 mg, 0.02 mmol). The desired product was obtained as a yellow solid (yield: 2.8 mg, 15%). ^{1}H-NMR (500 MHz, MeOD) δ: 7.43 (dd, *J*=7.1, 8.5 Hz, 2H), 7.00 (d, *J*=8.5 Hz, 2H), 6.94 (d, *J*=7.1 Hz, 2H), 4.94 (dd, *J*=5.5, 12.7 Hz, 2H), 3.86 (s, 4H), 3.52 (s, 8H), 3.40 (s, 8H), 2.80 - 2.57 (m, 6H), 2.04 - 1.98 (m, 2H). ^{13}C-NMR (101 MHz, MeOD) δ: 174.7, 173.5, 171.6, 170.6, 148.1, 137.2, 133.9, 112.1, 71.8, 71.2, 42.5, 40.4, 39.4, 32.1, 23.7. HR-MS: found 819.3005 $[M+H]^{+}$.

***N*^{1},*N*^{14}-bis(2-((2-(2,6-dioxopiperidin-3-yl)-1,3-dioxoisoindolin-4-yl)amino)ethyl)-3,6,9,12-tetraoxatetradecanediamide (29e)**

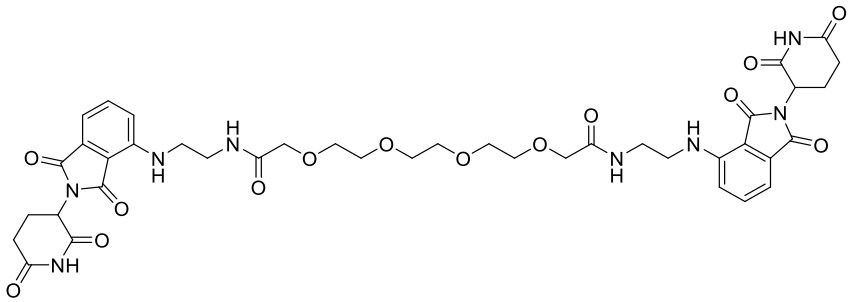

The title compound was obtained as side product from the synthesis of compound **13e** (yield: 2.4 mg, yellow solid). ^{1}H-NMR (400 MHz, MeOD) δ: 7.53 (dd, *J*=7.5, 8.4 Hz, 2H), 7.10 (d, *J*=8.6 Hz, 2H), 7.03 (d, *J*=7.1 Hz, 2H), 5.03 (dd, *J*=5.4, 12.2 Hz, 2H), 3.96 (s, 4H), 3.72 - 3.48 (m, 20H), 2.90 - 2.65 (m, 6H), 2.13 - 2.08 (m, 2H); ^{13}C-NMR (101 MHz, MeOD) δ: 174.6, 173.4, 171.5, 170.6, 169.2, 148.1, 137.2, 133.9, 112.1, 111.5, 71.9, 71.3, 71.2, 71.1, 42.5, 39.4, 32.2, 23.8. HR-MS: found 880.3389 $[M+NH_4]^{+}$.

***N*[1],*N*[17]-bis(2-((2-(2,6-dioxopiperidin-3-yl)-1,3-dioxoisoindolin-4-yl)amino)ethyl)-3,6,9,12,15-pentaoxaheptadecanediamide (29g)**

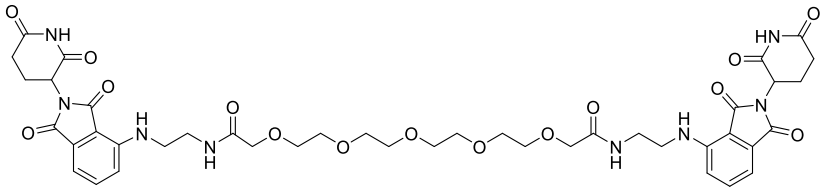

The title compound was prepared accordingly to **general method M**, starting from compound **5** (14.8 mg, 0.04 mmol) and compound **12g** (4.4 mg, 0.02 mmol). The desired product was obtained as a yellow solid (yield: 1.5 mg, 9%). ^{1}H-NMR (400 MHz, MeOD) δ: 7.53 (dd, *J*=7.1, 8.5 Hz, 2H), 7.11 (d, *J*=8.5 Hz, 2H), 7.04 (d, *J*=7.1 Hz, 2H), 5.04 (dd, *J*=5.5, 12.4 Hz, 2H), 3.96 (s, 4H), 3.60 - 3.49 (m, 24H), 2.86 - 2.68 (m, 6H), 2.14 - 2.06 (m, 2H). ^{13}C-NMR (101 MHz, MeOD) δ: 174.7, 173.5, 171.5, 170.6, 169.3, 148.1, 137.2, 134.0, 112.2, 111.5, 72.0, 71.4, 71.3, 71.1, 42.5, 40.5, 39.4, 32.2, 23.8. HR-MS: found 907.3451 $[M+H]^{+}$.

***N*[1],*N*[20]-bis(2-((2-(2,6-dioxopiperidin-3-yl)-1,3-dioxoisoindolin-4-yl)amino)ethyl)-3,6,9,12,15,18-hexaoxaicosanediamide (29c)**

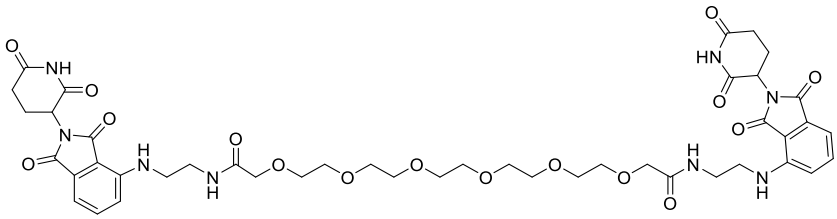

The title compound was obtained as side product from the synthesis of compound **13c** (yield: 1.0 mg, yellow solid). ^{1}H-NMR (400 MHz, MeOD) δ: 7.54 (dd, *J*=7.1, 8.5 Hz, 2H), 7.12 (d, *J*=8.5 Hz, 2H), 7.04 (d, *J*=7.1 Hz, 2H), 5.04 (dd, *J*=5.5, 12.4 Hz, 2H), 3.96 (s, 4H), 3.62 - 3.49 (m, 28H), 2.91 - 2.65 (m, 6H), 2.15 - 2.08 (m, 2H); ^{13}C-NMR (101 MHz, MeOD) δ: 174.7, 173.6, 171.5, 170.6, 169.3, 148.1, 137.2, 134.0, 112.1, 111.5, 72.0, 71.5, 71.4, 71.3, 71.1, 42.5, 39.4, 32.2, 23.8. HR-MS: found 968.4054 $[M+NH_4]^{+}$.

N^1,N^{29}-bis(2-((2-(2,6-dioxopiperidin-3-yl)-1,3-dioxoisoindolin-4-yl)amino)ethyl)-3,6,9,12,15,18,21,24,27-nonaoxanonacosanediamide (29d)

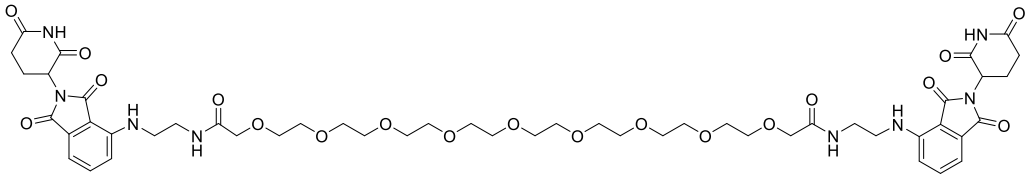

The title compound was obtained as side product from the synthesis of compound **13d** (yield: 2.5 mg, yellow solid). ^{1}H-NMR (400 MHz, MeOD) 7.55 (dd, *J*=7.1, 8.5 Hz, 2H), 7.14 (d, *J*=8.5 Hz, 2H), 7.05 (d, *J*=7.1 Hz, 2H), 5.04 (dd, *J*=5.3, 12.5 Hz, 2H), 3.96 (s, 4H), 3.65 - 3.48 (m, 42H), 2.91 - 2.66 (m, 6H), 2.14 - 2.08 (m, 2H); ^{13}C-NMR (101 MHz, MeOD) δ: 174.7, 173.6, 171.5, 170.6, 169.3, 148.1, 137.3, 134.0, 112.1, 111.5, 72.0, 71.5, 71.4, 71.3, 71.0, 42.4, 39.4, 32.2, 23.8. HR-MS: found 1100.4753 $[M+NH_4]^+$.

N^1,N^{20}-bis(2-((2-(2,6-dioxopiperidin-3-yl)-1,3-dioxoisoindolin-4-yl)amino)ethyl)-3,9,12,18-tetraoxaicosanediamide (29a)

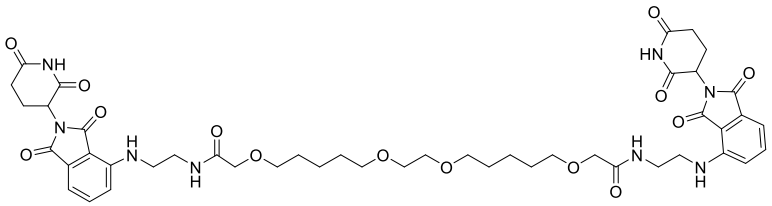

The title compound was prepared accordingly to **general method M**, starting from compound **5** (15 mg, 0.04 mmol) and compound **12a** (7.4 mg, 0.02 mmol). The desired product was obtained as a yellow solid (yield: 9.3 mg, 49%). ^{1}H-NMR (400 MHz, MeOD) δ: 7.44 (ddd, *J*=0.6, 7.1, 8.5 Hz, 2H), 7.02 (dd, *J*=0.6, 8.5 Hz, 2H), 6.94 (d, *J*=7.1 Hz, 2H), 4.95 (dd, *J*=5.4, 12.7 Hz, 2H), 3.78 (s, 4H), 3.44 (s, 4H), 3.39 (s, 8H), 3.35 (q, *J*=6.7 Hz, 8H), 2.80 - 2.56 (m, 6H), 2.04 - 1.96 (m, 2H), 1.53 - 1.42 (m, 8H), 1.32 - 1.26 (m, 4H). HR-MS: found 964.4409 $[M+H]^+$

2,2'-(hexane-1,6-diylbis(oxy))bis(N-(2-((2-(2,6-dioxopiperidin-3-yl)-1,3-dioxoisoindolin-4-yl)amino)ethyl)acetamide) (29b)

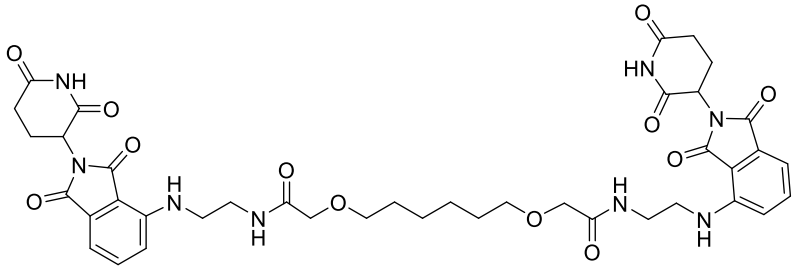

The title compound was obtained as side product from the synthesis of compound **13b** (yield: 1.2 mg, yellow solid). ^{1}H-NMR (400 MHz, MeOD) δ: 7.54 (2H, dd, *J*=7.1, 8.7 Hz), 7.12 (2H, d, *J*=8.7 Hz), 7.05 (2H, d, *J*=7.1 Hz), 5.04 (2H, dd, *J*=5.4, 12.5 Hz), 3.88 (4H, s), 3.52 - 3.41 (12H, m), 2.86 - 2.69 (6H, m), 2.13 - 2.07 (2H, m), 1.57 - 1.52 (4H, m), 1.33 - 1.31 (4H, m); ^{13}C-NMR (101 MHz, MeOD) δ: 174.6, 173.5, 171.5, 170.6, 169.3, 148.2, 137.2, 134.0, 112.2, 111.5, 72.8, 70.9, 42.6, 39.4, 32.2, 30.4, 26.8, 23.8. HR-MS: found 831.3361 $[M+H]^{+}$.

4,4'-(octane-1,8-diylbis(azanediyl))bis(2-(2,6-dioxopiperidin-3-yl)isoindoline-1,3-dione) (30a)

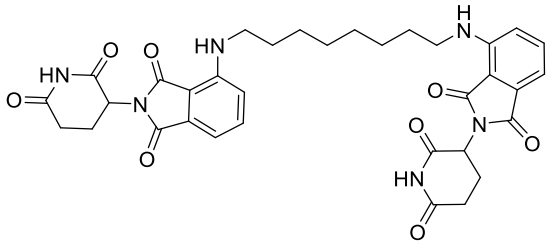

The title compound was prepared accordingly to **general method N**, starting from compound **4** (30 mg, 0.11 mmol) and octane-1,8-diamine (7.8 mg, 0.05 mmol). The title compound was obtained as a yellow solid (yield: 3.7 mg, 12%). ^{1}H-NMR (500 MHz, $CDCl_3$) δ: 8.10 (s, 1H), 8.05 (s, 1H), 7.46 (dd, *J*=7.1, 8.5 Hz, 2H), 7.06 (d, *J*=7.1 Hz, 2H), 6.86 (d, *J*=8.5 Hz, 2H), 6.22 (t, *J*=5.3 Hz, 2H), 4.89 (dd, *J*=5.3, 12.4 Hz, 2H), 3.24 (q, *J*=6.5 Hz, 4H), 2.88 - 2.66 (m, 6H), 2.13 - 2.07 (m, 2H), 1.67 - 1.61 (m, 4H), 1.43 - 1.32 (m, 8H); ^{13}C-NMR (101 MHz, $CDCl_3$) δ: 170.0, 169.6, 168.3, 167.6, 147.0, 136.1, 132.6, 116.6, 11.3, 109.9, 48.9, 42.6, 31.4, 29.2, 29.1, 26.8, 22.8. HR-MS: found 657.2680 $[M+H]^{+}$.

4,4'-((1,3-phenylenebis(methylene))bis(azanediyl))bis(2-(2,6-dioxopiperidin-3-yl)isoindoline-1,3-dione) (30b)

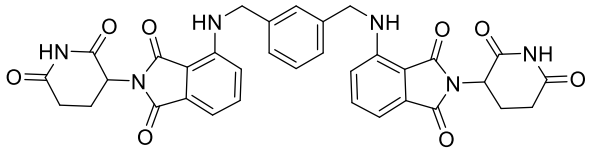

The title compound was prepared accordingly to **general method N**, starting from compound **4** (30 mg, 0.11 mmol) and 1,3-phenylenedimethanamine (7.4 mg, 0.05 mmol). The title compound was obtained as a yellow solid (yield: 7.0 mg, 20%). ^{1}H-NMR (500 MHz, $CDCl_3$) δ: 8.20 (s, 1H), 8.15 (s, 1H), 7.34 (t, *J*=7.8 Hz, 2H), 7.30 - 7.19 (m, 4H), 7.03 (d, *J*=6.9 Hz, 2H), 6.72 (dd, *J*=2.7, 8.8 Hz, 2H), 6.61 (q, *J*=5.4 Hz, 2H), 4.85 (t, *J*=9.2 Hz, 2H), 4.42 (d, *J*=5.7 Hz, 4H), 2.83 - 2.62 (m, 6H), 2.09 - 2.03 (m, 2H). ^{13}C-NMR (101 MHz, $CDCl_3$) δ: 171.1, 171.0, 169.5, 168.4, 167.5, 146.6, 138.6, 136.1, 132.5, 129.4, 126.4, 126.3, 125.5, 117.1, 112.1, 110.6, 49.0, 46.7, 31.4, 22.8. HR-MS: found 649.2067 $[M+H]^+$.

4,4'-(((1,3-phenylenebis(oxy))bis(ethane-2,1-diyl))bis(azanediyl))bis(2-(2,6-dioxopiperidin-3-yl)isoindoline-1,3-dione) (30c)

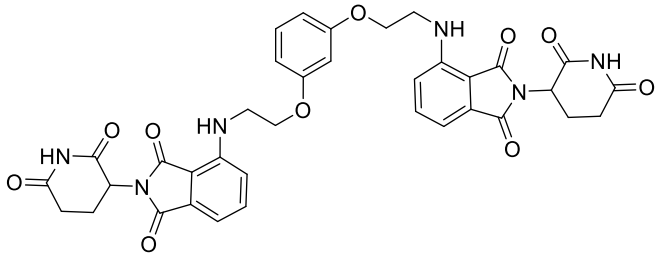

The title compound was prepared accordingly to **general method N**, starting from compound **4** (30 mg, 0.11 mmol) and 2,2'-(1,3-phenylenebis(oxy))bis(ethan-1-amine) (10.7 mg, 0.05 mmol). The title compound was obtained as a yellow solid (yield: 9 mg, 23%). ^{1}H-NMR (500 MHz, DMSO-d_6) δ: 11.09 (s, 2H), 7.50 (dd, *J*=7.3, 8.5 Hz, 2H), 7.15 (d, *J*=8.5 Hz, 2H), 7.06 - 7.02 (m, 2H), 6.95 - 6.91 (m, 4H), 6.77 - 6.73 (m, 2H), 5.03 (dd, *J*=5.4, 12.9 Hz, 2H), 4.16 (t, *J*=5.4 Hz, 4H), 3.67 - 3.60 (m, 4H), 2.90 - 2.82 (m, 2H), 2.59 - 2.52 (m, 3H), 2.49 - 2.42 (m 1H), 2.05 - 1.97 (m, 2H); HR-MS: found 709.2381 $[M+H]^+$.

4,4'-((1,4-phenylenebis(ethane-2,1-diyl))bis(azanediyl))bis(2-(2,6-dioxopiperidin-3-yl)isoindoline-1,3-dione) (30d)

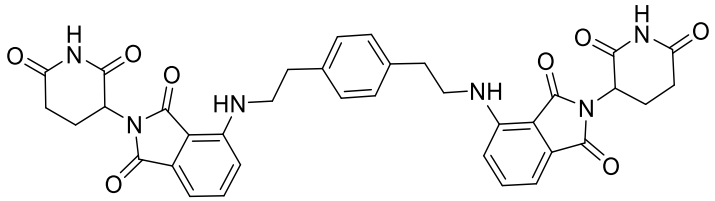

The title compound was prepared accordingly to **general method N**, starting from compound **4** (30 mg, 0.11 mmol) and 2,2'-(1,4-phenylene)bis(ethan-1-amine) (8.9 mg, 0.05 mmol). The title compound was obtained as a yellow solid (yield: 11 mg, 30%). ^{1}H-NMR (500 MHz, DMSO-d_6) δ: 11.11 (s, 2H), 7.59 (dd, *J*=7.1, 8.5 Hz, 2H), 7.26 (s, 4H), 7.16 (d, *J*=8.6 Hz, 2H), 7.04 (d, *J*=7.1 Hz, 2H), 6.59 (t, *J*=6.1 Hz, 2H), 5.05 (dd, *J*=5.5, 12.8 Hz, 2H), 3.56 - 3.49 (m, 4H), 2.90 - 2.83 (m, 4H), 2.62 - 2.52 (m, 4H), 2.06 - 1.98 (m, 2H). ^{13}C-NMR (101 MHz, DMSO- d_6) δ: 173.3, 170.6, 167.8, 146.7, 137.4, 136.8, 132.6, 129.3, 117.8, 111.1, 109.6, 49.0, 44.0, 34.9, 31.4, 22.6 HR-MS: found 677.2356 $[M+H]^+$.

4,4'-((cyclohexane-1,3-diylbis(methylene))bis(azanediyl))bis(2-(2,6-dioxopiperidin-3-yl)isoindoline-1,3-dione) (30e)

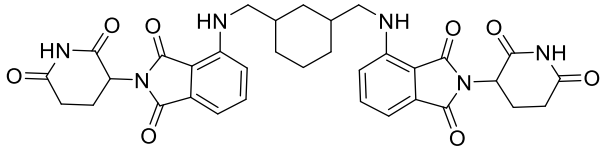

The title compound was prepared accordingly to **general method N**, starting from compound **4** (30 mg, 0.11 mmol) and cyclohexane-1,3-diyldimethanamine (7.7 mg, 0.05 mmol). The title compound was obtained as a yellow solid (yield: 4.6 mg, 13%). ^{1}H-NMR (500 MHz, DMSO) δ: 11.12 (s, 2H), 7.59 - 7.54 (m, 2H), 7.13 - 7.12 (m, 2H), 7.04 - 6.98 (m, 2H), 6.66 - 6.58 (m, 2H), 5.05 (dd, *J*=5.5, 12.9 Hz, 2H), 3.29 - 3.14 (m, 4H), 2.91 - 2.82 (m, 2H), 2.63 - 2.52 (m, 4H), 2.06 - 1.99 (m, 2H), 1.77 - 1.45 (m, 6H), 1.32 - 1.16 (m, 2H), 0.95 - 0.71 (m, 2H); ^{13}C-NMR (101 MHz, DMSO- d_6) δ: 173.3, 170.6, 169.5, 167.8, 147.1, 136.7, 132.6, 117.9, 110.8, 109.3, 49.0, 48.5, 37.4, 37.3, 35.0, 32.6, 31.4, 30.6, 29.3, 25.3, 22.6, 20.6. HR-MS: found 655.2529 $[M+H]^+$.

5.4.2 Biology

Cell Culture. HeLa (HeLa (ATCC® CCL2™) and 293 [HEK293] (ATCC® CRL1573™) cells were purchased from ATCC and cultured in DMEM medium (Gibco) supplemented with 10% FBS, 100 µg/mL penicillin/streptomycin and L-glutamine. Cells were grown at 37 °C and 5% CO_2 and were cultured for no more than 30 passages. All cell lines were routinely tested for mycoplasma contamination using MycoAlert kit from Lonza.

Testing compounds in cells. HeLa (5 x 105) and HEK293 (1 x 106) cells were seeded in standard 6-well plates (2 mL medium) overnight before treatment with compounds at the desired concentration, with a final DMSO concentration of 0.1% v/v. After the appropriate incubation time, cells were washed with DPBS (Gibco) and lysed using 85 µL RIPA buffer (Sigma-Aldrich) supplemented with cOmplete Mini EDTA-free protease inhibitor cocktail (Roche) and benzonase. Lysates were clarified by centrifugation (20000 g, 10 min, 4 °C) and the total protein content of the supernatant was quantified using a Bradford colorimetric assay or Pierce BCA assay. Samples were prepared using equal amounts of total protein in LDS sample buffer (Invitrogen).

Immunoblotting. Proteins were separated by SDS-PAGE on NuPage 4-12% Bis-Tris gels and transferred on Amersham Protran 0.45 NC nitrocellulose membrane (GE Healthcare) using wet transfer. Membranes were blocked using 5% w/v milk in Tris-buffered saline (TBS) with 0.1% Tween-20. Blots were probed using anti-VHL (CST-68547), anti-CRBN (Novus, NBP1-91810), anti-Tubulin hFAB-rhodamine (BioRad, 12004166) or anti β-actin (Cell Signaling Technology, 4970S, 13E5) primary antibodies, followed by incubation with secondary anti-Rabbit IRDye 800CW (ab216773) or anti-rabbit HRP-conjugated (CST7074) antibodies. Blots were developed using a Bio-Rad ChemiDoc MP Imaging System or the Amersham ECL Prime Western blotting detection kit and Amersham Hyperfilm ECL film, as appropriate. Band quantification was performed using the ImageJ software. Band intensities were normalized to the tubulin or actine loading control and reported as % of the average against 0.1% DMSO vehicle intensity. Degradation data was plotted and analyzed using Prism (Graphpad, version 6). DC50 values (concentration to reach 50% maximal degradation) were estimated by

fitting band intensity against log[concentration] with a one-site inhibition model. Apparent half-life values (time to reach 50% maximal degradation) were estimated by fitting band intensity against time using a single-phase exponential decay model.

5.5 References

(1) Girardini, M.; Maniaci, C.; Hughes, S. J.; Testa, A.; Ciulli, A. Cereblon versus VHL: Hijacking E3 Ligases against Each Other Using PROTACs. *Bioorg. Med. Chem.* **2019**, *27* (12), 2466–2479.

(2) Hershko, A.; Ciechanover, A. THE UBIQUITIN SYSTEM. Annual Review of Biochemistry, **1998**, Vol. 67: 425-479.

(3) Pickart, C. M. Mechanisms Underlying Ubiquitination. *Annu. Rev. Biochem.* **2001**, *70* (1), 503–533.

(4) Rousseau, A.; Bertolotti, A. Regulation of Proteasome Assembly and Activity in Health and Disease. *Nat. Rev. Mol. Cell Biol.* **2018**, *19* (11), 697–712.

(5) Bedford, L.; Paine, S.; Sheppard, P. W.; Mayer, R. J.; Roelofs, J. Assembly, Structure and Function of the 26S Proteasome. *Trends Cell Biol.* **2010**, *20* (7), 391–401.

(6) Lecker, S. H.; Goldberg, A. L.; Mitch, W. E. Protein Degradation by the Ubiquitin–Proteasome Pathway in Normal and Disease States. *J. Am. Soc. Nephrol.* **2006**, *17* (7), 1807–1819.

(7) Turcu, F. E. R.; Ventii, K. H.; Wilkinson, K. D. Regulation and Cellular Roles of Ubiquitin-Specific Deubiquitinating Enzymes. *Annu. Rev. Biochem.* **2009**, *78*, 363–397.

(8) Komander, D. The Emerging Complexity of Protein Ubiquitination. *Biochem. Soc. Trans.* **2009**, *37* (Pt 5), 937–953.

(9) Buetow, L.; Huang, D. T. Structural Insights into the Catalysis and Regulation of E3 Ubiquitin Ligases. *Nat. Rev. Mol. Cell Biol.* **2016**, *17* (10), 626–642.

(10) Morreale, F. E.; Walden, H. Types of Ubiquitin Ligases. *Cell* **2016**, *165* (1), 248.

(11) Deshaies, R. J.; Joazeiro, C. A. P. RING Domain E3 Ubiquitin Ligases. *Annu. Rev. Biochem.* **2009**, *78* (1), 399–434.

(12) Sarikas, A.; Hartmann, T.; Pan, Z.-Q. The Cullin Protein Family. *Genome Biol.* **2011**, *12* (4), 220.

(13) Nguyen, H. C.; Yang, H.; Fribourgh, J. L.; Wolfe, L. S.; Xiong, Y. Insights into Cullin-RING E3 Ubiquitin Ligase Recruitment: Structure of the VHL–EloBC–Cul2 Complex. *Struct. Lond. Engl. 1993* **2015**, *23* (3), 441–449.

(14) Schofield, C. J.; Ratcliffe, P. J. Oxygen Sensing by HIF Hydroxylases. *Nat. Rev. Mol. Cell Biol.* **2004**, *5* (5), 343–354.

(15) Buckley, D. L.; Van Molle, I.; Gareiss, P. C.; Tae, H. S.; Michel, J.; Noblin, D. J.; Jorgensen, W. L.; Ciulli, A.; Crews, C. M. Targeting the von Hippel–Lindau E3 Ubiquitin Ligase Using Small Molecules To Disrupt the VHL/HIF-1α Interaction. *J. Am. Chem. Soc.* **2012**, *134* (10), 4465–4468.

(16) The Nobel Prize in Physiology or Medicine 2019 https://www.nobelprize.org/prizes/medicine/2019/press-release.

(17) Fischer, E. S.; Böhm, K.; Lydeard, J. R.; Yang, H.; Stadler, M. B.; Cavadini, S.; Nagel, J.; Serluca, F.; Acker, V.; Lingaraju, G. M.; Tichkule, R.B.; Schebesta, M.; Forrester, C.; Schirle, M.; Hassiepen, U.; Ottl, J.; Hild, M.; Beckwith, R.E.J.; Harper J.W.; Jenkins J.L.; Thoma N.H. Structure of the DDB1-CRBN E3 Ubiquitin Ligase in Complex with Thalidomide. *Nature* **2014**, *512* (7512), 49–53.

(18) Higgins, J. J.; Hao, J.; Kosofsky, B. E.; Rajadhyaksha, A. M. Dysregulation of Large-Conductance Ca^{2+}-Activated K^{+} Channel Expression in Nonsyndromal Mental Retardation Due to a Cereblon p.R419X Mutation. *neurogenetics* **2008**, *9* (3), 219–223.

(19) Ito, T.; Suzuki, T.; Ando, H.; Ogura, T.; Hotta, K.; Imamura, J.; Yamaguchi Y.; Handa, H. Identification of a Primary Target of Thalidomide Teratogenicity. Science **2010**, 327 (5971), 1345-1350.

(20) Lee, K. M.; Jo, S.; Kim, H.; Lee, J.; Park, C.-S. Functional Modulation of AMP-Activated Protein Kinase by Cereblon. *Biochim. Biophys. Acta BBA - Mol. Cell Res.* **2011**, *1813* (3), 448–455.

(21) Kim, H. K.; Ko, T. H.; Nyamaa, B.; Lee, S. R.; Kim, N.; Ko, K. S.; Rhee, B. D.; Park, C.-S.; Nilius, B.; Han, J. Cereblon in Health and Disease. *Pflugers Arch.* **2016**, *468* (8), 1299–1309.

(22) Ong, J. Y.; Torres, J. Z. E3 Ubiquitin Ligases in Cancer and Their Pharmacological Targeting. *Ubiquitin Proteasome Syst. - Curr. Insights Mech. Cell. Regul. Dis.* **2019**.

(23) Dang, C. V.; Reddy, E. P.; Shokat, K. M.; Soucek, L. Drugging the “undruggable” Cancer Targets. *Nat. Rev. Cancer* **2017**, *17* (8), 502–508.

(24) Lai, A. C.; Crews, C. M. Induced Protein Degradation: An Emerging Drug Discovery Paradigm. *Nat. Rev. Drug Discov.* **2017**, *16* (2), 101–114.

(25) Pei, H.; Peng, Y.; Zhao, Q.; Chen, Y. Small Molecule PROTACs: An Emerging Technology for Targeted Therapy in Drug Discovery. *RSC Adv.* **2019**, *9* (30), 16967–16976.

(26) Pettersson, M.; Crews, C. M. PROteolysis TArgeting Chimeras (PROTACs) — Past, Present and Future. *Drug Discov. Today Technol.* **2019**, *31*, 15–27.

(27) Raina, K.; Lu, J.; Qian, Y.; Altieri, M.; Gordon, D.; Rossi, A. M. K.; Wang, J.; Chen, X.; Dong, H.; Siu, K.; Winkler, D.; Crew, A.P.; Crew, C.M.; Coleman, G.K. PROTAC-Induced BET Protein Degradation as a Therapy for Castration-Resistant Prostate Cancer. *Proc. Natl. Acad. Sci. U. S. A.* **2016**, *113* (26), 7124–7129.

(28) Zengerle, M.; Chan, K.-H.; Ciulli, A. Selective Small Molecule Induced Degradation of the BET Bromodomain Protein BRD4. *ACS Chem. Biol.* **2015**, *10* (8), 1770–1777.

(29) Gadd, M. S.; Testa, A.; Lucas, X.; Chan, K.-H.; Chen, W.; Lamont, D. J.; Zengerle, M.; Ciulli, A. Structural Basis of PROTAC Cooperative Recognition for Selective Protein Degradation. *Nat. Chem. Biol.* **2017**, *13* (5), 514–521.

(30) Winter, G.E.; Buckley, D.L.; Paulk, J.; Roberts J.M; Souza A.; Dhe-Paganon S.; Bradner, J.E. Phthalimide conjugation as a strategy for in vivo target protein degradation. *Science* **2015**, *348*, 1376-1381.

(31) Lu, J.; Qian, Y.; Altieri, M.; Dong, H.; Wang, J.; Raina, K.; Hines, J.; Winkler, J. D.; Crew, A. P.; Coleman, K.; Crew, M.C. Hijacking the E3 Ubiquitin Ligase Cereblon to Efficiently Target BRD4. *Chem. Biol.* **2015**, *22* (6), 755–763.

(32) Zoppi, V.; Hughes, S. J.; Maniaci, C.; Testa, A.; Gmaschitz, T.; Wieshofer, C.; Koegl, M.; Riching, K. M.; Daniels, D. L.; Spallarossa, A.; Ciulli, A. Iterative Design and Optimization of Initially Inactive Proteolysis Targeting Chimeras (PROTACs) Identify VZ185 as a Potent, Fast, and Selective von Hippel–Lindau (VHL) Based Dual Degrader Probe of BRD9 and BRD7. *J. Med. Chem.* **2019**, *62* (2), 699–726.

(33) Bondeson, D. P.; Mares, A.; Smith, I. E. D.; Ko, E.; Campos, S.; Miah, A. H.; Mulholland, K. E.; Routly, N.; Buckley, D. L.; Gustafson, J. L.; Zinn, N.; Grandi, P.; Shimamura, S.; Bergamini, G.; Faelt-Savitski, M., Bantscheff, M.; Cox, C.; Gordon, D. A.; Willard, R. R.; Flanagen, J. J.; Casillas, L. N.; Votta, B. J.; den Besten W.; Famm, K.; Kruidenier, L.; Carter, P.S.; Harling, J. D.; Churcher, I.; Crews, C. M. Catalytic in Vivo Protein Knockdown by Small-Molecule PROTACs. *Nat. Chem. Biol.* **2015**, *11* (8), 611–617.

(34) Lai, A. C.; Toure, M.; Hellerschmied, D.; Salami, J.; Jaime-Figueroa, S.; Ko, E.; Hines, J.; Crews, C. M. Modular PROTAC Design for the Degradation of Oncogenic BCR-ABL. *Angew. Chem. Int. Ed Engl.* **2016**, *55* (2), 807–810.

(35) Itoh, Y.; Ishikawa, M.; Naito, M.; Hashimoto, Y. Protein Knockdown Using Methyl Bestatin−Ligand Hybrid Molecules: Design and Synthesis of Inducers of Ubiquitination-Mediated Degradation of Cellular Retinoic Acid-Binding Proteins. *J. Am. Chem. Soc.* **2010**, *132* (16), 5820–5826.

(36) Maniaci, C.; Hughes, S. J.; Testa, A.; Chen, W.; Lamont, D. J.; Rocha, S.; Alessi, D.R.; Romeo, R.; Ciulli, A. Homo-PROTACs: bivalent small-molecule dimerizers of the VHL E3 ubiquitin ligase to induce self-degradation. *Nat. Commun.* ***2017****, 8* (1), 830.

(37) Steinebach, C.; Lindner, S.; Udeschi, N.D.; Mani, D. C.; Kehm, H.; Köpff, S.; Carr, S. A.; Gütschow, M.; Krönke, J. Homo-PROTACs for the Chemical Knockdown of Cereblon. *ACS Chem. Biol.* ***2018****, 13 (9) 2771-2782.*

(38) Galdeano, C.; Gadd, M. S.; Soares, P.; Scaffidi, S.; Van Molle, I.; Birced, I.; Hewitt, S.; Dias, D. M.; Ciulli, A. Structure-Guided Design and Optimization of Small Molecules Targeting the Protein-Protein Interaction between the von Hippel-Lindau (VHL) E3 Ubiquitin Ligase and the Hypoxia Inducible Factor (HIF) Alpha Subunit with in Vitro Nanomolar Affinities. *J. Med. Chem.* **2014**, *57* (20).

(39) Soares, P.; Gadd, M. S.; Frost, J.; Galdeano, C.; Ellis, L.; Epemolu, O.; Rocha, S.; Read, K. D.; Ciulli, A. Group-Based Optimization of Potent and Cell-Active Inhibitors of the von Hippel–Lindau (VHL) E3 Ubiquitin Ligase: Structure–Activity Relationships Leading to the Chemical Probe (2S,4R)-1-((S)-2-(1-Cyanocyclopropanecarboxamido)-3,3-Dimethylbutanoyl)-4-Hydroxy-N-(4-(4-Methylthiazol-5-Yl)Benzyl)Pyrrolidine-2-Carboxamide (VH298). *J. Med. Chem.* **2018**, *61* (2), 599–618.

(40) Shahbazi, S.; Peer, C. J.; Polizzotto, M. N.; Uldrick, T. S.; Roth, J.; Wyvill, K. M.; Aleman, K.; Zeldis, J. B.; Yarchoan, R.; Figg, W. D. A Sensitive and Robust HPLC Assay with Fluorescence Detection for the Quantification of Pomalidomide in Human Plasma for Pharmacokinetic Analyses. *J. Pharm. Biomed. Anal.* **2014**, *92*, 63–68.

(41) Roy, M. J.; Winkler, S.; Hughes, S. J.; Whitworth, C.; Galant, M.; Farnaby, W.; Rumpel, K.; Ciulli, A. SPR-Measured Dissociation Kinetics of PROTAC Ternary Complexes Influence Target Degradation Rate. *ACS Chem. Biol.* **2019**, *14* (3), 361–368.

(42) Riching, K. M.; Mahan, S.; Corona, C. R.; McDougall, M.; Vasta, J. D.; Robers, M. B.; Urh, M.; Daniels, D. L. Quantitative Live-Cell Kinetic Degradation and Mechanistic Profiling of PROTAC Mode of Action. *ACS Chem. Biol.* **2018**, *13* (9), 2758–2770.

(43) Chan, K.-H.; Zengerle, M.; Testa, A.; Ciulli, A. Impact of Target Warhead and Linkage Vector on Inducing Protein Degradation: Comparison of Bromodomain and Extra-Terminal (BET) Degraders Derived from Triazolodiazepine (JQ1) and Tetrahydroquinoline (I-BET726) BET Inhibitor Scaffolds. *J. Med. Chem.* **2018**, *61* (2), 504–513.

(44) Crew, A. P.; Raina, K.; Dong, H.; Qian, Y.; Wang, J.; Vigil, D.; Serebrenik, Y. V.; Hamman, B. D.; Morgan, A.; Ferraro, C.; Siu, K.; Neklesa, T. K., Winkler. J. D.; Coleman K. G. Identification and Characterization of Von Hippel-Lindau-Recruiting Proteolysis

Targeting Chimeras (PROTACs) of TANK-Binding Kinase 1. *J. Med. Chem.* **2018**, *61* (2), 583–598.

(45) Remillard, D.; Buckley, D. L.; Paulk, J.; Brien, G. L.; Sonnett, M.; Seo, H.-S.; Dastjerdi, S.; Wühr, M.; Dhe-Paganon, S.; Armstrong, S. A.; et al. Degradation of the BAF Complex Factor BRD9 by Heterobifunctional Ligands. *Angew. Chem. Int. Ed Engl.* **2017**, *56* (21), 5738–5743.

(46) An, S.; Fu, L. Small-Molecule PROTACs: An Emerging and Promising Approach for the Development of Targeted Therapy Drugs. *EBioMedicine* **2018**, *36*, 553–562.

(47) Knuf, E. C.; Jiang, J.-K.; Gin, M. S. Preparation of Discrete Oligoethers: Synthesis of Pentabutylene Glycol and Hexapropylene Glycol by Two Complementary Methods. *J. Org. Chem.* **2003**, *68* (23), 9166–9169.

(48) Accurso, A. A.; Delaney, M.; O'Brien, J.; Kim, H.; Iovine, P. M.; Díaz Díaz, D.; Finn, M. G. Improved Metal-Adhesive Polymers from Copper(I)-Catalyzed Azide-Alkyne Cycloaddition. *Chem. Weinh. Bergstr. Ger.* **2014**, *20* (34), 10710–10719.

(49) Burslem, G. M.; Ottis, P.; Jaime-Figueroa, S.; Morgan, A.; Cromm, P. M.; Toure, M.; Crews, C. M. Efficient Synthesis of Immunomodulatory Drug Analogues Enables Exploration of Structure–Degradation Relationships. *ChemMedChem* **2018**, *13* (15), 1508–1512.

(50) Maniaci, C. Design, Synthesis and Biological Evaluation of New Bifunctional Chemical Degrader Molecules (PROTACs) Targeting Hypoxia Signalling Pathway. **2017**, PhD Thesis, University of Messina.

(51) Paramanik, M.; Singh, R.; Mukhopadhyay, S.; Ghosh, S. K. Catalytic Nucleophilic Fluorination by an Imidazolium Ionic Liquid Possessing Trialkylphosphine Oxide Functionality. *J. Fluor. Chem.* **2015**, *178*, 47–55.

(52) Wittmann, V.; Takayama, S.; Gong, K. W.; Weitz-Schmidt, G.; Wong, C.-H. Ligand Recognition by E- and P-Selectin: Chemoenzymatic Synthesis and Inhibitory Activity of Bivalent Sialyl Lewis x Derivatives and Sialyl Lewis x Carboxylic Acids. *J. Org. Chem.* **1998**, *63* (15), 5137–5143.

(53) PATENT UY37728 (A), **2019**.

(54) Bright, S. A.; Brinkø, A.; Larsen, M. T.; Sinning, S.; Williams, D. C.; Jensen, H. H. Basic N-Interlinked Imipramines Show Apoptotic Activity against Malignant Cells Including Burkitt's Lymphoma. *Bioorg. Med. Chem. Lett.* **2013**, *23* (5), 1220–1224.

6. Conclusions

In this work, convergent medicinal chemistry approaches were explored to provide novel chemical tools for innovative therapeutic intervention against mycobacterial infections. In particular, the research was carried out *via* three main strategies: (i) a hit-to-lead optimization process of potent antitubercular hit compounds, (ii) the development of a non-cytotoxic efflux pump inhibitor, and (iii) the synthesis of small-peptide inhibitors of Pup/PafA interaction to evaluate the inhibition of protein degradation as an innovative antitubercular target.

The first approach, carried out through parallel Structure-Activity Relationships and Structure-Metabolism Relationships studies, allowed on one hand to explore the influence of various chemical modifications on the activity of the two promising parent compounds, and, on the other hand, to gain insights about the metabolic faith of these molecules in an *in vitro* model. The most abundant metabolites generated in Human Liver Microsomes were identified and the structure of the parent was accordingly modified to give more stable compounds. In some cases, cellular activity was maintained despite a slight increase of cytotoxicity could be noticed. The characterization of these compounds was then further enriched by the preliminary investigation of their mechanism of action.

The improvement of an in-house efflux pumps inhibitor was mainly focused on overcoming its cytotoxicity, *via* an investigation of the structure-activity/toxicity relationships. This led to the identification of the chemical features linked to the activity and those related to the cytotoxicity and to the development of a potent, non-cytotoxic inhibitor of *M. tuberculosis* efflux pumps.

Finally, peptidic sequences derived from pupylation agent Pup were tested for their ability to inhibit the Pup/PafA interaction, allowing to identify a promising peptide inhibitor. This study set the stage for further development of such inhibitors, that ideally should be shrunk in a small-molecule structure.

In conclusion, this thesis work meant to provide a set of molecules/chemical tools that, after proper development, might represent a solid base for future innovative antitubercular therapeutics.

7. Acknowledgements

I would like to acknowledge, at first, Prof. Gabriele Costantino, who gave me the possibility to carry out this extremely rewarding experience in his research group, for his support and precious advice. Dr Marco Pieroni is warmly acknowledged for his precious help during these three years and for the support in the thesis writing. Since the fairly high number of biological assays presented in this PhD thesis, several collaborators must be acknowledged for their inestimable contribution. MIC determinations presented in chapter 2 were performed by the research group headed by Maria Rosalia Pasca, University of Pavia. Preliminary studies on the mechanism of action were carried out by Dr Charles Omollo in the research group headed by Prof Digby Warner, University of Cape Town. Metabolic stability investigations were performed in collaboration with Prof Federica Vacondio and Dr Francesca Ferlenghi, University of Parma. Cytotoxicity assays were performed in collaboration with Prof Francesca Zimetti and Prof Maria Pia Adorni, University of Parma. All the biological assays reported in chapter 3 were performed by Dr Diana Machado in the group of Prof Miguel Viveiros, from the Universitade Nova de Lisboa. Biochemical evaluation of Pup/PafA interaction (chapter 4) was performed at the University of Piemonte Orientale in Novara, under the supervision of Prof Riccardo Miggiano e Prof Davide Ferraris. Prof Stefano Sforza, Prof Tullia Tedeschi and Dr Sofie Buhler are warmly acknowledged for their help in the synthesis of the peptide inhibitors. Finally, I would like to acknowledge all the members of the group of Prof Alessio Ciulli at the University of Dundee, where I have spent my period abroad. Their contribution has been instrumental to obtain the results presented in chapter 5 and to sustain my personal and professional growth. A warm acknowledge is due to the head of the group, Prof Alessio Ciulli, who gave the possibility to spend 10 months in his group where I have never missed his precious advises.

Appendix A.

1. Comparative identification of metabolites:

1.1 HR-MS spectra of the identified metabolites:

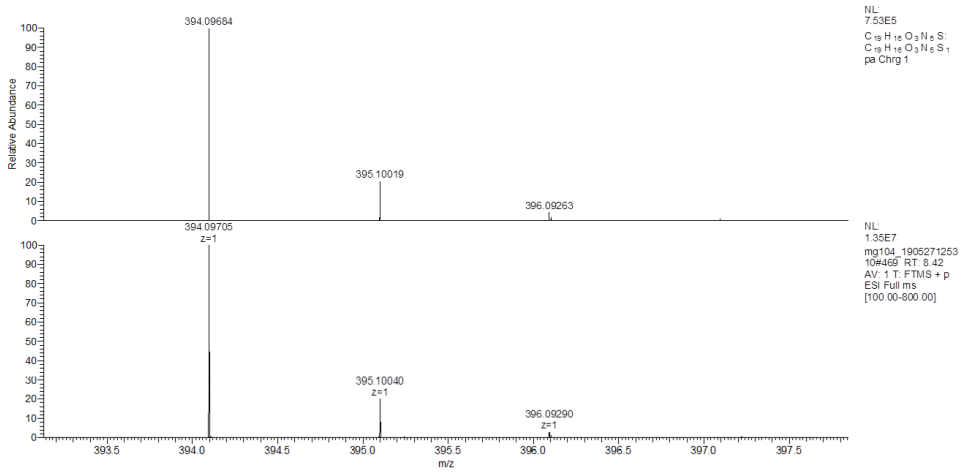

Figure 1S. *Calculated and experimental HR-MS spectra with relative abundance of compound* ***42h***

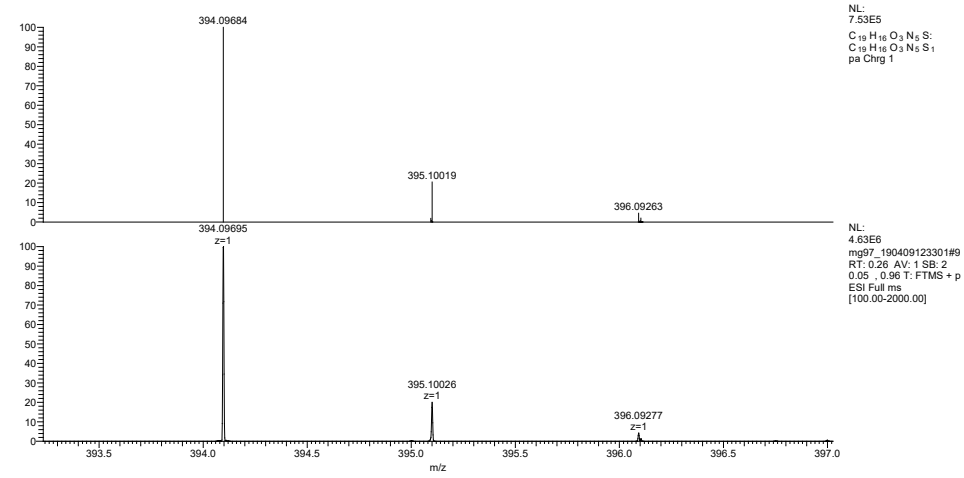

Figure 2S. *Calculated and experimental HR-MS spectra with relative abundance of compound* ***42e***

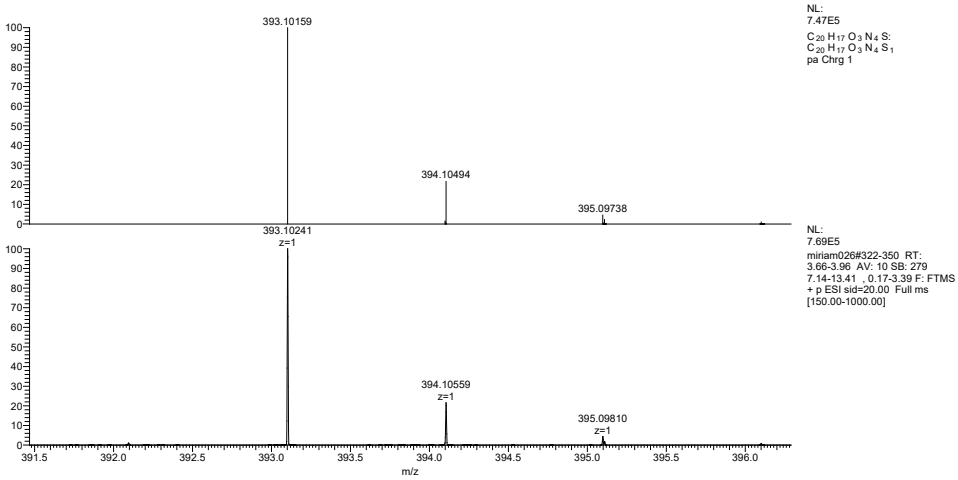

Figure 1S. *Calculated and experimental HR-MS spectra with relative abundance of compound* ***43h***

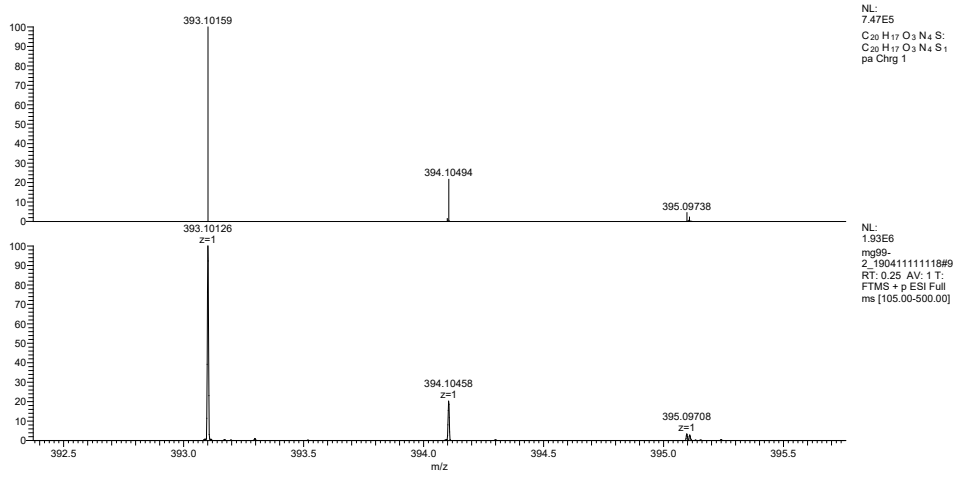

Figure 4S. *Calculated and experimental HR-MS spectra with relative abundance of compound* ***38***

1.2 MS/MS spectra:

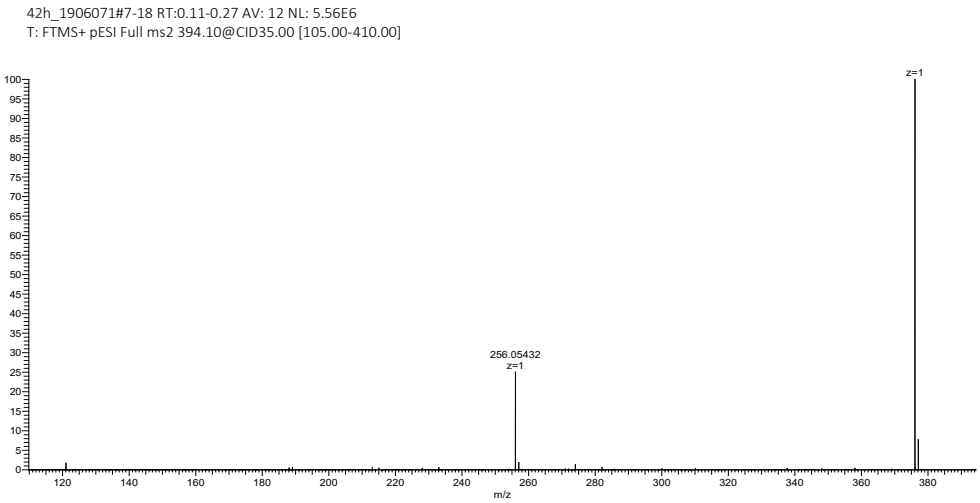

Figure 5S. *MS/MS spectrum of compound* ***42h***

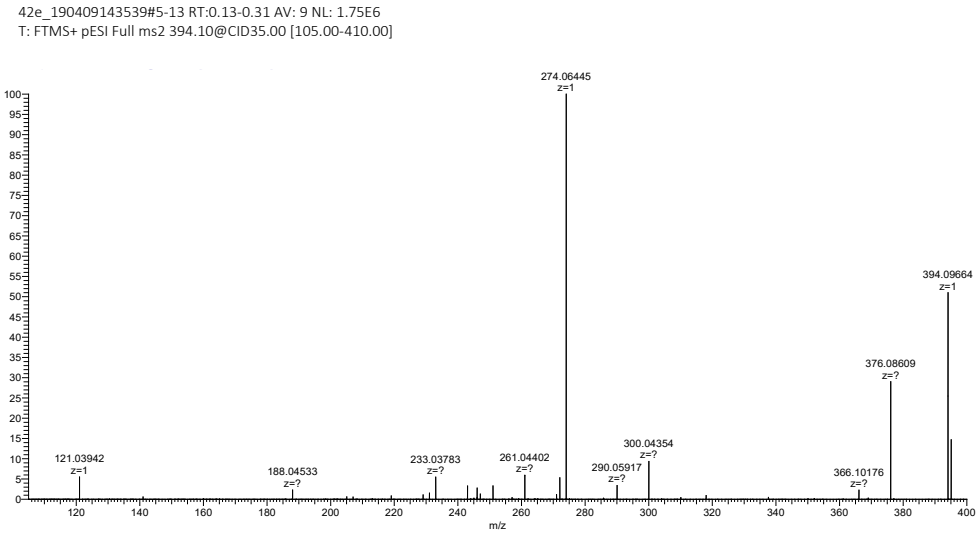

Figure 6S. *MS/MS spectrum of compound* ***42e***

42i_190718113134#10-19 RT:0.22-044 AV: 10 NL: 2.12E6
T: FTMS+ pESI Full ms2 394.10@CID35.00 [105.00-450.00]

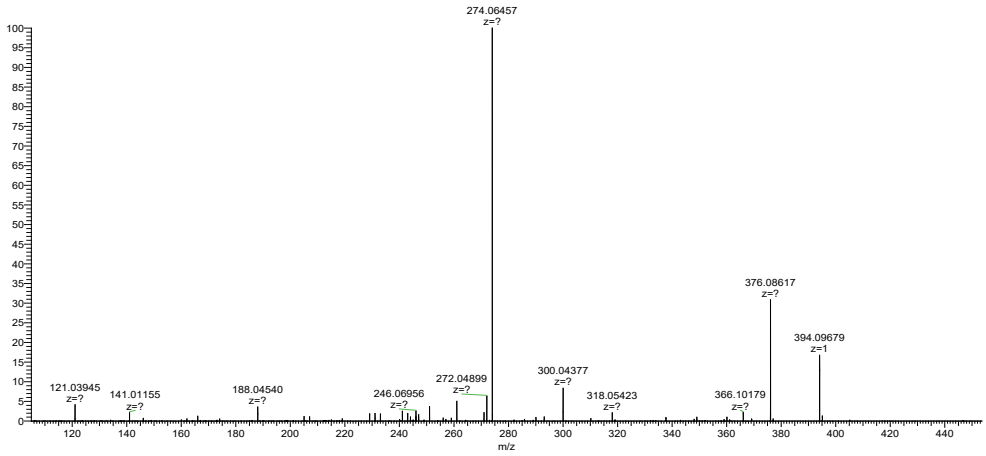

Figure 7S. *MS/MS spectrum of compound* ***42i***

43h_#312-367 RT:0.12-0.28 AV: 19 NL: 3.28E4
T: FTMS+ pESI Full ms2 393.09@CID35.00 [105.00-400.00]

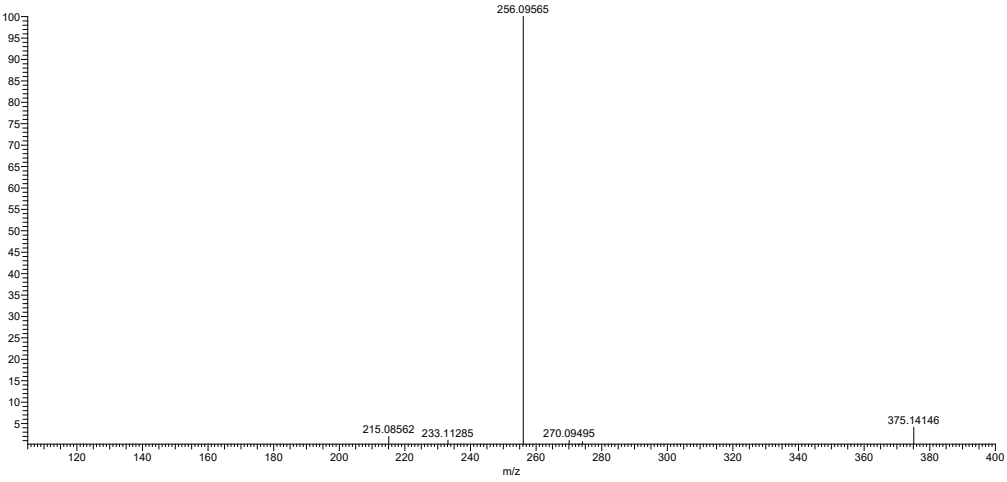

Figure 7S. *MS/MS spectrum of compound* ***43h***

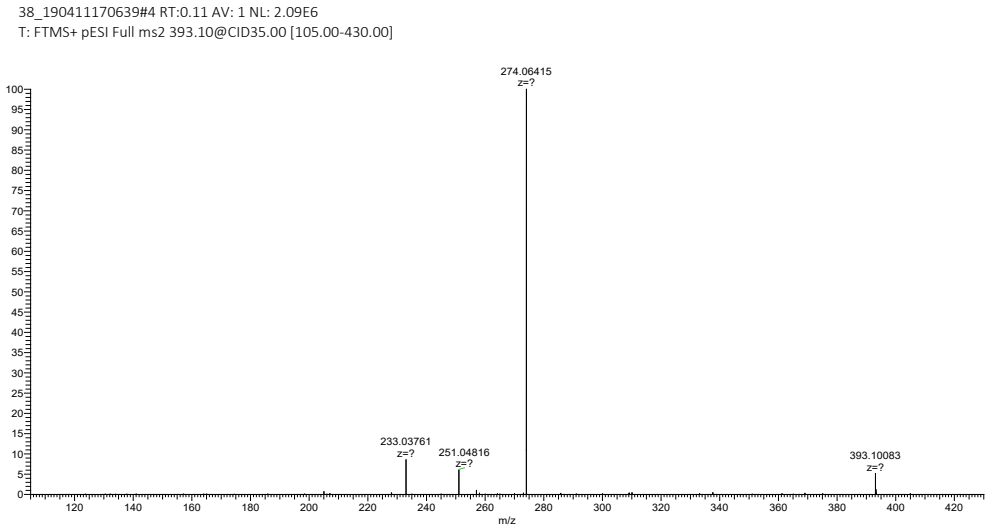

Figure 8S. *MS/MS spectrum of compound **38***

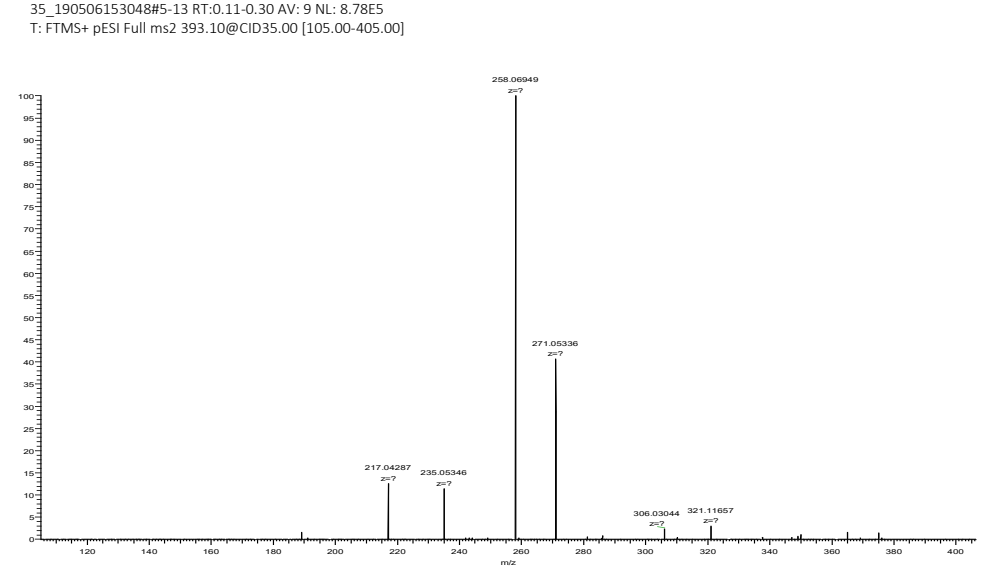

Figure 9S. *MS/MS spectrum of compound **35***

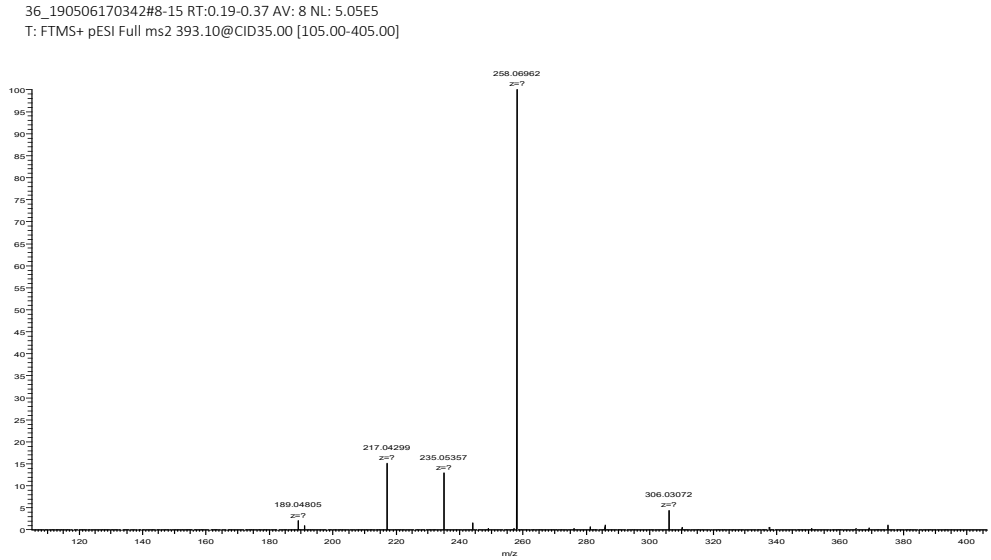

Figure 10S. *MS/MS spectrum of compound **36***

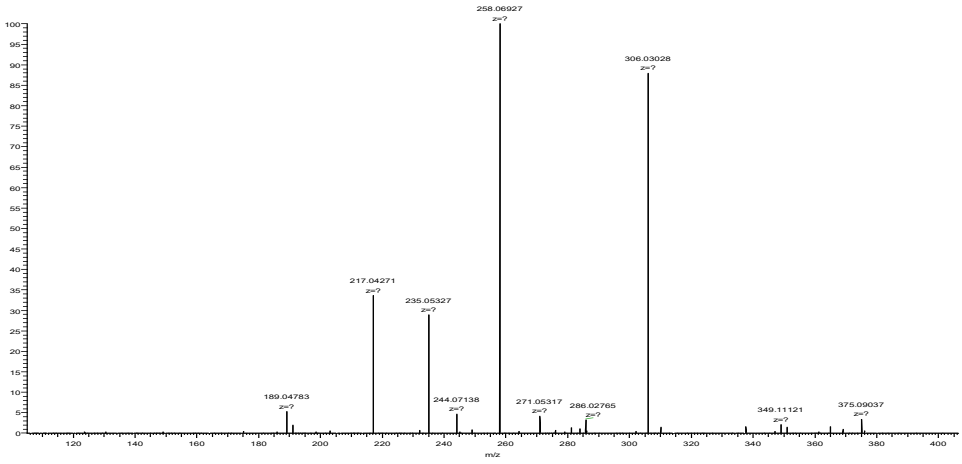

Figure 11S. *MS/MS spectrum of compound **37***

1.3 HPLC runs, retention times and coelutions

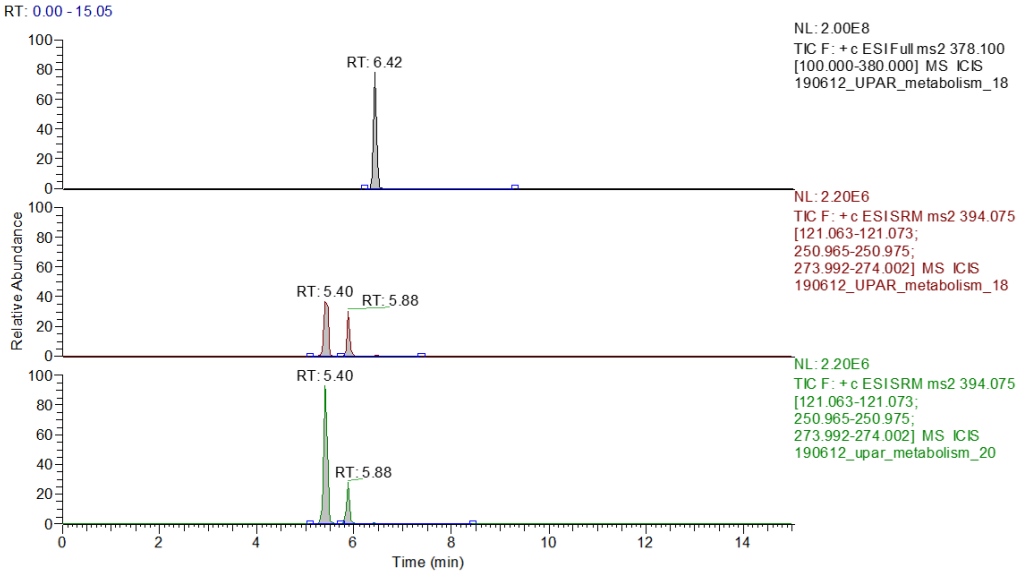

Figure 12S. *(A) Parent compound (UPAR-453) in incubation mixture eluting at 6.42 min in HLM incubate. (B) Metabolites M1 and M2 at m/z = 394 $[M+H]^+$ and retention time of 5.40 min and 5.88 min. (C) Co-elution in HLM Incubation mixture of M1 with a 500 nM concentration of* ***42h****.*

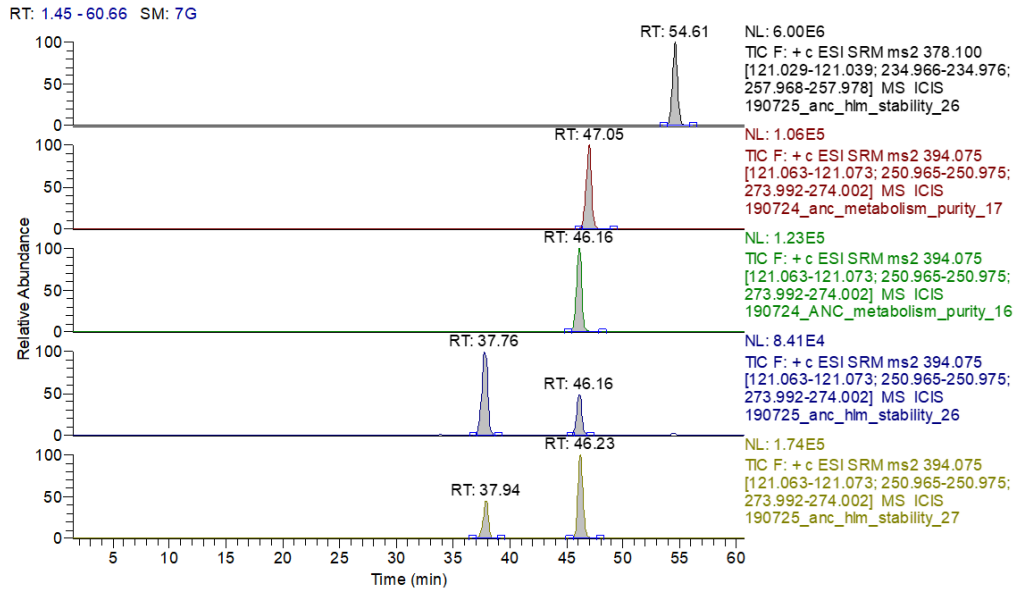

Figure 13S. *(A) Parent compound (UPAR-453) in HLM incubation mixture (RT: 54.6 min). (B) Elution of standard* ***42i*** *(RT=47.0 min). (C) Elution of standard* ***42e*** *(RT=46.1 min). (D) HLM Incubation mixture showing metabolites M1 (RT = 37.7 min) and M2 (RT = 46.1 min). (E) HLM Incubation mixture spiked with a 250 nM concentration of* ***42e****. For clarity purposes the 0-60 min of the 120 min HPLC-MS gradient were reported.*

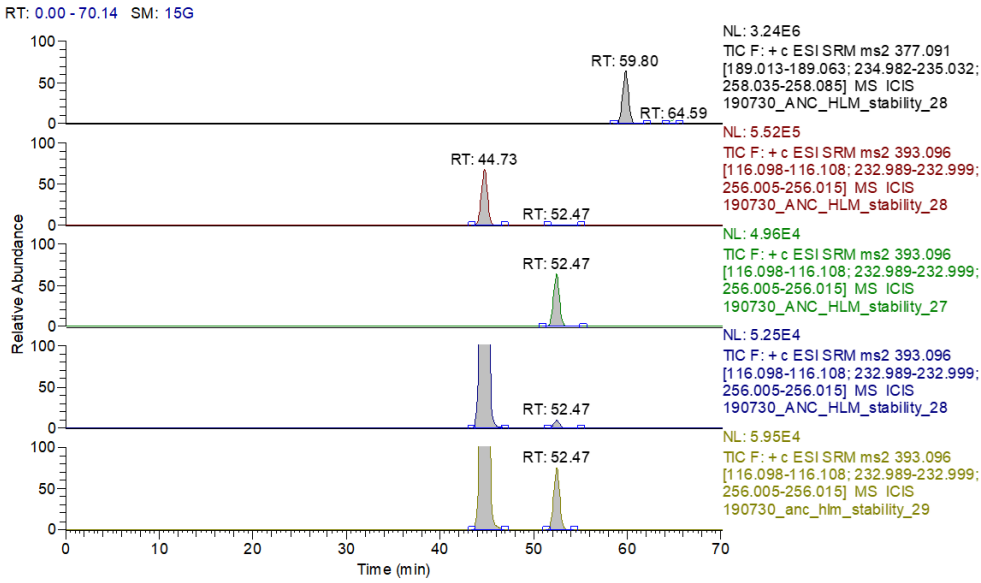

Figure 14S. *(A) Parent compound (UPAR-452) in HLM incubation mixture (RT: 59.9 min). (B) Elution of standard **43h** (RT=44.8 min). (C) Elution of standard **38** (RT=52.5 min). (D) HLM Incubation mixture showing metabolites M1 (RT = 44.7 min) and M2 (RT = 52.5 min). (E) HLM Incubation mixture spiked with a 250 nM concentration of **38**. For clarity purposes traces the 0-70 min of the 120 min HPLC-MS gradient were reported. Moreover, (D) and (E) traces were magnified to show the increase of metabolite M2 peak after **38** spike.*

Appendix B.

1. Supporting synthetic procedures

1,5-Bis(allyloxy)pentane (S1)

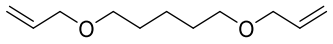

The title compound was synthesized as previously reported.[1] Analytical data matched those reported.

5-(Benzyloxy)pentan-1-ol (S2)

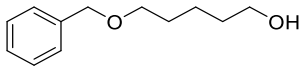

The title compound was synthesized as previously reported.[2] Analytical data matched those reported.

2-(2-(2-(Benzyloxy)ethoxy)ethoxy)ethyl methanesulfonate (S3)

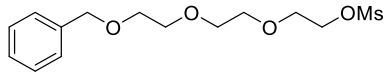

The title compound was obtained following the method previously reported.[3] Analytical data matched those reported.

1,18-Diphenyl-2,5,8,11,17-pentaoxaoctadecane (S4)

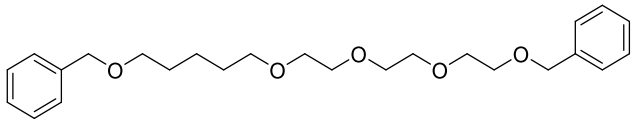

Compound **S2** (228.58 mg, 1.177 mmol, 2.5 eq) was added to a solution of NaHMDS 1M in THF (107 mg, 0.58 mL, 0.58 mmol, 1.25 eq.) at 0°C under N_2 atmosphere. Reaction mixture was stirred at r.t. for 1 h. After this time a solution of compound **S3** (150 mg, 0.47 mmol, 1 eq.) in DMF was added and the mixture was irradiated with microwave at 130°C for 2 h. After this time the solvent was evaporated, the reaction quenched with 5% aqueous $NaHSO_4$ and extracted with DCM (x3). Organic layers were collected, dried over $MgSO_4$, filtered and evaporated under reduced pressure. The crude was purified

by flash chromatography eluting from 0% to 50% v/v of ethyl acetate in heptane to yield the desired compound as an oil (114 mg, yield: 58%). ^{1}H-NMR (500 MHz, $CDCl_3$) δ: 7.28 - 7.19 (m, 10H), 4.49 (s, 2H), 4.43 (s, 2H), 3.62 - 3.54 (m, 10H), 3.51 - 3.48 (m, 2H), 3.43 - 3.36 (m, 4H), 1.61 - 1.48 (m, 4H), 1.42 - 1.31 (m, 2H).

(S)-1-((2R,3R,4S)-3-Fluoro-4-hydroxy-2-((4-(4-methylthiazol-5-yl)benzyl)carbamoyl)pyrrolidin-1-yl)-3,3-dimethyl-1-oxobutan-2-aminium chloride (S5)

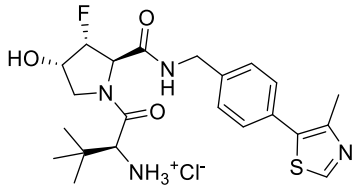

The title compound was prepared accordingly to PATENT WO 2018/051107 A1.

Analytical data matched those previously reported.

2. Supporting schemes

SI Scheme 1

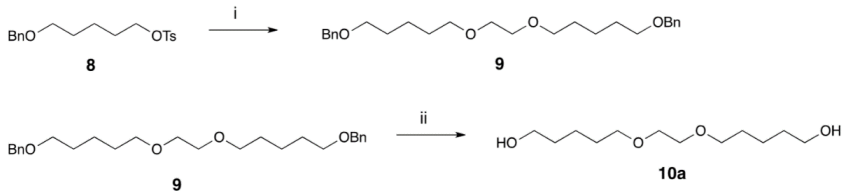

Scheme 2: *Synthesis of diol **10a**. i) ethylene glycol, NaH 60% dispersion in mineral oil, DMF dry, r.t to 50°C, O/N, 79%; ii) H_2, Pd/C, ethanol, r.t., quantitative.*

SI Scheme 2

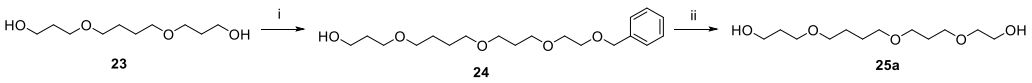

SI Scheme 2. *i) 50% NaOH aq., TBABr, TBAI, benzyl-2-bromo-ethylether, toluene, 48 h, r.t, 57%; ii) ethanol, H-cube machine: flow 1 mL/min, H_2, 10 atm, yield: 34%.*

SI Scheme 3

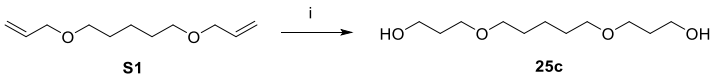

SI Scheme 3. *i) 9-BBN, dry THF, r.t., overnight, quenching mixture: MeOH, 30% NaOH aq., 30% H_2O_2 aq., 81%.*

SI Scheme 4

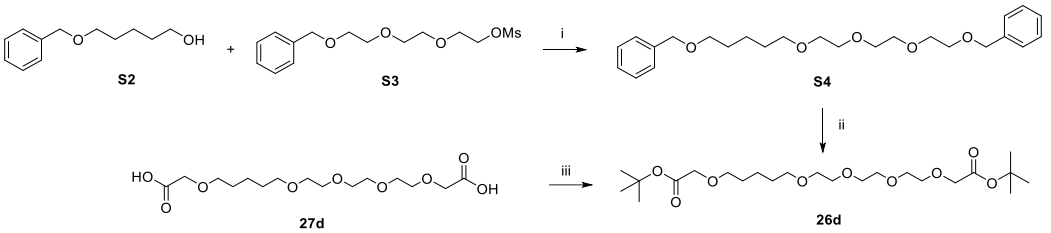

SI Scheme 4. *i) **S2**, NaHMDS 1M in THF, 0°C, N_2 atm, 1 h; then **S3**, dry DMF, 130°C, 2 h, 58%; ii) ethanol, H-cube machine: flow 1 mL/min, H_2, 10 atm; then, tert-butyl bromoacetate, TBABr, NaOH 37%, DCM, r.t, overnight, 47%; iii) 50% TFA in DCM, r.t, 1 h, quantitative.*

SI Scheme 5

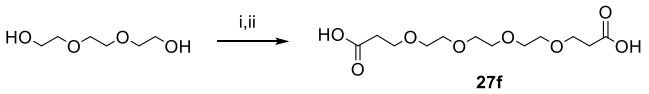

SI Scheme 5. *i) tert-butyl acrylate, TBABr, 50% NaOH (aq), DCM, r.t, overnight, 78%; ii) 50% TFA in DCM, r.t, 1 h, quantitative*

3. References

(1) Accurso, A. A.; Delaney, M.; O'Brien, J.; Kim, H.; Iovine, P. M.; Díaz Díaz, D.; Finn, M. G. Improved Metal-Adhesive Polymers from Copper(I)-Catalyzed Azide-Alkyne Cycloaddition. *Chem. Weinh. Bergstr. Ger.* **2014**, *20* (34), 10710–10719.

(2) Young, I. S.; Kerr, M. A. Total Synthesis of (+)-Nakadomarin A. *J. Am. Chem. Soc.* **2007**, *129* (5), 1465–1469.

(3) Bonnet, N.; O'Hagan, D.; Hähner, G. Ionic Strength Mediated Hydrophobic Force Switching of CF3-Terminated Ethylene Glycol Self-Assembled Monolayers (SAMs) on Gold. *Chem. Commun. Camb. Engl.* **2007**, No. 47, 5066–5068.